Biosynthesis of phenylphenalenone-type compounds in Haemodoraceae plants and their phytopathological role in the interaction *Musa* - *Mycosphaerella fijiensis*

Dissertation

(kumulativ)

Zur Erlangung des akademischen Grades

Doctor rerum naturalium (Dr. rer. nat.)

vorgelegt dem Rat der Chemisch-Geowissenschaftlichen Fakultät

der Friedrich-Schiller-Universität Jena

von Master of Science in Biotechnology,

William Fernando Hidalgo Bucheli

Geboren am 01. März 1981 in Pasto, Kolumbien

Gutachter:

1. Prof. Dr. Hans-Dieter Arndt	Institut für Organische Chemie und Makromoleculare Chemie, Friedrich Schiller University, Jena
2. PD Dr. Bernd Schneider	Research group Biosynthesis/NMR, Max Planck Institute for Chemical Ecology, Hans-Knöll Str. 8, Jena
3. Dr. Felipe Otálvaro Tamayo	Institute of Chemistry, Universidad de Antioquía, Medellín-Colombia.

Tag der Verteidigung: 14.10.2015

Contents

1. Introduction 1
   - 1.1 Taxonomic aspects of Musaceae 1
   - 1.2 Economic importance of banana 3
   - 1.3 Pest and diseases of banana 4
     - 1.3.1 Black Leaf Sigatoka Disease 5
     - 1.3.2 Chemical control 6
     - 1.3.3 Biological control 8
     - 1.3.4 Crop improvement 8
   - 1.4 *Musa-Mycosphaerella fijiensis* interaction 9
   - 1.5 Phenylphenalenones 12
     - 1.5.1 Natural occurrence 12
     - 1.5.2 Biosynthetic aspects 14
     - 1.5.3 Inducible metabolites in Musa 16
     - 1.5.4 Pharmacological activity 18
   - 1.6 Scope of this work 19

2. Overview of manuscripts 21

3. Biosynthesis of phenylphenalenones in Haemodoraceae plants
   - 3.1 4-Methoxycinnamic acid - An unusual phenylpropanoid involved in phenylphenalenone biosynthesis in *Anigozanthos preissii* 27
   - 3.2 Biosynthesis of tetraoxygenated phenylphenalenones in *Wachendorfia thyrsiflora* 35

4. Phenylphenalenones protect banana plants from infection by *Mycosphaerella fijiensis* and are deactivated by metabolic conversion 47

5. Synthesis of new antimicrobial compounds against *M. fijiensis*
5.1 Improved synthesis of 4-phenylphenalenones: the case of isoanigorufone and structural analogs 111
5.2 4-phenylphenalenones as a template for new photodynamic compounds against *Mycosphaerella fijiensis* 121

6. Discussion 127
6.1 General discussion 127
6.2 Biosynthesis of phenylphenalenones in Haemodoraceae plants 128
6.3 Phenylphenalenones involved in chemical defense of *Musa* 130
6.4 Design of new antimicrobial compounds against *M. fijiensis* 140

7. Summary 143
Zusammenfassung

References 149

Acknowledgements 162

Curriculum vitae 164

Selbständigkeitserklärung 169

Erklärung 170

Abbreviations

1D	One-dimensional
2D	Two-dimensional
ANOVA	Analysis of variance
BLSD	Black Leaf Sigatoka Disease
c.v	clon variety
$CDCl_3$	deuterated chloroform
CIRAD	Agricultural Research for Development
COSY	correlated spectroscopy
DAD	diode array detector
DMSO	dimethyl sulphoxide
dpi	Days post inoculation
EIMS	electron impact mass spectrometry
ESI-MS	Electrospray ionization mass spectrometry
FAO	Food and Agriculture Organization of the United Nations
FHIA	Fundación Hondureña de Investigación Agrícola
Fig	Figure
FRAC	Fungicide Resistance Action Committee
ha	Hectare
HMBC	Heteronuclear multiple-bond correlation
HPLC	High performance liquid chromatography
HRESIMS	high resolution electrospray ionisation mass spectrometry
HSQC	Heteronuclear single quantum coherence spectroscopy
Hz	Hertz
IITA	International Institute of Tropical Agriculture
INIBAP	International Network for the Improvement of Banana and Plantain
J	Coupling constant
KTR	Khai Thong Ruang
LC-MS	Liquid chromatography coupled with mass spectrometry
m/z	mass-to-charge ratio

MeOH-*d4*	deuterated methanol
min	minute
NMR	Nuclear magnetic resonance
NOESY	Nuclear Overhauser enhancement spectroscopy
OECD	Organization for Economic Co-operation and Development
OGTR	Office of the Gene Technology Regulator
OMT	S-adenosyl-methionine-dependent *O*-methyltransferases
PAL	Phenylalanine ammonia-lyase
PCA	Principal Component analysis
PDA	Potato dextrose agar
ppm	parts per million
PR protein	Pathogenesis-related protein
RP	Reverse phase
R_t	Retention time
SAM	S-adenosylmethionine
SE	Standard error
TAL	Tyrosine ammonia-lyase
TFA	Trifluoroacetic acid
TMS	trimethylsilane
TSP	trimethylsilyl propanoic acid
UV	Ultraviolet / Unit variance
UV-VIS	Ultraviolet and visible
δ	Chemical shift

Chapter 1

1. Introduction

Plants produce an enormous variety of natural products named "secondary metabolites" with high structural diversity. During the last decades, the ecological role of secondary metabolites and their importance for the producing organisms has been continuously disclosed. It is intriguing that many if not all of these metabolites can play a role in plant chemical ecology, i.e. the interaction between plants and their biotic and abiotic environment (Osbourn & Lanzotti 2009). According to the biosynthetic origin, secondary metabolites can be divided in four different groups: alkaloids, phenylpropanoids, polyketides, and terpenoids. Among them, phenolic compounds derived from the phenylpropanoid pathway fulfill a broad spectrum of ecological roles in plants. Phenolics are among the major classes of natural products involved in the plant's response to abiotic environmental stresses such as light, temperature, and nutrient deficiency, and biotic challenges such as pathogen infection, and herbivore attacks (Ramawat & Mérillon 2013). Phenylphenalenones, a class of secondary metabolites produced in a few plant families, constitute the base of the present work. In this regard, biosynthetic studies in Haemodoraceae plants, their role in the plant defense of the Musaceae plant family as well as design of new antifungal agents were covered as the major goals in this project. A brief introduction into the main topics covered in the present project is described as follows.

1.1 Taxonomic aspects of Musaceae

The banana family (Musaceae), monocotyledonous plants belonging to the order Zingiberales in the clade commelinids, has been conventionally divided into the three genera *Musa*, *Ensete* and *Musella* (Christelova, et al. 2011) with 41 currently accepted species (Liu, et al. 2010). The 35 species of the genus *Musa* mainly occur in areas of tropical Asia; *Ensete* (5 species) is discontinuously distributed in Africa and Asia while *Musella*, a monotypic genus, is domestic to the southwestern China (Christelova, et al. 2011). The name of the genus *Musa* is thought to be derived from the Arabic name for the plant (*mouz*) in honour of Antonius Musa, physician to Octavius Augustus, first emperor of Rome (Hyam & Pankhurst 1995). This genus is

currently sub-divided into four sections, *Eumusa* (containing the majority of species) and *Rhodochlamys* with a basic chromosome number of $2n = 22$, *Australimusa* ($2n = 20$) and *Callimusa* ($2n = 20$) (Li, et al. 2010; Christelova, et al. 2011).

Bananas (*Musa* spp.) are giant perennial herbs with a pseudostem consisting of leafs sheaths and an underground true stem (corm) cultivated throughout the humid tropics and subtropics in Latin America, Africa and Asia. The vast majority of cultivated bananas are derived from inter- and intraspecific crosses between two diploid ($2n = 2x = 22$) wild species, *Musa acuminata* (with a genome designation AA) and *Musa balbisiana* (genome designation BB) (Heslop-Harrison & Schwarzacher 2007) and differ from their wild relatives by being seedless and parthenocarpic (development of the ovary of a flower into a fruit without fertilization) (Swennen, et al. 1995). Many of the domesticated bananas are triploid, $2n = 3x = 33$, with a genome constitution of AAA (sweet desert bananas), AAB or ABB (most of them starchy plantains that are cooked before become edible) (Simmonds & Shepherd 1955; Swennen, et al. 1995). Fig. 1 summarizes a sectional classification of *Musa* species with common banana cultivars used in commercial agriculture.

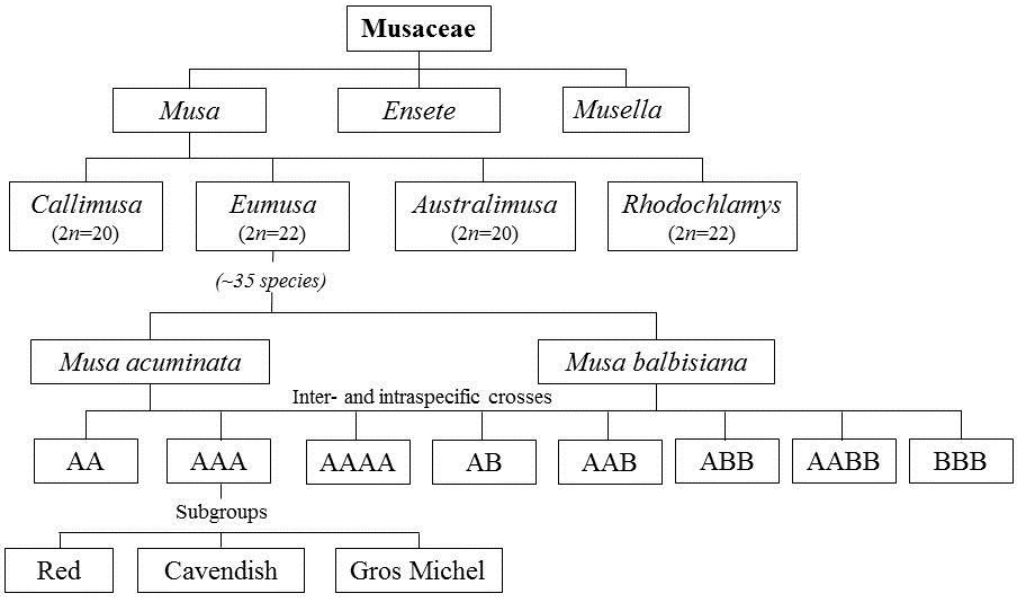

Fig. 1. Musaceae family with the subdivision of *Musa* genus.

1.2 Economic importance of banana

Bananas and plantains constitute the fourth most important staple fruit worldwide (after rice, wheat and maize) with a global production of more than 100 million metric tons in 2012 produced by nearly 130 countries, ranking first among all varieties of fruits produced (FAO 2013; FAO 2015). The total production of banana provides a significant source of income, food and nutrition for more than 400 million people, particularly in Africa, where its consumption is close to 1 Kg per person per day. Uganda is the largest producer of banana and plantain in Africa, followed by Rwanda, Ghana, Nigeria and Cameroon (INIBAP 1989; IITA 2015); whereas the major sweet banana producing countries are India and Brazil but mostly for domestic consumption (OGTR 2008).

However, around 17 % of total production of banana is intended for exporting to foreign markets annually where Ecuador with a portion of 31%, Philippines (11%), Costa Rica (10%), Colombia (10%) and Guatemala (8%) cover nearly 70% of the total international trade of banana and plantains. Latin America contributes with two-thirds to the total banana export to Europe and the United States (FAO 2013; Potts et al. 2014). Among the whole group of banana plants, the Cavendish subgroup (triploid genotype AAA) represented by the *Musa* varieties 'Grand Nain', 'Williams', 'Robusta', 'Poyo', 'Dwarf Cavendish' and 'Valery', is the most widely grown group of edible bananas which represent over 40% of these fruits produced worldwide. Their good yield, post-harvest characteristics, nutritional value and palatability meet with the international standards for their acceptance and marketing (Ploetz et al. 2007). Companies such as Chiquita Brands International (Ohio, USA), Dole Food Company (California, USA), Fresh Del Monte Produce (Florida, USA), Fyffes (Dublin, Ireland) and Grupo Noboa S.A. (Guayaquil, Ecuador) are the major agricultural trader on the global market of bananas (Potts et al. 2014).

Nevertheless, bananas are not only appealing for human consumption and commercialization but also constitute a host crop for many microorganism and herbivores, which since several decades are headache-markers both for smallholders as well as for large banana farmers. The agricultural practice in the production of banana as a monoculture together with the use of genetically identical clones derived from a single triploid genotype (Cavendish AAA) has

the disadvantage of promoting rapid proliferation of pathogens (Bairu et al. 2006; Dita et al. 2013). Some of the diseases in banana caused by bacteria, fungi, viruses and herbivores are discussed in the following section.

Along with the use of banana as a nutritive fruit, some *Musa* varieties are used in the fermentation of juice (beer bananas) or even used for frying and commercialized as banana chips. Furthermore, plants belonging to the section *Australimusa* (e.g. *Musa textilis*) are currently used in the papermaking and clothes industry due to the high content of fiber (Heslop-Harrison & Schwarzacher 2007; OGTR 2008). Furthermore, leaves of banana plants are used in some countries (e.g. Ecuador, Colombia and Costa Rica) as plates for eating or wrapping food for steaming during the preparation of gastronomic dishes.

1.3 Pests and diseases of banana

As mentioned above, the production of banana is strongly affected by a broad range of viruses, bacteria, fungi and other pests. *Banana bunchy top virus* (BBTV) causing the banana bunchy top disease (Elayabalan et al. 2015), the bacteria *Ralstonia solanacearum* (Moko's disease) (Munar-Vivas et al. 2010; Albuquerque et al. 2014), *Fusarium oxysporum* f.sp. *cubense* (fungus causing the Panama disease) (García-Bastidas et al. 2014), the burrowing nematode *Radopholus similis* (Sarah 1999), the banana borer *Cosmopolites sordidus* (Coleoptera: Curculionoidea, Dryphthoridae) (OECD 2009) and the Sigatoka disease complex of banana which involve three related ascomycetous fungi, *Mycosphaerella eumusae* (causal agent of eumusae leaf spot disease), *M. musicola* (yellow Sigatoka disease) and *M. fijiensis* (black leaf streak disease, BLSD) (Arzanlou et al. 2007) are among the most serious agronomical problems that threat the production of banana worldwide.

Since the interaction between *Musa* and *M. fijiensis* comprises part of the study in the present doctoral dissertation, this pathosystem will be described in more detail.

1.3.1 Black Leaf Streak Disease (BLSD)

Mycosphaerella fijiensis Morelet (anamorph: *Paracercospora fijiensis* (Morelet) Deighton), the causal agent of the BLSD, is a haploid, hemibiotrophic ascomycete fungus belonging to the class Dothideomycetes, order Capnodiales and family Mycosphaerellaceae. The disease cycle in its host consists of four distinct stages that include spore germination, penetration through stomata, symptom development and spore production (Churchill 2011). *M. fijiensis* produces conidias and ascospores (Fig. 2,a). Both spores can germinate and be infective under optimal conditions of high relative humidity (90-100%) or a film of water on the leaf surface and temperatures in the range of 25-30°C (Jacome & Schuh 1992). However, ascospores are considered as the most epidemiological agent since they can become wind-borne within infected plantations and spread the disease through long distances while conidia are associated with local spread of the disease and are important during heavy dews and intermittent showers (Ploetz 2001; Marín et al. 2003).

After a period of epiphytic fungal growth of two or three days, germ tubes penetrate plant stomata mainly on the lower (abaxial) leaf surface due to the greater abundance of stomata on this area (Carlier et al. 2002; Pérez-Vicente 2012). Once inside, the hypha grows through the mesophyll cells up to reach the palisade layer without the formation of haustoria. The period of biotrophy can last two or more weeks (depending plant maturation) before any initial symptom can be observed (Churchill 2011). According to the progress of the disease symptoms, several BLSD stages have well been described by Meredith and Lawrence (Meredith & Lawrence 1969) and Fouré (Fouré 1987) and summarized as follows:

Stage 1: Depigmentation mark (whitish or yellow) followed by red-brown specks only on the lower surface
Stage 2: Red-brown streaks on both sides of the leaf
Stage 3: Wider streaks. Color starts changing from red to dark brown
Stage 4: Dark brown (lower) to black (upper) spots
Stage 5: Black spot with chlorotic halo. Lesion is slightly depressed.

Stage 6: Center of spot dries out and becomes whitish to gray. Spot is surrounded by a dark brown to black border and further depressed.

Conidia (asexual spore) produced by structures named "conidiophores" are located on the abaxial side of the leaf while ascospores (sexual spore) are released by structures called "pseudothecia" placed on both surfaces of the leaf. Both spores can concurrently be produced in the infected leaves at the first stage of the disease but, in the last stages (late necrotrophic stage), ascospores are produced and dispersed wind-borne to other plantations (Marín et al. 2003).

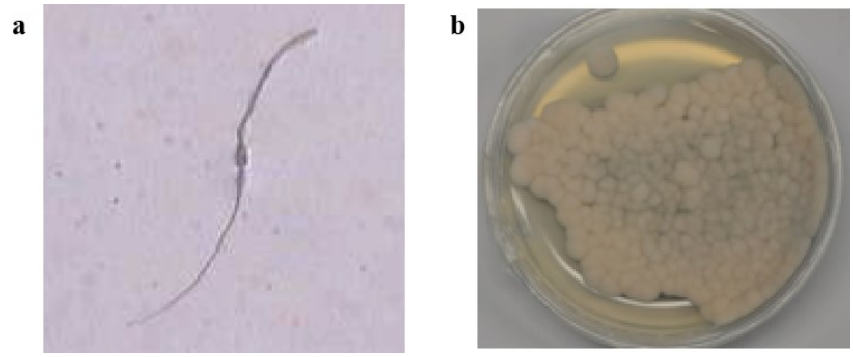

Fig. 2. Pane a. Ascospore (sexual spore) of *Mycosphaerella fijiensis*. Panel b: Plate showing fungal colony of *M. fijiensis* strain Ca10_13 (growth media PDA). Photos taken by W. Hidalgo

As mentioned above, most of the commercial *Musa* varieties are susceptible to *M. fijiensis* and the disease can affect banana production through significant reduction of the photosynthetic leaf area, yield losses of 50% or more, premature fruit ripening and serious defects in the exported fruit (Ploetz 2001). Several methods used to control this disease will be discussed below.

1.3.2 Chemical control

The use of chemicals is still the most effective method to control BLSD worldwide. Frequently, its control requires about 12-15 applications annually of systemic and protectant fungicides that are used in an alternated mode as a part of a strategy to prevent the fungicide resistance. The costs to control the disease by this method have been estimated to be nearly 20% of the final retail price of the banana fruit in the importing countries. Thus, chemical treatments

affect enormously the revenues of the small-holder farmers who grow this crop (Ploetz 2001; Ploetz et al. 2007).

Protectant fungicides such as mancozed and chlorothalonil are used to control BLSD. However, systemic fungicides have provided better control than the former due to their ability to penetrate the leaf cuticle, to undergo translocation, and inhibit the pathogen inside the plant. Benzimidazoles (e.g. benomyl), triazoles (e.g. propiconazole, bitertanol), strobilurins (e.g. azoxystrobin, trifloxystrobin) and morpholines (e.g. tridemorph) are among the main classes of systemic fungicides currently used for BLSD control (Fig. 3).

However, as a consequence of the extensive application in banana plantations, concomitant resistance to fungicides has been generated by *M. fijiensis*. To a certain extent this is due to the increased abuse in the application of fungicides as a last option for avoiding large reduction in crop yields by this pathogen (range from 12-25 L ha^{-1}) (Ploetz 2000; Etebu & Young-Harry 2011; Martínez-Bolaños et al. 2012).

Therefore, alternate application of fungicides with different mode of action or application in a mixture can minimize the risk of microbial resistance. Such strategies have been implemented under an integrated disease management and strict fungicide application program (FRAC 2014).

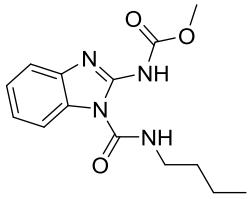

Benomyl

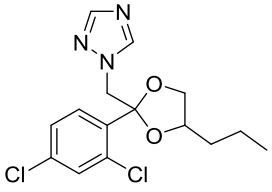

Propiconazole

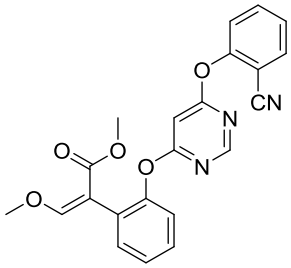

Azoxystrobin

Fig. 3. Chemical structures of the most common fungicides used in the control of BLSD

1.3.3 Biological control

As an environmental-friendly alternative, the use of microorganisms which are able to inhibit the development of *M. fijiensis* has emerged. As examples, the fungus *Trichoderma spp.* (Castro et al. 2015) and bacteria such as *Serratia marcescens* (Gutiérrez et al. 2015) have been tested under *in vitro* conditions as well as in planta for evaluating their properties. The selection of these microorganisms has been focused on the ability to produce hydrolytic enzymes such as glucanases and chitinases which are able to degrade the fungal cell wall of *M. fijiensis* (González et al. 1996).

Nevertheless, the results have not been entirely satisfactory since the inhibition of *M. fijiensis* proliferation is not comparable with the use of the fungicides.

1.3.4 Crop improvement

The development of *Musa* varieties resistant to the BLSD through conventional breeding has been considered an additional tool in controlling this disease. Therefore, some research centers such as Fundación Hondureña de Investigaciones Agrícolas (FHIA, Honduras), International Institute of Tropical Agriculture (IITA, Nigeria) and Centre of Coopération Internationale en Recherche Agronomique pour le Developpement (CIRAD-FLHOR, France) have developed some tetraploid varieties (e.g. FHIA-01, FHIA-18) of *Musa* conferring resistance to BLSD (Table 1) but, there still are some issues concerning the premature senescence, leaf and fruit drop, weak pseudostems and undesirable seed production in the fruit that need to be improved (OGTR 2008).

On the other hand, since the genome of *Musa* plant (D'Hont et al. 2012) has been recently sequenced, it becomes more fascinating to deepen the knowledge about the molecular bases of the *Musa* - *M. fijiensis* pathosystem. Molecular research on the expression of genes encoding chitinases, stilbene synthases, defensing antimicrobial peptides, and non-specific lipid-transfer proteins, have been successfully carried out and corresponding genetically modified *Musa* plants expressing resistance against *M. fijiensis* under glasshouse or climatic chamber conditions have

been established (Sági 2003; Vishnevetsky et al. 2011; Kovacs et al. 2013). However, experiments under outdoor conditions are required in order to evaluate characteristics such as fruit quality, crop yield, and environmental safety.

In the future, the breeding programs will continue to play an important role in the development of resistant cultivars against several pathogens. Resistant cultivars will contribute to the subsistence agriculture and help to avoid the use of the costly chemical control that in fact has become less appealing to consumers in the importing countries.

Table 1. *Musa* varieties with different levels of resistance against *M. fijiensis*.

Musa variety	Genome	Level of Resistance	*Musa* variety	Genome	Level of Resistance
Calcutta 4	AA	HR	Fougamou	ABB	PR
Tuu gia	AA	HR	Yangambi	AAA	HR
M.a. burmanica	AA	HR	Grand Nain	AAA	HS
Bocadillo	AA	S	Gross Michel	AAA	HS
Niyarma yik	AA	S	Balbisiana	BB	HR
Pelipita	ABB	PR	Manzano	AAB	HS
FHIA-01	AAAB	HR	FHIA-18	AAAB	PR

HR: Highly resistant; HS: Highly susceptible; PR: partial resistant; S: susceptible

1.4 *Musa-Mycosphaerella fijiensis* interaction

The interaction between *Musa* and *M. fijiensis* is governed both by the genotype of the host and the pathogen, along with a complex exchange of signals and responses occurring under given environmental conditions. Once ascospores or conidia from *M. fijiensis* get in contact with the leaf surface of the host plant, a series of biochemical events determine the success of the fungal colonization (Beveraggi et al. 1995; Hoss et al. 2000). According to this initial step of the pathogenesis, *Musa* varieties have been classified into three main categories: 1. Highly resistant (HR) *Musa* varieties are able to arrest the microbial growth in an early stage of the interaction (incompatible interaction); 2. Partially resistant (PR) *Musa* varieties allow the disease to progress

slowly (compatible interaction); 3. Susceptible (S) *Musa* varieties are unable to prevent the disease to progress fast and, as a consequence of the infection, the plant dies (compatible interaction) (Table 1) (Fouré 1993; Ortíz & Vuylsteke 1994; Lepoivre et al. 2002).

In the *Musa* resistance, several characteristic biochemical patterns play an important role after the early recognition of the pathogen. Triggering the plant defense mechanisms with the expression of pathogenesis-related proteins (PR-proteins such as chitinases and glucanases) (Lepoivre et al. 1993; Torres, et al. 2012), reinforcement of preformed substances (Hoss et al. 2000) and biosynthesis of phytoalexins (Quiñones et al. 2000) and phytoanticipins (Cruz-Cruz et al. 2010) seem to be the most important mechanisms behind the success of counteracting the fungal invader.

Nevertheless, little is known about the factors that contribute to the early pathogen recognition in incompatible interactions. With the identification and characterization of the metabolites 2,4,8-trihydroxytetralone (2,4,8-THT), 5-hydroxy-1,4-naphthalenedione (juglone), 4-hydroxyscytalone, 3-carboxy-3-hydroxycinnamic acid, isoochracinic acid (Stierle et al. 1991) and a metabolite named 'fijiensis' (Upadhyay et al. 1990) isolated from *in vitro* cultures of *M. fijiensis*, new hypotheses were proposed due to strong phytotoxic activity displayed by these metabolites on banana leaves under laboratory conditions. Further studies reported that 2,4,8-THT and juglone affected enormously the chloroplast of the *Musa* leaves, thereby identifying the site of action of these compounds. In addition, detailed experiments by spreading juglone on the surface of two *Musa* varieties, Fougamou (partial resistance) and Grand Nain (highly susceptible), demonstrated that Fougamou responded more quickly than the susceptible plant, supporting the hypothesis that differential response in the host is consistently correlated with relative levels of susceptibility or partial resistant to BLSD (Stierle et al. 1991). Taking into account that such compounds are recognized shunt metabolites of fungal melanin biosynthetic pathways (Langfelder et al. 2003), further experiments were executed with the intention to prove the role of melanin metabolites in the disease development. Therefore, *in vitro* cultures of *M. fijiensis* were incubated with tricyclazole, an inhibitor of the melanin biosynthetic pathway, and afterwards inoculated into leaves of *Musa* plants. The results showed that the fungal strain treated with tricyclazole was able to develop faster and more substantial symptoms than the

untreated fungal inoculum used as a control, supporting the above mentioned findings on the role of melanin shunt metabolites in BLSD development (Hoss et al. 2000). An enhanced production of 2,4,8-THT was also observed when *in vitro* cultures of *M. fijiensis* were treated with intercellular extracts from highly resistant *Musa* varieties. However, this was not the case when *M. fijiensis* was treated with extracts from susceptible *Musa* plants, suggesting the role of plant metabolites in modulating the metabolism in *M. fijiensis* (Hoss et al. 2000).

Recent molecular genomic analyses have shown that fungal protein effectors from *M. fijiensis* can also mediate virulence in the host. The functional effectors Avr4 and Ecp2 identified in the tomato pathogen *Cladosporium fulvum* are also present in *M. fijiensis*. While the effector Avr4 protects the fungal cells against hydrolysis by plant chitinases (through binding to chitin), Ecp2 seems to be correlated with the hypersensitivity response in resistant tomato plants (Stergiopoulos et al. 2010). However, there is not much evidence whether these effectors behave similar in *Musa* - *M. fijiensis* interaction and therefore, further work is currently in progress in order to clarify the role of specialized metabolites and effector proteins in the *Musa*-*M. fijiensis* pathosystem.

Phenylalanine-ammonia-lyase (PAL), the enzyme responsible for the first step in the phenylpropanoid pathway, converts L-phenylalanine into *(E)*-cinnamic acid which is then used for further synthesis of diverse plant secondary metabolites such as flavonoids, coumarins, stilbenes and the cell wall polymer lignin (Alvarez et al. 2013). Therefore, activation of PAL has been extensively studied for playing a role in plant resistance against pathogens (Chandra et al. 2007; Chang et al. 2008; Malencic et al., 2013; Manosalva et al. 2013), in plant development and environmental stresses (Wen et al. 2008; Capanoglu et al. 2012; Wada et al. 2014). Induction of PAL activity in an early stage of the interaction between *Musa* and *M. fijiensis* has been correlated with resistant traits of the plant against this pathogen (Torres et al. 2012; Alvarez et al. 2013) and also against nematodes (Wuyts et al. 2006). On the other hand, polycyclic phenolic compounds named phenylphenalenones have been reported for being induced metabolites of *Musa* plants once the plant recognize the microbial invader. Since these metabolites exhibited antimicrobial and nematicidal activities under *in vitro* assays, they have been considered as phytoalexins of the genus *Musa* (Luis et al. 1993; Luis et al. 1995; Hölscher et al. 2014). In

addition, previous reports also correlated the production of phenylphenalenones with the resistance of some *Musa* varieties (Otálvaro et al. 2002; Otálvaro et al. 2007). Therefore, there must be a direct correlation between the early induction of PAL and the increasing biosynthetic rate of the production of phenylphenalenones during the plant-pathogen interaction. Thus, phenylphenalenones may play a critical role during the plant defenses of *Musa* against pathogens and pests. A section covering different aspects of phenylphenalenones will be discussed in more detail in the context of the present research.

1.5 Phenylphenalenones

1.5.1 Natural occurrence

Phenylphenalenone-type compounds are a class of polycyclic aromatic compounds found in Haemodoraceae, Pontederiaceae, Strelitziaceae and Musaceae plant families (Munde et al. 2011; Hölscher et al. 2015). After the first phenylphenalenone named haemocorin was isolated from the higher plant *Haemodorum corymbosum* (Cooke & Segal 1955), to date more than 140 phenylphenalenone-type compounds have been isolated and identified from the monocotyledoneous plant families above mentioned (Hölscher et al. 2015). Their chemical structure consists of a tricyclic phenalene nucleus with ketone functionality (on ring A or B) and a lateral phenyl ring. Nevertheless, some phenalenones (lacking the lateral phenyl ring) have been isolated from *Musa* plants (Otálvaro et al. 2007). The variation of the substitution pattern of the lateral phenyl ring, location of the ketone group and the oxidation pattern on the phenylphenalenone molecule makes them a diverse group of metabolites. Each of the phenylphenalenone-producing plant species confers characteristic structural features to “their” phenylphenalenones (Fig. 4).

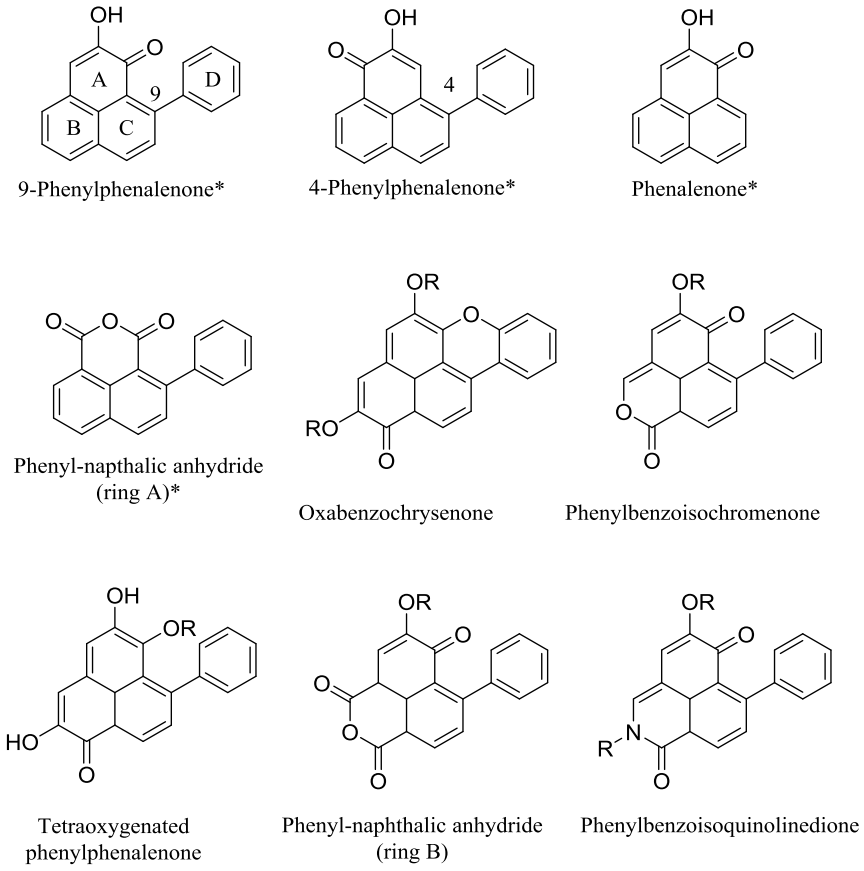

Fig. 4. General structures of phenalenone and phenylphenalenone-type compounds. * Identified in *Musa* plants

On the other hand, phenalenone derivatives have been reported from microbial sources, especially from Hypomycetous (genera *Penicillium, Fusicoccun, Giesmaniella* and *Verticillium*) and Dyscomycetous fungi. However, their structures differ greatly from the metabolites found in higher plants since fungal phenalenones biosynthetically originate from the acetate-polymalonate pathway (Fig. 5) (Elsebai et al. 2014; Nazir et al. 2015) while the plant phenalenones are derived from the phenylpropanoid pathway (Thomas 1971; Hölscher & Schneider 1995).

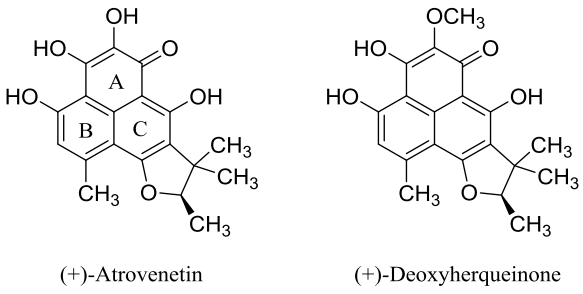

Fig. 5. The first natural phenalenone derivatives isolated from the fungus *Penicillium atrovenetum*.

1.5.2 Biosynthetic aspects

Previous biosynthetic studies have confirmed that phenylphenalenones are formed by condensation of two units of phenylpropanoids with one unit of malonate through a diarylheptanoid intermediate (Fig. 6) (Thomas 1971; Hölscher & Schneider 1995). It was found that the enzymes phenylalanine ammonia lyase (PAL) and tyrosine ammonia lyase (TAL) catalyze a reaction converting L-phenylalanine and L-tyrosine into the corresponding phenylpropanoids cinnamic acid and *p*-coumaric, respectively, which then are incorporated into the diarylheptanoid intermediate followed by an intramolecular cyclo-addition step (catalyzed by a hypothetical Diels-Alderase) for ending up in the formation of the phenylphenalenone (Fig. 6) (Thomas 1971; Kamo et al. 2000; Munde et al. 2011).

Biosynthesis of phenylphenalenones in Haemodoraceae plants

Biosynthetic studies of phenylphenalenones have been carried out mostly in Haemodoraceae plants, e.g. *Anigozanthos preissii* and *Wachendorfia thyrsiflora*, basically because these metabolites are constitutively produced in *in vitro* root cultures of those plant species which make them desirable and suitable biological systems for deciphering new insights into the biosynthetic context of phenylphenalenones (Hölscher & Schneider 1995; Schmitt et al. 2000; Opitz 2002). In this regard, *A. preissii* has not only been the chosen plant system for exploring the potential diarylheptanoid intermediates involved in the biosynthesis of phenylphenalenones but also for studying the substitution pattern of the lateral phenyl ring of these metabolites (Fig. 7) (Schmitt et al. 2000) and even to determine the sequence of the biosynthetic origin of the oxygen functions in such molecules (Munde et al. 2011).

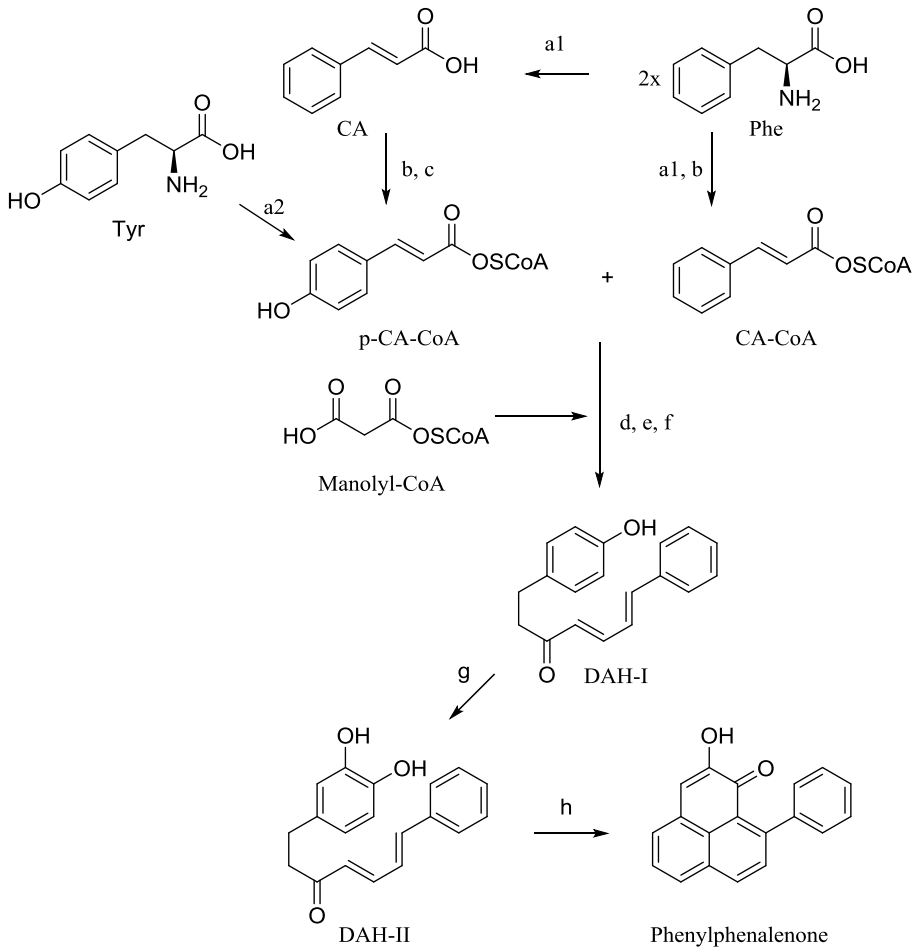

Fig. 6. Biosynthesis of phenylphenalenones through the general diarylheptanoid pathway. Enzymatic conversions catalyzed by (a1) phenylalanine ammonia lyase (PAL), (a2) tyrosine ammonia lyase (TAL), (b) cinnamate 4-hydroxylase (C4H), (c) CoA ligase, (d) polyketide synthase type III, (e) putative reductase, (f) putative dehydrogenase, (g) putative CYP or phenol oxidase, (h) putative cyclase (possibly through Diels-Alderase). Phe: L-phenylalanine; Tyr: L-tyrosine; CA: cinnamic acid; CA-CoA: cinnamoyl-CoA; pCA-CoA: *p*-coumaroyl-CoA; DAH-I: Diarylheptanoid I; DAH-II: Diarylheptanoid II (Munde et al. 2011).

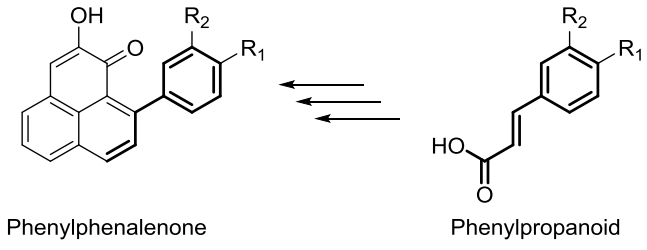

Fig. 7. Biosynthetic studies on the substitution pattern of the lateral phenyl ring in the phenylphenalenone by feeding experiments in *A. preissii* with ^{13}C-labelled phenylpropanoid precursors. Possible combinations of R_1 = -OH with R_2 = -H, -OH and –OCH_3 have been reported.

Biosynthetic studies of phenylphenalenones in Musa plants

In lesser extent, biosynthetic studies of 9-phenylphenalenones have also been performed in *Musa* plants after induction with biotic or abiotic stresses. Although their biosynthesis almost follows the general phenylpropanoid pathway as described in Haemodoraceae plants, the formation of 4-phenylphenalenones, which are typical of the *Musa* genus, and phenalenones still remain unclear (Kamo et al. 1998; Otálvaro 2004). After the isolation of 1,2,3-trihydroxy-2,3-dihydro-phenylphenalene from rhizomes of *Musa acuminata* Grand Nain infected with *Fusarium oxysporum*, it was suggested that this metabolite must be a key intermediate in the biosynthesis of 4- and 9-phenylphenalenones in *Musa*. In this case, oxidation and dehydration of compounds of the 1,2,3-triol type result in the formation of 4-phenylphenalenones (Fig. 8) (Luis et al. 1995; Otálvaro et al. 2002).

However, an alternative route for the synthesis of 4- and 9-phenylphenalenones was also proposed by Kamo et al. (Kamo et al. 2000) according with their findings (Fig. 8). Furthermore, isotopic labelling experiments with [2',3',5',6'–$^{2}H_4$]hydroxyanigorufone (a 9-phenylphenalenone) and its homologous counterpart [2',3',5',6'–$^{2}H_4$]irenolone (a 4-phenylphenalenone) administered to banana fruits infected with conidia of *Colletotrichum musae* demonstrated that naphthalic anhydride derivatives were likely oxidation products from 9-phenylphenalenones rather than their counterpart 4-phenylphenalenones by a putative decarboxylase (Fig. 8) (Kamo et al. 2000).

On the other hand, *O*-methylation during the biosynthesis of phenylphenalenones has been recently reported to occur *via* catalysis by *S*-adenosyl methionine-dependent *O*-methyltransferases in *Musa* plants as well as in *W. thyrsiflora* (Otálvaro et al. 2010).

1.5.3 Inducible metabolites in *Musa* plants

Phenylphenalenones have been reported for being induced metabolites in *Musa* plants after biotic stresses, treatment with elicitors (Luis et al. 1993), wounding (Kamo et al. 1998) or interaction with non-pathogenic microorganisms (Jitsaeng & Schneider 2010). Antimicrobial properties of these metabolites have been demonstrated against fungal pathogens such as *M.*

fijiensis (Quiñones et al. 2000; Otálvaro et al. 2007)*, Colletotrichum musae* (Hirai et al. 1994; Kamo et al. 2001) and *Fusarium oxysporum* (Luis et al. 1995), the causing agents of Black Leaf Sigatoka Disease, anthracnose disease and Panama disease, respectively, in Banana crops. Nematicidal activity has recently reported against *Radopholus similis*, the burrowing nematode of banana plants (Hölscher et al. 2014). Therefore, phenylphenalenones are well recognized as phytoalexins of genus *Musa*.

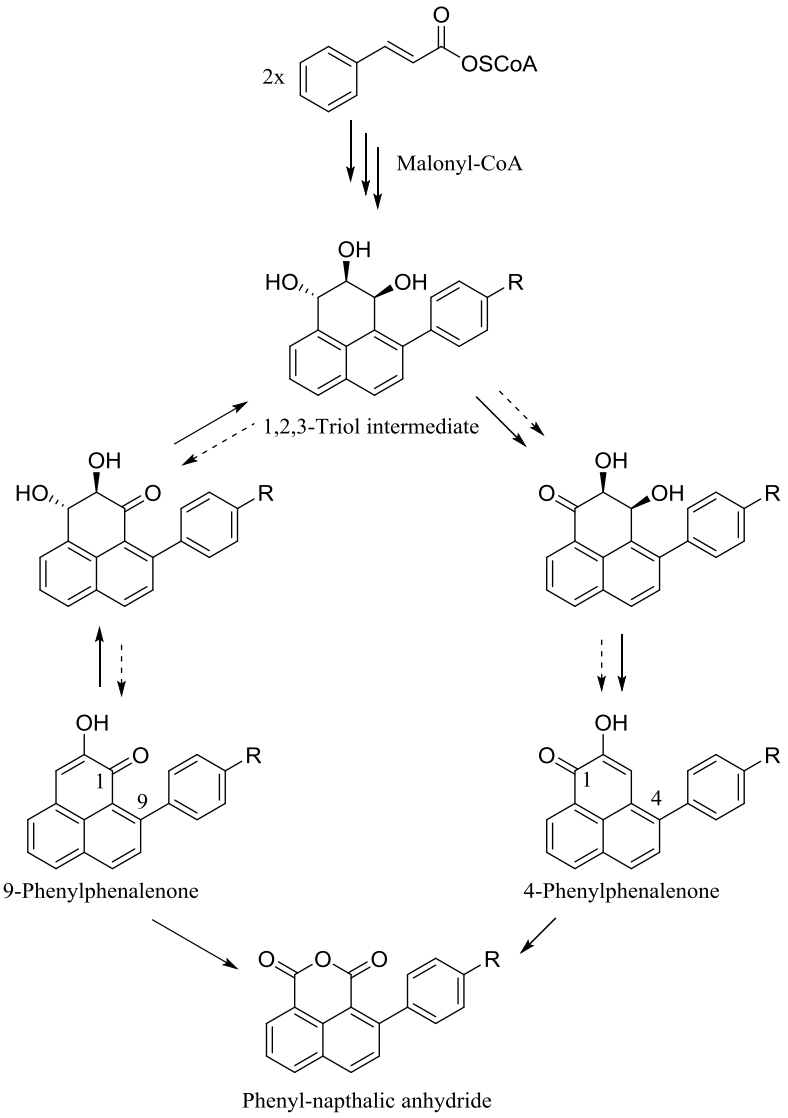

Fig. 8. Hypothetical biosynthesis of 4- and 9-phenylphenalenones as proposed by Luis et al. (Luis et al. 1995) (shown by solid arrows) and Kamo et al. (Kamo et al. 1998) (shown by dashed arrows). Phenyl naphthalic anhydrides are represented as oxidized products mainly from 9-phenylphenalenones.

To date, there are no reports about the mechanism of action of phenylphenalenones on the target sites in the microbial organism and therefore, investigations in this field are needed in order to unravel the role of these metabolites as phytoalexins. Nevertheless, it has been suggested that phenylphenalenones could act through a dual mode of action against *M. fijiensis*: (I) they inhibit the fungal growth even without illumination; (II) when irradiated with light, an enhanced inhibition of the fungal growth was observed in the *in vitro* fungus-phenylphenalenone incubation system, where a photodynamic mode of action by light-induced singlet oxygen production could affect the microbial survival (Lazzaro et al. 2004; Flors & Nonell 2006; Hidalgo et al. 2009; Bucher et al. 2014).

1.5.4 Pharmacological activity

Haemocorin, a metabolite isolated from the rhizome of *Haemodorum corymbosum*, was the first phenalenone assessed for antitumor (Schwenk 1962) and antimicrobial activities (Narasimhachari et al. 1968). To date, several studies have been reported on the biological properties of some natural and synthetic phenylphenalenone- and phenalenone-type compounds. For example, anigorufone and methoxyanigorufone exhibited leishmanicidal activity on both parasite *Leishmania donovani* promatigotes and *L. infantum* amastigotes (Luque-Ortega et al. 2004). Natural and synthetic phenylphenalenones displayed considerable effects against the malaria parasite *Plasmodium falciparum* (Gutierrez et al. 2013) and relevant forms of trypanosomiasis (e.g. Chaga's disease) and leishmaniasis (Rosquete et al. 2010). New phenalenone derivatives isolated from the fungus *Coniothyrium cereal* exhibited considerable antimicrobial activity against *Staphylococcus aureus* and potent inhibition of human leukocyte elastase (HLE) (Elsebai et al. 2011). Sculezonone-A and Sculezonone-B, two phenalenones isolated from the fungus *Penicillium sp.*, displayed inhibition on eukaryotic DNA polymerases, a target biomolecules in cancer chemotherapy (Perpelescu et al. 2002). In addition, studies on disruption of biofilms of human pathogens have also been reported by using light activated photosensitizers (synthetic phenalenones) as lethal phototoxicity treatment (Cieplik et al. 2013; Spath et al. 2014).

1.6 Scope of this work

Little is known about the ecological role of phenylphenalenones in Haemodoraceae and Musaceae plant families. These specialized metabolites are constitutively biosynthesized in Haemodoraceae plants whereas in the Musaceae family, they are induced metabolites after biotic or abiotic environmental stresses. Plants such as *Anigozanthos preissii*, *Wachendorfia thyrsiflora* and *Xiphidium caeruleum* (Haemodoraceae plants), are suitable biological systems for going ahead into biosynthetic studies of phenylphenalenones. Therefore, precursor-product relationships in the biosynthesis of phenylphenalenones have been explored in this work both in *Anigozanthos preissii* (Chapter 3.1) and *Wachendorfia thyrsiflora* (Chapter 3.2). On the other hand, *Musa* (Banana) plants seems to be well suitable to study the ecological relevance of phenylphenalenones as phytoalexins against pathogens, especially in the interaction with the ascomycete fungus *Mycosphaerella fijiensis*, etiological agent of the most detrimental disease in banana crops named Black Leaf Streak Disease (BLSD). Since several authors have correlated the production of these specialized metabolites with the resistance of some *Musa* varieties against *M. fijiensis*, this section of the project was aimed for exploring the metabolic chemical responses of two *Musa* varieties: the susceptible 'Williams' and the resistant 'Khai Thong Ruang' ('KTR') during the interaction with the fungal pathogen causing of BLSD (Chapter 4). During several decades, natural products have been proven valuable for diverse applications in medicine, agriculture and pigments industry. However, the major relevance has been addressed towards developing new drugs as challenges against human diseases. In agriculture, pathogens and pests are serious problems that cause large losses in the production of several crops and thereby, control management by application of fungicides and pesticides are one of the main ways for crop protection. Commercial banana plantations are susceptible to diseases caused by fungal pathogens and application of fungicides is still the best choice for controlling the banana production. However, the abuse of such applications has led to another serious problem, namely the resistance against fungicides developed by the fungus. Thus, the design of new antifungal agents has become a big challenge for this particular issue. Therefore, the final part of the thesis was aimed to explore phenylphenalenones as a template for the synthesis of new antifungal agents with dual mode of action (Chapter 5.1 and 5.2).

Chapter 2

Overview of manuscripts

Biosynthesis of phenylphenalenones in Haemodoraceae plants (see Chapters 3.1 and 3.2)

3.1 4-Methoxycinnamic acid - An unusual phenylpropanoid involved in phenylphenalenone biosynthesis in *Anigozanthos preissii.* William Hidalgo, Marco Kai, Bernd Schneider. *Phytochemistry* (2015), Volume 13, pp 68-73. Reprint License Number: 3651741394073

In vitro root cultures of *Anigozanthos preissii* and *Wachendorfia thyrsiflora* (Haemodoraceae) are suitable biological systems for studying the biosynthesis of phenylphenalenones. Here we report the usage of these root cultures to investigate precursor-product relationships between phenylpropanoids and phenylphenalenones having identical substitution patterns of the phenyl rings. Four phenylpropanoic acids, including ferulic acid and the unusual 4-methoxycinnamic acid, were used in ^{13}C-labeled form as substrates to study incorporation into phenylphenalenones. In addition to the previously reported 2-hydroxy-9-(4'-hydroxy-3'-methoxyphenyl)-1*H*-phenalen-1-one (trivial name musanolone F), 2-hydroxy-9-(4'-methoxyphenyl)-1*H*-phenalen-1-one (proposed trivial name 4'-*O*-methylanigorufone) was found as a biosynthetic product in *A. preissii*. 4'-Methoxycinnamic acid was biosynthetically incorporated as an intact unit including its 4'-*O*-methyl substituent at the lateral phenyl ring. 4'-*O*-methylanigorufone is reported here for the first time as a natural product.

Author contributions

Research conceived by: Schneider B, Hidalgo W (40%)
Experiments designed by: Schneider B, Hidalgo W (60%)
Experiments conducted by: Kai M, Hidalgo W (85%)
Data analysis performed by: Kai M, Schneider B, Hidalgo W (80%)
Manuscript written: Schneider B, Hidalgo W (50%)

3.2 Biosynthesis of tetraoxygenated phenylphenalenones in *Wachendorfia thyrsiflora*. Tobias Munde, Silke Brand, William Hidalgo, Ravi K. Maddula, Aleš Svatoš, Bernd Schneider. *Phytochemistry* (2013), Volume 91, pp 165-176. Reprint License Number: 3645790959465

The biosynthetic origin of 1,2,5,6-tetraoxygenated phenylphenalenones and the sequence according to which their oxygen functionalities are introduced during the biosynthesis in *Wachendorfia thyrsiflora* were studied using two approaches. (1) Oxygenated phenylpropanoids were probed as substrates of recombinant *W. thyrsiflora* polyketide synthase 1 (WtPKS1), which is involved in the diarylheptanoid and phenylphenalenone biosynthetic pathways, (2) Root cultures of *W. thyrsiflora* were incubated with ^{13}C-labelled precursors in an $^{18}O_2$ atmosphere to observe incorporation of the two isotopes at defined biosynthetic steps. NMR- and HRESIMS-based analyses were used to unravel the isotopologue composition of the biosynthetic products, lachnanthoside aglycone and its allophanyl glucoside. Current results suggest that the oxygen atoms decorating the phenalenone tricycle are introduced at different biosynthetic stages in the sequence O-1 → O-2 → O-5. In addition, the incubation of *W. thyrsiflora* root cultures with ^{13}C-labelled lachnanthocarpone established a direct biosynthetic precursor–product relationship with 1,2,5,6-tetraoxygenated phenylphenalenones.

Author contributions

Research conceived by: Munde T, Brand S, Svatos A, Schneider B, Hidalgo W (30%)
Experiments designed by: Munde T, Brand S, Schneider B, Hidalgo W (30%)
Experiments conducted by: Munde T, Brand S, Maddula R.K, Hidalgo W (30%)
Data analysis performed by: Munde T, Brand S, Maddula R.K, Hidalgo W (30%)
Manuscript written: Munde T, Schneider B, Hidalgo W (25%)

Phenylphenalenones in the *Musa - M. fijiensis* interaction (see Chapter 4)

Phenylphenalenones protect banana plants from infection by *Mycosphaerella fijiensis* and are deactivated by metabolic conversion. William Hidalgo, Jima Chandran, Riya Menezes, Felipe Otálvaro, Bernd Schneider. *Plant, Cell & Environment* (in press). doi: 10.1111/pce.12630 Reprint License Number: 3734700406554

Phenylphenalenones, polycyclic aromatic natural products from some monocotyledonous plants, are known as phytoalexins in banana (*Musa* spp.). In this study, ^{1}H NMR-based metabolomics along with liquid chromatography and mass spectrometry were used to explore the chemical responses of the susceptible 'Williams' and the resistant 'KTR' *Musa* varieties to the ascomycete fungus *Mycosphaerella fijiensis*, the agent of the Black Leaf Sigatoka Disease. Principal component analysis discriminated strongly between infected and non-infected plant tissue, mainly due to specialized metabolism induced in response to the fungus. Phenylphenalenones are among the major induced compounds, and the resistance level of the plants was correlated with the progress of the disease. However, a virulent strain of *M. fijiensis* was able to overcome plant resistance by converting phenylphenalenones to sulfate conjugates. Here we report the first metabolic detoxification of fungitoxic phenylphenalenones to evade the chemical defense of *Musa* plants.

Author contributions

Research conceived by: Schneider B, Hidalgo W (50%)
Experiments designed by: Schneider B, Hidalgo W (80%)
Experiments conducted by: Schneider B, Hidalgo W (90%)
Data analysis performed by: Chandran J, Menezes R, Otálvaro F, Schneider B, Hidalgo W (80%)
Manuscript written: Schneider B, Hidalgo W (60%)

Synthesis of phenylphenalenone derivatives exhibiting antifungal properties (see Chapter 5.1 and 5.2)

5.1 Improved synthesis of 4-phenylphenalenones: the case of isoanigorufone and structural analogs. Marisol Cano, Carlos Rojas, William Hidalgo, Jairo Sáez, Jesús Gil, Bernd Schneider, Felipe Otálvaro. *Tetrahedron Letters* (2012), Volume 54, pp 351-354. Reprint License Number: 3645791120811

2-Hydroxy-4-phenyl-1*H*-phenalen-1-one (isoanigorufone, **1**), a phytoalexin exclusive of Musaceae, was synthesized starting from 3-(2-hydroxynaphthalen-1-yl)propanenitrile in nine steps in an overall yield of 10%. Hydrolysis of ethyl 3-(2-phenylnaphthalen-1-yl)propanoate obtained from Suzuki–Miyaura coupling between the parent triflate and phenylboronic acid afforded the corresponding propionic acid which, after Friedel–Crafts acylation and bromine-mediated dehydrogenation, was subjected to Yang–Finnegan epoxidation to furnish **1**. The preparation of analogs using this procedure is also discussed.

Author contributions

Research conceived by: Cano M, Sáez J, Gil J, Schneider B, Otálvaro F, Hidalgo W (25%)
Experiments designed by: Cano M, Rojas C, Otálvaro F, Hidalgo W (30%)
Experiments conducted by: Cano M, Rojas C, Otálvaro F, Hidalgo W (30%)
Data analysis performed by: Cano M, Rojas C, Schneider B, Otálvaro F, Hidalgo W (30%)
Manuscript written: Schneider B, Otálvaro F, Hidalgo W (15%)

5.2 4-Phenylphenalenones as a template for new photodynamic compounds against *Mycosphaerella fijiensis*. William Hidalgo, Marisol Cano, Manuela Arbelaez, Edwin Zarrazola, Jesús Gil, Bernd Schneider and Felipe Otálvaro. *Pest Management Science*. (in press). doi: 10.1002/ps.4055. Reprint License Number: 3645791438987

Evaluation of 4-phenylphenalenones and structural analogues against the fungal pathogen *Mycosphaerella fijiensis* (causal agent of black sigatoka disease in bananas) under light-controlled conditions uncovered some key structural features for the design of photodynamic compounds. Structure–activity relationship analysis revealed the importance of a chromophoric aryl-ketone and a steroidomimetic structural motif in the activity of the assayed compounds. The results pointed to 1,2-dihydro-3*H*-naphtho[2′,1′:3,4]cyclohepta[1,2-*b*]furan-3-one, which displayed an activity in the range of propiconazole but with photodynamic behaviour. The present work demonstrates that 1,2-dihydro-3*H*-naphtho[2′,1′:3,4]cyclohepta[1,2-*b*]heterocyclic-3-one derivatives can be used as potential lead compounds for the development of fungicides, relying on a dual mode of action.

Author contributions

Research conceived by: Cano M, Arbelaez M, Gil J, Schneider B, Otálvaro F, Hidalgo W (50%)
Experiments designed by: Cano M, Arbelaez M, Gil J, Schneider B, Otálvaro F, Hidalgo W (50%)
Experiments conducted by: Cano M, Arbelaez M, Otálvaro F, Hidalgo W (50%)
Data analysis performed by: Cano M, Zarrazola E, Schneider B, Otálvaro F, Hidalgo W (70%)
Manuscript written: Schneider B, Otálvaro F, Hidalgo W (30%)

Chapter 3

Biosynthesis of phenylphenalenones in Haemodoraceae plants

3.1 4-Methoxycinnamic acid - An unusual phenylpropanoid involved in phenylphenalenone biosynthesis in *Anigozanthos preissii.* ……..27

3.2 Biosynthesis of tetraoxygenated phenylphenalenones in *Wachendorfia thyrsiflora*……35

Phytochemistry 13 (2015) 68–73

Contents lists available at ScienceDirect

Phytochemistry

journal homepage: www.elsevier.com/locate/phytochem

4-Methoxycinnamic acid – An unusual phenylpropanoid involved in phenylphenalenone biosynthesis in *Anigozanthos preissii*

William Hidalgo, Marco Kai, Bernd Schneider *

Max-Planck Institut für Chemische Ökologie, Beutenberg Campus, Hans-Knöll-Strasse 8, 07745 Jena, Germany

ARTICLE INFO

Article history:
Received 6 February 2015
Received in revised form 22 May 2015
Accepted 26 May 2015

Keywords:
Anigozanthos preissii
Wachendorfia thyrsiflora
Biosynthesis
Haemodoraceae
Labeling
Nuclear magnetic resonance
Phenylphenalenones
Phenylpropanoids

ABSTRACT

In vitro root cultures of *Anigozanthos preissii* and *Wachendorfia thyrsiflora* (Haemodoraceae) are suitable biological systems for studying the biosynthesis of phenylphenalenones. Here we report how we used these root cultures to investigate precursor–product relationships between phenylpropanoids and phenylphenalenones whose phenyl rings share identical substitution patterns. Four phenylpropanoic acids, including ferulic acid and the unusual 4-methoxycinnamic acid, were used in ^{13}C-labeled form as substrates to study their incorporation into phenylphenalenones. In addition to the previously reported 2-hydroxy-9-(4′-hydroxy-3′-methoxyphenyl)-1*H*-phenalen-1-one (trivial name musanolone F), 2-hydroxy-9-(4′-methoxyphenyl)-1*H*-phenalen-1-one (proposed trivial name 4′-methoxyanigorufone) was found as a biosynthetic product in *A. preissii*. The carbon skeleton of 4′-methoxycinnamic acid was biosynthetically incorporated as an intact unit including its 4′-*O*-methyl substituent at the lateral phenyl ring. 4′-Methoxyanigorufone is reported here for the first time as a natural product.

1. Introduction

Phenylphenalenones are a characteristic class of secondary metabolites occurring in the monocotyledoneous plant families Haemodoraceae, Pontederiaceae, Strelitziaceae and Musaceae (Munde et al., 2013). They are polycyclic aromatic compounds consisting of a tricyclic phenalene core structure with a keto functional group and a lateral phenyl ring (ring D) (see structure in Table 1). Because of their fungicidal (Otálvaro et al., 2007; Hidalgo et al., 2009) and nematicidal properties (Hölscher et al., 2014) and their inducibility after pathogen/herbivore attack (Luis et al., 1994; Jitsaeng and Schneider, 2010; Otálvaro et al., 2010), phenylphenalenones play an important role as phytoalexins in the chemical defense of *Musa* plants. The physiological and/or ecological importance of these metabolites in the three other plant families has yet to be explored, although their antioxidant capacity could be one of the reasons they are produced (Blokhina et al., 2003; Duque et al., 2010; Brewer, 2011).

Previous biosynthetic studies have demonstrated that phenylphenalenone-type compounds are formed by the condensation of two phenylpropanoids merged with one malonate unit through the diarylheptanoid pathway. The variable substitution pattern of the lateral phenyl ring (ring D: unsubstituted phenyl; 4′-hydroxyphenyl; 3′,4′-dihydroxyphenyl; 3′-methoxy-4′-hydroxyphenyl) contributes to the structural diversity of the phenylphenalenones (Hölscher and Schneider, 1995a,b; Schmitt et al., 2000). As previously demonstrated in *Anigozanthos preissii*, the substitution pattern of ring D reflects the substitution pattern of the phenylpropanoid precursors (Schmitt et al., 2000). Four phenylpropanoids have been identified so far as precursors of a C-9 moiety comprising ring D and three adjacent carbon atoms C-7 to C-9 of the phenalenone tricycle (for details see Table 1). In the case of 4′-*O*-methylirenolone, which has a methoxy group in position 4′ of ring D, the actual phenylpropanoid precursor could not be determined because 4′-methoxycinnamic acid (**2**), when administered to *in vitro* plants of *Musa acuminata*, was demethylated and further converted to 3′,4′-methylenedioxyphenylpropanoic acid (Otálvaro et al., 2010). Hence, due to their strong demethylation capacity for exogenously supplied 4′-methoxycinnamic acid, *Musa* plants seemed to be unsuitable for studying the suggested biosynthetic precursor–product relationship between methoxyphenylpropanoids and phenylphenalenones with methoxy-substituted ring D, such as 4′-*O*-methylirenolone.

In vitro root cultures of *A. preissii* and *Wachendorfia thyrsiflora* (both belonging to the Haemodoraceae plant family), which are suitable biological systems for studying the biosynthesis of phenylphenalenones (Hölscher and Schneider, 1995b; Schmitt et al., 2000; Munde et al., 2013), produce pairs of phenylpropanoids

* Corresponding author.
E-mail address: schneider@ice.mpg.de (B. Schneider).

http://dx.doi.org/10.1016/j.phytochem.2015.05.017
0031-9422/

Table 1
Examples of phenylpropanoids and phenylphenalenones sharing the same substitution pattern of the phenyl ring.

	Phenylpropanoic acids			Phenylphenalenones	
Part A					
R_1	R_2				
H	H	Cinnamic acid	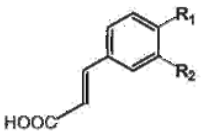	Anigorufone	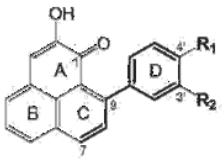
OH	H	4-Coumaric acid		Hydroxyanigorufone	
OH	OH	Caffeic acid		Dihydroxyanigorufone	
OH	OCH_3	Ferulic acid (**1**)		Musanolone F (**3**)	
Part B					
R					
H	4-Coumaric acid (+SAM)		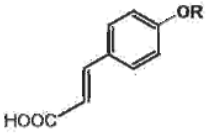	4′-*O*-Methylirenolone	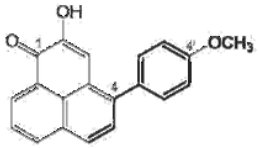
CH_3	4′-Methoxy-cinnamic acid (**2**)				

Part A: Moieties shown in bold are linked by confirmed biosynthetic precursor–product relationships (Schmitt et al., 2000). Part B: The precursor of 4′-*O*-methylirenolone in *M. acuminata* is uncertain. For details see text and Otálvaro et al. (2010).
SAM = *S*-adenosyl-L-methionine.

and phenylphenalenones with corresponding methoxy-substituted phenyl ring substitutions. Here we report the ^{1}H NMR and HPLC-guided identification of phenylpropanoic acids using an isotope dilution approach. In the second part of this work, we offer evidence for a precursor–product relationship by administering the ^{13}C-labeled phenylpropanoids then isolating the resulting phenylphenalenones and analyzing its ^{13}C enrichment by ^{13}C NMR and HRMS.

2. Results and discussion

2.1. Detection of phenylpropanoic acids in plant root cultures

In vitro root cultures of *A. preissii* and *W. thyrsiflora* are rich sources of phenylphenalenones (Hölscher and Schneider, 1997; Opitz et al., 2002; Opitz and Schneider, 2003; Fang et al., 2011) and therefore were selected for the present study. However, only one compound of that type, 2-hydroxy-9-(4′-hydroxy-3′-methoxyphenyl)-1*H*-phenalen-1-one (musanolone F (**3**)), which has a methoxylated lateral phenyl ring D, was reported from *A. preissii* (Schmitt et al., 2000). Musanolone F (**3**) is biosynthetically derived from ferulic acid (**1**), which is an abundant phenylpropanoic acid in *A. preissii* (Schmitt and Schneider, 2001). Most of the phenylphenalenones occurring in *W. thyrsiflora* have an unsubstituted ring D (Fang et al., 2011, 2012), and no compound with a methoxy substituent in ring D has yet been reported from this plant. Also no data about the occurrence of phenylpropanoic acids in *W. thyrsiflora* are available.

We synthesized [2-^{13}C]ferulic acid ([2-^{13}C]-**1**), [2-^{13}C]isoferulic acid, [2-^{13}C]4′-methoxycinnamic acid ([2-^{13}C]-**2**), and [2-^{13}C]3′,4′-methylenedioxycinnamic acid and used an isotope dilution approach to analyze the two plant systems for the occurrence of these phenylpropanoic acids. Although compound **1** is widely distributed in plants (Kroon and Williamson, 1999) including *A. preissii* (Schmitt and Schneider, 2001), isoferulic acid and 4′-methoxycinnamic acid (**2**) are rarely found in plants (Liu et al., 1999; Sobolev et al., 2006; Kuddus et al., 2010). Free 3′,4′-methylenedioxycinnamic acid has to our knowledge been identified only in *Piper philippinum* (Chen et al., 2007) and *M. acuminata* (Otálvaro et al., 2010). The four [2-^{13}C]-labeled phenylpropanoids were separately administered to the two *in vitro*-root cultures. ^{1}H NMR and HPLC-guided isolation was used to identify ^{13}C-labeled phenylpropanoic acids and their unlabeled native counterparts in the crude root extracts of both cultures.

The fingerprint signals of H-2 of the *E*-configured double bonds (J_{H2-H3} = 16 Hz) and their ^{13}C satellite signals (J_{C2-H2} = 161 Hz) were used to detect isotopologue mixtures of non-metabolized [2-^{13}C]-phenylpropanoids together with the unlabeled counterparts in the plant extracts. Using this approach, the natural occurrence of free ferulic acid (**1**) was confirmed in root cultures of *A. preissii* and detected for the first time in root cultures of *W. thyrsiflora* (Fig. 1A and B). 4′-Methoxycinnamic acid (**2**) was found in *A. preissii* but not in *W. thyrsiflora* (data not shown). Isoferulic acid and 3′,4′-methylenedioxy phenylpropanoic acid were not detectable in either of the two root cultures.

Moreover, the proportion of [2-^{13}C]-labeled and unlabeled phenylpropanoids was determined from the integral ratio of the doublets of H-2 and the ^{13}C satellite signals in the ^{1}H NMR spectra (Schneider et al., 2003). Since the feeding experiments with *A. preissii* and *W. thyrsiflora* were performed under identical conditions, the integral ratios suggested a lower endogenous level of free ferulic acid (**1**) in *W. thyrsiflora* (ratio ^{13}C-labeled: unlabeled 8.0:1) compared to *A. preissii* (2.7:1). The isotopologue ratio of [2-^{13}C]-**2** to unlabeled **2** (natural abundance ^{13}C contents) in *A. preissii* was found to be 8.1:1 under the experimental conditions.

As ferulic acid (**1**) is a common cell wall lignin component (Buanafina, 2009), the proportion of this phenylpropanoic acid potentially available for the biosynthesis of phenylphenalenones is difficult to estimate. Unlike ferulic acid (**1**), 4′-methoxycinnamic acid (**2**) seems not to be used as a precursor in major plant metabolic pathways such as lignin formation. Therefore, all of the endogenous pool found in *A. preissii* should be available for the biosynthesis of phenylphenalenones. Hence, our search for methoxyphenylphenalenones and their biosynthesis was focused on *A. preissii*.

2.2. Detection and biosynthesis of methoxyphenylphenalenones in plant root cultures

The administration of [2-^{13}C]ferulic acid (**1**) and [2-^{13}C]4′-methoxycinnamic acid (**2**) resulted in their successful incorporation into the corresponding phenylphenalenones from *A. preissii*, whereas no incorporation of **1** into any phenylphenalenone was detected in the case of *W. thyrsiflora*. Musanolone F (**3**) was the

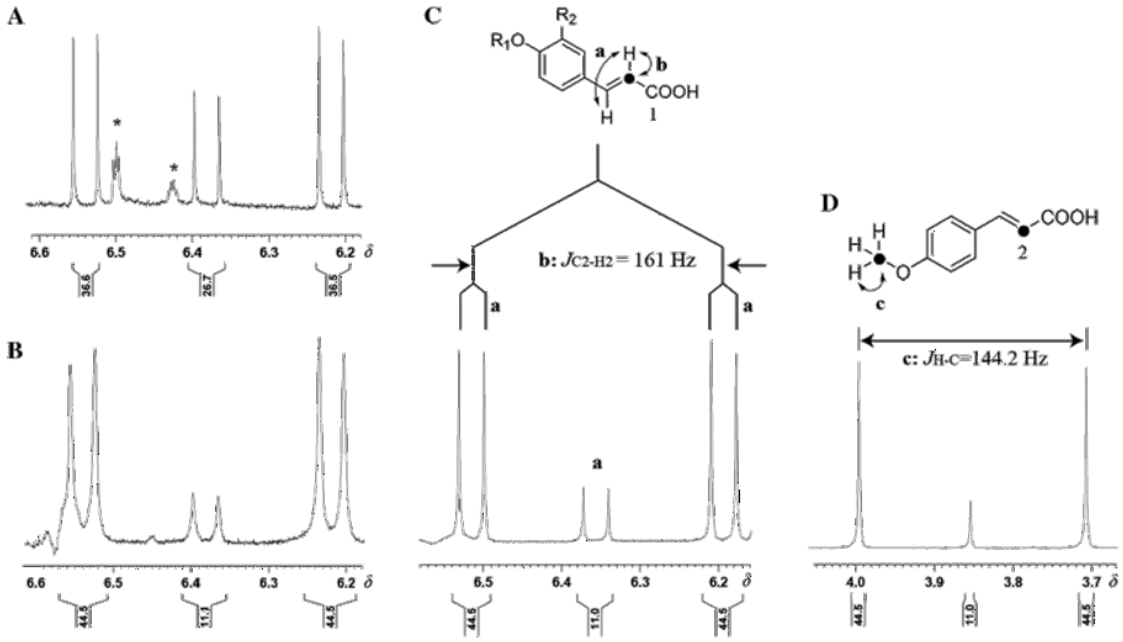

Fig. 1. Partial ^{1}H NMR spectra (500 MHz, MeOH-d_4) displaying signals of isotopologue mixtures of unlabeled (natural abundance ^{13}C) and ^{13}C-labeled phenylpropanoic acids: Panels (A) and (B): H-2-signals of ferulic acid (**1**) (R_1 = H, R_2 = OCH_3) from *in vitro* root cultures of *A. preissii* and *W. thyrsiflora*, respectively, incubated with [2-^{13}C]-**1**. Panel (C): H-2-signal 4′-methoxycinnamic acid (**2**) (R_1 = CH_3, R_2 = H) from root cultures of *A. preissii* incubated with [2-^{13}C,4′-O$^{13}CH_3$]-**2**). Panel (D): *O*-Methyl signal of **2** (R_1 = CH_3, R_2 = H) from root cultures of *A. preissii* incubated with [2-^{13}C,4′-O$^{13}CH_3$]-**2**). Integral values are given at the bottom of each spectrum. The structure drawing and splitting lines in panels (C) and (D) explain the spin–spin coupling pattern of the signals of ^{13}C-labeled and unlabeled isotopologues. For details, see text. ● = ^{13}C. * = signals of contaminations.

only phenylphenalenone isolated after *A. preissii* was incubated with [2-^{13}C]-**1**, and its ^{13}C NMR spectra as well as the isotopologue analysis by HRESIMS (data not shown) are in accordance with the data previously reported (Schmitt et al., 2000). This leads us to conclude that the characteristic 3′-OMe, 4′-OH substitution pattern found in ring D of **3** is derived from **1**.

The incubation of *A. preissii* root cultures with [2-^{13}C]4′-methoxycinnamic acid (**2**) and ^{13}C NMR-guided fractionation indicated that an unknown metabolite had been enriched with ^{13}C (Fig. S1). This metabolite, which was subjected to HPLC-guided isolation, was finally identified by 1D and 2D NMR and mass spectrometry as 2-hydroxy-9-(4′-methoxyphenyl)-1*H*-phenale-1-one (**4**). This compound, for which we propose the trivial name 4′-methoxyanigorufone, was previously synthesized and characterized by spectroscopic methods (Cooke and Dagley, 1978) and also found in *Musella lasiocarpa* (D. Hölscher, personal communication). Here **4** is reported for the first time as a naturally occurring phenylphenalenone. The ^{13}C NMR spectrum of **4** showed an enhanced signal at δ 132.6 of C-8 in the phenylphenalenone skeleton (Fig. 2, panel b), and the isotopologue analysis carried out by HRESIMS indicated the enrichment of 53.7% ^{13}C singly labeled molecule of [8-^{13}C]2-hydroxy-9-(4′-methoxyphenyl)-1*H*-phenale-1-one (**4**) biosynthesized from the administered [2-^{13}C]-labeled precursor **2** (Table 2).

This result clearly indicates a precursor–product relationship between 4′-methoxycinnamic acid (**2**) and the new phenylphenalenone (**4**). However, it opens the question whether **2** was incorporated (after being activated to the SCoA ester) as an intact unit into 4′-methoxydiarylheptanoid and, further, whether **2** was incorporated into the phenylphenalenone **4** (early *O*-methylation; route *i* in Fig. 3). Alternatively an *O*-demethylation of 4′-methoxycinnamic acid (**2**) could have been involved (route *ii* in Fig. 3); such an *O*-demethylation could have led to 4-coumaric acid which has been reported for being a precursor of the lateral phenyl ring in the phenylphenalenone skeleton (Funk and Brodelius, 1990; Hölscher and Schneider, 1995a). Route *ii* would require re-methylation of the 4′-OH group, probably at the stage of hydroxyanigorufone (late *O*-methylation) or the 4′-hydroxydiarylheptanoid (Fig. 3). This option was considered because in *M. acuminata*, the *O*-demethylation of 4′-methoxycinnamic acid (**2**) was reported; however, no conclusive evidence was provided about whether the 4′-*O*-methyl group of 4′-*O*-methylirenolone, an isomer of **4**, is the result of an early or a late *O*-methylation (Otálvaro et al., 2010).

In order to investigate the demethylation of 4′-methoxycinnamic acid (**2**) and to check which of the two routes, *i* or *ii*, is operating in *A. preissii*, [2-^{13}C,4′-O$^{13}CH_3$]-**2** was synthesized; this compound contains 99% ^{13}C enrichment in both positions, at C-2 of the carbon skeleton and in the 4′-*O*-methyl group. The specific ^{13}C enrichment at C-2 was employed to verify that the C-9 phenylpropanoid skeleton had been incorporated through the established general biosynthetic pathway; the label of the 4′-*O*-methyl group was used to check for a possible 4′-*O*-demethylation step. Thus, after the incubation of *A. preissii* root cultures with [2-^{13}C,4′-O$^{13}CH_3$]-**2**, a part of the substrate was isolated from this feeding experiment again and analyzed by ^{1}H NMR and HRESIMS to see what part of it was labeled. The integrals of the central and ^{13}C satellite signals of H-2 (δ 6.36) and the OCH_3 signal (δ 3.85) in the ^{1}H NMR spectrum (Fig. 1C and D) showed 89% ^{13}C in each of the two labeled positions, thus ruling out the possibility that the label in the OCH_3 group was lost through a hypothetical demethylation/remethylation mechanism (Fig. 3). The isotope enrichment determined by ^{1}H NMR was in good agreement with that found for the abundance of the double-labeled isotopologue [2-^{13}C,4′-O$^{13}CH_3$]-**2** of 84.4% found by HRESIMS (Table 3), although no single labeled isotopologues [2-^{13}C]-**2** and [4′-O$^{13}CH_3$]-**2** were detected.

As expected, the administration of [2-^{13}C,4′-O$^{13}CH_3$]-**2** to the root cultures of *A. preissii* also resulted in the formation of metabolite **4**, which was isolated and analyzed by NMR and HRESIMS. The

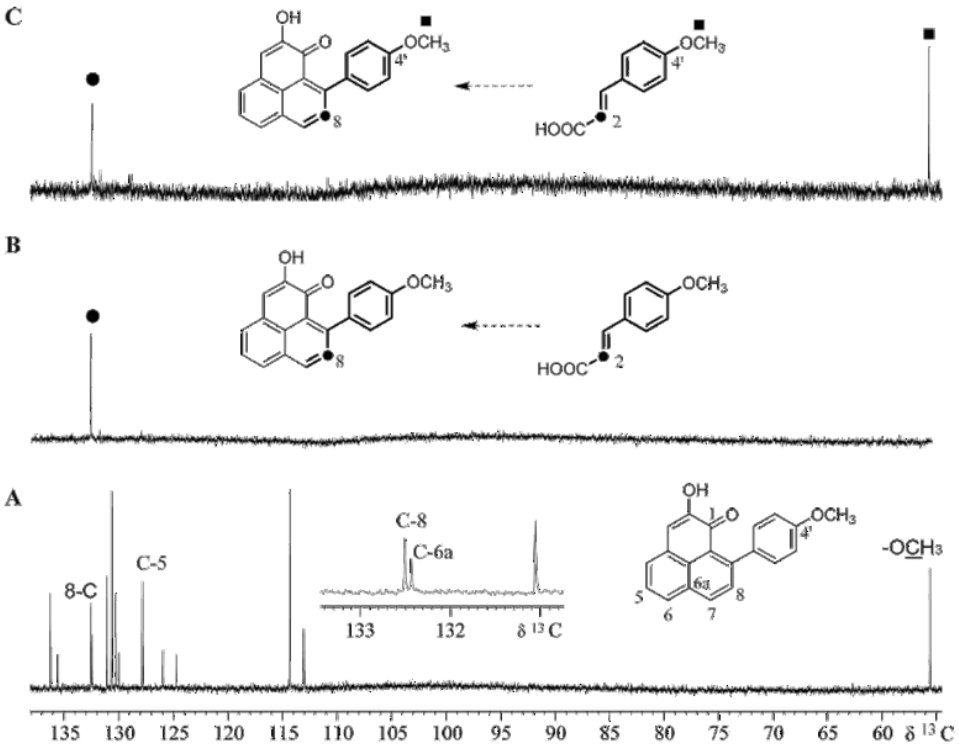

Fig. 2. Partial ^{13}C NMR spectra (125 MHz, acetone-d_6) of 2-hydroxy-9-(4′-methoxyphenyl)-1*H*-phenale-1-one (**4**) from root cultures of *A. preissii*. (a) Spectrum of unlabeled reference. (b) Isotope enrichment of **4** in position C-8 upon the incorporation of [2-^{13}C]4′-methoxycinnamic acid ([2-^{13}C]-**2**). (c) Isotope enrichment of **4** in position C-8 and in the *O*-methyl carbon atom upon the incorporation of [2-^{13}C,O$^{13}CH_3$]4′-methoxycinnamic acid ([2-^{13}C,O$^{13}CH_3$]-**2**). ●, ■ = Signal of the ^{13}C-enriched of C-8 and the 4′-*O*-methyl group, respectively.

Table 2
Isotopologue composition of 2-hydroxy-9-(4′-methoxyphenyl)-1*H*-phenalen-1-one (**4**) in root cultures of *A. preissii*, determined by HRESIMS after incubation with [2-^{13}C]-**2** and [2-^{13}C,O$^{13}CH_3$]-**2**, respectively.

Formula	*m/z* [M+H]$^+$ (calcd.)	Isotopologue analysis of compound **4** after incorporation of					
		Unlabeled **2** (reference)		[2-^{13}C]-**2**		[2-^{13}C,O$^{13}CH_3$]-**2**	
		m/z [M+H]$^+$ (found)	Relative abundance (%)	*m/z* [M+H]$^+$ (found)	Relative abundance (%)	*m/z* [M+H]$^+$ (found)	Relative abundance (%)
$C_{20}H_{15}O_3^+$	303.1021	303.1016	**80.3**	303.1018	33.6	303.1019	35.9
$C_{19}{}^{13}CH_{15}O_3^+$	304.1055	304.1051	17.6	304.1053	**53.7**	304.1051	7.5
$C_{18}{}^{13}C_2H_{15}O_3^+$	305.1088	305.1084	1.9	305.1085	12.3	305.1086	**45.9**
$C_{17}{}^{13}C_3H_{15}O_3^+$	306.1122	306.1118	0.2	306.1120	0.4	306.1118	10.7

^{13}C NMR spectrum of [2-^{13}C,4′-O$^{13}CH_3$]-**4** obtained from this experiment displayed two equally enhanced signals at δ 132.6 and δ 55.6, corresponding to an identical degree of ^{13}C enrichment at C-8 and 4′-OCH_3 (Fig. 2, panel c); this enrichment proved that the intact 4′-methoxycinnamic acid was incorporated as a unit into phenylphenalenone **4**. Additionally, the isotopologue analysis by HRESIMS showed 45.9% relative abundance of the doubly ^{13}C-labeled isotopologue (Table 2). Hence, route *i* in Fig. 3 represents the actual biosynthetic pathway of this metabolite.

3. Conclusions

Biosynthetic precursor–product relationships have been demonstrated in *A. preissii* between ferulic acid (**1**) and musanolone F (**3**) and between 4′-methoxycinnamic acid (**2**), which is a rare phenylpropanoid, and 4′-methoxyanigorufone (**4**). This finding clearly shows that in root cultures of this plant the substitution pattern at the lateral phenyl ring (ring D) of phenylphenalenones reflects the existence of the corresponding phenylpropanoids in the plant tissue. 4′-Methoxyanigorufone (**4**) is reported here for the first time as a natural product. The involvement of 4′-methoxycinnamic acid (**2**) in the phenylphenalenone biosynthesis represents an extension of the general phenylpropanoid pathway (Noel et al., 2005; Vogt, 2010). Thus, route *i* (Fig. 3) requires a new CoA ligase or an additional function for a promiscuous 4-coumarate CoA-ligase. This work also demonstrates the potential power of isotopically labeled compounds as a tool, not only in the elucidation of biosynthetic pathways but also in the detection and quantification of naturally occurring minor metabolites.

4. Experimental

4.1. General experimental procedures

^1H NMR, ^{13}C NMR, ^1H–^1H COSY, HMBC, and HSQC spectra were measured on a Bruker Avance 500 NMR spectrometer (Bruker

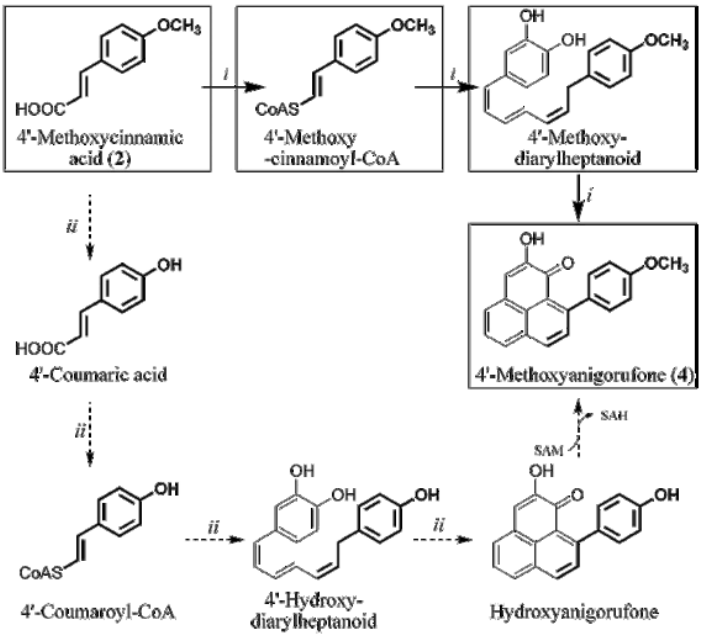

Fig. 3. Hypothetical biosynthetic pathways of 2-hydroxy-9-(4′-methoxyphenyl)-1*H*-phenalen-1-one (4). (i) Early 4′-*O*-methylation, (ii) late 4′-*O*-methylation. The phenylpropanoid unit is highlighted in bold. SAM: *S*-adenosyl-L-methionine; SAH: *S*-adenosylhomocysteine.

Table 3
Isotopologue composition of 4′-methoxycinnamic acid (2) determined by HRESIMS. The isotopologue mixture of 2 was isolated after feeding experiments to *in vitro* root cultures of *A. preissii* and compared with the data from untreated root cultures of the same plant (control).

Formula	*m/z* $[M+H]^+$ (calcd.)	Isotopologue analysis of compound 2 isolated from			
		Control plant		After incubation with [2-^{13}C,O^{13}CH$_3$]-2	
		m/z $[M+H]^+$ (found)	Relative abundance (%)	*m/z* $[M+H]^+$ (found)	Relative abundance (%)
$C_{10}H_9O_3^-$	177.0557	177.0551	96.3	177.0553	14.2
$C_9{}^{13}CH_9O_3^-$	178.0591	178.0587	3.6	178.0585	0.1
$C_9{}^{13}C_2H_9O_3^-$	179.0624	179.0622	0.1	179.0619	84.4
$C_7{}^{13}C_3H_9O_3^-$	180.0658	n.d.	n.d.	180.0655	1.3

n.d.: not detected.

Biospin, Karlsruhe, Germany), operating at 500.13 MHz for ^{1}H and 125.75 MHz for ^{13}C. A TCI cryoprobe (5 mm) was used to measure spectra at 300 K. Tetramethyl silane was used as an internal standard for referencing ^{1}H and ^{13}C NMR spectra. Electrospray ionization mass spectra (ESIMS) and LC–ESIMS were recorded on a Bruker Esquire 3000 ion trap mass spectrometer (Bruker Daltonics, Bremen, Germany). HRESIMS was recorded on a UPLC–MS/MS system consisting of an Ultimate 3000 series RSLC (Dionex, Idstein, Germany) system, and an Orbitrap mass spectrometer (Thermo Fisher Scientific, Bremen, Germany). Analytical and semipreparative HPLC was performed on an Agilent series HP1100 (binary pump G1312A; auto sampler G1367A; diode array detector G1315A; connected to fraction collector Advantec CHF122SB) using a LiChrospher RP18e column (5 µm, 250 × 10 mm) and a linear gradient MeOH-0.1% aq. trifluoroacetic acid from 35% to 100% in 25 min (flow rate 0.8 mL/min; monitoring wavelength 254 nm). The UV spectra were recorded by the DAD during analytical HPLC.

4.2. Plant material

Sterile root cultures of *A. preissii* (L.) and *W. thyrsiflora* L. were established as previously described (Hölscher and Schneider, 1997) and maintained in liquid MS medium (100 mL) in conical flasks (300 mL) on a gyratory shaker (85 rpm) at 23 °C under permanent light conditions (4.4 µmol m^{-2} s^{-1}). Three days before the precursor was administered, the cultured roots were transferred to fresh medium.

4.3. Reagents and the chemical synthesis of the ^{13}C-labeled precursors

The [2-^{13}C]hydroxycinnamic acids ([2-^{13}C]ferulic acid ([2-^{13}C]-**1**), [2-^{13}C]isoferulic acid, [2-^{13}C]4-methoxycinnamic acid ([2-^{13}C]-**2**), [2-^{13}C]4-coumaric acid and [2-^{13}C]3,4-methylenedioxy cinnamic acid) were prepared from the corresponding substituted benzaldehyde (0.33 mmol; Sigma–Aldrich, ⩾95.0%) (vanillin, isovanillin, anisaldehyde, 4-hydroxybenzaldehyde, piperonal) with [2-^{13}C]malonic acid (99% ^{13}C; 0.72 mmol; Deutero GmbH, Kastellaun, Germany) in a Knoevenagel reaction. The ^{13}C-methylated [2-^{13}C,4′-O^{13}CH$_3$]4-methoxycinnamic acid ([2-^{13}C,4′-O^{13}CH$_3$]-**2**) was synthesized by refluxing [2-^{13}C]4-coumaric acid (10 mg, 0.061 mmol), K_2CO_3 (10 mg), and $^{13}CH_3I$ (20 µL, 0.32 mmol, 99 atom% ^{13}C Sigma–Aldrich) in acetone (5 mL) for 4 h in order to yield 8.7 mg (79%) of the desired compound.

4.4. Feeding experiments, extraction and isolation of phenylphenalenones

Each ^{13}C-labeled compound (10 μmol) was dissolved in an EtOH:H_2O 4:1 solution (1 mL) and passed through a membrane filter (0.1 μm diameter) before being administered to the root culture. The incubation time was 4 d; afterwards, the roots (ca. 20 g fresh weigh) were frozen in liquid N_2, ground and extracted with methanol at room temperature for 1 h (3 × 100 mL). The solvent was removed by evaporation under vacuum pressure (<40 °C), and the crude extract was fractionated by partitioning between *n*-hexane–H_2O, CH_2Cl_2–H_2O and EtOAc–H_2O. The ^{13}C NMR labeling experiment was used to identify metabolites specifically enriched by the incorporation of the labeled precursor. Musanolone F (**3**, R_t 20.9 min) and 2-hydroxy-9-(4′-methoxyphenyl)-1*H*-phenalen-1-one (**4**, R_t 23.9 min), the products derived from successful incorporation, were isolated by semipreparative HPLC as described above. The analytical data of compound **3** exactly matched those of musanolone F available in our in-house database.

4.5. 2-Hydroxy-9-(4′-methoxyphenyl)-1*H*-phenalen-1-one (4)

The ^{1}H and ^{13}C NMR spectra of compound **4** resembled that of hydroxyanigorufone, which was previously reported from *A. preissii* root cultures (Hölscher and Schneider, 1997). The only exception was an additional singlet in the ^{1}H NMR spectrum (δ 3.89) and a corresponding signal in the ^{13}C NMR spectrum (δ 55.6), suggesting an *O*-methyl group was attached to one of the hydroxyl groups at 2-OH or 4′-OH. An HMBC cross-peak between the ^{1}H NMR signal of the *O*-methyl group and C-4′ (δ 160.3) of the lateral phenyl ring clearly indicated the methoxy group was attached to the *p*-position of ring D. ^{1}H,^{1}H-COSY and HSQC spectra, in addition to HMBC data, allowed all ^{1}H and ^{13}C chemical shifts to be assigned. Based on the above NMR data and combined with HRESIMS (Table 2), the structure of compound **4** was elucidated as 2-hydroxy-9-(4′-methoxyphenyl)-1*H*-phenalen-1-one. ^{1}H NMR (500 MHz, acetone-d_6): δ 8.39 (1H, d, J = 8.3 Hz, H-7), 8.08 (1H, d, J = 8.2 Hz, H-4), 7.87 (1H, d, J = 7.2 Hz, H-6), 7.68 (1H, dd, J = 8.2, 7.2 Hz, H-5), 7.64 (1H, d, J = 8.3 Hz, H-8), 7.34 (2H, d-like, J = 8.8 Hz, H-2′/6′), 7.18 (1H, s, H-3), 7.02 (2H, d-like, J = 8.8 Hz, H-3′/5′), 3.89 (3H, s, 4′-OCH_3); ^{13}C NMR (125 MHz, acetone-d_6): δ 180.9 (C-1), 160.3 (C-4′), 151.5 (C-2), 149.3 (C-9), 136.3 (C-7), 135.6 (C-1′), 132.6 (C-8), 132.5 (C-6a), 131.1 (C-6), 130.7 (C-2′/6′), 130.3 (C-4), 130.0 (C-3a), 127.9 (C-5), 126.0 (C-9b), 124.8 (C-9a), 114.4 (C-3′/5′), 113.1 (C-3), 55.6 (4′-OCH_3). UV (MeOH–H_2O): λ_{max} 265, 315, 371, 420 nm.

Acknowledgments

We thank COLCIENCIAS (Colombia) for a scholarship to W.H., the Max Planck Institute for Chemical Ecology for financial support and Emily Wheeler for editorial assistance.

Appendix A. Supplementary data

Supplementary data associated with this article can be found, in the online version, at http://dx.doi.org/10.1016/j.phytochem.2015.05.017.

References

Blokhina, O., Virolainen, E., Fagerstedt, K.V., 2003. Antioxidants, oxidative damage and oxygen deprivation stress: a review. Ann. Bot. 91, 179–194.

Brewer, M.S., 2011. Natural antioxidants: sources, compounds, mechanisms of action, and potential applications. Compr. Rev. Food Sci. F. 10, 221–247.

Buanafina, M.M.D., 2009. Feruloylation in grasses: current and future perspectives. Mol. Plant 2, 861–872.

Chen, Y.C., Liao, C.H., Chen, I.S., 2007. Lignans, an amide and anti-platelet activities from *Piper philippinum*. Phytochemistry 68, 2101–2111.

Cooke, R.G., Dagley, I.J., 1978. Coloring matters of Australian plants. 20. Synthesis of hydroxyanigorufone and related phenalenones. Aust. J. Chem. 31, 193–197.

Duque, L., Restrepo, C., Saez, J., Gil, J., Schneider, B., Otálvaro, F., 2010. Synthesis of musafluorone: a naphthoxanthenone isolated from *Musa acuminata*. Tetrahedron Lett. 51, 4640–4643.

Fang, J.J., Paetz, C., Hölscher, D., Munde, T., Schneider, B., 2011. Phenylphenalenones and related natural products from *Wachendorfia thyrsiflora* L. Phytochem. Lett. 4, 203–208.

Fang, J.J., Kai, M., Schneider, B., 2012. Phytochemical profile of aerial parts and roots of *Wachendorfia thyrsiflora* L. studied by LC-DAD-SPE-NMR. Phytochemistry 81, 144–152.

Funk, C., Brodelius, P.E., 1990. Phenylpropanoid metabolism in suspension-cultures of Vanilla planifolia Andr. 3: Conversion of 4-methoxycinnamic acids into 4-hydroxybenzoic acids. Plant Physiol. 94, 102–108.

Hidalgo, W., Duque, L., Saez, J., Arango, R., Gil, J., Rojano, B., Schneider, B., Otálvaro, F., 2009. Structure activity relationship in the interaction of substituted perinaphthenones with *Mycosphaerella fijiensis*. J. Agric. Food Chem. 57, 7417–7421.

Hölscher, D., Schneider, B., 1995a. The biosynthetic origin of the central one-carbon unit of phenylphenalenones in *Anigozanthos preissii*. Nat. Prod. Lett. 7, 177–182.

Hölscher, D., Schneider, B., 1995b. A diarylheptanoid intermediate in the biosynthesis of phenylphenalenones in *Anigozanthos preissii*. J. Chem. Soc., Chem. Commun., 525–526.

Hölscher, D., Schneider, B., 1997. Phenylphenalenones from root cultures of *Anigozanthos preissii*. Phytochemistry 45, 87–91.

Hölscher, D., Dhakshinamoorthy, S., Alexandrov, T., Becker, M., Bretschneider, T., Buerkert, A., Crecelius, A.C., De Waele, D., Elsen, A., Heckel, D.G., Heklau, H., Hertweck, C., Kai, M., Knop, K., Krafft, C., Maddula, R.K., Matthaus, C., Popp, J., Schneider, B., Schubert, U.S., Sikora, R.A., Svatoš, A., Swennen, R.L., 2014. Phenalenone-type phytoalexins mediate resistance of banana plants (Musa spp.) to the burrowing nematode *Radopholus similis*. Proc. Natl. Acad. Sci. U.S.A. 111, 105–110.

Jitsaeng, K., Schneider, B., 2010. Metabolic profiling of *Musa acuminata* challenged with *Sporobolomyces salmonicolor*. Phytochem. Lett. 3, 84–87.

Kroon, P.A., Williamson, G., 1999. Hydroxycinnamates in plants and food: current and future perspectives. J. Sci. Food Agric. 79, 355–361.

Kuddus, M.R., Rumi, F., Kaisar, M.A., Hasan, C.M., Rashid, M.A., 2010. Trans-isoferulic acid from *Curcuma longa*. B. Latinoam. Caribe Pl. 9, 319–321.

Liu, I.M., Chi, T.C., Hsu, F.L., Chen, C.F., Cheng, J.T., 1999. Isoferulic acid as active principle from the rhizoma of *Cimicifuga dahurica* to lower plasma glucose in diabetic rats. Planta Med. 65, 712–714.

Luis, J.G., Fletcher, W.Q., Echeverri, F., Grillo, T.A., 1994. Phenalenone-type phytoalexins from *Musa acuminata*. Synthesis of 4-phenylphenalenones. Tetrahedron 50, 10963–10970.

Munde, T., Brand, S., Hidalgo, W., Maddula, R.K., Svatoš, A., Schneider, B., 2013. Biosynthesis of tetraoxygenated phenylphenalenones in *Wachendorfia thyrsiflora*. Phytochemistry 91, 165–176.

Noel, J.P., Austin, M.B., Bomati, E.K., 2005. Structure–function relationships in plant phenylpropanoid biosynthesis. Curr. Opin. Plant Biol. 8, 249–253.

Opitz, S., Schneider, B., 2003. Oxidative biosynthesis of phenylbenzoisochromenones from phenylphenalenones. Phytochemistry 62, 307–312.

Opitz, S., Otálvaro, F., Echeverri, F., Quiñones, W., Schneider, B., 2002. Isomeric oxabenzochrysenones from *Musa acuminata* and *Wachendorfia thyrsiflora*. Nat. Prod. Lett. 16, 335–338.

Otálvaro, F., Nanclares, J., Vasquez, L.E., Quiñones, W., Echeverri, F., Arango, R., Schneider, B., 2007. Phenalenone-type compounds from *Musa acuminata* var. "Yangambi km 5" (AAA) and their activity against *Mycosphaerella fijiensis*. J. Nat. Prod. 70, 887–890.

Otálvaro, F., Jitsaeng, K., Munde, T., Echeverri, F., Quiñones, W., Schneider, B., 2010. *O*-Methylation of phenylphenalenone phytoalexins in *Musa acuminata* and *Wachendorfia thyrsiflora*. Phytochemistry 71, 206–213.

Schmitt, B., Schneider, B., 2001. Phenylpropanoid interconversion in *Anigozanthos preissii* observed by high-performance liquid chromatography–nuclear magnetic resonance spectroscopy. Phytochem. Anal. 12, 43–47.

Schmitt, B., Hölscher, D., Schneider, B., 2000. Variability of phenylpropanoid precursors in the biosynthesis of phenylphenalenones in *Anigozanthos preissii*. Phytochemistry 53, 331–337.

Schneider, B., Gershenzon, J., Graser, G., Hölscher, D., Schmitt, B., 2003. One-dimensional ^{13}C NMR and HPLC-^{1}H NMR techniques for observing carbon-13 and deuterium labelling in biosynthetic studies. Phytochem. Rev., 31–43

Sobolev, V.S., Horn, B.W., Potter, T.L., Deyrup, S.T., Gloer, J.B., 2006. Production of stilbenoids and phenolic acids by the peanut plant at early stages of growth. J. Agric. Food Chem. 54, 3505–3511.

Vogt, T., 2010. Phenylpropanoid biosynthesis. Mol. Plant 3, 2–20.

Appendix. Supplementary information

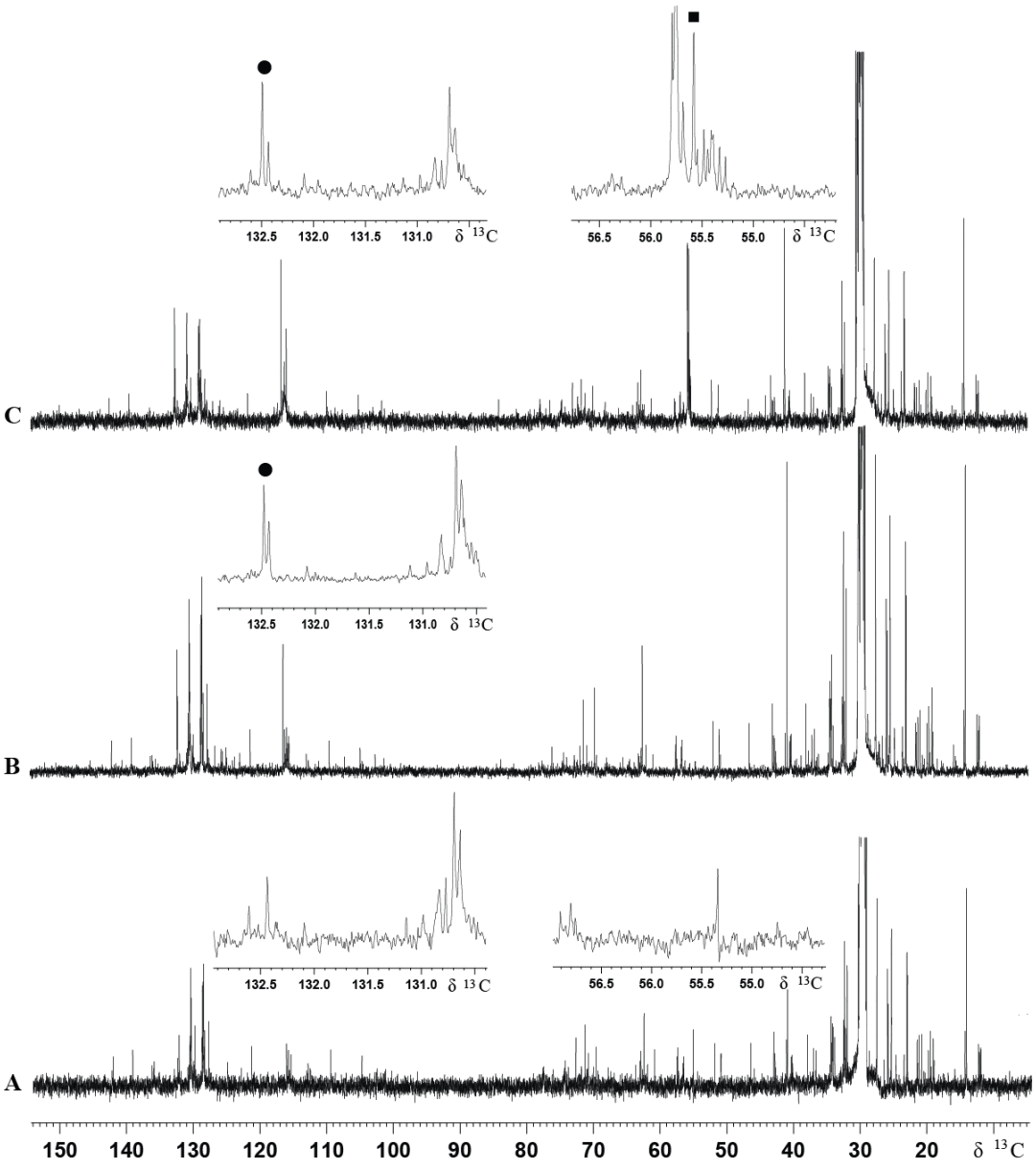

Figure S1. Partial ^{13}C-NMR spectra (125 MHz, acetone-d_6) of the *n*-hexane extract of root cultures from *Anigozanthos preissii*. Panel A, control root culture. Panel B shows the ^{13}C-enhanced signal (see expanded region) of C-8 of 2-hydroxy-9-(4'-methoxyphenyl)-1*H*-phenale-1-one (**4**) after incubation with [2-^{13}C]-**2**. Panels C shows the ^{13}C-enhanced signals (see expanded regions) of C-8 and 4'-OCH_3 of **4** after incubation with [2-^{13}C,O$^{13}CH_3$]-2, respectively. *= signal of the ^{13}C-enrichtment. *= signal of the ^{13}C-enrichment.

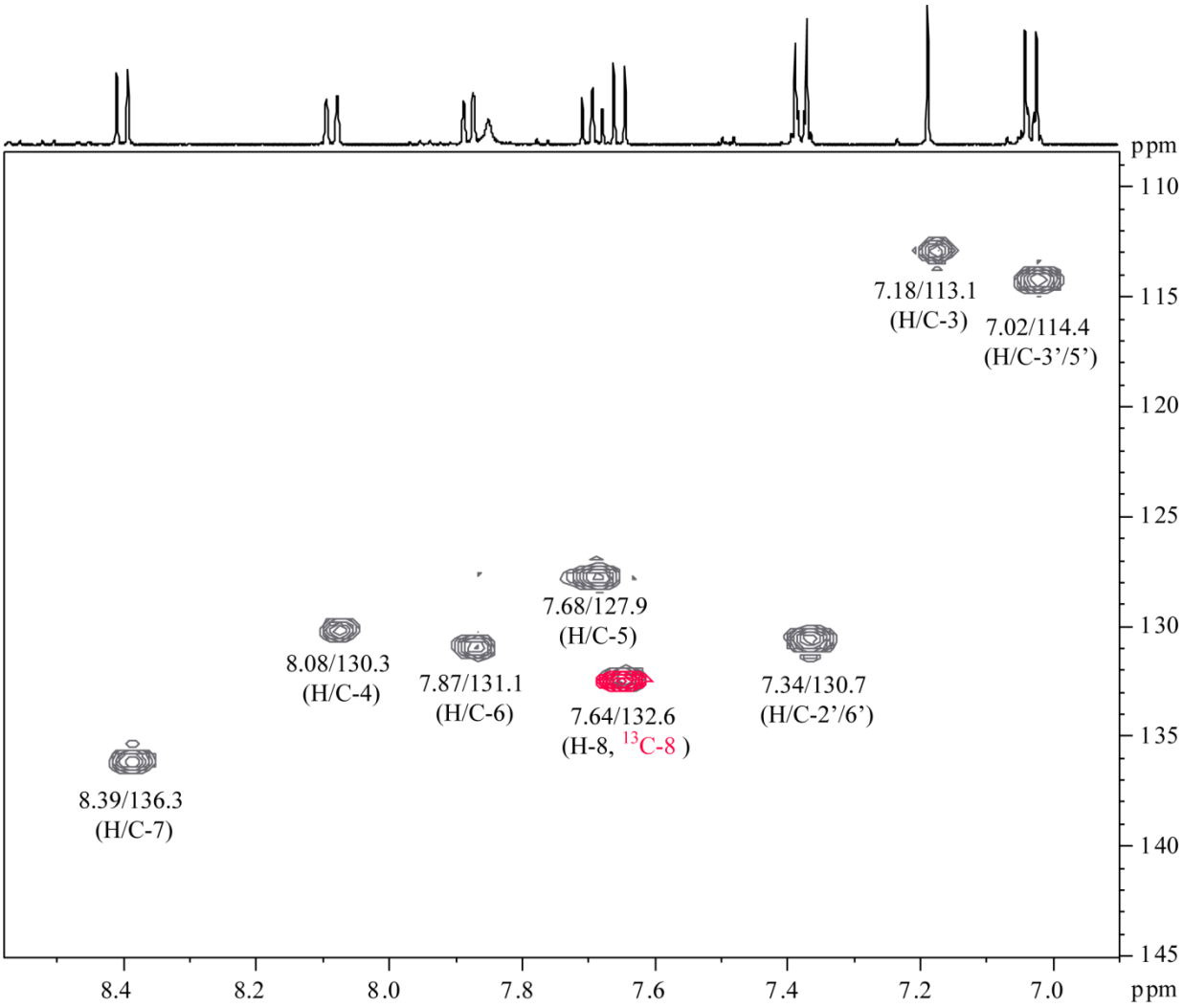

Figure S2. Superimposed HSQC spectra (500 MHz, acetone-d_6) of labeled and 2-hydroxy-9-(4'-methoxyphenyl)-1*H*-phenale-1-one (**4**) obtained after incubation of *Anigozanthos preissii* root cultures with [2-^{13}C]-**2**. Gray spectrum: unlabeled **4**; red spectrum: [8-^{13}C]-**4**, displaying only the signal to H/C-8 (threshold adjusted).

Phytochemistry 91 (2013) 165–176

Contents lists available at SciVerse ScienceDirect

Phytochemistry

journal homepage: www.elsevier.com/locate/phytochem

Biosynthesis of tetraoxygenated phenylphenalenones in *Wachendorfia thyrsiflora*

Tobias Munde, Silke Brand, William Hidalgo, Ravi K. Maddula, Aleš Svatoš, Bernd Schneider *

Max Planck Institute for Chemical Ecology, Beutenberg Campus, Hans-Knöll-Straße 8, D-07745 Jena, Germany

ARTICLE INFO

Article history:
Available online 17 March 2012

Dedicated to the memory of Meinhart H. Zenk.

Keywords:
Wachendorfia thyrsiflora
Diarylheptanoids
Haemodoraceae
Isotope-induced chemical shift
Isotope effect
Isotopologues
Labelling
Nuclear magnetic resonance
Oxygen-18
Phenylphenalenones

ABSTRACT

The biosynthetic origin of 1,2,5,6-tetraoxygenated phenylphenalenones and the sequence according to which their oxygen functionalities are introduced during the biosynthesis in *Wachendorfia thyrsiflora* were studied using two approaches. (1) Oxygenated phenylpropanoids were probed as substrates of recombinant *W. thyrsiflora* polyketide synthase 1 (WtPKS1), which is involved in the diarylheptanoid and phenylphenalenone biosynthetic pathways, (2) Root cultures of *W. thyrsiflora* were incubated with ^{13}C-labelled precursors in an $^{18}O_2$ atmosphere to observe incorporation of the two isotopes at defined biosynthetic steps. NMR- and HRESIMS-based analyses were used to unravel the isotopologue composition of the biosynthetic products, lachnanthoside aglycone and its allophanyl glucoside. Current results suggest that the oxygen atoms decorating the phenalenone tricycle are introduced at different biosynthetic stages in the sequence *O*-1 → *O*-2 → *O*-5. In addition, the incubation of *W. thyrsiflora* root cultures with ^{13}C-labelled lachnanthocarpone established a direct biosynthetic precursor–product relationship with 1,2,5,6-tetraoxygenated phenylphenalenones.

1. Introduction

Phenylphenalenones are a group of polycyclic natural products occurring in the Musaceae (banana) (Luis et al., 1994; Kamo et al., 1998; Hölscher and Schneider, 1998; Otálvaro et al., 2007) and related plant families Strelitziaceae (*Strelitzia reginae*, the bird of paradise plant) (Hölscher and Schneider, 2000), Haemodoraceae (e.g. *Anigozanthos* species, the kangaroo paw) (Cooke and Thomas, 1975; Hölscher and Schneider, 1997; Hölscher and Schneider, 1999; Opitz et al., 2002), and Pontederiaceae (e.g. *Eichhornia crassipes*, the water hyacynth) (DellaGreca et al., 2008; Hölscher and Schneider, 2005). Bioassay studies have demonstrated the antifungal properties of (phenyl)phenalenones (Quiñones et al., 2000; Otálvaro et al., 2007). The remarkable structural diversity of phenylphenalenones is mainly due to their variable oxygenation pattern. Anigorufone (**3a**) (Fig. 1), which occurs in most phenylphenalenone-producing plants, is one of the simplest 2-hydroxy-9-phenylphenalen-1-ones. Recently, the biosynthetic origin of the 1-keto-2-hydroxy motif of phenylphenalenones was elaborated using ^{13}C/^{18}O labelling experiments and isotopologue analysis based on nuclear magnetic resonance (NMR) spectroscopy and high resolution electro-spray mass spectrometry (HRESIMS) (Munde et al., 2011). It was shown that the hydroxyl group at C-2 of 9-phenylphenalenones had been introduced at the stage of a linear diarylheptanoid, and the carbonyl oxygen atom originated from the hydroxyl group of the 4-coumaroyl moiety.

Not only 2-hydroxy-9-phenylphenalen-1-ones such as anigorufone (**3a**) but also compounds such as lachnanthoside aglycone (**2a**) and its allophanyl glucoside (**1a**) (Fig. 1) with two more hydroxyl groups in the phenalenone nucleus occur in *Wachendorfia thyrsiflora* (Fang et al., 2011), *Xiphidium caeruleum* (Opitz et al., 2002) and some other Haemodoraceae (Cooke and Edwards, 1980). One of the additional oxygen atoms is located at C-6, and, in most phenylphenalenones, the other atom is attached to C-5 but can also be found at C-4. The oxygen functionality at C-6 very likely comes from the carbonyl thioester of 4-coumaroyl–CoA, which in the course of phenylphenalenone biosynthesis condenses with a diketide to form a diarylheptanoid (Brand et al., 2006). Unlike the origin of the oxygen atom at C-6, nothing is known about the introduction of the oxygen at C-5.

In order to probe for the origin of the oxygen functionalities and the sequence according to which they are introduced to the phenylphenalenone scaffold in *W. thyrsiflora*, two independent approaches were used. First, the substrate specificity of WtPKS1 was investigated. The recombinant enzyme was incubated with α-oxygenated phenylpropanoyl *N*-acetyl cysteamine (NAC) derivatives [phenylpyruvoyl–NAC, 3-(4-hydroxyphenyl)pyruvoyl–NAC, (*R*)- and (*S*)-phenyllactoyl–NAC), (*R*)- and (*S*)-3-(4-hydroxyphenyl) lactoyl–NAC] as mimics of the corresponding CoA esters.

In a second approach, root cultures of *W. thyrsiflora* were supplemented with [2-^{13}C]L-phenylalanine ([2-^{13}C]Phe), [2-^{13}C]4-coumaric

* Corresponding author. Tel.: +49 3641 571600; fax: +49 3641 571601.
E-mail address: schneider@ice.mpg.de (B. Schneider).

0031-9422/$ - see front matter © 2012 Elsevier Ltd. All rights reserved.
doi:10.1016/j.phytochem.2012.02.020

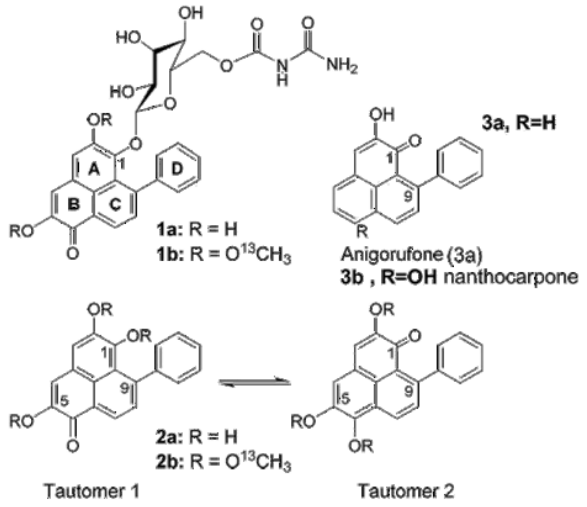

Fig. 1. Structures of 1,2,5,6-tetraoxygenated phenylphenalenones used as target compounds to study biosynthetic oxygenation in root cultures of *W. thyrsiflora* and anigorufone; the last compound exemplifies a 2-hydroxy-9-phenylphenalen-1-one. Because of tautomerism of **2a**, the carbonyl group of **2a**/**2b** appears at different positions in the phenalenone tricycle. For simplicity, the position *peri* to the phenyl ring is designated C-1 in the text and in structure drawings of all tautomeric 1,2,5,6-tetraoxygenated phenylphenalenones, regardless if this position is bearing a keto or hydroxyl functionality. Thus, the numbering used in this paper is different from that used in chemical names, which are as follows: **1a**, 6-*O*-[(6″-*O*-allophanyl-ß-D-glucopyranosyl]-2,5-dihydroxy-7-phenylphenalen-1-one; **1b**, 6-*O*-[(6″-*O*-allophanyl-ß-D-glucopyranosyl]-2,5-dimethoxy-7-phenylphenalen-1-one; **2a**, two tautomers of lachnanthoside aglycone, 2,5,6-trihydroxy-9-phenylphenalen-1-one and 2,5,6-trihydroxy-7-phenylphenalen-1-one; **2b**, two tri-*O*-methyl derivatives of lachnanthoside aglycone, [2,5,6-($O^{13}CH_3$)$_3$]2,5,6-trimethoxy-9-phenylphenalen-1-one and [2,5,6-($O^{13}CH_3$)$_3$]2,5,6-trimethoxy-7-phenylphenalen-1-one.

acid ([2-^{13}C]CA), and two ^{13}C-labelled diarylheptanoids, [6-^{13}C](4*E*,6*E*)-1-(4-hydroxyphenyl)-7-phenylhepta-4,6-dien-3-one (DAH-I), and [6-^{13}C](4*E*,6*E*)-1-(3,4-dihydroxyphenyl)-7-phenylhepta-4,6-dien-3-one (DAH-II), and simultaneously incubated in an $^{18}O_2$ atmosphere. Phenylphenalenones isolated from these precursor administration experiments were subjected to NMR- and HRESIMS-based isotopologue analysis. The results of the enzymatic studies and labelling experiments are discussed with respect to the biosynthetic sequence according to which oxygen functionalities are introduced to the phenylphenalenone scaffold.

In addition, a 1,2,6-trioxygenated phenylphenalenone, lachnanthocarpone (**3b**), which is a potential biosynthetic precursor of tetraoxygenated phenylphenalenones, was administered in ^{13}C-labelled form to probe for direct precursor–product relationships.

2. Results

2.1. α-Oxygenated phenylpropanoids are substrates of WtPKS1 in vitro

In *W. thyrsiflora*, WtPKS1 (Genbank™ accession number AY727928) catalyzes the condensation of a phenylpropanoyl–CoA with one malonyl–CoA to form a diketide. The diketide is then condensed with another phenylpropanoyl–CoA to form a diarylheptanoid, which is further processed to form phenylphenalenones (Brand et al., 2006). As shown by competitive precursor administration experiments (Schmitt and Schneider, 1999) (which indicated reversible conversion of phenylpropionic acid and cinnamic acid) and as discussed by Brand et al. (2006), 4-coumaroyl–CoA seems to be the starter substrate of WtPKS1 *in vivo*. *In vitro*, however, WtPKS1 accepts various phenylpropanoyl–CoAs, including phenylpyruvoyl–CoA, as starter units. Hypothetically, an α-oxygenated 3-(4-hydroxyphenyl)propanoyl–CoA could function as a substrate of WtPKS1. If the hypothetical biosynthetic pathway shown in Fig. 2 operated in *W. thyrsiflora*, the α-oxygen of the phenylpropanoid side chain would end up at C-5 of the phenylphenalenone skeleton.

N-Acetyl cysteamine (NAC) esters have been reported instead of CoA esters to be the starter substrates of polyketide synthases (Cane et al., 1991; Jacobs et al., 1991). Therefore, activated NAC esters of (*R*)- and (*S*)-phenyllactate, (*R*)- and (*S*)-3-(4-hydroxyphenyl)lactate, phenylpyruvate and 3-(4-hydroxyphenyl)pyruvate were synthesized according to reported procedures (Gilbert et al., 1995; Pohl et al., 1998) and, instead of CoA esters, assayed with WtPKS1. Activated phenylpropionyl- and cinnamoyl derivatives were used as reference substrates to compare the relative activities obtained for the incubation of WtPKS1 with NAC esters and with CoA esters (Table 1). In a previous study, the phenylpropionyl–CoA ester was among the best substrates *in vitro* and the cinnamoyl–CoA ester was among the poorest (Brand et al., 2006). Assay conditions optimized for phenylpropionyl–CoA as a starter substrate were used as previously reported (see Experimental).

Although the relative reactivity of WtPKS1 with NAC esters was drastically reduced compared to CoA esters, products of enzymatic conversion were still readily detectable, demonstrating that the NAC esters are useful starter substrates. In all experiments, [2-^{14}C]malonyl–CoA was used as the extender substrate. The products were detected in the assay by their UV absorption at 280 nm and the radiolabel originating from [2-^{14}C]malonyl–CoA. With (*S*)-phenyllactoyl–NAC as a starter substrate, the condensation product with two malonyl–CoA units was identified as (*S*)-6-[1-hydroxy-2-(4-hydroxyphenyl)ethyl]-4-hydroxy-2*H*-pyran-2-one (**4**, R_t 28.2 min) by LCESIMS (*m/z* 249 $[M+H]^+$) (see Fig. 3b). A minor, according to its retention time, slightly more polar product was tentatively assigned to benzalacetone. According to LCESIMS data and the long retention times, the structures of enzymatic condensations with starter substrates possessing an unsubstituted phenyl ring were identified as (*R*)-6-(1-hydroxy-2-phenyl)ethyl-4-hydroxy-2*H*-pyran-2-one (**5**) (37.7 min, *m/z* 231 $[M-H]^-$), (*S*)-6-(1-hydroxy-2-phenyl)ethyl-4-hydroxy-2*H*-pyran-2-one (**6**) (37.7 min, *m/z* 231 $[M-H]^-$), and (*E*)-6-(1-hydroxy-2-phenyl)ethenyl-4-hydroxy-2*H*-pyran-2-one (**7**) (38.8 min, *m/z* 231 $[M+H]^+$) (Fig. 3).

WtPKS1 converts (*S*)-phenyllactoyl–NAC to the pyrone (**6**; rel. activity 101%) (Fig. 4) as efficient as phenylpropionyl–NAC (100%). In contrast, WtPKS1 was much less active (51%) with the *R*-enantiomer, (*R*)-phenyllactoyl–NAC, to produce **5**. With (*S*)-3-(4-hydroxyphenyl)lactoyl–NAC, a substrate having a hydroxyl group in 4-position of the phenyl ring, the activity of WtPKS1 was reduced to 34% compared to the non-hydroxylated substrate, (*S*)-phenyllactoyl–NAC, although it was still better accepted than cinnamoyl–NAC (24%). Phenylpyruvoyl–NAC (30%) is nearly as efficiently accepted as (*S*)-3-(4-hydroxyphenyl)lactoyl–NAC (34%). No product formation was observed with 3-(4-hydroxyphenyl)pyruvoyl–NAC and (*R*)-3-(4-hydroxyphenyl)lactoyl–NAC.

Pyrones have been formed by WtPKS1 *in vitro* (in addition to benzalacetones) from phenylpropanoids, but the products *in vivo* are diketides, which are converted to diarylheptanoids and, further downstream in the biosynthetic pathway, to phenylphenalenones. Hence, the formation of pyrones as a result of *in vitro* incubation experiments of WtPKS1 with α-oxygenated phenylpropanoid–NAC thioesters shows that some of them have the potential to function as precursors of the diarylheptanoid/phenylphenalenone biosynthesis. However, since the results with PKS type III enzymes *in vitro* generally do not provide convincing clues for the activity of the protein *in vivo*, alternative approaches were used to confirm or disprove the outcome of the enzymatic experiments.

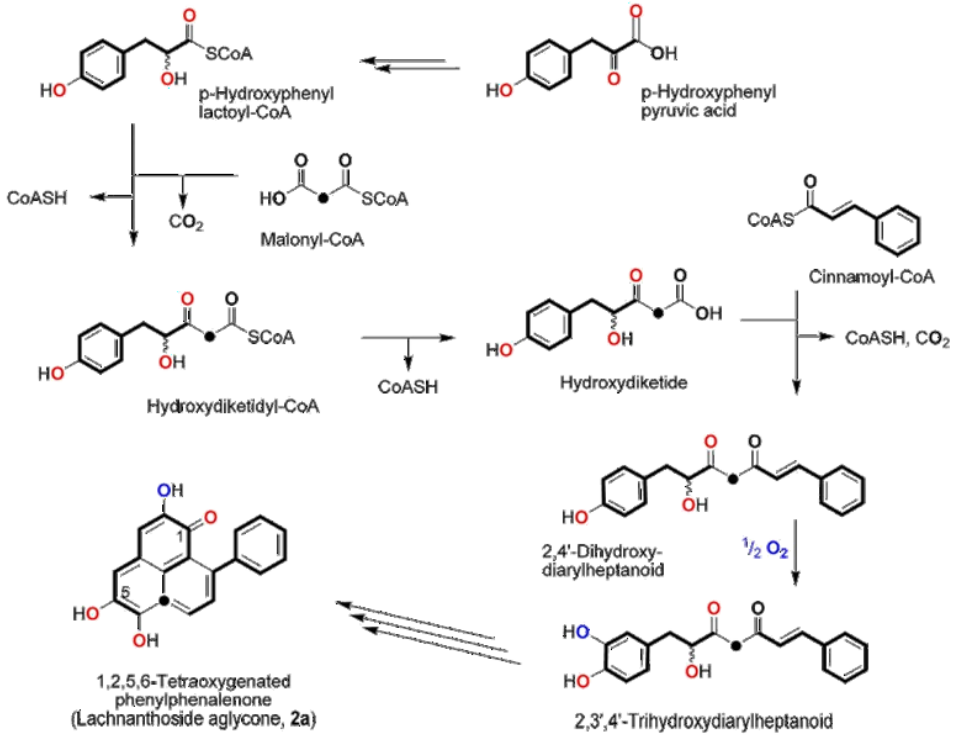

Fig. 2. Hypothetical "early hydroxylation" biosynthesis of 1,2,5,6-tetraoxygenated phenylphenalenones as probed by the incubation of WtPKS1 with α-oxygenated phenylpropanoyl thioesters and incubation of *W. thyrsiflora* root cultures with the corresponding ^{13}C-labelled precursors. The hypothetical fate of oxygen atoms is coded by color. Oxygen atoms which are suggested to be kept during phenylphenalenone biosynthesis are highlighted in red; lost oxygen atoms are displayed in bold; and oxygen atoms incorporated from O_2 are highlighted in blue. Phenylpropanoid units are marked with bold C–C bonds. ● indicates the origin of the marked atom from C-2 of malonate (Hölscher and Schneider, 1995b).

Table 1
Relative activities of WtPKS1 for cinnamoyl- and phenylpropionyl-CoA and -NAC esters as starter substrates.

Starter substrate	Relative activity [%]
Cinnamoyl-CoA	8
Cinnamoyl-NAC	2
Phenylpropionyl-CoA	100
Phenylpropionyl-NAC	7

See experimental section for conditions.

2.2. Early precursor administration experiments

Three ^{13}C-labelled α-oxygenated 3-(4-hydroxyphenyl)propanoic acids, [2-^{13}C](*S*)-3-(4-hydroxyphenyl)lactic acid, [2-^{13}C](*R*)-3-(4-hydroxyphenyl)lactic acid, and [2-^{13}C]3-(4-hydroxyphenyl) pyruvic acid, were synthesized and administered to root cultures of *W. thyrsiflora* in order to probe for their incorporation into phenylphenalenones. However, enhancement of ^{13}C signals was observed neither in the NMR spectra of the root extracts nor in isolated lachnanthoside aglycone (**2a**) and its allophanyl glucoside (**1a**). As shown by HPLC of aliquots taken regularly from the medium, significant absorption of the α-oxygenated precursor into the roots did not take place. Therefore, the results of these precursor administration experiments were inconclusive, and the biosynthesis of 2-oxygenated diarylheptanoids and 5-oxygenated phenylphenalenones remained unclear.

2.3. HRESIMS- and NMR-based $^{13}C/^{18}O$ isotopologue analysis

Unlike the administration of α-oxygenated 3-(4-hydroxyphenyl)propanoic acids, precursor administration experiments with radio-labelled phenylalanine and **4**-coumaric acid showed that the label in the medium decreased within 1 day to 84% for [2,3,4,5,6-^{3}H]Phe (1.5 mg, 0.37 kBq) and 43% for [U-^{14}C]CA (1.5 mg, 0.34 kBq), suggesting absorption into the root tissue. The absorption of L-Phe and hydroxycinnamic acids from the medium into the cultured roots is consistent with previous studies, in which the corresponding ^{13}C-labelled precursors were smoothly incorporated into phenylphenalenones in *W. thyrsiflora* (Opitz and Schneider, 2003; Brand et al., 2006) and root cultures of the related species, *Anigozanthos preissii* (Hölscher and Schneider, 1995b; Schmitt et al., 2000).

Recent $^{13}C/^{18}O$ labelling experiments have demonstrated the usefulness of isotopologue analysis to infer the biosynthetic origin of the oxygen atoms in positions 1 and 2 of simple phenylphenalenones (Munde et al., 2011). Thus, $^{13}C/^{18}O$-labelled isotopologues of compounds **1a** and **2a** from *W. thyrsiflora* were also considered to encode useful biosynthetic information about the sequence according to which oxygen functionalities are introduced into phenylphenalenones.

The administration of ^{13}C-labelled precursors to root cultures, which were simultaneously incubated in an $^{18}O_2$ atmosphere, followed by the isolation of phenylphenalenones **1a** and **2a**, and *O*-$^{13}CH_3$-methylation of the hydroxyl groups, was used to confirm the previously reported origin of the 1-keto-2-hydroxy motif

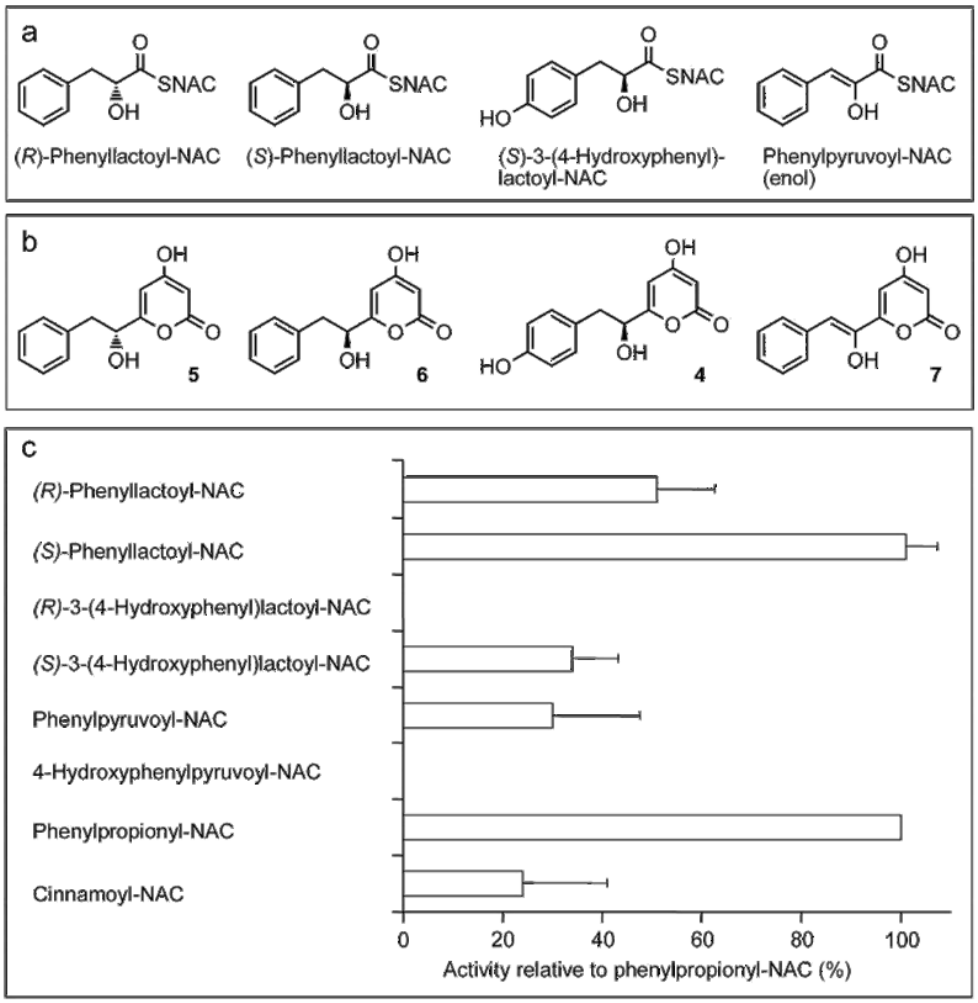

Fig. 3. (a) Starter substrates and (b) their corresponding products formed by incubation with [2-^{14}C]malonyl–CoA and WtPKS1. Products of two condensations are (*S*)-6-[1-hydroxy-2-(4-hydroxyphenyl)ethyl]-4-hydroxy-2*H*-pyran-2-one (**4**), (*R*)-6-(1-hydroxy-2-phenyl)ethyl-4-hydroxy-2*H*-pyran-2-one (**5**), (*S*)-6-(1-hydroxy-2-phenyl)ethyl-4-hydroxy-2*H*-pyran-2-one (**6**), and (*E*)-6-(1-hydroxy-2-phenyl)ethenyl-4-hydroxy-2*H*-pyran-2-one (**7**). (c) Enzymatic activity of WtPKS1 with different NAC esters, relative to the activity with phenylpropionyl–NAC (100%). Mean values of three experiments.

(Munde et al., 2011) by NMR and MS. Whether the additional oxygen atoms in positions 5 and 6 of 1,2,5,6-tetraoxygenated phenylphenalenones **1a** and **2a** are incorporated as a unit with α-oxygenated 4-hydroxyphenylpropanoids or come from an alternative late hydroxylation was the subject of the double labelling experiments.

[2-^{13}C]Phe, [2-^{13}C]CA, [6-^{13}C]DAH-I, and [6-^{13}C]DAH-II were used as ^{13}C-labelled precursors. Labels derived from [2-^{13}C]Phe into C-5 and C-8 (for a comment on numbering see caption of Fig. 1) of the allophanyl glycoside **1a** were reportedly incorporated (Brand et al., 2006) and confirmed in the present investigation for [2-^{13}C]Phe and [2-^{13}C]CA as precursors of phenylphenalenones in *W. thyrsiflora* (data not shown). ^{18}O-induced ^{13}C NMR signals of C-2 and C-5 of **1a** were not detected, indicating the low level of ^{18}O that was incorporated. In order to enhance the sensitivity with which ^{18}O is detected by isotope-induced ^{13}C NMR signals, samples of the target compound obtained from precursor administration experiments were methylated with $^{13}CH_2N_2$, thus attaching a ^{13}C atom to each hydroxyl group, including those groups containing ^{18}O atoms incorporated from atmospheric $^{18}O_2$. The ^{13}C NMR spectra of the 2,5-di-O$^{13}CH_3$ derivative **1b** obtained from [2-^{13}C]Phe and [2-^{13}C]CA, respectively, exhibited weak but distinct 2-^{18}O$^{13}CH_3$ and 5-^{18}O$^{13}CH_3$ signals; these were shifted to a slightly higher field compared to the large 2-^{16}O$^{13}CH_3$ ($^1\Delta\delta^{18}O(^{13}C) = -29$ ppb) and 5-^{16}O$^{13}CH_3$ signals ($^1\Delta\delta^{18}O(^{13}C) = -25$ ppb) (Fig. 4, a and b). The Δδ values are in the order of magnitude of α-induced isotope shifts (Risley and van Etten, 1990). ^{18}O-induced ^{13}C NMR shifts of the same magnitude were also observed for C-2 and C-5 of compound **1b** after administering [6-^{13}C]DAH-I and [6-^{13}C]DAH-II (Fig. 4, c and d). These results demonstrated that the two hydroxyl groups at C-2 and C-5 of **1a/b** are derived from atmospheric oxygen. The sequence of oxygen incorporation, however, remained unknown because the ^{13}C NMR spectra suggested that the occurrence of ^{18}O in positions 2 and 5 seems to be independent of the administered precursor (Fig. 4). The reason that ^{18}O appeared to be attached to C-2 and C-5, regardless of the administered precursor, is that NMR of isotopologue mixtures does not necessarily distinguish between individual isotopologues, i.e.,

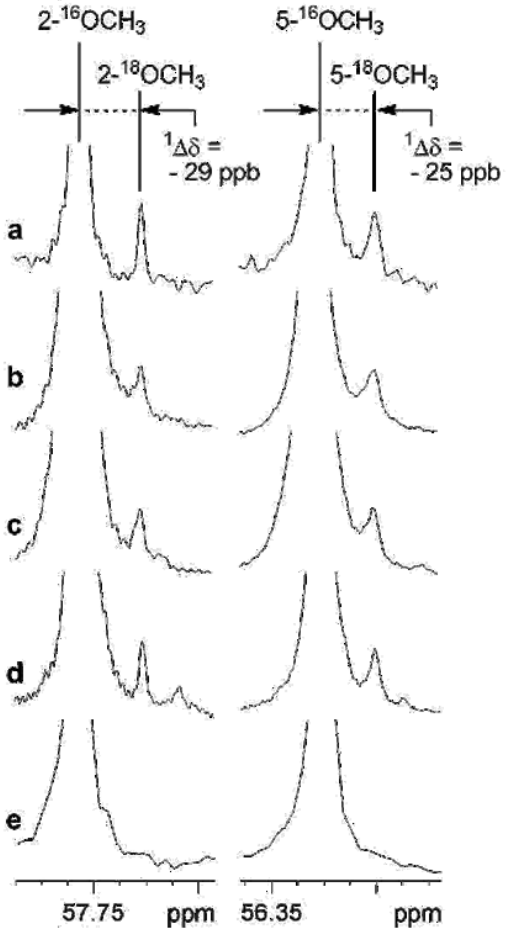

Fig. 4. Partial ^{13}C NMR spectra (125 MHz, acetone-d_6, regions of *O*-methyl signals) of compound **1b** prepared from **1a** by *O*-methylation using $^{13}CH_2N_2$ (99% ^{13}C). Samples of compound **1a** were obtained from *W. thyrsiflora* root cultures incubated in an atmosphere of $^{18}O_2$ and supplemented with ^{13}C-labelled precursors: (a) [2-^{13}C]Phe, (b) [2-^{13}C]CA, (c) [6-^{13}C]DAH-I, (d) [6-^{13}C]DAH-II. Spectrum (e) was recorded from unlabelled **1b** (reference).

it was not always evident from the NMR spectra whether the label belongs to the same or different isotopologues. This was the case because heavy isotopes used for labelling did not show isotope-induced shifts (e.g. 2-^{18}O and 5-^{13}C) or interact through spin–spin coupling (^{13}C-5 and ^{13}C-8) if they were located in remote positions.

Furthermore, differences in the uptake and transportation of precursors, pool size perturbation (Munde et al., 2011), and the low accuracy with which small $^{18}O^{13}CH_3$ signals versus large $^{16}O^{13}CH_3$ signals in the ^{13}C NMR spectra were integrated also made it difficult to quantify isotopologues and understand the sequence of ^{18}O incorporation. Moreover, ^{18}O-induced shifts were not observed for C-1 (in **1a/b** substituted with *O*-allophanyl-glc) and C-6 (C = O) because *O*-methylation with $^{13}CH_2N_2$ was impossible in these positions. Thus, NMR-based quantitative isotopologue analysis was supplemented by mass spectrometry, especially to determine $^{13}C/^{18}O$-labelled isotopologues.

According to the NMR spectroscopic results, the incorporation of ^{13}C from labelled precursors and ^{18}O from the gas phase (Fig. 4) into the allophanyl glucoside **1a** was low, suggesting large proportions of unlabelled and singly labelled (^{18}O or ^{13}C) isotopologues. This was confirmed by analysis of HRESIMS data (Table 2) of the di-O$^{13}CH_3$ derivative **1b** of the biosynthetically obtained allophanyl glucoside **1a**. Approximately 76% to 78% of the target molecules accounted for the isotopologues **1bA** and another approximately 20% were natural abundance isotopologues, mainly due to 1.1% ^{13}C in non-enriched positions of the molecule (not shown in Table 2). In addition to isotopologue **1bA** containing ^{13}C only in the diazomethane-derived *O*-methyl groups, isotopologue groups **B – H** were identified in the case of compound **1b**.

The isotopologues of group **1bB** contained one additional ^{13}C either at C-5 or C-8 but did not incorporate ^{18}O and therefore were not useful for studying oxygenation. Unlike **1bB**, the isotopologues **1bC**, **1bE**, and **1bG** did not contain ^{13}C, except in the diazomethane-derived O$^{13}CH_3$ group, but incorporated one (**1bC**), two (**1bE**), or three ^{18}O atoms (**1bG**), respectively, from the gas phase, demonstrating that the experimental system works. The value of isotopologues containing only ^{18}O for determining the sequence of oxygenation was limited because they were not formed from the ^{13}C-labelled precursors. The isotopologue group **1bH** was also unable to provide new information about the sequence of oxygenation because, except for the carbonyl oxygen at C-6 (which was derived from the carbonyl oxygen of phenylpropanoic acid), ^{16}O atoms of the oxygen functionalities were uniformly substituted by ^{18}O.

Therefore, to understand how the ^{18}O is incorporated, only the isotopologue groups **1bD** and **1bF** had to be considered; these groups possess one ^{13}C atom in the carbon skeleton and either one (**1bD**) or two ^{18}O atoms (**1bF**) in the functional groups. As previously reported (Brand et al., 2006) and confirmed here by means

Table 2
$^{13}C/^{18}O$ Isotopologue composition of labelled **1b** as determined by HRESIMS (positive ion mode) and ^{13}C NMR (125 MHz). Compound **1a** was isolated from root cultures of *W. thyrsiflora* after these were incubated with ^{13}C-labelled precursors ([2-^{13}C]Phe, [2-^{13}C]CA, [6-^{13}C]DAH-I, [6-^{13}C]DAH-II) in an atmosphere of $^{18}O_2$ followed by *O*-methylation with $^{13}CH_2N_2$ to afford **1b**.

Isotopologue							Isotopologue of **1b** obtained from the experiment with							
							[2-^{13}C]Phe		[2-^{13}C]CA		[6-^{13}C]DAH-I		[6-^{13}C]DAH-II	
No.	Molecular composition of aglycone cation					*m/z* $[M+H]^+$ (calcd.)	*m/z* $[M+H]^+$ (found)	Relative abundance (%)[a]	*m/z* $[M+H]^+$ (found)	Relative abundance (%)[a]	*m/z* $[M+H]^+$ (found)	Relative abundance (%)[a]	*m/z* $[M+H]^+$ (found)	Relative abundance (%)[a]
	^{12}C	^{13}C	^{1}H	^{16}O	^{18}O									
1bA	19	2	17	4	0	335.1188	335.1201	78.22	335.1202	78.46	335.1201	76.20	335.1197	76.27
1bB	18	3	17	4	0	336.1222	336.1232	0.55	–	0.00	336.1233	1.22	336.1227	2.06
1bC	19	2	17	3	1	337.1231	337.1254	0.42	337.1256	0.07	337.1256	0.83	337.1252	0.26
1bD	18	3	17	3	1	338.1264	338.1273	0.41	338.1274	0.29	**338.1275**	**0.98**	**338.1269**	**0.42**
1bE	19	2	17	2	2	339.1273	339.1285	0.19	339.1283	0.51	339.1283	0.46	339.1276	0.66
1bF	18	3	17	2	2	340.1307	340.1315	0.33	340.1316	0.28	**340.1314**	**0.21**	–	0.00
1bG	19	2	17	1	3	341.1316	341.1345	0.10	341.1326	0.81	341.1325	0.44	341.1318	0.82
1bH	18	3	17	1	3	342.1349	342.1358	0.11	–	0.00	–	0.00	–	0.00

[a] Isotopologues containing the level of naturally abundant ^{13}C were eliminated.

of analysis of ^{13}C NMR and HSQC spectra (data not shown), ^{13}C from [2-^{13}C]Phe appears at C-5 or C-8. The experiment with [2-^{13}C]CA had similar results, although the formation of [8-^{13}C]-isotopologues was not possible in this case and the ^{13}C-label had to have been located exclusively at C-5. The NMR-spectroscopic detection of ^{18}O in 2-OH and/or 5-OH (Fig. 4) and HRESIMS data (Table 2) in the experiments with [2-^{13}C]Phe and [2-^{13}C]CA did not clarify whether 2-OH or 5-OH comes first, i.e., the introduction of the oxygen functionality at C-2 may occur before or after oxygenation at C-5.

Evidence for the sequence according to which oxygen functionalities are introduced into the phenylphenalenone skeleton came from the administration of diarylheptanoids ([6-^{13}C]DAH-I and -II) and $^{18}O_2$. The ^{13}C labelling of C-6 in the linear seven-carbon-chain of the diarylheptanoids determined that only isotopologues of **1a** with a single ^{13}C atom, namely those at C-8, could be formed, which after O-[^{13}C]methylation using diazomethane results in the di-O$^{13}CH_3$ derivative **1b**. Therefore, ^{18}O incorporation and O-[^{13}C]methylation could result in isotopologues of the subgroups **1bB**, **1bD**, **1bF**, and **1bH**; of these, as noted above, only **1bD** and **1bF** were useful here.

In the experiment with [6-^{13}C]DAH-I, isotopologues of the **1bD** group possess one ^{18}O, which may be attached to C-2 (isotopologue **1bD-2**) or C-5 (isotopologue **1bD-5**). As determined by HRESIMS, the isotopologue **1bD** group was formed more efficiently (relative abundance ~1%; Table 2) than were the other $^{13}C/^{18}O$-labelled isotopologues, **1bF** and **1bH**. Although not fully conclusive, the abundance of **1bD** may suggest that the incorporation of ^{18}O takes place late in the biosynthetic pathway, and it seems unlikely that an α-oxygenated phenylpropanoid (early oxidation) would be used. The occurrence of isotopologue **1bF**, though present in a small quantity (0.21%) in the experiment with DAH-I, confirmed this suggestion. Since 8-^{13}C in **1bF** comes from [6-^{13}C]DAH-I, which has two unlabelled oxygen atoms (^{16}O) that end up at C-1 and C-6 of **1bF**, the two "new" oxygen atoms at C-2 and C-5 must be ^{18}O. This finding rules out the possibility that an α-oxygenated phenylpropanoid is a precursor. Thus, one ^{18}O atom was incorporated from the atmosphere to DAH-I and another ^{18}O atom was incorporated downstream in the pathway (Fig. 5). The product of the hydroxylation of DAH-I is likely DAH-II, a compound that was previously found to be an excellent precursor of phenylphenalenones (Hölscher and Schneider, 1995a).

In addition to resulting in some singly labelled isotopologues, the administration of [6-^{13}C]DAH-II in an ^{18}O atmosphere produced **1bD**, the only $^{13}C/^{18}O$ labelled isotopologue (Table 2). [6-^{13}C]DAH-II was already oxygenated at the positions, which in **1aD** and **1bD** ended up in the carbonyl group (C-6) and in the oxygen functionalities at C-1 and C-2, respectively. Therefore, the simultaneous occurrence of ^{18}O in positions 1, 5, and 6 and ^{13}C in C-8 was impossible. Only the isotopologue [8-^{13}C,5-$^{18}OCH_3$]-**1a** (**1aD-5**), containing ^{18}O at C-5 as the exclusive labelled oxygen, could be formed in the experiment with [6-^{13}C]DAH-II.

The complete amount (0.42%) of **1bD** (Table 2) generated by derivatization with $^{13}CH_2N_2$ was therefore attributed to a single isotopologue [8-^{13}C,5-$^{18}O^{13}CH_3$,2-$^{16}O^{13}CH_3$]-**1** (**1bD-5**). The formation

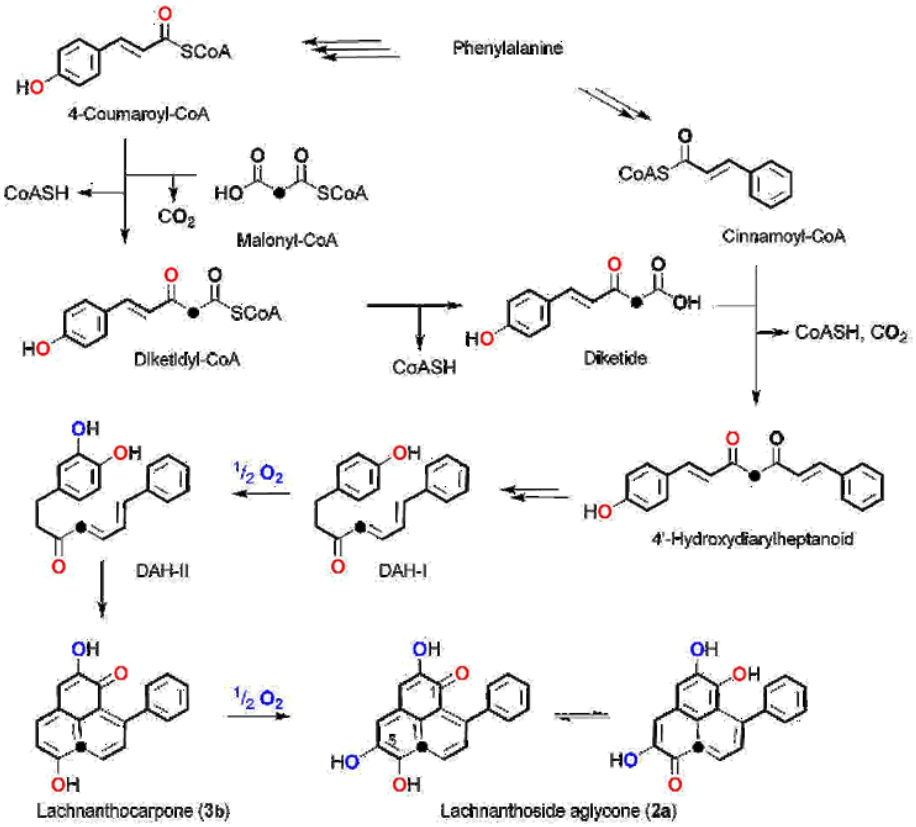

Fig. 5. "Late hydroxylation" biosynthetic pathway of 1,2,5,6-tetraoxygenated phenylphenalenones as evident from $^{18}O/^{13}C$-labelling experiments. The fate of oxygen atoms is coded by color. Oxygen atoms which are suggested to retain from the phenylpropanoid precursor through the entire phenylphenalenone biosynthesis are highlighted in red; lost oxygen atoms are displayed in bold, and oxygen atoms incorporated from O_2 are highlighted in blue. Phenylpropanoid units are marked with bold C–C bonds. ● indicates the origin of the marked atom from C-2 of malonate (Hölscher and Schneider, 1995b).

of isotopologues **1bF** and **1bH** was not possible from [6-^{13}C]DAH-II and indeed was not observed. This result provided evidence that the oxygen atom at C-5 of phenylphenalenones is introduced late in biosynthesis, probably by hydroxylation of lachnanthocarpone (Fig. 5).

In addition to compound **1a**, lachnanthoside aglycone (**2a**) was isolated from root cultures, which were administered with [2-^{13}C]Phe, [2-^{13}C]CA, [6-^{13}C]DAH-I and [6-^{13}C]DAH-II, respectively, and simultaneously incubated under an ^{18}O atmosphere. Again, as observed by ^{13}C NMR and HRESIMS analysis of non-derivatized tautomeric **2a** and its O^{13}CH$_3$-derivatives **2b**, isotope enrichment was low in experiments with all precursors, and the data obtained with [2-^{13}C]Phe, [2-^{13}C]CA, and [6-^{13}C]DAH-I were not conclusive (data not shown). However, ^{13}C/^{18}O-labelled tautomers of lachnanthoside aglycone were detected after the administration of [6-^{13}C]DAH-II and ^{18}O$_2$ and were quantified after *O*-methylation with ^{13}CH$_2$N$_2$ as isotopologues **2bD** (Table 3). The occurrence of ^{18}O in **2bD** from the experiment with [6-^{13}C]DAH-II again indicated the incorporation of the oxygen into position 5 late in biosynthesis (Fig. 5). This confirmed the result, which was found for the allophanyl glucoside **1a** and, after *O*-methylation, for **1b**.

2.4. Administration of [phenyl-^{13}C$_6$]lachanthocarpone

After evidence for late oxygenation at C-5 had been obtained by ^{13}C/^{18}O stable isotope labelling experiments, lachnanthocarpone (**3b**) was considered a good candidate to function as the immediate precursor of the 1,2,5,6-tetraoxygenated phenylphenalenone **2a**. Compound **3b** has been previously reported as a constituent of *W. paniculata* (Edwards, 1974). In order to probe for a precursor–product relationship, [*phenyl*-^{13}C$_6$]lachanthocarpone (**3b**) (Otálvaro et al., 2004) was administered to root cultures of *W. thyrsiflora* as described in Experimental, after which compounds **1a** and **2a** were isolated. The NMR spectrum of **1a** (Fig. 6) showed low but significant ^{13}C enrichment in the lateral phenyl ring. The enhancement of the

Table 3
^{13}C/^{18}O Isotopologue composition of the tri-O^{13}CH$_3$ derivatives **2b** was determined by HRESIMS (positive ion mode) and ^{13}C NMR (125 MHz). Lachnanthoside aglycone (**2a**) was isolated from the root cultures of *W. thyrsiflora* after these were incubated with [6-^{13}C]DAH-II in an atmosphere of ^{18}O$_2$ followed by *O*-methylation with ^{13}CH$_2$N$_2$ to afford two derivatives of **2b**.

Isotopologue							Isotopologues of **2b** obtained from the experiment with [6-^{13}C]DAH-II			
							Tri-O^{13}CH$_3$ derivative 1 (1-OH, 6-C = O)		Tri-O^{13}CH$_3$ derivative 2 (1-C = O, 6-OH)	
No.	Molecular composition of molecular cation[a]					*m/z* [M + H]$^+$ (calcd.)	*m/z* [M + H]$^+$ (found)	Relative abundance (%)[b]	*m/z* [M + H]$^+$ (found)	Relative abundance (%)[b]
	^{12}C	^{13}C	^{1}H	^{16}O	^{18}O					
2bA	19	3	18	4	0	372.1204	372.1208	78.67	372.1205	78.49
2bB	18	4	18	4	0	373.1237	373.1238	0.76	373.1235	0.77
2bC	19	3	18	3	1	374.1247	374.1258	0.53	374.1255	0.77
2bD	18	4	18	3	1	375.1279	**375.1278**	**0.20**	**375.1276**	**0.10**
2bE	19	3	18	2	2	376.1288	376.1288	0.15	376.1282	0.18

Isotopologue groups **2bF** (^{12}C$_{18}$^{13}C$_4$^{1}H$_{18}$^{16}O$_2$^{18}O$_2$Na$^+$) and **2bG** (^{12}C$_{19}$^{13}C$_3$^{1}H$_{18}$^{16}O$_2$^{16}O$_2$Na$^+$) were not detected.
[a] Molecular ions were observed as sodium adducts.
[b] Isotopologues containing the level of naturally abundant ^{13}C were eliminated.

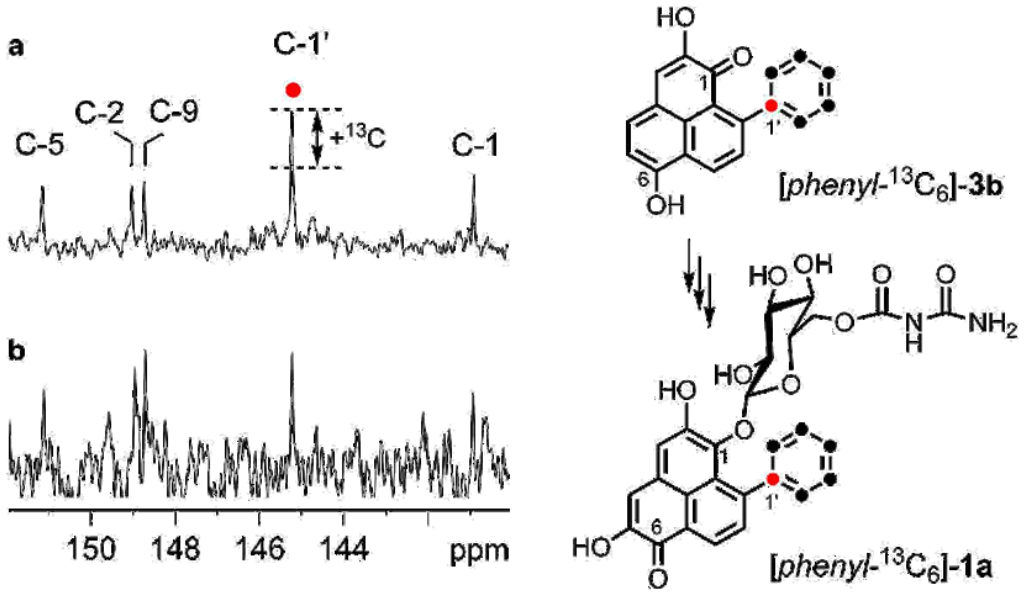

Fig. 6. Partial ^{13}C NMR spectra (125 MHz, acetone-d_6, region of quaternary carbon signals) of **1a** obtained from *W. thyrsiflora* fed with (a) [*phenyl*-^{13}C$_6$]lachnanthocarpone (**3b**). The spectrum shows an enhanced signal for C-1', indicating that ^{13}C was incorporated from the labelled precursor. Spectrum (b) was recorded from unlabelled **1a** (reference). For the numbering of carbon atoms, see also the legend for Fig 1. Red dot: positions enriched with ^{13}C, corresponding signal of [*phenyl*-^{13}C$_6$]**1a** shown in spectrum (a). Black dots: positions enriched with ^{13}C (signals not shown in ^{13}C NMR spectra).

^{13}C NMR signal of the quaternary C-1 in the spectrum (a) compared to the corresponding signal in spectrum (b) of the non-labelled reference indicates ^{13}C-enrichment of this particular carbon atom. The signals of other phenyl carbon atoms of **1a** (C-2'-C-6') (not shown) were enriched as well but are less descriptive due to overlap with other ^{13}C resonances, signal broadening, and magnetic inequivalence (Opitz et al., 2002). In addition to ^{13}C NMR, HRESIMS indicated $^{13}C_6$-labelled isotopologues of **1a** ($[C_{21}{}^{13}C_6H_{25}O_{11}N_2]^+$, found: 559.1654, calcd: 559.1537), confirming labelling of the lateral phenyl ring. The ^{13}C enrichment of 2.0% is in the same order of magnitude as determined by ^{13}C NMR (Fig. 6). HRESIMS also established biosynthetic $^{13}C_6$-labelling of lachnanthoside aglycone (**2a**) (2.0% ^{13}C enrichment, $[C_{13}{}^{13}C_6H_{13}O_4]^+$, found: 311.1006, calcd: 311.1015) from [*phenyl*–$^{13}C_6$]lachnanthocarpone (**3b**) as a precursor. Unfortunately the amount of **2a** was insufficient for recording a ^{13}C NMR spectrum.

3. Discussion

Recombinant *W. thyrsiflora* polyketide synthase 1 (WtPKS1) accepts a wide variety of aromatic and aliphatic starter CoA esters, including phenylpropionyl–CoA and side-chain unsaturated phenylpropanoyl–CoA. This substrate specificity is consistent with the occurrence of 2-hydroxy-9-phenylphenalen-1-one (anigorufone **3a**) and its 2-*O*-methyl derivative (methoxyanigorufone), which in addition to other Haemodoracae, also occur in *W. thyrsiflora* (Fang et al., 2011). However, the most abundant constitutive phenylphenalones of whole plants and cultured roots of *W. thyrsiflora* not only contain the 1-keto-2-hydroxy motif, which is typical of simple phenylphenalenones, but are also oxygenated in additional positions. According to the occurrence of such 1,2,5,6-tetraoxygenated phenylphenalenones and the availability of root cultures, *W. thyrsiflora* was used to investigate the biosynthetic origin of the oxygen functionalities in the tricyclic phenalenone part of phenylphenalenones.

The administration of [1-^{13}C]phenylalanine to *A. preissii* root cultures has demonstrated (Opitz and Schneider, 2003) that the carbon atoms C-6 and C-7 (using the numbering scheme shown in Fig. 1) of phenylphenalenones are derived from C-1 of the phenylpropanoid precursors, and, although this has not been examined experimentally, it is very likely that the carbonyl in position 6 of 1,2,5,6-tetraoxygenated phenylphenalenones comes from the carboxyl group of the precursor forming the A/B ring. Moreover, the carbonyl oxygen atom of 9-phenylphenalenones (e.g. anigorufone **3a**) is derived from the hydroxyl group of 4-coumaroyl–CoA (Munde et al., 2011) as is the oxygen at C-1 of 1,2,5,6-tetraoxygenated phenylphenalenones (e.g. **1a**). Unlike the oxygen atoms at C-1 and C-6, the hydroxyl groups at C-2 and C-5 of compounds **1a** (and **2a**) do not come from the usual phenylpropanoid precursor, 4-coumaroyl–CoA. The introduction of the 2-OH group of anigorufone **3a** from atmospheric oxygen at the stage of DAH-I was established from $^{13}C/^{18}O$-labelling experiments with root cultures of *A. preissii* (Munde et al., 2011). Our results confirm that the 2-OH of 1,2,5,6-tetraoxygenated phenylphenalenones was also inserted at the stage of DAH-I.

Two pathways, an early and a late oxygenation pathway, for understanding the introduction of the oxygen atom at C-5 seemed possible. According to one, this oxygen could be introduced early in the biosynthesis as a unit with an α-oxygenated phenylpropanoid (Fig. 2). 3-(4-Hydroxyphenyl)pyruvic acid or 3-(4-hydroxyphenyl)lactic acid are putative intermediates of this pathway, and the activated esters, e.g. 3-(4-hydroxyphenyl)lactoyl–CoA, could be substrates of the PKS type III enzyme catalyzing the condensation with malonyl–CoA. WtPKS1 was an excellent candidate enzyme for this reaction because it shows broad substrate specificity and, among other starter substrates, also accepted phenylpyruvoyl–CoA, although the hydroxylated pyrone was produced instead of a diarylheptanoid *in vitro* (Brand et al., 2006). Indeed, α-oxygenated 4-hydroxyphenylpropanoids were accepted by WtPKS1, which is the first report of utilization of such substrates by PKS type III enzymes (Fig. 3). However, labelling experiments did not confirm the origin of the oxygen at C-5 from such substrates.

An alternative biosynthetic possibility was that not only the oxygen at C-2 of phenylphenalenones but also the oxygen at C-5 could be introduced at the stage of diarylheptanoids, more specifically to C-2 of the linear carbon chain of DAH-II. However, the question whether the oxygen ending up at C-5 of **1a** is introduced at the stage of DAH-II or further downstream in biosynthesis, after cyclization had yielded the phenalenone tricycle, finally was determined by administering [*phenyl*–$^{13}C_6$]lachnanthocarpone (**3b**) to root cultures of *W. thyrsiflora*. The incorporation of **3b** into lachnanthoside aglycone (**2a**) and its allophanyl glucoside **1a** proved conclusively that the hydroxylation at C-5 of the phenylphenalenone skeleton was the final step of the biosynthesis of 1,2,5,6-tetraoxygenated phenylphenalenones. However, formation of tetraoxygenated phenylphenalenones through additional routes cannot be excluded from this experiment.

The relatively low isotopic enrichment of **1a** and **2a** from atmospheric ^{18}O and ^{13}C-labelled precursors suggests the slow biosynthetic flux into phenylphenalenones in *W. thyrsiflora*. This seems to be a consequence of the constitutive character of the target compounds. Unlike the formation of anigorufone and methoxyanigorufone, the biosynthesis of compounds **1a** and **2a** is not inducible in *W. thyrsiflora* (Schüler et al., 2004; Brand et al., 2006), and the major proportion of these compounds is already present in the root cultures before incubation with labelled compounds starts. In order to detect low isotope enrichment with ^{18}O, the recently reported approach (Munde et al., 2011) of attaching O-$^{13}CH_3$ groups to the hydroxyl functionalities of phenylphenalenones by means of $^{13}CH_2N_2$, followed by recording isotope-induced ^{13}C NMR shifts of the obtained O-$^{13}CH_3$ derivatives, was used. In addition, HRESIMS was employed for isotopologue analysis. The synthesis of the substrates and labeled precursors has been reported in the Experimental and of [*phenyl*–$^{13}C_6$]lachnanthocarpone by Otálvaro et al. (2004).

4. Conclusions

The present work extends previously reported results on the biosynthetic origin of the oxygen functionalities of phenylphenalenones (Fig. 7). $^{13}C/^{18}O$ labelling together with sensitivity-enhanced NMR detection of isotope-induced chemical shift changes of $^{13}CH_2N_2$-derived O$^{13}CH_3$ groups and HRESIMS-based isotopologue analysis have been used successfully to probe the origin of oxygen functionalities and the biosynthetic sequence according to which oxygen functionalities are introduced to the polyoxygenated phenylphenalenone scaffold in root cultures of *W. thyrsiflora*.

The oxygen atoms, except those at C-6, of 1,2,5,6-tetraoxygenated phenylphenalenones were incorporated from atmospheric oxygen at different biosynthetic stages. The oxygen atoms ending up in C-1 and C-6 are incorporated together with the 4-coumaroyl unit (Fig. 7, panel b). Thereafter, the hydroxyl group in position 2 is introduced at the stage of DAH-I (Fig. 5). Isotope labelling experiments showed that the hydroxyl group in position 5 is introduced late in phenylphenalenone biosynthesis, at the stage of lachnanthocarpone (**3b**). Thus, not only the 4-coumaroyl–CoA-derived oxygen at C-1, which is introduced by cinnamate-4-hydroxylase, but also the oxygen atoms at C-2 and C-5 of the phenalenone tricycle are suggested to be the result of monooxygenase-catalyzed reactions. From the data obtained, the "late hydroxylation"

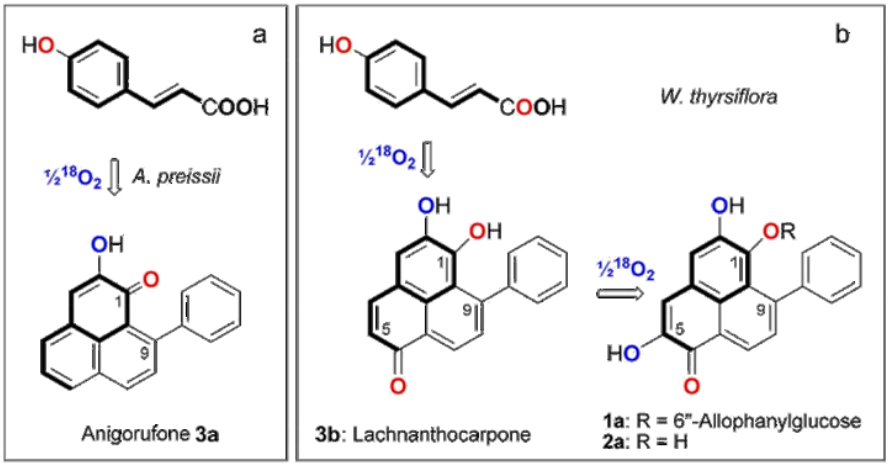

Fig. 7. Origin of oxygen atoms in anigorufone in root cultures of *A. preissii* (Munde et al., 2011) and compound **1a** in root cultures of *W. thyrsiflora*. The hydroxyl group at C-2 of **1a** is incorporated at the stage of linear diarylheptanoids (**DAH-I**) before the hydroxyl group at C-5, which is introduced into lachnanthocarpone (**3**). The fate of oxygen atoms is coded by color. Oxygen atoms which are retained from 4-coumaric acid are highlighted in red; oxygen atoms lost during phenylphenalenone biosynthesis are displayed in bold, and oxygen atoms incorporated from $^{18}O_2$ are highlighted in blue. The 4-coumaroyl unit is marked with bold C–C bonds.

pathway, as shown in Fig. 5, was concluded for 1,2,5,6-tetraoxygenated phenylphenalenones.

5. Experimental

5.1. General experimental procedures

^{1}H NMR and ^{13}C NMR of samples from biosynthetic incorporation experiments were measured on a Bruker AV 500 spectrometer (Bruker, Rheinstetten, Germany) equipped with a 5 mm TCI CryoProbe™. The Bruker pulse sequence zgpg30 (power-gated decoupling; 30° flip angle; relaxation delay 2 s) was used for recording ^{13}C spectra. A Bruker DRX 500 and a Bruker AV 400 NMR spectrometer were used to measure NMR spectra of synthetic phenylpropanoic acids and NAC diketide thioesters. Acetone-d_6, MeOH-d_4 and $CDCl_3$ were used as NMR solvents. Chemical shifts are given in δ values. Tetramethylsilane (TMS) was used as an internal standard for referencing ^{1}H and ^{13}C NMR spectra.

The LC-MS/MS system used for HRESIMS measurements consisted of an Ultimate3000 series RSLC (Dionex) system and an LTQ-Orbitrap XL mass spectrometer (Thermo Fisher Scientific, Bremen, Germany). UPLC was performed using an Acclaim C18 column (150 × 2.1 mm, 2.2 µm, Dionex, Germany) at a constant flow rate of 300 µL min^{-1} using a binary solvent system: Solvent A, H_2O with 0.1% HCOOH and solvent B, MeCN with 0.1% HCOOH. The UPLC gradient system started with 20% B and increased linearly to 95% B in 6 min; from there it was held for 4 min, then brought back to the initial conditions and held for 4 more min in order to re-equilibrate the column for the next injection. Full-scan mass spectra were generated using 30,000 m/Δm resolving power, and for MS2 (CID) experiments the resolution power was set to 7500 m/Δm. The mass accuracy was better than 3 ppm for MS and MS2 experiments. LCESIMS for substrate incubation with WtPKS1 were obtained using a Micromass Quattro II tandem quadrupole mass spectrometer (Micromass Ltd., Manchester, UK) operating in both positive and negative ion modes. Enzymatic products were separated on a C18-RP column. Details were reported elsewhere (Brand et al., 2006).

Preparative HPLC was performed on a Merck–Hitachi LiChrograph chromatography system (L-6200A gradient pump, L-4250 UV/Vis detector). Flow rate 3.5 ml min^{-1}; UV detection at 254 nm. Semipreparative and analytical HPLC was performed on an Agilent (Palo Alto, CA, USA) series HP1100 (binary pump G1312A; auto sampler G1313A; diode array detector G1315B, 200–700 nm). Flow rate 0.8 ml min^{-1}; monitoring wavelength 254 nm.

5.2. Plant material and culture conditions

Root cultures of *W. thyrsiflora* were established from seeds as previously described for root cultures of *A. preissii* (Hölscher and Schneider, 1997). Sterile cultures were grown in liquid M3 (Murashige and Skoog, 1962) medium (100 ml) in conical flasks (volume 250 ml) on a gyratory shaker (85 rpm) at 23 °C under permanent diffuse light (4.4 µmol m^{-2} s^{-1}) until they reached a fresh mass of up to 40 g. Three days before labelled precursors were administered, the *in vitro*-cultured roots were transferred into fresh medium.

5.3. Synthetic procedures and analytical data

5.3.1. Synthesis of activated ester derivatives

Phenylpropanoyl–CoA esters were prepared according to the method described by Wang et al. (2000), using RP-18 cartridges (LiChrolut®, VWR Darmstadt, Germany) in a modified purification procedure (Beuerle and Pichersky, 2002). 3-(4-Hydroxyphenyl) pyruvic acid and (*R*)- and (*S*)-3-(4-hydroxyphenyl)lactic acids were prepared as described below for the ^{13}C-labelled compounds. The same procedure was used to prepare phenylpyruvic acid, and (*R*)- and (*S*)-phenyl)lactic acids. To synthesize the *N*-acetyl cysteamine derivatives, the corresponding acid (cinnamic acid, phenylpropionic acid, phenylpyruvic acid, 3-(4-hydroxyphenyl)pyruvic acid, (*R*)- and (*S*)-phenyllactic acid, (*R*)- and (*S*)-3-(4-hydroxyphenyl)lactic acid) was dissolved in CH_3CN. Dicyclohexyl-carbodiimide, *N*-hydroxy-1,2,3-benzotriazole (both equimolar) and *N*-acetylcysteamine (in threefold molar excess) were added and the mixture was stirred overnight. The yield after purification by preparative HPLC was 82% for phenylpropionyl–NAC and up to 67% for *R*- and *S*-phenyl lactoyl–NAC's and phenylpyruvoyl–NAC. The 4-hydroxyphenyllactic and -pyruvic acids were protected using the tetrahydropyranyl group (Parham and Anderson, 1948). Pyridinium 4-toluenesulfonate (5 mg, 4 d, 5 ml THF) was used for deprotection. In the latter

case the total yields were very low (1%) but still more than sufficient for the enzyme assays.

5.3.2. Analytical data of N-acetyl cysteamine derivatives

Cinnamoyl-*N*-acetylcysteamine. ^{1}H NMR (500 MHz, MeOH-d_4): δ 7.63 (1H, d, J = 15.9 Hz), 7.63 (2H, m, H-2/6), 7.41 (3H, m, H-3/5, H-4), 6.87 (1H, d, J = 15.9 Hz, H-8), 3.39 (2H, t, J = 6.7 Hz, H-12), 3.13 (2H, t, J = 6.7 Hz, H-11), 1.93 (3H, s, C-15).

Phenylpropionyl-*N*-acetylcysteamine. ^{1}H NMR (500 MHz, MeOH-d_4): δ 7.25 (2H, m, H-3/5), 7.18 (3H, m, H-2/6, H-4), 3.29 (2H, t, J = 6.7 Hz; H-12), 2.98 (2H, t, J = 6.7 Hz, H-11), 2.94 (2H, m, H-8), 2.88 (2H, m, H-7), 1.90 (3H, s, H-15).

Phenylpyruvoyl-*N*-acetylcysteamine. ^{1}H NMR (500 MHz, $CDCl_3$): δ 7.97 (2H, dd, J = 8.0 Hz, 1.5 Hz, H-2/6), 7.60 (1H, dt, J = 8.0 Hz, 1.5 Hz, H-4), 7.47 (2H, t, J = 8.0 Hz, H-3/5), 3.84 (0.8 H, s, H-7, signal intensity reduced due to H/D exchange), 3.54 (2 H, q, H-12), 3.24 (2H, t, J = 6.5 Hz, H-11), 1.98 (3H, s, H-15).

3-(4-Hydroxyphenyl)pyruvoyl-*N*-acetylcysteamine. ^{1}H NMR (500 MHz, acetone-d_6): δ 7.62 (2H, d, J = 8.8 Hz, H-2/6), 6.92 (2H, d, J = 8.8 Hz, H-3/5), 3.36 (2H, dt, J = 6.7, 5.9 Hz, H-12), 3.09 (2H, t, J = 6.7 Hz, H-11), 1.87 (3H, s, H-15). H-7 not detected due to H/D exchange.

(*R*)-Phenyllactoyl-*N*-acetylcysteamine. ^{1}H NMR (500 MHz, $CDCl_3$): δ 7.32 (2H, m, H-3/5), 7.28 (1H, m, H-4), 7.25 (2H, m, H-2/6), 4.49 (1H, dd, J = 7.7, 4.3 Hz, H-8), 3.42 (2H, m, H-12), 3.18 (1H, dd, J = 14.2, 4.3 Hz, H-7a), 3.04 (2H, dt, J = 6.3, 1.5 Hz, H-11), 2.98 (1H, dd, J = 14.2, 7.7 Hz, H-7b) 1.96 (3H, s, H-15).

(*S*)-Phenyllactoyl-*N*-acetylcysteamine. ^{1}H NMR (500 MHz, $CDCl_3$): δ 7.32 (2H, m, H-3/5), 7.28 (1H, m, H-4), 7.25 (2H, m, H-2/6), 4.49 (1H, dd, J = 7.7, 4.3 Hz, H-8), 3.42 (2H, m, H-12), 3.18 (1H, dd, J = 14.2, 4.3 Hz, H-7a), 3.04 (2H, m, H-11), 2.98 (1H, dd, J = 14.2, 7.7 Hz, H-7b) 1.96 (3H, s, H-15).

(*R*)-4-Hydroxyphenyllactoyl-*N*-acetylcysteamine. ^{1}H NMR (500 MHz, acetone-d_6): δ 7.24 (2H, d, J = 8.5 Hz, H-2/6), 6.92 (2H, d, J = 8.5 Hz, H-3/5), 5.45 (1H, dd, J = 8.7, 4.4 Hz, H-8), 3.44 (2H, dt, J = 6.8, 5.8 Hz, H-12), 3.24 (1H, dd, J = 14.2, 4.4 Hz, H-7a), 3.15 (2H, dt, J = 6.8, 2.9 Hz, H-11), 3.11 (1H, dd, J = 14.2, 8.7 Hz, H-7b), 1.86 (3H, s, H-15).

(*S*)-4-Hydroxyphenyllactoyl-*N*-acetylcysteamine. ^{1}H NMR (500 MHz, MeOH-d_4): δ 7.05 (2H, d, J = 8.3 Hz, H-2/6), 6.69 (2H, d, J = 8.3 Hz, H-3/5), 4.25 (1H, dd, J = 8.7, 4.0 Hz, H-8), 3.29 (2H, overlap, H-12), 2.98 (1H, dd, J = 14.2 Hz, 4.0 Hz, H-7a), 2.95 (2H, dt, J = 6.7, 1.9 Hz, H-11), 2.73 (1H, dd, J = 14.2, 8.7 Hz, H-7b), 1.92 (3H, s, H-15).

5.4. Labelled compounds

5.4.1. Origin and synthesis of labelled compounds

[1-^{13}C]L-Phenylalanine (99% ^{13}C) and [2-^{13}C]malonic acid (99% ^{13}C) were purchased from Deutero GmbH (Castellaun, Germany). $^{18}O_2$ (95%) was from EurisoTop (Saarbrücken, Germany). [2,3,4,5,6-^{3}H]L-Phenylalanine, [U-^{14}C]4-coumaric acid, and [2-^{14}C]malonyl–CoA were from Hartmann Analytic (Braunschweig, Germany). [2-^{13}C]4-Coumaric acid (99% ^{13}C) was synthesized from 4-hydroxybenzaldehyde and [2-^{13}C]malonic acid using the Knoevenagel condensation. [2-^{13}C]3-(4-Hydroxyphenyl)pyruvic acid was synthesized under an Ar atmosphere from [2-^{13}C]tyrosine (99% ^{13}C, 0.3 g, 1.6 mmol), dimethylaminopyridine (DMAP, 9.9 mg) and $(CF_3CO)_2O$ TFA, (4 ml, 28.8 mmol) by refluxing for 20 h. After evaporation, the residue was reconstituted with HCl (10 ml, 1%) and stirred for 12 h at room temperature. After 12 h at 4 °C the precipitate was filtered, washed with cold H_2O, and dried over (P_4O_{10}) to obtain the product (0.24 g, 81%). [2-^{13}C](*R*)- and [2-^{13}C](*S*)-3-(4-hydroxyphenyl)lactic acids were prepared from [2-^{13}C]3-(4-hydroxyphenyl)pyruvic acid using (–)-diisopinocampheyl chloroborane [(–)DIP-Cl] and (+)-diisopinocampheyl chloroborane [(+)DIP-Cl], respectively. Et_3N (77 μl, 0.55 mmol) was added at −20 °C to a solution of [2-^{13}C](4-hydroxyphenyl)pyruvic acid (100 mg, 0.55 mmol) in THF (10 ml). After 5 min, a solution of (–)DIP-Cl or (+)DIP-Cl (0.3 g, 0.94 mmol) in THF was added dropwise to the mixture. The solution was stirred for 8 h at room temperature and then quenched with 2 N NaOH (1.2 ml) and H_2O (0.6 ml). The combined aqueous fractions obtained from extraction of the aqueous phase with *t*-butylmethyl ether (2×) and the organic phase with H_2O (2×) were acidified to pH 1 with 2 N HCl and extracted with EtOAc. Evaporation to dryness yielded [2-^{13}C](*R*)-3-(4-hydroxyphenyl)lactic acid (65%) and [2-^{13}C](*S*)-3-(4-hydroxyphenyl)lactic acid (65%), respectively. [6-^{13}C]1-(4-Hydroxyphenyl)-7-phenylhepta-4,6-dien-1-one ([6-^{13}C]DAH-I) and [6-^{13}C]1-(3,4-dihydroxyphenyl)-7-phenylhepta-4,6-dien-1-one ([6-^{13}C]DAH-II) were synthesized according to a previously reported procedure (Baranovsky et al., 2003; Munde et al., 2011). The synthesis of [*phenyl*-$^{13}C_6$]lachnanthocarpone **3b** (99% ^{13}C) was reported previously (Otálvaro et al., 2004).

5.4.2. Analytical data of synthetic labelled compounds

[2-^{13}C]3-(4-Hydroxyphenyl)pyruvic acid. ^{1}H NMR (500 MHz, MeOH-d_4): δ 7.63 (d, J = 8.8 Hz, 2H, H-2'/6'), 6.75 (d, J = 8.8 Hz, 2H, H-3'/5'), 6.44 (d, $^2J_{H\text{-}C}$ = 2.5 Hz, 1H, H-3); ^{13}C NMR (125 MHz, MeOH-d_4): δ 169.1 (C-1), 158.3 (C-4'), 140.1 (C-2, signal enhanced due to ^{13}C enrichment), 132.4 (C-2'/6'), 128.0 (C-1'), 116.2 (C-3'/5'), 112.6 (C-3). EIMS *m/z* (rel. int.): 181 [M$^+$] (16), 135 (20), 107 (100), 77 (17).

[2-^{13}C](*R*)-3-(4-Hydroxyphenyl)lactic acid. ^{1}H NMR (500 MHz, MeOH-d_4): δ 7.08 (d, J = 8.5 Hz, 2H; H-2'/6'), 6.70 (d, J = 8.5 Hz, 2H; H-3'/5'), 4.26 (dd, $^3J_{H\text{-}2\text{-}H\text{-}3b}$ = 7.8 Hz, $^3J_{H\text{-}2\text{-}H\text{-}3a}$ = 4.0 Hz, $^1J_{H\text{-}2\text{-}C\text{-}2}$ = 145.5 Hz, 1H; H-2), 3.01 (dd, $^3J_{H\text{-}3a\text{-}H\text{-}2}$ = 4.0 Hz, $^2J_{H\text{-}3a\text{-}H\text{-}3b}$ = 14.0 Hz, 1H; H-3a), 2.80 (dd, $^3J_{H\text{-}3b\text{-}H\text{-}2}$ = 7.8 Hz, $^2J_{H\text{-}3b\text{-}H\text{-}3a}$ = 14.0 Hz, 1H; H-3b); ^{13}C NMR (125 MHz, MeOH-d_4): δ 174.1 (C-1), 157.1 (C-4'), 131.7 (C-2'/6'), 129.9 (C-1'), 116.1 (C-3'/5'), 74.1 (C-2, signal enhanced due to ^{13}C enrichment), 40.9 (C-3). EIMS *m/z* (rel. int.): 183 [M$^+$] (9), 107 (100), 77 (10).

[2-^{13}C](*S*)-3-(4-Hydroxyphenyl)lactic acid. ^{1}H NMR (400 MHz, MeOH-d_4): δ 7.08 (d, J = 8.5 Hz, 2H; H-2'/6'), 6.70 (d, J = 8.5 Hz, 2H; H-3'/5'), 4.26 (dd, $^3J_{H\text{-}2\text{-}H\text{-}3b}$ = 7.8 Hz, $^3J_{H\text{-}2\text{-}H\text{-}3a}$ = 4.4 Hz, $^1J_{H\text{-}2\text{-}C\text{-}2}$ = 145.5 Hz, 1H; H-2), 3.01 (dd, $^3J_{H\text{-}3a\text{-}H\text{-}2}$ = 4.0 Hz, $^2J_{H\text{-}3a\text{-}C\text{-}3b}$ = 14.0 Hz, 1H; H-3a), 2.80 (dd, $^3J_{H\text{-}3b\text{-}H\text{-}2}$ = 7.8 Hz, $^2J_{H\text{-}3b\text{-}H\text{-}a}$ = 14.0 Hz, 1H; H-3b); ^{13}C NMR (100 MHz, MeOH-d_4): δ 174.9 (C-1), 155.8 (C-4'), 130.3 (C-2'/6'), 128.3 (C-1'), 114.7 (C-3'/5'), 71.8 (C-2, signal enhanced due to ^{13}C enrichment), 39.7 (C-3). EIMS *m/z* (rel. int.): 183 [M$^+$] (13), 107 (100), 77 (5).

5.5. Enzyme assay

Assay conditions were previously reported (Brand et al., 2006). In brief, the phenylpropanoyl starter substrates (50 μM), [2-^{14}C]malonyl–CoA (80 μM, 0.17 kBq nmol^{-1}) and the recombinant WtPKS1 protein (20 μg) (EMBL/DDBJ/GenBank™ database accession number AY727928) were added to the buffer (0.1 M Hepes, pH 6.85; assay volume 100 μl) and incubated for 1 h at 37 °C. Products were extracted with (2 × 200 μl) EtOAc. The combined EtOAc extracts were evaporated, reconstituted in MeOH (20 μl), and analyzed by reversed-phase HPLC using a Supelcosil LC18 column, 250 × 2.1 mm i.d. (Sigma–Aldrich, Taufkirchen, Germany), solvent A: H_2O containing 0.1% TFA, solvent B: MeCN, gradient: 10% to 50% solvent B over 40 min at a flow rate of 0.25 ml min^{-1}. Enzyme products were detected at 280 nm and, after adding scintillation liquid (Ultima-Flo AP, 1 ml min^{-1}, Perkin Elmer), by radioactivity monitoring using a flow scintillation analyzer (Canberra-Packard, Dreieich, Germany). For NMR and MS analysis, the assays were scaled up 10 to 18-fold, with the appropriate amount of unlabelled malonyl–CoA.

5.6. Administration of labelled precursors

The administered amounts of labelled compounds were as follows: [2-^{13}C](*S*)-3-(4-hydroxyphenyl)lactic acid (3.0 mg), [2-^{13}C](*R*)-3-(4-hydroxyphenyl)lactic acid (3.0 mg), [2-^{13}C]-3-(4-hydroxyphenyl)pyruvic acid (3.0 mg), [2-^{13}C]Phe (3.5 mg), [2-^{13}C]CA (2.7 mg), [6-^{13}C]DAH-I (3.5 mg), [6-^{13}C]DAH-II (3.5 mg), and [*phenyl*-$^{13}C_6$]lachnanthocarpone **3b** (2.2 mg). Compounds were administered to *W. thyrsiflora* root cultures (100 ml medium) as an ethanolic solution (1 ml) through a sterile membrane filter. For incubation with $^{18}O_2$, the conical flask containing the root culture was connected through a three-way cock to a vacuum pump and an $^{18}O_2$ reservoir. The normal atmosphere was removed from the incubation flask under vacuum (72 mbar) and $^{18}O_2$ filled from the scaled reservoir. The incubation flask was also connected to a tube containing NaOH for trapping metabolically formed CO_2 from cultured roots. The incubation time was 4–5 days except in the $^{18}O_2$ incubation experiments (7 days) under continuous shaking (85 rpm). The administration of radio-labelled [2,3,4, 5,6-^{3}H]Phe (1.5 mg, 0.37 kBq) and [U-^{14}C]CA (1.5 mg, 0.34 kBq) in absorption experiments was carried out under conditions otherwise identical to experiments using stable isotope labelling.

5.7. Extraction, purification and derivatization of compounds 1a and 2a

Cultured roots were taken from the medium, shock-frozen by liquid nitrogen, ground, and extracted with MeOH at room temperature. The extract was evaporated to dryness (<40 °C), and the residue subjected to liquid–liquid separation between *n*-hexane–H_2O, CH_2Cl_2–H_2O and EtOAc–H_2O. The organic phases were subjected to preparative HPLC on a LiChrospher RP18 column (10 μm, 250 × 10 mm). A linear gradient MeCN–H_2O from 10% to 50% MeCN in 40 min (method a) and MeCN–H_2O (0.1% TFA in H_2O), 30% to 75% MeCN in 35 min (method b) was used. Pure **1a** and **2a** were obtained from the CH_2Cl_2 and ethyl acetate extracts at R_t 13.0 min (method a) and R_t 16.0 min (method b), respectively. The pure products **1a** and **2a** were analyzed by NMR and HRESIMS. Compounds obtained from $^{12}C/^{18}O$ double-labelling experiments were methylated using an ethereal solution of [^{13}C]diazomethane, which was prepared from *N*-[^{13}C]methyl-*N*-nitroso-*p*-toluenesulfonamide using a standard procedure. Semipreparative HPLC on a LiChrospher RP18 column (5 μm, 250 × 10 mm) was used to purify the *O*-methyl derivatives **1b** and **2b**. Method c: linear gradient MeCN–H_2O (0.1% TFA) from 40% to 60% MeCN in 20 min and method d: linear gradient MeCN–H_2O (0.1% TFA) from 40% to 75% MeCN in 30 min were used. Pure **1b** was obtained with method c at R_t 15.7 min and two *O*-methyl derivatives **2b** with method d at R_t 13.4 and 13.8 min.

5.8. Analytical data of biosynthetic products and their O-methyl derivatives

6-*O*-[(6''-*O*-Allophanyl)-β-D-glucopyranosyl]-2,5-dihydroxy-7-phenylphenalen-1-one (**1a**): HPLC (method a): UV (MeCN–H_2O) λ_{max} 211, 279, 378, 477 nm; ^{1}H NMR (500 MHz, MeOH-d_4): δ 2.36 (dd, *J* = 7.9, 9.0 Hz, 1H, H-2''), 3.04 (dd, *J* = 9.0, 9.3 Hz, 1H, H-4''), 3.09 (ddd, *J* = 2.2, 6.5, 9.0 Hz, 1H, H-5''), 3.19 (dd, *J* = 9.0, 9.3 Hz, 1H, H-3''), 3.96 (dd, *J* = 2.2, 11.8 Hz, 1H, H-6''b), 4.18 (dd, *J* = 6.5, 11.8 Hz, 1H, H-6''a), 4.67 (d, *J* = 7.9 Hz, 1H, H-1''), 7.04 (s, 1H, H-3), 7.22 (br, 1H, H-5'), 7.33 (br, 2H, H-4', H-2''), 7.39 (br, 1H, H-6'), 7.43 (br, 1H, H-3'), 7.46 (s, 1H, H-4), 7.54 (d, *J* = 7.6 Hz, 1H, H-8), 8.47 (d, *J* = 7.6 Hz, 1H, H-9); ^{13}C NMR (125 MHz, MeOH-d_4): δ 64.9 (C-6''), 71.1 (C-4''), 74.6 (C-2''), 75.2 (C-5''), 77.6 (C-3''), 104.1 (C-1'') 116.3 (C-3), 121.7 (C-9b), 124.2 (C-4), 127.3 (C-2'), 127.8 (C-6[a], C-4') 128.3 (C-6'), 128.5 (C-3a), 128.6 (C-9), 130.0 (C-9a), 130.7 (C-3'), 131.8 (C-5'), 132.3 (C-8), 141.0 (C-6), 145.3 (C-1'), 148.8 (C-7), 149.0 (C-5), 151.2 (C-2), 169.3 (C-1'''), 171.5 (C-2'''), 182.2 (C-1). Please note different carbon atom numbering of **1a** in the text and figures.

2,5,6-Trihydroxy-9-phenylphenalen-1-one (**2a**): HPLC (gradient b): UV (MeCN–H_2O) λ_{max} 208, 278, 374 nm; ^{1}H NMR (500 MHz, acetone-d_6): δ 7.36 (s, 1H, H-3), 7.38–7.44 (m, 5H, H-2' to H-6'), 7.54 (d, *J* = 8.2 Hz, 1H, H-8), 7.84 (s, 1H, H-4), 8.66 (d, *J* = 8.2 Hz, 1H, H-9); ^{13}C NMR (125 MHz, acetone-d_6): δ 112.9 (C-3), 118.4 (C-3a), 120.7 (C-9b), 122.7 (C-4), 125.4 (C-9a), 126.9 (C-4'), 128.2 (C-3'/5'), 129.1 (C-2'/6'), 129.2 (C-9), 129.9 (C-6a), 130.6 (C-8), 139.0 (C-6), 144.2 (C-1'), 147.3 (C-7), 149.0 (C-5), 150.7 (C-2), 178.4 (C-1).

[2,5-di-O^{13}CH$_3$]6-*O*-[(6''-*O*-Allophanyl)-β-D-glucopyranosyl]-2,5-methoxy-7-phenylphenalen-1-one (**1b**): HPLC (gradient c): UV (MeCN–H_2O) λ_{max} 201, 279, 374 nm; ^{1}H NMR (500 MHz, MeOH-d_4): δ 2.05 (dd, *J* = 7.7, 9.3 Hz, 1H, H-2''), 2.97 (ddd, *J* = 2.3, 5.6, 9.7 Hz, 1H, H-5''), 3.03 (dd, *J* = 8.7, 9.7 Hz, 1H, H-4''), 3.21 (dd, *J* = 8.7, 9.3 Hz, 1H, H-3''), 3.45 (dd, *J* = 5.6, 11.9 Hz, 1H, H-6''a), 3.60 (dd, *J* = 2.3, 11.9 Hz, 1H, H-6''b), 3.99 (s, $^1J_{H-C}$ = 145.0 Hz, 3H, 2-O^{13}*CH*$_3$), 4.05 (s, $^1J_{H-C}$ = 145.0 Hz, 3H, 5-O^{13}*CH*$_3$), 5.11 (d, *J* = 7.7 Hz, 1H, H-1''), 7.29 (s, 1H, H-3), 7.32 (br, 1H, H-5'), 7.38 (br, 2H, H-2' and H-4'), 7.44 (br, 1H, H-6'), 7.50 (br, 1H, H-3'), 7.55 (d, *J* = 7.6 Hz, 1H, H-8), 7.86 (s, 1H, H-4), 8.56 (d, *J* = 7.6 Hz, 1H, H-9); ^{13}C NMR (125 MHz, MeOH-d_4): δ 56.31 (2-^{18}O^{13}CH$_3$, $^1\Delta\delta$ ^{18}O(^{13}C)=−25 ppb), 56.34 (2-^{16}O^{13}CH$_3$), 57.73 (5-^{18}O^{13}CH$_3$, $^1\Delta\delta$ ^{18}O(^{13}C)=−29 ppb), 57.76 (5-^{16}O^{13}CH$_3$), 62.8 (C-6''), 71.5 (C-4''), 74.6 (C-2''), 77.8 (C-5''), 78.2 (C-3''), 103.0 (C-1''), 115.6 (C-3), 121.4 (C-9b), 122.3 (C-4), 126.6 (C-3a), 128.0 (C-6a, C-2', C-4'), 128.6 (C-9), 128.9 (C-6'), 129.5 (C-9a), 129.7 (C-3'), 130.3 (C-5'), 132.6 (C-8), 143.6 (C-6), 145.8 (C-1'), 149.7 (C-7), 151.4 (C-5), 153.7 (C-2), 169.3 (C-1'''), 171.5 (C-2'''), 179.2 (C-1). Please note different carbon atom numbering of **1b** in the text and figures.

[2,5,6-tri-O^{13}CH$_3$]2,5,6-Trimethoxy-7-phenylphenalen-1-one (**2b**, R_t 13.8 min): HPLC (gradient d): R_t 13.8 min, UV (MeCN–H_2O) λ_{max} 208, 279, 373 nm; ^{1}H NMR (500 MHz, acetone-d_6): δ 3.27 (s, $^1J_{H-C}$ = 144.7 Hz, 3H, 6-O^{13}*CH*$_3$), 3.93 (s, $^1J_{H-C}$ = 144.5 Hz, 3H, 2-O^{13}*CH*$_3$), 4.03 (s, $^1J_{H-C}$ = 144.6 Hz, 3H, 5-O^{13}*CH*$_3$), 7.22 (s, 1H, H-3), 7.39-7.47 (br, 5H, H-2' to H-6'), 7.56 (d, *J* = 7.5 Hz, 1H, H-8), 7.86 (s, 1H, H-4), 8.49 (d, *J* = 8.5 Hz, 1H, H-9); ^{13}C NMR (125 MHz, acetone-d_6): δ 55.7 (2-^{16}O^{13}CH$_3$), 57.2 (5-^{16}O^{13}CH$_3$), 60.64 (6-^{18}O^{13}CH$_3$, $^1\Delta\delta$ ^{18}O(^{13}C)=−28 ppb), 60.67 (6-^{16}O^{13}CH$_3$), 114.1 (C-3), 119.9 (C-4), 121.9 (C-9b), 125.9 (C-3a), 127.2 (C-9a), 127.4 (C-4'), 127.8 (C-3'/C-5'), 128.2 (C-9), 129.3 (C-2'/C-6'), 129.9 (C-6a), 131.3 (C-8), 144.7 (C-1'), 146.9 (C-7), 146.6 (C-6), 151.5 (C-5), 153.4 (C-2), 179.6 (C-1). Please note different carbon atom numbering in the text and figures.

[2,5,6-tri-O^{13}CH$_3$]2,5,6-Trimethoxy-9-phenylphenalen-1-one (**2b**, R_t 13.4 min): HPLC (gradient d): UV (MeCN–H_2O) λ_{max} 209, 277, 374 nm; ^{1}H NMR (500 MHz, acetone-d_6): δ 3.84 (s, $^1J_{H-C}$ = 144.5 Hz, 3H, 2-O^{13}*CH*$_3$), 4.10 (s, $^1J_{H-C}$ = 144.8 Hz, 3H, 6-O^{13}*CH*$_3$), 4.11 (s, $^1J_{H-C}$ = 144.7 Hz, 3H, 5-O^{13}*CH*$_3$), 7.12 (s, 1H, H-3), 7.34 - 7.45 (br, 5H, H-2' to H-6'), 7.56 (d, *J* = 8.5 Hz, 1H, H-8), 7.82 (s, 1H, H-4), 8.52 (d, *J* = 8.5 Hz, 1H, H-7); ^{13}C NMR (125 MHz, acetone-d_6): δ 55.8 (2-^{16}O^{13}CH$_3$), 57.24 (5-^{18}O^{13}CH$_3$, $^1\Delta\delta$ ^{18}O(^{13}C)=−28 ppb), 57.27 (5-^{16}O^{13}CH$_3$), 61.9 (6-^{16}O^{13}CH$_3$), 112.2 (C-3), 119.6 (C-4), 121.9 (C-6b), 126.3 (C-3a), 127.5 (C-4'), 128.4 (C-7), 128.6 (C-6a), 128.8 (C-3'/C-5'), 129.0 (C-2'/C-6'), 129.9 (C-9a), 132.2 (C-8), 144.3 (C-1'), 144.8 (C-6), 145.8 (C-5), 146.5 (C-9), 153.9 (C-2), 179.8 (C-1).

Acknowledgments

The authors thank the Deutsche Forschungsgemeinschaft for financial support, and Emily Wheeler for editorial assistance.

References

Baranovsky, A., Schmitt, B., Fowler, D.J., Schneider, B., 2003. Synthesis of new biosynthetically important diarylheptanoids and their oxa- and fluoro analogues by three different strategies. Synth. Commun. 33, 1019–1045.

Beuerle, T., Pichersky, E., 2002. Enzymatic synthesis and purification of aromatic coenzyme A esters. Arch. Biochem. Biophys. 302, 305–312.

Brand, S., Hölscher, D., Schierhorn, A., Svatoš, A., Schröder, J., Schneider, B., 2006. A type III polyketide synthase from *Wachendorfia thyrsiflora* and its role in diarylheptanoid and phenylphenalenone biosynthesis. Planta 224, 413–428.

Cane, D.E., Prabhakaran, P.C., Tan, W.T., Ott, W.R., 1991. Macrolide biosynthesis. 6. Mechanism of polyketide chain elongation. Tetrahedron Lett. 32, 5457–5460.

Cooke, R.G., Thomas, R.L., 1975. Colouring matters of Australian plants. XVIII. Constituents of *Anigozanthos rufus*. Aust. J. Chem. 28, 1053–1057.

Cooke, R.G., Edwards, J.M., 1980. Naturally occurring phenalenones and related compounds. Prog. Chem. Org. Nat. Prod. 40, 153–190.

DellaGreca, M., Previtera, L., Zarrelli, A., 2008. Revised structures of phenylphenalene derivatives from *Eichhornia crassipes*. Tetrahedron Lett. 49, 3268–3272.

Edwards, J.M., 1974. Phenylphenalenones from *Wachendorfia* species. Phytochemistry 13, 290–291.

Fang, J., Paetz, C., Hölscher, D., Munde, T., Schneider, B., 2011. Phenylphenalenones and related natural products from *Wachendorfia thyrsiflora*. Phytochem. Lett. 4, 203–208.

Gilbert, I.H., Ginty, M., Oneill, J.A., Simpson, T.J., Staunton, J., Willis, C.L., 1995. Synthesis of beta-keto and alpha, beta-unsaturated *N*-acetylcysteamine thioesters. Bioorg. Med. Chem. Lett. 5, 1587–1590.

Hölscher, D., Schneider, B., 1995a. A diarylheptanoid intermediate in the biosynthesis of phenylphenalenones in *Anigozanthos preissii*. J. Chem. Soc. Chem. Commun., 525–526.

Hölscher, D., Schneider, B., 1995b. The biosynthetic origin of the central one-carbon unit of phenylphenalenones in *Anigozanthos preissi*. Nat. Prod. Lett. 7, 177–182.

Hölscher, D., Schneider, B., 1997. Phenylphenalenones from root cultures of *Anigozanthos preissii*. Phytochemistry 45, 87–91.

Hölscher, D., Schneider, B., 1998. Phenylphenalenones from *Ensete ventricosum*. Phytochemistry 49, 2155–2157.

Hölscher, D., Schneider, B., 1999. HPLC-NMR analysis of phenylphenalenones and a stilbene from *Anigozanthos flavidus*. Phytochemistry 50, 155–161.

Hölscher, D., Schneider, B., 2000. Phenalenones from *Strelitzia reginae*. J. Nat. Prod. 63, 1027–1028.

Hölscher, D., Schneider, B., 2005. The biosynthesis of 8-phenylphenalenones from *Eichhornia crassipes* involves a putative aryl migration step. Phytochemistry 66, 59–64.

Jacobs, A., Staunton, J., Sutkowski, A.C., 1991. Aspyrone biosynthesis in *Aspergillus melleus*: identification of the intermediates formed on the polyketide synthase (PKS) in the first chain extension cycle leading to crotonate. J. Chem Soc. Chem. Commun. 16, 1113–1114.

Kamo, T., Kato, N., Hirai, N., Tsuda, M., Fujioka, D., Ohigashi, H., 1998. Phenylphenalenone-type phytoalexins from unripe Bungulan banana fruit. Biosci. Biotechnol. Biochem. 62, 95–101.

Luis, J.G., Fletcher, W.Q., Echeverri, F., Grillo, T.A., 1994. Phenalenone-type phytoalexins from *Musa acuminata*. Synthesis of 4-phenyl-phenalenones. Tetrahedron 50, 10963–10970.

Munde, T., Maddula, R.K., Svatoš, A., Schneider, B., 2011. The biosynthetic origin of oxygen functions in phenylphenalenones of *Anigozanthos preissii* inferred from NMR- and HRMS-based isotopologue analysis. Phytochemistry 72, 49–58.

Murashige, T., Skoog, F., 1962. A revised medium for rapid growth and bioassays with tobacco tissue cultures. Physiol. Plant. 15, 473–497.

Opitz, S., Hölscher, D., Oldham, N.J., Bartram, S., Schneider, B., 2002. Phenylphenalenone-related compounds. Chemotaxonomic markers of the Haemodoraceae from *Xiphidium caeruleum*. J. Nat. Prod. 65, 1122–1130.

Opitz, S., Schneider, B., 2003. Oxidative biosynthesis of phenylbenzoisochromenones from phenylphenalenones. Phytochemistry 62, 307–312.

Otálvaro, F., Nanclares, J., Vásquez, L.E., Quiñónes, W., Echeverri, F., Arango, R., Schneider, B., 2007. Phenalenone-type compounds from *Musa acuminata* var. "Yangambi km 5" (AAA) and their activity against *Mycosphaerella fijiensis*. J. Nat. Prod. 70, 887–890.

Otálvaro, F., Quiñónes, W., Echeverri, F., Schneider, B., 2004. Synthesis of [*phenyl*-$^{13}C_6$]lachnanthocarpone and other ^{13}C-labelled phenylphenalenones. J. Labelled. Compd. Radiopharm. 47, 147–159.

Parham, W.E., Anderson, E.L., 1948. The protection of hydroxyl groups. J. Am. Chem. Soc. 70, 4187–4189.

Pohl, N.L., Gokhale, R.S., Cane, D.E., Khosla, C., 1998. Synthesis and incorporation of an *N*-acetylcysteamine analogue of methylmalonyl-CoA by a modular polyketide synthase. J. Am. Chem. Soc. 120, 11206–11207.

Quiñones, W., Escobar, G., Echeverri, F., Torres, F., Rosero, Y., Arango, V., Cardona, G., Gallego, A., 2000. Synthesis and antifungal activity of Musa phytoalexins and structural analogs. Molecules 5, 974–980.

Risley, J.M., Van Etten, R.L., 1990. Properties and chemical applications of ^{18}O isotopic shifts in ^{13}C and ^{15}N nuclear magnetic resonance spectroscopy. In: Diehl, P., Fluck, E., Günther, H., Kosfeld, R., Seelig, J. (Eds.), Isotope Effects in NMR Spectroscopy. Springer, Berlin, pp. 81–168.

Schmitt, B., Schneider, B., 1999. Dihydrocinnamic acids are involved in the biosynthesis of phenylphenalenones in *Anigozanthos preissii*. Phytochemistry 52, 45–53.

Schmitt, B., Hölscher, D., Schneider, B., 2000. Variability of phenylpropanoid precursors in the biosynthesis of phenylphenalenones in *Anigozanthos preissii*. Phytochemistry 53, 331–337.

Schüler, G., Mithöfer, A., Baldwin, I.T., Berger, S., Ebel, J., Santos, J.G., Herrmann, G., Hölscher, D., Kramell, R., Kutchan, T., Maucher, H., Schneider, B., Stenzel, I., Wasternack, C., Boland, W., 2004. Coronalon: a powerful tool in plant stress physiology. FEBS Lett. 563, 17–22.

Wang, C.Z., Maier, U.H., Zenk, M.H., 2000. Synthesis of 3,3',5-trihydroxybiphenyl-2-carboxylic acid, a component of the bitterest natural product amarogentin and its coenzyme A and *N*-acetyl cysteamine thiol esters. J. Nat. Prod. 63, 371–374.

Chapter 4

Phenylphenalenones protect banana plants from infection by *Mycosphaerella fijiensis* and are deactivated by metabolic conversion

William Hidalgo[1], Jima N. Chandran[1], Riya C. Menezes[1], Felipe Otálvaro[2] and Bernd Schneider[1]*

[1]*Max-Planck Institut für Chemische Ökologie, Beutenberg Campus, Hans-Knöll-Strasse 8, 07745, Jena, Germany*
[2]*Instituto de Química-Universidad de Antioquia, Calle 67# 53-108, A.A. 1226, Medellín, Colombia*

*Corresponding author:
Bernd Schneider
Max-Planck-Institute for Chemical Ecology,
Hans-Knöll-Str. 8,
07745 Jena, Germany
Email: schneider@ice.mpg.de

ABSTRACT

Phenylphenalenones, polycyclic aromatic natural products from some monocotyledonous plants, are known as phytoalexins in banana (*Musa* spp.). In this study, ^{1}H NMR-based metabolomics along with liquid chromatography and mass spectrometry were used to explore the chemical responses of the susceptible 'Williams' and the resistant 'Khai Thong Ruang' *Musa* varieties to the ascomycete fungus *Mycosphaerella fijiensis*, the agent of the Black Leaf Sigatoka Disease. Principal component analysis discriminated strongly between infected and non-infected plant tissue, mainly due to specialized metabolism induced in response to the fungus.

Phenylphenalenones are among the major induced compounds, and the resistance level of the plants was correlated with the progress of the disease. However, a virulent strain of *M. fijiensis* was able to overcome plant resistance by converting phenylphenalenones to sulfate conjugates. Here we report the first metabolic detoxification of fungitoxic phenylphenalenones to evade the chemical defense of *Musa* plants.

Key-words: Musa; *Mycosphaerella fijiensis;* detoxification; metabolomics; phenylphenalenones; sulfate conjugates.

INTRODUCTION

Bananas and plantains constitute the fourth most important staple fruit worldwide with a global production of more than 100 million metric tons in 2012; they rank first among all varieties of fruits produced (Food and Agriculture Organization of the United Nations-FAO 2013; 2015). The revenues from trading these fruits internationally represent an important economical income for several tropical and subtropical developing countries (FAO 2014). However, their production is often affected not only by herbivores such as *Radopholus similis,* which cause the burrowing nematode disease (Chabrier & Queneherve 2003), but also by several pathogens: *Ralstonia solanacearum* (Race 2) causes the Moko's disease (Sequeira 1998); *Fusarium oxysporum* f. sp. *cubense* causes Panama's disease (Ploetz 2006); and the Sigatoka disease complex of banana, involving three related ascomycetous fungi *Mycosphaerella musicola*, *M. eumusae* and *M. fijiensis.* Among these fungi, *M. fijiensis* causes the most detrimental disease in banana, Black Leaf Streak Disease (BLSD) (Arzanlou *et al.* 2007; Etebu & Young-Harry 2011).

Cavendish bananas, belonging to the subgroup AAA, are among the most frequently consumed commercial banana crops due to their sweetness and testability and the nutritional value of the fruit. However, they are highly susceptible to BLSD. Although several efforts have been made to breed *Musa* hybrids resistant to pathogens, the banana fruit for each cultivar type still does not meet consumers' expectations (Heslop-Harrison 2011; Kovacs *et al.* 2013; Perrier, *et al.* 2011; Vishnevetsky *et al.* 2011). Therefore, chemical treatments through the application of

fungicides (such as benomyl, propiconazole and azoxystrobin) remain the most effective method to control this disease. As a consequence of poor agricultural management practices, namely, the blanket application of fungicides to avoid reduction in crop yields by fungal infections, banana plants have developed widespread resistance to fungicides. As a result, such reinforced microbial resistance has brought enormous losses in the commercial banana trade (Etebu & Young-Harry 2011; Martinez-Bolaños *et al.* 2012; Ploetz 2000).

Understanding the physiological responses triggered in resistant *Musa* plants during their interaction with pathogens, especially with *M. fijiensis*, will allow scientists to search for new strategies that can lead towards the control of pests without damaging the environment. Thus, several biochemical traits in *Musa* have been recognized to play a role during the pathogenesis. Among these, strengthened physical barriers through lignin biosynthesis, along with induction of pathogenesis-related (PR) proteins, hypersensitivity response (HR) and production of phytoalexins, constitute the basis for the broad resistance of *Musa* plants to pathogens and herbivores (Dhakshinamoorthy *et al.* 2014; Hölscher *et al.* 2014; Otálvaro et al. 2007; Torres *et al.* 2012; Vaganan *et al.* 2014; Wang *et al.* 2015). Phenylphenalenones, a group of polycyclic aromatic compounds found in Haemodoraceae, Pontederiaceae, Strelitziaceae and Musaceae plant families (Munde *et al.* 2013), act as phytoalexins in the *Musa* genus because they are induced either in the leaves as well in the roots of *Musa* plants that are affected by biotic or abiotic factors. In addition, their strong antimicrobial and nematicidal properties have made them valuable to researchers attempting to explain the chemical basis for the resistance of some cultivars of *Musa* (Hölscher *et al.* 2014; Jitsaeng & Schneider 2010; Quiñones *et al.* 2000).

As some phenylphenalenones have recently been identified at the cellular level in the stomata of *Musa* leaves (Hölscher *et al.* 2015), this experimental system has become attractive for exploring the plant-pathogen interaction in more detail. Furthermore, metabolomic analyses that use Nuclear Magnetic Resonance (NMR) and Mass Spectrometry (MS) have been demonstrated to be powerful tools for analyzing host metabolic pathways that are triggered by pathogens (Ali *et al.* 2009; López-Gresa *et al.* 2010; Parker *et al.* 2009). The research reported in this study aimed to elucidate and explore the metabolic changes behind the *Musa*-*M. fijiensis* interaction, which is correlated with host resistance and pathogen virulence. Thus, chemical

responses from the susceptible 'Williams' (*Musa* spp. AAA group) (Jones 2000) and the resistant 'Khai Thong Ruang' (*Musa* spp. AAA Ibota group) varieties in the interaction with *M. fijiensis*, strain E22 'sensitive' and strain Ca10_13 'tolerant' to the fungicide propiconazole, were probed by using ^{1}H NMR-based metabolomics along with HPLC-DAD analysis.

MATERIALS AND METHODS

Plant material

In vitro plants of *Musa acuminata* var. 'Williams' (AAA, Cavendish subgroup) were provided by Universidad Católica de Oriente – Rio Negro (Antioquía, Colombia) and *in vitro* plants of *Musa acuminata* var. 'Khai Thong Ruang' (AAA, Ibota subgroup) was originally provided by the International Transit Centre (ITC), Bioversity International, Katholieke Universiteit Leuven, Belgium (Leuven, Belgium). Plants were propagated and cultured individually in medium B5Z according to the standard procedures (Banerjee and Delanghe 1985) and maintained at 26°C under 12 h photoperiod conditions until they reached a height of 10-12 cm (4-5 weeks). Plants were further transferred to 10 cm diameter plant pots containing sterile soil of a mixture of KTS (Klasmann-Ton-Substrat) : vermiculite 2-3 mm : sand 0.7-1.2 mm : perlite (in a ratio 2:1:1:2) with fertilizer Oscomote Exact 19-9-12 (333 mg L^{-1} soil), and each plant received a dose of Ferty 3 (0.1%, Planta Düngemittel GmbH Regenstauf, Germany) every week. The plants were maintained in an incubation chamber, Percival Model AR-95HILX (CLF Plant Climatics, Emersacker, Germany) at a temperature of 26/23°C (day/night), 70% humidity and 12 h photoperiod for one month. Then the plants were transferred to 4 L plant pots under the same soil conditions and kept for three months before the infection experiments began.

Fungal organisms

Mycosphaerella fijiensis strains voucher E22 and voucher Ca10_13 were provided by Dr. Gert Kema from the Plant Research International (Wageningen, The Netherlands) and maintained in solid Potato Dextrose Agar medium (PDA, emended with 100 µg mL^{-1} ampicillin), at 25°C under dark conditions for 15 d. They were further cryo-preserved according with the

INIBAP technical guidelines (Carlier 2002) until the inoculum for the infection protocol and bioassays was prepared.

Analytical equipment

1D- and 2D NMR experiments were carried out in a Bruker Avance 500 NMR spectrometer (Bruker Biospin, Karlsruhe, Germany), operating frequency 500.13 MHz for ^{1}H and 125.75 MHz for ^{13}C. A TCI cryoprobe (5 mm) was used to measure spectra at 300 K. Tetramethyl silane (TMS) (0.05%) was used as an internal standard for referencing ^{1}H and ^{13}C NMR spectra unless otherwise indicated. 1D NOESY experiments were performed using a Bruker Avance III HD 700 NMR spectrometer, operating frequency 700 MHz for ^{1}H. A TCI H-C/N-D 1.7 mm microcryoprobe was used to measure spectra at 298 K. NMR spectrometers were controlled with Bruker Topspin v2.1 and v3.2 software for the 500 MHz- and 700 MHz instruments, respectively. Electrospray ionization mass spectra (ESIMS) and LC-ESIMS were recorded on a Bruker Esquire 3000 ion trap mass spectrometer (Bruker Daltonics, Bremen, Germany). HRESIMS was recorded on UHPLC system of the Ultimate 3000 series RSLC (Dionex, Sunnyvale, CA, USA) connected to a LTQ-Orbitrap XL mass spectrometer (Thermo Fisher Scientific, Bremen, Germany). Analytical and semipreparative HPLC was performed on an Agilent series HP1100 (binary pump G1312A; auto sampler G1367A; diode array detector G1315A) (Agilent Technologies, Waldbronn, Germany). The UV spectra were recorded by the diode array detector (DAD) during analytical HPLC. The semipreparative HPLC system was coupled with the fraction collector CHF 122SB ADVANTEC.

Metabolomics analysis

Fungal inoculum preparation. The standard protocol reported by Abadie (Abadie *et al.* 2008) was used with slight modifications. Briefly, *M. fijiensis* strain E22 kept in glycerol (15%) at -80°C was placed in PDA medium and incubated at 25°C under dark conditions for 20 d. Afterwards, the fungal mycelium was cut off from the agar medium and transferred to Petri dishes with sterile V8 juice agar (containing 300 mL of vegetable juice V8, 3g $CaCO_3$, 20 g of agar and 700 mL water) and incubated for 15 d under 12 h photoperiod. Four plugs of fungal

mycelium were cut off from the Petri dish and placed in a Falcon tube (50 mL) containing 25 mL of sterile water for further shaking in a vortex mixer for 2 min followed by ultrasound for 1 min. An aliquot of 2 mL was transferred to Petri dishes with sporulation V8 juice agar (containing 100 mL of vegetable juice V8, 0.2 g $CaCO_3$, 20 g of agar and 900 mL water, pH adjusted at 6.0) and incubated at 25°C under continuous cool white light conditions for 15 d. Sterile water (~ 2 mL x 3) was added to the sporulation culture, and conidia were removed by brushing the colonies' surface with a sterile camel's hair brush. The concentration of conidia was calculated by using a Neubauer chamber and adjusted to a final concentration of $1x10^4$ conidia mL^{-1} with sterile water (containing 0.1% of Tween 20) and used to further inoculate the *Musa* plants.

Artificial mock-inoculation of Musa plants. Three-months-old *Musa acuminata* plants of the susceptible variety 'Williams' and the resistant variety 'Khai Thong Ruang' ('KTR') were used for the infection experiment. A volume of 2 mL of the fungal inoculum was spread on the left-half side of the lower surface (abaxial side) of the second youngest unfolded leaf of each *Musa* plant using a camel's hair brush. The mock-inoculated plants were kept at room temperature (~ 20°C) for 2 h, while the microbial suspension was dried and then returned to the climate chamber under the conditions described above. The relative humidity was initially set at 90% and after the first week of incubation was maintained at 80%. A sterile solution of 0.1% Tween 20 (without fungal inoculum) was spread to *Musa* plants of each variety and used as a control. Four biological replicates of both treated and control *Musa* plants of each variety were used for the study.

Harvesting plant tissue. The infected *Musa* plants of each variety were harvested at 35 days post inoculation (dpi) once the plants developed visual BLSD symptoms on the upper side of the leaf. Four sections of each infected plant were collected as follows (Fig. 2): 1) necrotic plant tissue "sample A"; 2) asymptomatic tissue from the treated half of the leaf "sample B"; 3) healthy tissue from the non-treated half of the infected leaf "sample D" and 4) non-treated leaves from the treated plant "sample E". Plants without fungal treatment were used as a control, "sample C". Each specimen was cut off under visual inspection (using a binocular loupe), immediately frozen in liquid nitrogen and stored in a pre-cooled sterile Eppendorf tube (2 mL lock-safe Eppendorf tubes) until further lyophilized in a freeze drier for 72 h. Ceramic beads (0.7

mm diam.) were added to each tube and the plant material was ground by shaking it for 3 min in a paint shaker (Skandex SO-10M, Sassenheim, The Netherlands). The samples were then stored in a desiccator until they were used for analysis (not longer than 48 h).

Sample preparation for NMR analysis. A protocol established by Kim and coworkers (Kim *et al.* 2010) was adapted with some modifications. Briefly, 25 mg of dried and ground plant specimens were transferred to an Eppendorf tube to which was added 0.8 mL of MeOD-d_4 with 0.2 mL of KH_2PO_4 buffer in D_2O (pH 6.0) containing 0.05% trimethylsilyl propanoic acid (TSP) as internal standard. The solution was vortexed (1 min) and sonicated for 15 min at room temperature followed by a centrifugation step at 13.000 rpm for 15 min. The supernatant (600 µL) was directly transferred to a 5 mm NMR tube for further analysis.

NMR data analysis. ^{1}H NMR spectra were recorded using a standard one-dimensional pulse sequence with water suppression (PURGE), with 256 transients (scans) with 64 k data points and a spectral width of 15 ppm using a 30° flip-angle, a 4.43 s acquisition time, and a recycle delay of 2.0 s. Fourier transformation was applied to cumulative free induction decay (FID) with exponential line broadening of 0.3 Hz. All spectra were manually phased, baseline-corrected and calibrated to TSP (δ 0.0). The ^{1}H NMR spectra were reduced to 1586 sequentially integrated regions ("buckets") of 0.005 ppm width, from δ 0.5-8.7 and the data were scaled to total intensity using AMIX version 3.9.11 software (Bruker BioSpin, Rheinstetten, Germany). Regions from δ 3.32-3.25 and δ 5.0-4.8 were excluded before the bucketing analysis, and the whole dataset was exported as a text file (.txt). Principal component analysis (PCA) of the data was performed with SIMCA-P version 13.0 software (UMETRICS Company, Umeå, Sweden), and eight PCs were processed to meet 96% of the explained variance. Pareto- or unit variance (UV)-scaling was applied to the data before PCA analysis.

Analysis of inducible phenylphenalenones in *Musa* during pathogen attack

Phytochemical analysis of infected Musa *plants.* The crude extract from sample "A" of the variety 'KTR' (42.1 mg) and variety 'Williams' (34.3 mg) 35 dpi with the fungus was used to isolate the major metabolites induced during the pathogenesis. Briefly, the crude extract was

cleaned up by using solid-phase extraction (SPE, Chromabond C18ec-octadecyl modified silica, 500 mg absorbent weight, endcapped, Macherey-Nagel, Düren, Germany) before analysis by HPLC. The methanolic extract after SPE was dried under a stream of nitrogen and redissolved in methanol to a final concentration of 10 mg mL^{-1}. An aliquot of 5 µL of methanolic solution was injected into semipreparative HPLC. Separation was achieved on a Hibar column RP-18e (Purospher STAR, 250-4.6 mm, 5 µm particle size). Water with 0.05% TFA (solvent A) and a mixture of methanol:acetonitrile (1:1) with 0.05% TFA (solvent B) were used as a mobile phase. The elution profile was: 0 min - 0% (B), 60 min - 45% (B), 90-110 min - 65% (B), 115-125 min - 80% (B), 130-140 min - 100% (B). The mobile phase flow rate was 1 mL min^{-1}. Column temperature was maintained at 30°C. A wavelength at 254 nm was used for monitoring the chromatographic traces (HPLC method A). Further purification was carried on a LiChrospher 100 RP-18 column (250x4mm, 5 µm particle size) with water (0.1% TFA) and acetonitrile (solvent B) as a mobile phase. Flow rate of 1 ml min^{-1} and a linear gradient from 0 min (35% B) to 40 min (100% B) was used.

The crude extract of sample "D" (asymptomatic area of infected plant) of the variety 'Williams' (18.2 mg) was processed following the same procedure as described before. Separation of the major compound was achieved by semipreparative HPLC using a LiChrospher 100 RP-18 column (250x4 mm, 5 µm particle size). Water with 0.1% TFA (solvent A) and methanol (solvent B) were used as the mobile phase. The elution gradient was from 0 min (0% B), 12 min (45% B), 17 min (100% B), to 25 min (100% B). Column temperature was kept at 30°C. The monitored wavelength was 254 nm. 1D- and 2D NMR experiments were carried out for the metabolites isolated.

Infection, sample preparation and disease rating. *Musa* plants of both varieties ('Williams' and 'KTR') were raised and treated with the fungus according to the conditions of the infection protocol with the fungus as described above with few modifications. In this case, 5 mL of the fungal inoculum was spread on the whole (abaxial) lower surface of the second youngest unfolded leaf of each *Musa* plant using a camel's hair brush. Three areas of 4x4 cm^2 were randomly traced with a permanent marker (Faber-Castell Multimark 1523 permanent) on the upper surface of the infected leaf for determining the severity of the fungal pathogen over time.

The average number and area of the symptoms were evaluated on the delimited area at 25 and 50 dpi with the fungus in order to determine the progress of the disease. Conidia of *Mycosphaerella fijiensis* strains E22 and Ca10_13, differing in their tolerance to the fungicide propiconazole (Fig. 8), were chosen as infective propagules for both *Musa* varieties in separate experiments. The infected plant tissue (sample A, Fig. 2) was collected and processed as described above. The experimental design consisted of six biological replicates of each plant variety per time assessed. Three plants without fungal inoculation were used as control (5 mL of water with 0.1% Tween 20).

Quantification by HPLC-DAD analysis. 9-Phenylphenalenone was synthesized according to the protocol reported by Otálvaro et al. (Otálvaro et al. 2004) extensively purified by chromatographic techniques (column chromatography, TLC preparative, semipreparative HPLC) up to a purity >98% (UV 254 and 280 nm) and used as internal standard (IS) for quantification of phenylphenalenones. A total of 25 mg of the infected dried and ground tissue was transferred into 0.8 mL methanol with 0.2 mL phosphate buffer and 0.1 mL of a 9-phenylphenalenone solution of 550 ppm (final concentration: 0.05 mg mL^{-1}) for extraction and cleaning procedures as described above, except that a SPE cartridge of 200 mg was used instead of a 500 mg SPE cartridge. The final extract was resuspended in 1 mL of a mixture of methanol:acetonitrile (1:1) and passed through a filter (0.45 µm); the final solution (5 µL) was injected into the HPLC using method A. The average of the peak integral value of three injections from each sample was used for quantification. Calibration curves of the phenylphenalenones and structural analogues (compounds **1-5**, **7**, **9-13**, **15** isolated and in-house synthetic standards, purity > 98% checked by LC-MS, UV 254-280 nm) were generated using six standard solutions of each compound in the range of 0.1-1.5 mM (each solution containing the internal standard at A concentration of 0.05 mg/mL). An aliquot of 5 µL of each standard solution was injected in triplicate into the HPLC using method A. The average area of the peak integral value of each concentration was calculated from the triplicate data, and a linear regression equation was obtained by plotting the peak areas (y) versus the injected amounts (x) of each standard compounds. The linearity for each compound was evaluated by the correlation coefficient ($r^2 \geq 0.9967$). The lower limit of quantification was 0.013 nmol per injection (based on the signal/noise ratio of approximately 10:1 extracted from the HPLC trace at 254 nm). Compounds **6**, **8** and **14** (Table 2) were

quantified based on the relative response factor of hydroxyanigorufone (**5**), since the UV absorption of this compound at 254 nm was very similar to compounds **6**, **8** and **14**. The relative response factor of hydroxyanigorufone (**5**) was 0.5, as calculated relative to the internal standard, 9-phenylphenalenone.

Antifungal bioassay

A microtiter well method developed by Peláez (Peláez 2006) was used with some modifications (Hidalgo *et al.* 2009). Briefly, *M. fijiensis* strains (voucher E22 and Ca10_13) grown for 15-17 days at 26°C±1 in potato dextrose agar – PDA (Fluka Analytical, Steinheim, Germany) was used for preparing the fungal inoculum. Mycelium of the culture was scraped with a smear loop and sterile water, and the dense suspension obtained was then fragmented in a vortex mixer with glass beads of 4±0.3 mm diameter (Carl Roth GmbH Germany) followed by filtration through four layers of sterile cheesecloth to obtain uniform myceliar fragments. The concentration of the inoculum was counted under a light microscope using a Neubauer hematocytometer (Marienfeld, Germany) and adjusted to $2x10^5$ mycelial fragments mL^{-1} with sterile water. Sterile microtiter plates 96 well-F (Sarstedt AG & Co, Germany) were used for the biological incubation. Each well was filled with 50 µL of Sabouraud broth (Fluka Analytical, St. Louis, USA), 50 µL of the fungal inoculum (described above) and 50 µL of the corresponding compound to be assessed. Concentrations ranging from 1 to 100 ppm of each compound were prepared in aqueous dimethyl sulfoxide (12% DMSO, BioReagent for molecular biology, Sigma-Aldrich, ≥99.9%) and passed through a filter (0.1 µm, hydrophilic polyethersulfone membrane sterile, PALL Life Sciences, Ann Arbor, USA) before to be administered to the incubation system. The culture medium (50 µL; Sabouraud), 50 µL of inoculum and 50 µL of aqueous DMSO (12%, sterile) was used as a reference for growth control. Propiconazole (Fluka Analytical, 98.4%) was used as a positive control. The same procedure was applied for the negative control except that the inoculum solution was replaced by sterile water. The microplates were incubated under darkness or a photoperiod for 8 d (logarithmic growth phase of the fungi) at 25°C in an incubation chamber. For the light-controlled experiments, the plates were placed at a distance of 1 m and irradiated by two cool white light tubes (Sylvania luxline Plus T8 36W/840, Großschirma, Germany) during 12 h d^{-1}. Both experiments (darkness and photoperiod)

were carried out simultaneously. The absorbance for the optical density (OD_{595nm}) was recorded by a spectrophotometer (TECAN infinite M200 built it with a multiple reads per well, Crailsheim, Germany) at time 0 and 8 days after incubation in order to measure the mycelia growth. The experimental design consisted of three biological replicates (including three technical replicates). The IC_{50} value was calculated by plotting the mycelial growth (data previously normalized to the reference control) against the logarithm of each concentration of the compound assessed.

Phenylphenalenone metabolism

The antimicrobial activity of phenylphenalenones and derivatives depends on the chemical structure of the compound (Hidalgo *et al.* 2009; Otálvaro *et al.* 2007). In order to test whether the survival of *M. fijiensis* to the incubation with certain phenylphenalenones is in part due to the ability to metabolize or degrade them, an experimental approach was set up including several parameters to be analyzed during *in vitro* interaction the fungal pathogen and the phenylphenalenone. Thus, seven phenylphenalenone-type compounds covering a range from weak to strong antifungal activity against *M. fijiensis* were selected for this analysis. The protocol used for the antifungal bioassay was adapted with some modifications. The fungal inoculum was prepared and adjusted to a final concentration of $3x10^5$ mycelial fragments mL^{-1} in identical conditions as has been described above. Sabouraud broth (600 µL, Fluka Analytical, Germany) with 600 µL of the fungal inoculum and 60 µL of each concentration of the compound to be assessed was incubated in a sterile Eppendorf tube (Safe-Lock tubes, 2.0 mL, Eppendorf, Hamburg-Germany) containing five sterile ceramic beads (0.7 mm diam.). Three solutions of each compound at 210, 420 and 840 ppm were prepared in dimethyl sulfoxide (DMSO, BioReagent for molecular biology, Sigma-Aldrich, ≥99.9%) to achieve a final concentration of 10, 20 and 40 ppm in the incubation system, respectively (maximum concentration of DMSO in the system: 4.7%). Sabouraud broth (600 µL) with 600 µL of the fungal inoculum and 60 µL of DMSO (0.1 µm filtered) was used as control growth. Similarly, 600 µL of Sabouraud broth with 600 µL of sterile water and 60 µL of each compound solution (at each concentration) were prepared in order to ensure a comparable analysis with the treated samples. Ten replicates of control growth, reference compounds and treated samples were used for reproducibility purposes

and additional analysis. The samples were maintained at 25°C, shaken at 150 rpm under dark conditions and incubated for 8 d (logarithmic growth phase). Fungal biomass, soluble protein, ergosterol production and quantification of each phenylphenalenone either in the culture medium as well as in fungal mycelium were analyzed as follows.

Biomass quantification

After the microbial incubation, the fungal mycelium was completely removed from each tube and transferred to a new sterile Eppendorf tube. The fungal biomass was washed with 500 µL (x 3) phosphate-buffered saline (sterile PBS, pH 7.4, 10% DMSO) and centrifuged at 13.000 rpm for 10 min, and the supernatant was poured off and collected for further analysis. A final rinse was followed with 500 µL of sterile water, and the mycelium was immediately frozen in liquid nitrogen and lyophilized in a freeze drier for 48 h. The biomass was left for 24 h in a desiccator before being weighed in a microbalance Mettler Toledo XP26 (0.001 mg readability).

Soluble protein quantification

The protein quantification was carried out by the Bradford method. Briefly, after 8 d of incubation with the fungus, 120 µL of each culture medium (control growth, negative controls and treated samples) was placed in a sterile microtiter 96-well plate and mixed with 120 µL of Coomassie reagent (Coomassie Protein Assay Reagent, Thermo Scientific, Rockford, IL, U.S.A), then allowed to react for 15 min followed by reading the absorbance at 595 nm as indicated by the manufacturer. Three technical replicates of each sample were measured, and the average was used for quantification. The protein concentration was calculated from a calibration curve with bovine gamma globulin as standard.

Ergosterol quantification

The fungal biomass obtained either from control as well as material treated with phenylphenalenones (n = 4) was ground in a paint shaker using stainless steel beads (1.4 mm diam., Carl ROTH, Karlsruhe, Germany) and 0.7 mg was weighed, transferred to an Eppendorf

tube (2 mL Lock-safe Eppendorf tube) and subjected to saponification with 1.5 mL of methanolic solution of KOH (0.1 M) followed by heating at 70°C and shaking at 600 rpm for 10 min (Eppendorf Thermomixer comfort 1.5 mL, Eppendorf AG, Hamburg, Germany). The reaction was left at room temperature, and then the tubes were centrifuged at 10.000 rpm for 10 min and the supernatant transferred to a 4 mL glass vial. Distillated water (1 mL) was added to the methanolic extract solution along with 1 mL of diethyl ether for liquid-liquid extraction. The ether phase was poured off and two additional extractions with diethyl ether were repeated. The organic phase were pooled and evaporated under a stream of nitrogen. The raw extract was re-suspended in 60 µL of $CDCl_3$. ^1H NMR spectra were recorded in a Bruker Avance 700 MHz spectrometer using a standard 1D NOESY pulse sequence with water suppression, with 512 transients (scans) with 32 k data points and a spectral width of 15 ppm using a 30° flip-angle, a 1.46 s acquisition time, and a recycle delay of 2.0 s. Fourier transformation was applied to cumulative FID with exponential line broadening of 0.3 Hz. All spectra were manually phased, baseline corrected and calibrated to TMS (δ 0.0). Ergosterol was quantified using ERETIC2 software built-in in Topspin v3.2 (calibration method). Ergosterol 13.35 µM (purity >98%) in $CDCl_3$ was used as standard for the calibration procedure. The singlet signal at δ 0.63 which integrates for the protons of the methyl group attached to C-13 was used for quantification. A minimal signal-noise ratio of 80:1 was calculated. A T_1 relaxation time of 349.3 ms was determined for the signal at δ 0.63, and $5xT_1$ was setup as a repetition time. Five standard solutions of ergosterol in the range 0.01 - 2.0 mM were prepared and evaluated for the accuracy of the molar quantification method. An area of at least five times the full-width at half-height (FWHH) of the ^1H NMR signal was integrated and considered for the quantification. Absolute error below 2.34% was determined. This value is in agreement with validation methods using NMR spectroscopy (Pauli *et al.* 2005).

Quantification of metabolized phenylphenalenones

To quantify phenylpenalenones, the culture medium was extracted with ethyl acetate (500 µL x 5) by shaking for 10 min, and centrifuged at 7.000 rpm for 5 min. The organic phase was collected in a glass vial of 4 mL for further dryness under a stream of nitrogen. The extract was resuspended in 50 µL of methanol, and an aliquot of 5 µL of this solution was injected into

HPLC. Separation was achieved in a Hibar column RP-18e (Purospher STAR, 250-4.6 mm, 5 μm particle size) using water (0.1% TFA, solvent A) and methanol (solvent B) as a mobile phase. A linear gradient was used from 0 min (40% B), 20 min (100% B), 27 min (100% B). The monitor wavelength was set at 254 nm (HPLC method B). The analysis was carried out by triplicate injections of each sample and reference controls. A coefficient correlation $r^2 \geq 0.9997$ was determined by plotting the peak area (average data) versus the concentration of each reference compound. The data were normalized by comparing the peak area of the compounds (average data) of the treated sample against the peak area (average data) of the reference compound. The limit of quantification (LOQ) calculated for the phenylphenalenones was used as described above.

To quantify phenylpenalenones in the mycelium, fungal biomass was collected and lyophilized as described above. Methanol (1 ml, HPLC gradient grade) was added to the fungal mycelium (0.7 mg), shaken at 650 rpm for 15 min at room temperature and centrifuged at 10.000 rpm during 10 min at 4°C. The extraction was repeated twice with the same procedure, and the organic extracts were pooled and evaporated under stream of nitrogen gas. The final crude extract was resuspended in 50 μL of methanol, and an aliquot of 5 μL was injected into the HPLC system using method B (described above). Triplicate analysis was conducted and the data were normalized to the reference controls as was described above.

Analysis of phenylphenalenone metabolites

In order to investigate the products derived from the metabolism of phenylphenalenones by the fungus *M. fijiensis*, an up-scaled incubation system with anigorufone (**9**) as reference compound was implemented. Thus, the fungal inoculum ($3x10^5$ mycelial fragments mL^{-1}) of the *M. fijiensis* strain Ca10_13 was prepared as described above. A volume of 5 mL of inoculum was added to 50 mL of saboraoud medium (sterile, incubation in Erlenmeyer flask vol. 100 mL), and 2.38 mL of a solution of 1.5 M of anigorufone (prepared in 20% DMSO and passed through 0.1 μm sterile filter) was added. A parallel experiment without any treatment was used to control fungal growth (2.38 mL of a solution 20% of sterile DMSO was added). The incubation was carried out at 25°C, shaken at 150 rpm in a rotatory shaker under darkness for 12 d. Afterwards,

the fungal biomass together with the culture medium was transferred to sterile Falcon tubes (50 mL) for further centrifugation at 12.000 rpm during 15 min. The supernatant was poured off to a new sterile Falcon tube (50 mL) and the mycelium was washed twice with 30 mL of PBS (pH 7.4) and rinsed with 30 mL sterile water (10% DMSO). A centrifugation step was used in each wash, and the supernatants transferred to new sterile Falcon tube (vol. 50 mL). Both fungal mycelium as well as the supernatants were frozen in liquid nitrogen, lyophilized for 72 h and then kept in a desiccator until further analysis. The lyophilized supernatants were resuspended in 5 mL of methanol and injected into LC-MS system using a LiChrosphere 100 column RP-18 (250 - 4 mm, 5 μm particle size) with water (0.1% formic acid, solvent A) and methanol (0.1% formic acid, solvent B) as a mobile phase. A linear gradient was used from 0 min, 40% B; 20 min, 100% B; 30 min, 100% B. The fungal biomass (1.3 g dried weight) contained in a Falcon tube was ground using stainless steel beads (1.4 mm diam.) and shaken in a paint shaker (Skandex SO-10M, Sassenheim, The Netherlands) for 5 min. Methanol (10 mL x 3) was used for extraction by shaking for 10 min followed by centrifugation. The methanolic fraction was passed through a sterile membrane filter (0.45 μm) and evaporated under a nitrogen steam. The crude extract was resuspended in methanol (5 mg mL^{-1}), and 5 μL was injected into LC-MS system using the parameters described above.

The methanolic extracts either from mycelium as well as from culture medium incubated with phenylphenalenones **5**, **7**, **9**–**12** (Table 2) were analyzed with a UHPLC-ESI-MS. Phenylphenalenones were separated using an Acclaim C18 column (150 × 2.1 mm, 2.2 μm, Dionex, Sunnyvale, CA, USA) with a flow rate of 300 μl min^{-1} in a binary solvent system of water (solvent A) and acetonitrile (solvent B) (hypergrade for LC MS, Merck, Darmstadt, Germany), both containing 0.1% (v/v) formic acid (eluent additive for LC–MS, Sigma Aldrich, Steinheim, Germany). Separation was accomplished using a gradient as follows: linear increase from 0% B to 100% B within 15 min – 100% B constant for 5 min – equilibration time at 0% B for 5 min. ESI source parameters were set to 4 kV for spray voltage, 35 V for transfer capillary voltage at a capillary temperature of 275 °C. The samples were measured in positive and negative ion mode in the mass range of *m*/*z* 100 to 2000 using 30,000 m/Δm resolving power in the Orbitrap mass analyzer. Data were interpreted using XCALIBUR software (Thermo Fisher Scientific, Waltham, MA, USA).

Statistical analysis

Unless otherwise stated, statistical tests were carried out with Sigma Plot 12.0 (SYSTAT Software Inc., San Jose, CA, USA) using analysis of variance. Leven's and Shapiro-Wilk tests were applied to determine error variance and normality of the data, respectively. Holm-Sidak *post hoc* test was used for pairwise or multiple comparison. Datasets that did not fulfill the assumptions for ANOVA were natural log-, decimal log-, root square- or rank-transformed before analysis. A non-parametric Kruskal-Wallis one-way ANOVA on ranks was applied for variables that did not meet the normality assumption.

RESULTS

Differential responses of the interaction *Musa* - *M. fijiensis* detected by principal component analysis

In order to explore whether the susceptible *Musa* variety 'Williams' and the resistant variety 'Khai Thong Ruang' (KTR) respond differently to infection with the phytopathogenic ascomycete fungus *Mycosphaerella fijiensis*, *in vitro* plants of the two varieties were treated with conidia of the strain E22 as described in Materials and Methods. The progress of the development of the BLSD was observed by inspecting the leaf surface of the two *Musa* varieties using a binocular loupe. Initially, both the susceptible variety 'Williams' and the resistant variety 'KTR' developed similar symptoms at the site of treatment (Table S1). When BLSD symptoms of the treated plants, according to the classification by Fouré et al. (1987), reached a dimension similar to the stages 2 and 3, the necrotic zones (sample A) and healthy zones (B) of treated half of the leave were probed (Fig. 2C). Simultaneously, further samples were taken from the non-treated half of each treated leaf (D), non-treated leaves of the treated plants (E) and untreated plants (control, C). When ^{1}H NMR spectra of crude extracts of necrotic tissue (A) were compared with spectra of non-necrotic tissue (D) from the same treated leaf and the control plant (C) (Fig. 1), signals of aromatic metabolites were more pronounced in the extracts of leaf areas where the fungal infection had taken place than in extracts of samples taken from "healthy zones". This was

observed both for 'Williams' and 'KTR'. ^{1}H NMR spectra of samples B and E (not shown in Fig. 1) closely resembled those of (C).

The ^{1}H NMR spectra of all extracts are not much different in the regions of primary metabolites such as carbohydrates and amino acids (0.5-5.0 ppm, Fig. 1). However, the aromatic regions (6.0-9.0 ppm, Fig. 1) of the spectra exhibited not only largely enhanced signals obtained from the necrotic zones of infected leaves (A) but, compared to the spectra from extracts of non-treated tissues, also a significantly increased number of signals.

Thus, qualitative and quantitative gains in metabolic activity were observed in the infected zones of the plant and could be interpreted as a response to the pathogen attack. Therefore, it was thought that identification and quantification of the major metabolites produced while the BLSD ran its course would provide insight into the role and turnover of inducible natural products in this plant.

An NMR-based metabolomic analysis was carried out to gain information about metabolic changes occurring in *Musa* plants under attack by the pathogen. The full ^{1}H NMR spectra were used for understanding whether differences other than in the aromatic compounds exist between infected (A), non-infected (B, D and E) and control (C) *Musa* plant samples (Fig. 2 c). According to the score plots of principal component analysis (PCA, Fig. 2 a,b), the samples from BLSD-infected necrotic leaf zones (A, red) were clearly discriminated from those of the control group (C, green) by the first principal component (Fig. 2 a,b), mainly owing to aromatic compounds. Interestingly, the other non-infected plant sections (asymptomatic areas B, non-treated leaf areas D and E) obtained from plants treated with conidia of *M. fijiensis* E22 (Fig. 2c) appeared also separated in the PCA (blue, orange and gold) from the group of control *Musa* plants (green).

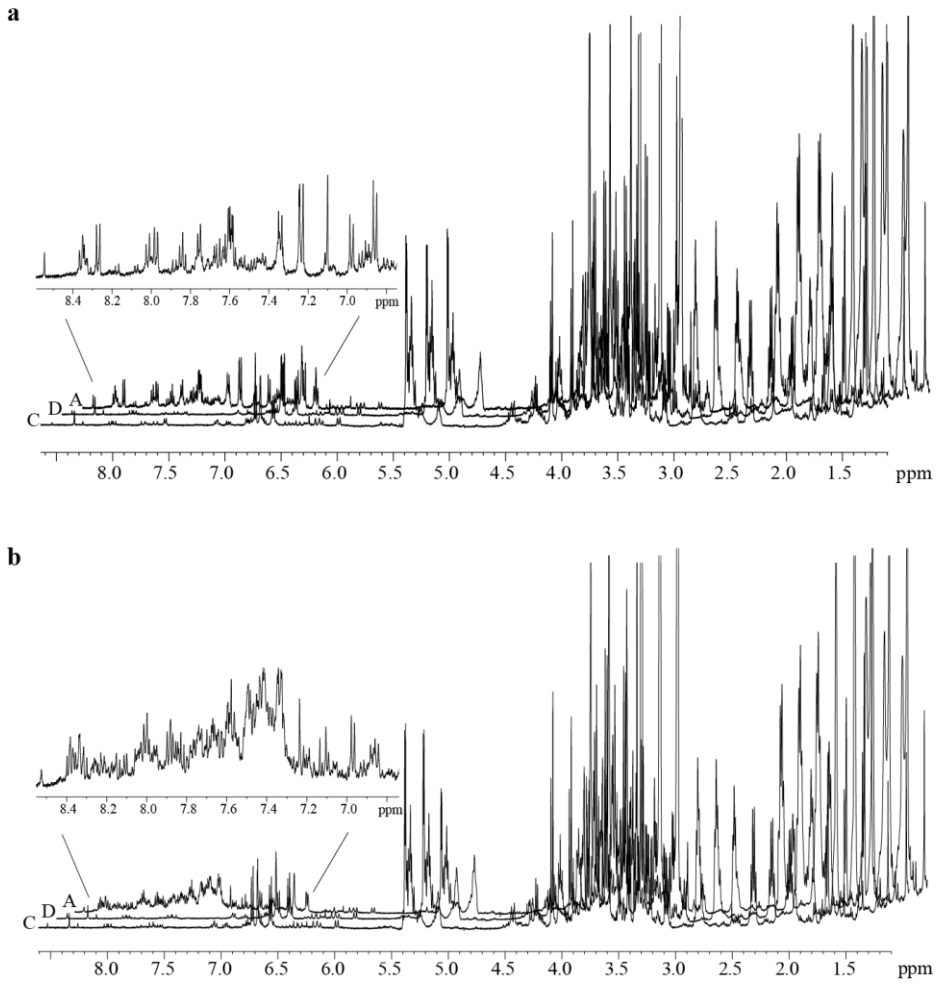

Fig. 1. ^{1}H NMR spectra (500 MHz, MeOH-d_4) of crude extracts of *Musa* leaf tissues from varieties 'Williams' (panel a) and 'KTR' (panel b). Extracts were prepared from necrotic areas of the infected half (A, see Fig. 2), the non-infected half (D) of a leaf treated with *M. fijiensis* strain E22, and a leaf of an untreated control plant (C) were taken 35 d after inoculation with fungal conidia. The extensions show the ^{1}H NMR signals of induced phenolics in the necrotic leaf areas (A). Spectral intensities were scaled with the signal of TSP, which was added as an internal standard.

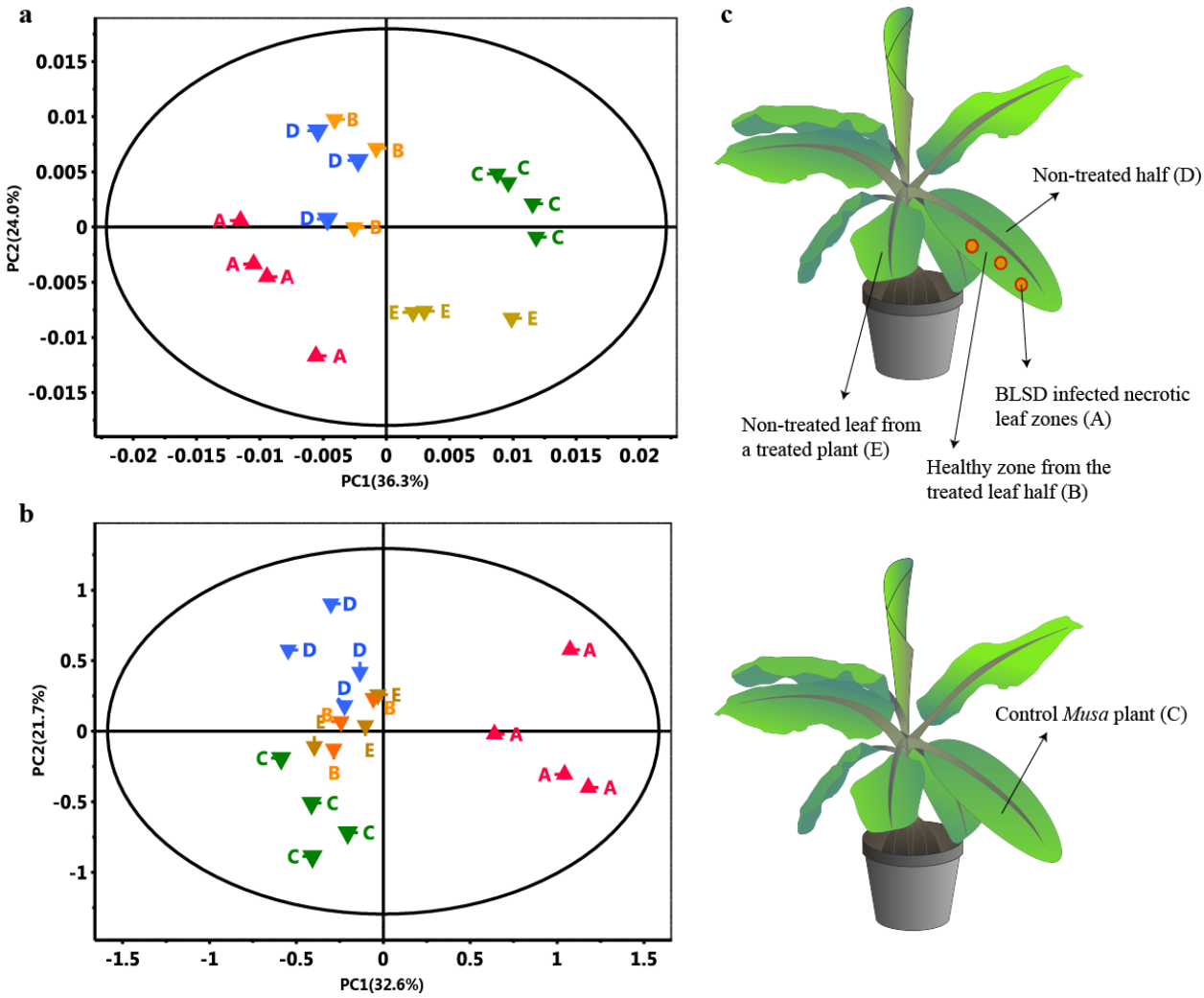

Fig. 2. Score plots of PC1 vs. PC2 of 8-component PCA model of the region 0.5-8.7 ppm of the ^{1}H NMR spectra (500 MHz) of samples A to E (0.005 ppm buckets). Regions 3.25-3.32 ppm and 4.8-5.0 ppm were excluded; data were normalized to total intensity of the spectrum. Panel **a**: 'Williams variety' (Pareto scaling was applied with $r^2 = 0.903$ of PCA model). Panel b: 'KTR' variety (unit variance scaling was applied with $r^2 = 0.854$ of PCA model). Panel **c**: sketch of the sampling procedure: A: BLSD-infected necrotic leaf zones; B: healthy zones from the treated leaf half; C: control *Musa* plant; D: non-treated half of a treated leaf; E: non-treated leaf from a treated plant.

With the intention of detecting the signals in the spectra that contribute to the differences between samples, 1D- and 2D NMR analysis was carried out along with comparisons to reference compounds and previously reported data (Franzyk *et al.* 2004; Huang *et al.* 2004; Kashiwada *et al.* 1988; Kim *et al.* 2010; Liang *et al.* 2006; Lu & Foo 2003; Najbjerg *et al.* 2011; Ramsay *et al.* 2014; Shimomura *et al.* 1987; Strack *et al.* 1989). This allowed the identification of the metabolites summarized in the Table 1. Taking the information from the PCA, including consideration of the metabolites identified, the corresponding loading plots were constructed (Fig. 3). For both *Musa* varieties, the red-orange color in the scale of the loading plots demonstrated that the phenolic metabolites, which are up-regulated in infected tissue, permit the infected tissue to be discriminated from the non-infected plant sections (Fig. 3).

Interestingly, the level of the 1-*O*-p-coumaroyl-β-D-glucoside was lower in infected tissue than in healthy tissue, perhaps due to consumption in specialized metabolism, which was triggered to produce phenylphenalenones (Table 1) such as irenolone and hydroxyanigorufone, already reported as phytoalexins of *Musa* plants (Luis, *et al.* 1993, 1994, 1995). Further, among the identified metabolites, dopamine, a well-known catecholamine in banana fruits (Kanazawa & Sakakibara 2000), and 2-(3,4-dihydroxyphenyl)ethyl β-D-glucopyranoside (common name dopaol β-D-glucoside), which is reported here for a first time as a metabolite from *Musa* plants, allowed the treated tissue to be discriminated from the untreated *Musa* tissue (for relevant resonances in the ^{1}H NMR spectrum see the region between 6.5-6.9 ppm in Fig. 2 a,b).

Surprisingly, a detailed analysis of ^{1}H NMR spectra of all extracts of 'Williams' and 'KTR' showed that dopamine was present in infected leaves and in control plants. While control samples contained only traces of dopaol β-D-glucoside (Fig. 4c), its level almost equaled that of dopamine in the necrotic tissue of treated plants (Fig. 4a). In non-infected zones from (B), (D) and (E) samples of both varieties, the level of the glucoside clearly exceeded the level of dopamine, which was detectable only in very low levels (Fig. 4b). This finding confirms the significance of dopaol β-D-glucoside in the differences observed by the PCA analysis.

According to the accumulation of dopaol β-D-glucoside in the different leaf areas of *Musa* plants treated with conidia of *M. fijiensis* but not in the control plant, this compound could be

considered a phytoalexin; phytoalexins are produced in those areas of a plant where the pathogen has not been yet spread but which might already have received electrophysiological or chemical signals. Therefore, the antifungal property of dopaol β-D-glucoside was assayed against *M. fijiensis* in an *in vitro* experiment. However, antimicrobial inhibition was not observed, and the weak activity was comparable to that obtained for dopamine in the same assay (Fig. S2), ruling out the function as a phytoalexin. Thus, the biological function of this compound in the *Musa* - *M. fijiensis* pathosystem remains to be investigated, including its potential role in signaling.

In addition, the roots of infected and control plants were evaluated in both *Musa* varieties in order to check if specialized metabolites were observed in the roots as they were in the leaves. However, no differences between control and treated plants were found (data not shown), supporting the hypothesis that after *Musa* leaves are treated with the conidia of *M. fijiensis*, chemical defenses are activated mainly in the above-ground plant parts, especially at the infection site.

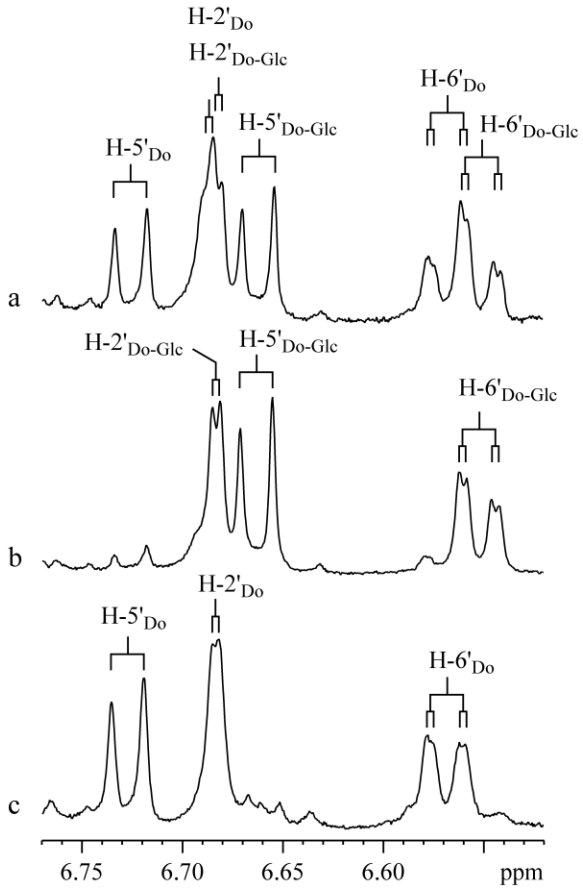

Fig. 4. Partial ^{1}H NMR spectra showing the aromatic signals of dopamine and dopaol-β-D-glucoside in **a**: infected leaf areas (A, see Fig. 2); **b**: non-infected areas from (D); **c**: control *Musa* 'Williams' variety. ^{1}H NMR spectra of (B) and (E) (not shown) resembled those of (D). Similar results were observable for the 'KTR' variety. Do: dopamine; Do-Glc: dopaol-β-D-glucoside

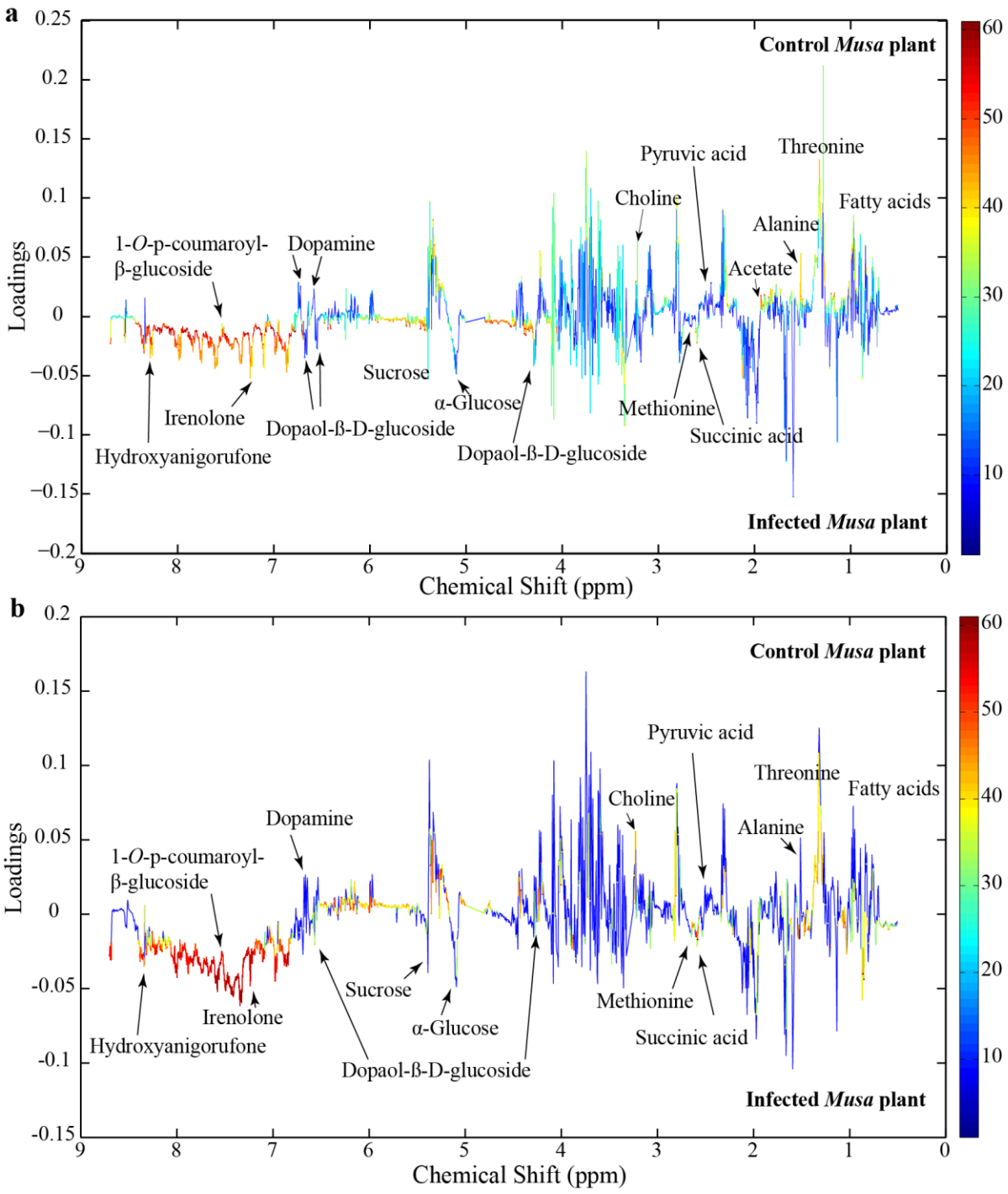

Fig. 3. Loading plots for PCA model shown in Fig. 2a and 2b displaying the regions of the metabolites with strong influence (in red and orange) and the metabolites with less influence (light blue and dark blue) during the group discrimination observed in the PCA analysis. Panel **a**: 'Williams' and panel **b**: 'KTR' *Musa* varieties.

Table 1. Metabolites identified by 1D- and 2D-NMR analysis in *Musa* varieties 'Williams' and 'KTR' and their up- and down-regulation after infection with *M. fijiensis* E22 as inferred from the corresponding loading plots.

Entry	Metabolite[e]	Position H/C	NMR data		Assigned with	Changes after infection with *M. fijiensis* E22 in *Musa*:[d]	
			δ ^{1}H (mult., *J* [Hz])	δ ^{13}C		'Williams'	'KTR'
1	Fatty acids	-CH_3 -CH_3	0.88 (t, 7.5) 0.95 (t, 7.5)	13.1 13.3	HSQC	↓	↓
2	Lactic acid	-CH_3 H/C-2	1.29[c] 4.09	22.3 71.8	HSQC, HMBC	nd	nd
3	Acetic acid	-CH_3 -COOH	1.93 (s)	25.9 175.9	HSQC, HMBC	↓	nd
4	Succinic acid	H/C-2, 3 -COOH	2.59 (s)	31.6 177.0	HSQC, HMBC	↑	↑
5	Pyruvic acid	- CH_3 -COOH (α) -COOH (β)	2.35 (s)	29.5 180.3 203.7	HSQC, HMBC	↓	↓
6	Choline	H/C-1 H/C-2 -$N^{+}(CH_3)_3$	3.5 (dd, 3.3, 5.0) 4.07 (m) 3.2 (s)	73.1 58.3 53.2	HSQC, HMBC	↓	↓
7	Glucose	CH-1	5.1 (d, 3.8)	92.3	HSQC, TOCSY	↑	↑
8	Sucrose	CH-1 CH-1'	5.39 (d, 3.7) 4.09 (d, 8.5)	92.3 77.7	HSQC, TOCSY	↑	↑
9	L-Alanine[a]	-CH_3 H/C-2	1.46 (d, 7.3) 3.59[c]	15.9 54.6	HSQC, COSY	↓	↓
10	L-Methionine[a]	H/C-2 H/C-4 H/C-3	3.81[c] 2.63 (dd, 7.8, 7.9) 2.19[c]	55.0 32.5 31.6	HSQC, COSY	↑	↑

		-CH_3	2.09[c]	17.9			
11	L-Threonine[a]	-CH_3 H/C-2 H/C-3 -COOH	1.3 (s) 3.55 (d, 3.5) 4.26[c]	22.2 60.7 68.6 173.6	HSQC, HMBC	↓	↓
12	Dopamine[a]	H/C-5' H/C-2' H/C-6'	6.72 (d, 8.0) 6.69 (d, 1.9) 6.56 (d, 7.9)	115.2 115.3 119.5	HSQC	↓	↓
13	Dopaol-β-D-glucoside[b]	H/C-2' H/C-5' H/C-6' H/C-8'a	6.68 (d, 1.9) 6.65 (d, 7.9) 6.54 (dd, 1.9. 7.9) 3.17 (dd, 8.9, 9.1)	115.7 114.6 119.6 73.6	HSQC, HMBC	↑	↑
14	(*E*)-Caffeoyl malate	H/C-2 H/C-3 H/C-5' H/C-6' H/C-7' H/C-8'	5.32[c] 2.94 (dd, 3.1, 15.9) 2.83 (dd, 8.3, 15.5) 6.79 (d, 8.0) 6.95 (d, 2.0, 8.2) 7.57 (d, 16.0) 6.29 (d, 16.0)	71.9 39.6 115.1 121.5 145.4 114.1	HSQC, HMBC, TOCSY	nd	nd
15	(*E*)-Coumaroyl malate	H/C-2 H/C-3 H/C-2'/6' H/C-3'/5' H/C-7'	5.32[c] 2.94 (dd, 3.1, 16.0) 2.83 (dd, 8.3, 16.0) 7.47 (d, 8.8) 6.8 (d, 8.9) 7.65 (d, 16.0)	71.9 39.6 131.2 145.6	HSQC, HMBC, TOCSY	nd	nd
16	1'-*O*-(*E)*-(4-Coumaroyl)-β-glucoside	H/C-3'/5' H/C-2'/6' H/C-7' H/C-8'	6.8 (d, 8.6) 7.52 (d, 8.6) 7.73 (d, 16.0) 6.44 (d, 16.0)	115.3 130.2 148.8 112.7	HSQC, HMBC, TOCSY, COSY	↓	↓
17	2-*O*-p-(*E*)-Coumaroyl glucose	H/C-7' H/C-8'	7.62 (d, 16.0) 6.34 (d, 16.0)	145.5 114.2	HSQC, HMBC	nd	nd
18	Irenolone	H/C-3'/5' H/C-2'/6'	6.96 (d, 8.1) 7.34 (d, 8.4)	115.4 131.5	HSQC, HMBC	↑	↑

19	Hydroxyanigorufone	H/C-2'/6' H/C-3'/5' H/C-7	7.23 (d, 8.5) 6.85 (d, 8.5) 8.27 (d, 8.4)	130.6 115.5 136.1	HSQC, HMBC	↑	↑

[a] Metabolites identified by comparing NMR data with authentic standards

[b] Metabolite isolated and 1D- and 2D-NMR data are matched with the data reported in the literature (Franzyk *et al.,* 2004)

[c] Signals or multiplicities were not determined because of signal overlap.

[d] (↑) or (↓): up- or down-regulation of metabolites.

[e] Chemical structures are shown in Fig. S1

Identification and quantification of induced defense metabolites in *Musa* after infection with *M. fijiensis*

Phytochemical analysis of infected Musa plants. Among the up-regulated metabolites found by means of the above-described metabolomic approach, only a small number of phenolic compounds were identified (Table 1, entry 12-19). However, the many overlapping signals in the overcrowded aromatic region in the ^{1}H NMR spectra (Fig. 1) suggested more up-regulated phenolics occur in these crude samples, especially in the 'KTR' variety, and made the identification of the signals difficult even using 2D NMR experiments.

Therefore, a conventional phytochemical analysis of the infected leaves of both *Musa* cultivars showing BLSD symptoms (35 days post inoculation (dpi)) was carried out in order to identify the metabolites produced in response to the pathogen attack. HPLC-guided isolation together with 1D- and 2D NMR spectroscopy and HRMS analysis allowed the identification of fifteen phenylphenalenone-type compounds or structural analogues in the resistant variety 'KTR' while ten were found in the susceptible variety 'Williams' (Table 2). Among these compounds are irenolone (**4**) and hydroxyanigorufone (**5**), which have been identified in the metabolomic approach. Further compounds such as 2-(4′-hydroxyphenyl)-naphthalic anhydride (**1**), methoxyanigorufone (**7**) and anigorufone (**9**) have been reported to be strongly toxic to fungi (Hirai *et al.* 1994; Kamo *et al.* 1998; Lazzaro *et al.* 2004; Luis *et al.* 1995; Otálvaro *et al.* 2002, 2007). The ^{1}H NMR spectra of the compounds from the infected *Musa* leaves matched those of authentic in-house standards, and HRMS spectra were fully consistent with the suggested structures.

All compounds, except compound **10**, are known natural products and have been identified from *Musa* plants (Kamo *et al.* 1998, 1998; Liu *et al.* 2014; Luis *et al.* 1993, 1994, 1995, 1999; Otálvaro *et al.* 2002). Unfortunately, some minor compounds remained unidentified due to the limited amount isolated and/or to insufficient chemical stability during the isolation procedure (data not shown). Their role in the plant defense therefore remains unclear.

Table 2. Phenylphenalenones isolated by HPLC and identified by 1D- and 2D NMR spectroscopy and HRMS from 'KTR' leaves after infection with *M. fijiensis* strain E22. Occurrence of the metabolites is represented by (+) or absence/not detectable (-).

Peak	R_t (min)	Compound	Chemical structure	Occurrence in *Musa*	
				'Williams'	'KTR'
1	74.77	2-(4'-Hydroxyphenyl)-1,8-naphthalic anhydride	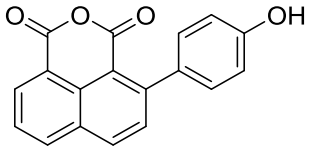	+	+
2	82.12	*trans*-2,3-Dihydro-2,3-dihydroxy-9-phenylphenalenone	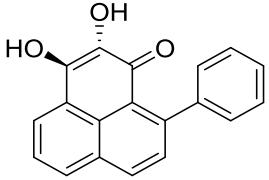	+	+
3	85.30	2-Phenyl-1,8-naphthalic anhydride	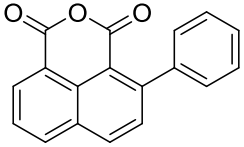	+	+
4	87.81	2-Hydroxy-4-(4′-hydroxyphenyl)-1*H*-phenalen-1-one (irenolone)	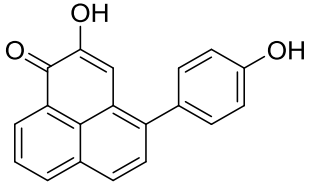	+	+
5	89.35	2-Hydroxy-9-(4′-hydroxyphenyl)-1*H*-phenalen-1-one (hydroxyanigorufone)	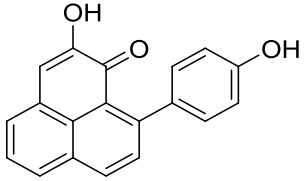	+	+

6	89.99	2-Methoxy-9-(4'-hydroxyphenyl)-1*H*-phenalen-1-one	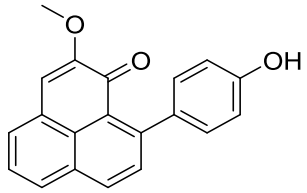	-	+
7	101.62	Methoxyanigorufone	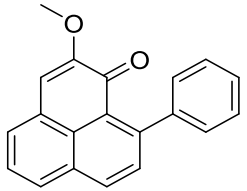	-	+
8	102.92	Dihydroxyanigorootin	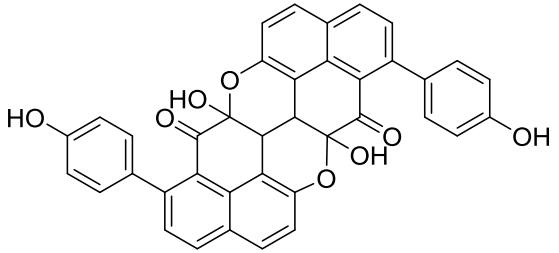	+	+
9	104.20	Anigorufone	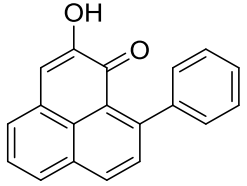	+	+
10	105.89	2-Hydroxy-9-(4'-methoxyphenyl)-1*H*-phenalen-1-one (4′-*O*-methylanigorufone)	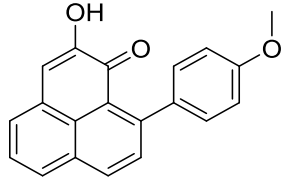	-	+
11	107.55	Isoanigorufone	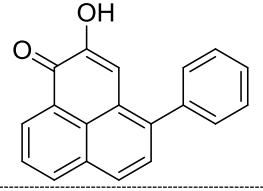	-	+

12	108.84	2-Hydroxy-4-(4'-methoxyphenyl)-1*H*-phenalen-1-one (4′-*O*-methylirenolone)	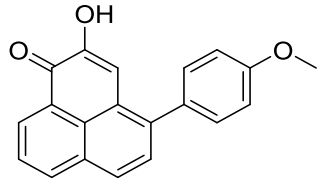	+	+
13	118.98	3,3′-bis-Hydroxyanigorufone	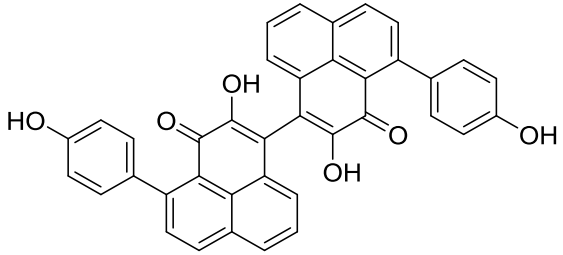	+	+
14	120.64	Hydroxyanigorootin	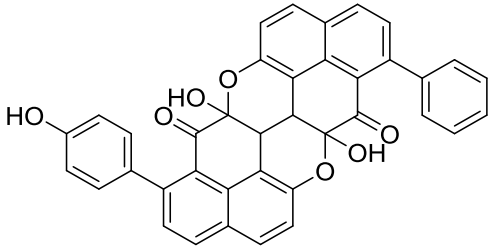	-	+
15	121.94	Anigorootin	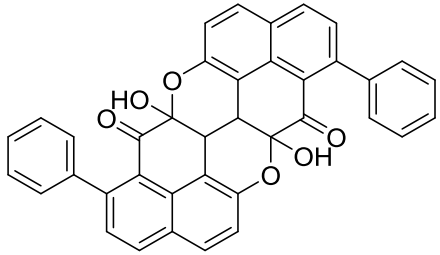	+	+

Quantification of phenylphenalenone-type compounds based on the progress of the disease. In order to study the hypothetical correlation between the virulence of *M. fijiensis* to *Musa* plants and the formation of phenylphenalenones, *in vitro* plants of 'Williams' and 'KTR' were treated in independent experiments with the fungal strains, E22 and Ca10_13, after which the symptoms were evaluated and the leaf tissues quantitatively analyzed for the presence of phenylphenalenones. The two *M. fijiensis* strains were chosen according to their different tolerance (Ca10_13) or susceptibility (E22) to the fungicide propiconazole, and their conidia were used as infective propagules for exploring differential responses of susceptible and resistant *Musa* varieties. The virulence of the two strains was evaluated by visually inspecting the number and area of the lesions on the surface of the *Musa* leaves at different time points after infection (Fig. 5). At early stages of infection, the resistant variety 'KTR' exhibited some symptoms characterized by small red specks (~1 mm diam.) on the lower surface of the leaf in response to each *M. fijiensis* strain, E22 and Ca10_13; these symptoms were stronger compared to symptoms observed in the susceptible 'Williams' variety (Table S1). This was evident by symptom-free leaves in 'Williams' at 8 dpi. The further development of the BLSD symptoms is clearly different for the infection of the two *Musa* varieties treated with the strain E22 or Ca10_13. While the number and area of the lesions constantly increased in 'Williams', these symptoms remained almost unaltered on the leaves of 'KTR' after infection with E22 but increased after infection with Ca10_13, reaching severe damage after 50 dpi (Fig. 5, Table S1).

After evaluating the BLSD symptoms, an HPLC-DAD approach was applied to quantify the inducible phenylphenalenone-type compounds produced by the two *Musa* varieties 'Williams' and 'KTR' during their response to the pathogen. The concentration of phenylphenalenones was determined either in an early stage (25 dpi) or a later stage (50 dpi) of the disease. The results for the 'KTR' variety (Fig. 6a) showed irenolone (**4**) as the major metabolite, with a concentration exceeding 25 nmol mg^{-1} DW. Metabolites **2**, **4**, **7**, **9**, **11** and **12** were produced in a concentration >10 nmol mg^{-1} DW. All other compounds were produced in a concentration range between 1.5 and 9.5 nmol mg^{-1} DW.

A significant increase in the concentration of compounds **6**, **10**, and **13** - **15** ($p<0.001$) during the observed period of time from 25 to 50 dpi was found when the 'KTR' plants were

treated with *M. fijiensis* strain E22. In contrast, compounds **5** (hydroxyanigorufone) and **9** (anigorufone) were significantly reduced in concentration between 25 and 50 dpi ($p<0.001$) (Fig. 6a). When the plants were treated with *M. fijiensis* strain Ca10_13, mainly compounds **4** and **14** but also **8, 10** and **15** were significantly induced at 50 dpi while metabolite **9** again was found to be significantly reduced ($p<0.001$).

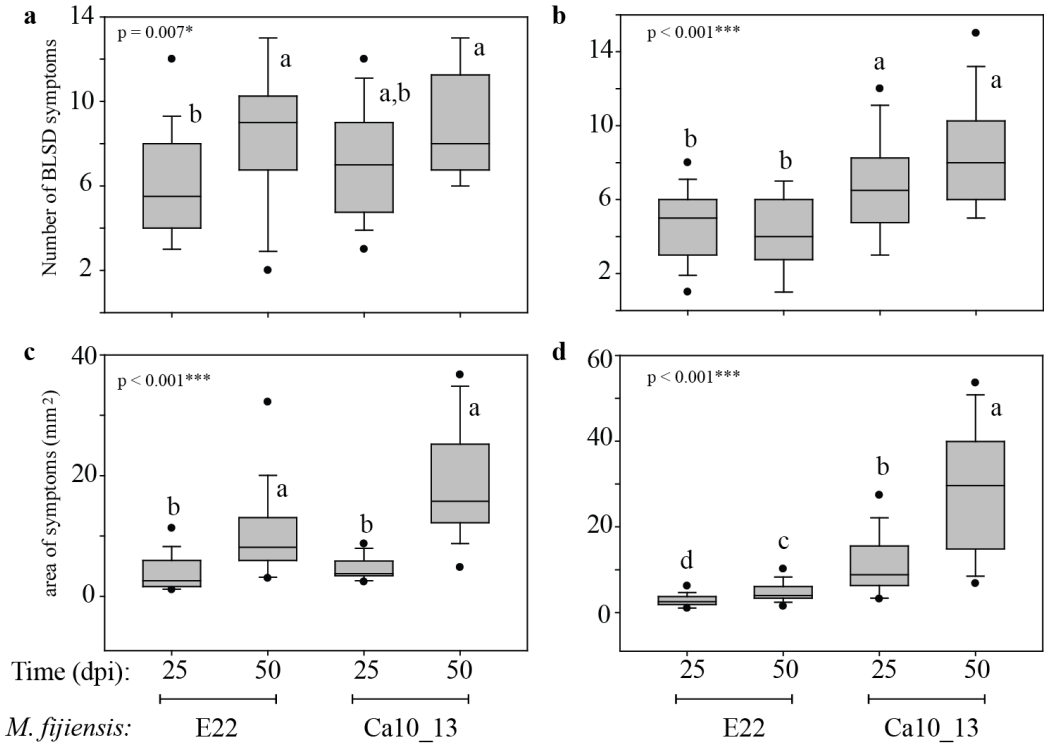

Fig. 5. Number and area of BLSD symptoms determined for *Musa* 'Williams' (panels **a** and **c**) and 'KTR' (panels **b** and **d**) varieties during the interaction with *M. fijiensis* strain E22 and Ca10_13. Letters a – d in the box-plot indicate significant differences among the treatments. One-way ANOVA, $p<0.001$=***, $p<0.05$=*.

The *Musa* 'KTR' variety reacted differently to the infection by each fungal strain. Overall, a significant increase in the production of compounds **2**, **3**, **4**, **12** and **14** were observed during the response against the strain Ca10_13, while compounds **6**, **7**, **9** and **11** were more induced by the infection with the strain E22 when compared with Ca10_13 ($p<0.001$).

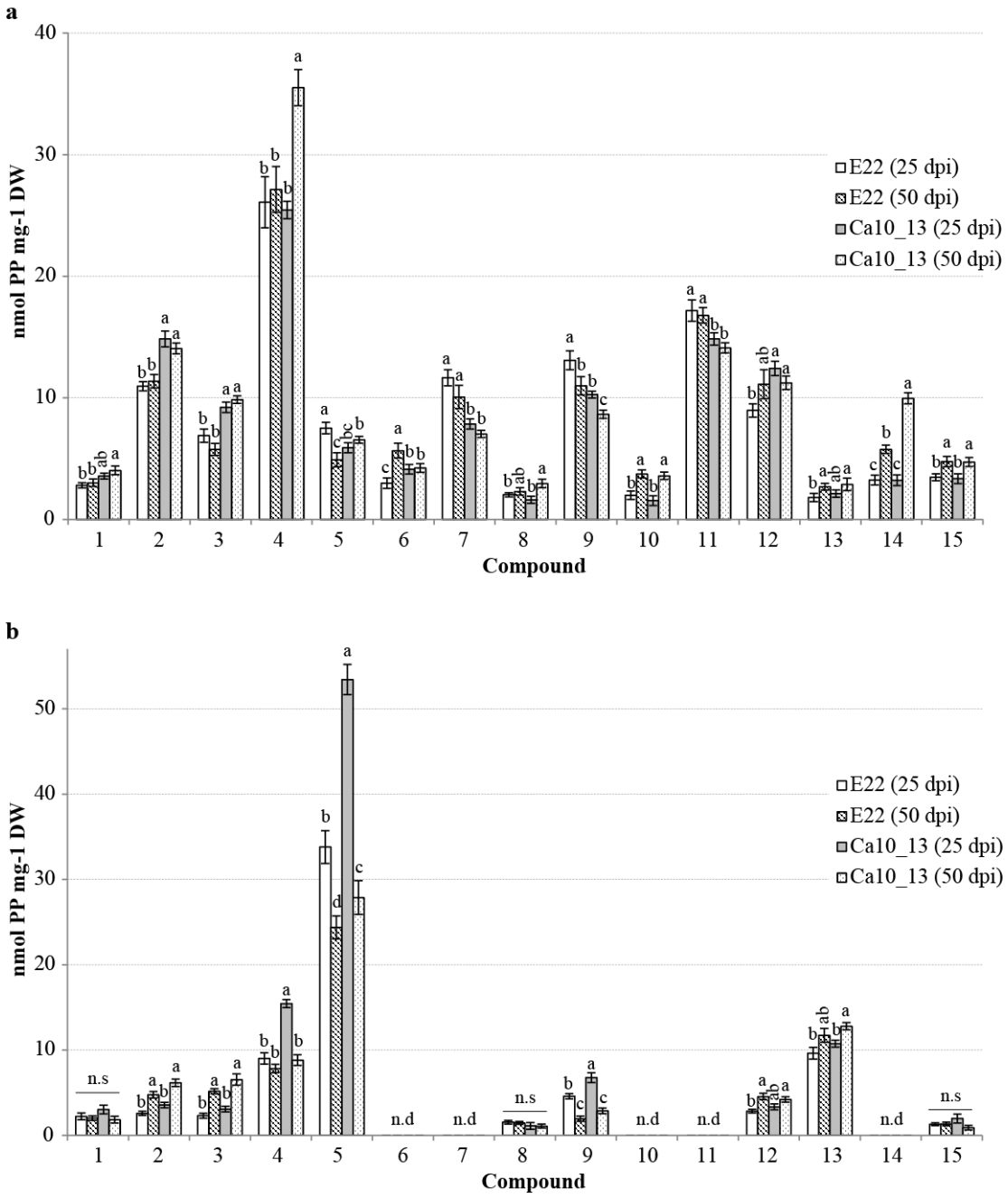

Fig. 6. Quantification of the phenylphenalenones (nmol PP mg^{-1} DW) identified in 'KTR' (panel **a**) and 'Williams' (panel **b**) varieties after infection with *M. fijiensis* strain E22 at 25 and 50 dpi and with *M. fijiensis* strain Ca10_13 at 25 and 50 dpi. Letters a - d indicate significant differences among treatments within the specified time (dpi) and compound (Three-Way ANOVA, Holm-Sidak *post hoc* test: $P<0.05$; n.s: not significant), n.d: not detectable. For chemical structures of compounds **1** – **15**, see Table 2.

Like 'KTR', the variety 'Williams' also exhibited one dominant metabolite in addition to a number of medium-concentrated and minor compounds. However, unlike 'KTR', which mainly produced irenolone (**4**), its positional isomer, hydroxyanigorufone (**5**) was the major compound in 'Williams' (25-52 nmol mg^{-1} DW) (Fig. 6b). Only two further compounds, **4** and **13**, also exceeded the concentration of 10 nmol mg^{-1} DW, while compounds **1**-**3**, **8**, **9**, **12**, and **15** remained below that level and were produced in the range of 1.3-8.5 nmol mg^{-1} DW.

According to the statistical analysis, a significant increase in the time-dependent induction of metabolites **2** and **3** were observed at 50 dpi, independently of the fungal strain used for the infection. Compounds **12** and **13** followed an induction pattern similar to that of **2** and **3** when the plant was treated with *M. fijiensis* strains E22 and Ca10_13, respectively. In contrast, the concentration of compounds **4**, **5** and **9** was dramatically reduced during the time BLSD developed, which is when the strain Ca10_13 was used ($p<0.001$). A remarkable drop of the concentration of hydroxyanigorufone (**5**) from ~ 52 to ~ 27 nmol mg^{-1} DW was observed between 25 and 50 dpi. Similar results were found for compounds **5** and **9** after infection with strain E22 (Fig. 6b). The *de novo* biosynthesis of metabolites **1**, **8**, and **15** remained almost unaffected both by the time point evaluated and by the fungal strain.

An overall overview of the total content of phenylphenalenones (and structural analogues) by the two *Musa* varieties was obtained by adding up the amount of each metabolite per mg of plant dry material. Thus, both after inoculation with the strain E22 and the strain Ca10_13, the susceptible variety 'Williams' produced lower levels of phenylphenalenones compared to the resistant variety 'KTR' (Fig. 7). For treatment with E22, ~ 68 nmol mg^{-1} DW were found in 'Williams' and ~ 120 nmol mg^{-1} DW were found in 'KTR'. No significant statistical differences in the total phenylphenalenone content were detected between plants at 25 dpi showing early BLSD symptoms and plants at 50 dpi showing stronger symptoms. However, large differences in total phenylphenalenone concentration between the early (25 dpi) and the late stage of the disease (50 dpi) were observed for both *Musa* varieties when infected with the *M. fijiensis* strain Ca10_13. However, 'Williams' and 'KTR' responded differently as the disease progressed. While the PP content in 'Williams' dropped significantly from ~ 100 nmol mg^{-1} DW at 25 dpi to ~ 70 nmol mg^{-1} DW at 50 dpi, the PP content in 'KTR' increased from ~ 120 to ~ 140 nmol mg^{-1} DW (Fig. 7).

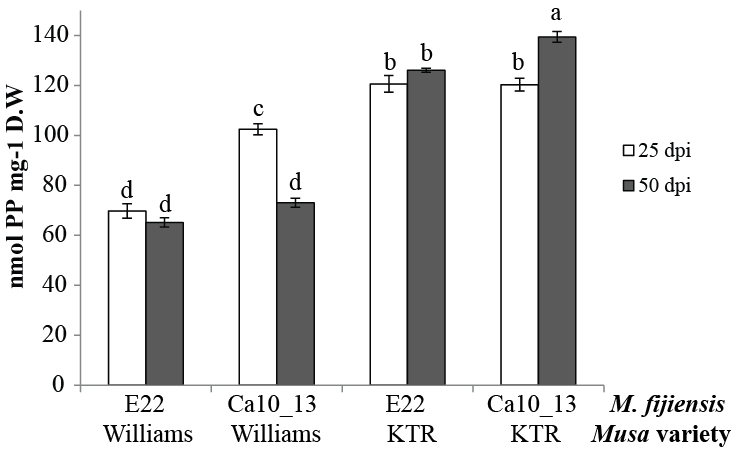

Fig.7. Total content of phenylphenalenone-type compounds (PP) produced by the *Musa* varieties 'Williams' and 'KTR' during 25 and 50 dpi with two different *M. fijiensis* strains. Letters a - d indicate significant differences among treatments (One-Way ANOVA, Holm-Sidak *post hoc* test: $P<0.001$).

Antifungal bioassay of the major phenylphenalenones

The major phenylphenalenone-type compounds identified in both *Musa* plants were assayed for their antifungal properties against the two *M. fijiensis* strains E22 and Ca10_13 used in this study. The half maximal inhibitory concentration (IC_{50}) values were generated using the method reported by Peláez et al. (Peláez *et al.* 2006) with modifications as described in Materials and Methods and using propiconazole as a positive control. The results showed that both fungal strains were sensitive not only to the commercial fungicide propiconazole but, though to a different extent, also to most of the phenylphenalenone-type compounds assessed. Among compounds **3** – **5**, **7**, **9** – **11**, **14**, and **15** tested, only hydroxyanigorootin (**14**) and 2-phenyl-1,8-napthalic anhydride (**3**) did not display significant inhibitory activity against both *M. fijiensis* strains. Most of the IC_{50} values were found to be in the range between ~ 0.05 and ~ 0.15 mM (Fig. 8). Isoanigorufone (**11**), a 4-phenylphenalenone found in the resistant variety 'KTR' but not in susceptible 'Williams', displayed antimycotic activity in $IC_{50\text{-}E22}$ = 0.032±0.002 mM under light conditions. This value represented the best antifungal bioactivity among all the compounds tested. The antimicrobial activity of irenolone (**4**), hydroxyanigorufone (**5**) and 4′-methoxyirenolone (**12**) against both *M. fijiensis* strains also increased significantly when the

experiments were carried out under light-controlled conditions ($p<0.05$). The antifungal activity of anigorufone (**9**) and methoxyanigorufone (**7**) was also significantly light-dependent but only in response to *M. fijiensis* Ca10_13 ($p<0.05$) (Fig. 8). The results also showed that *M. fijiensis* Ca10_13 was not only tolerant to propiconazole but also to the phenylphenalenones assessed in this study. This became especially evident by comparing the growth of the strain E22 treated with anigorufone (**9**), irenolone (**4**) (under darkness only, $p<0.05$) and methoxyanigorufone (**7**) (under darkness and photoperiod treatments, $p<0.001$) with the growth of the strain Ca10_13 under the same conditions (Fig. 8).

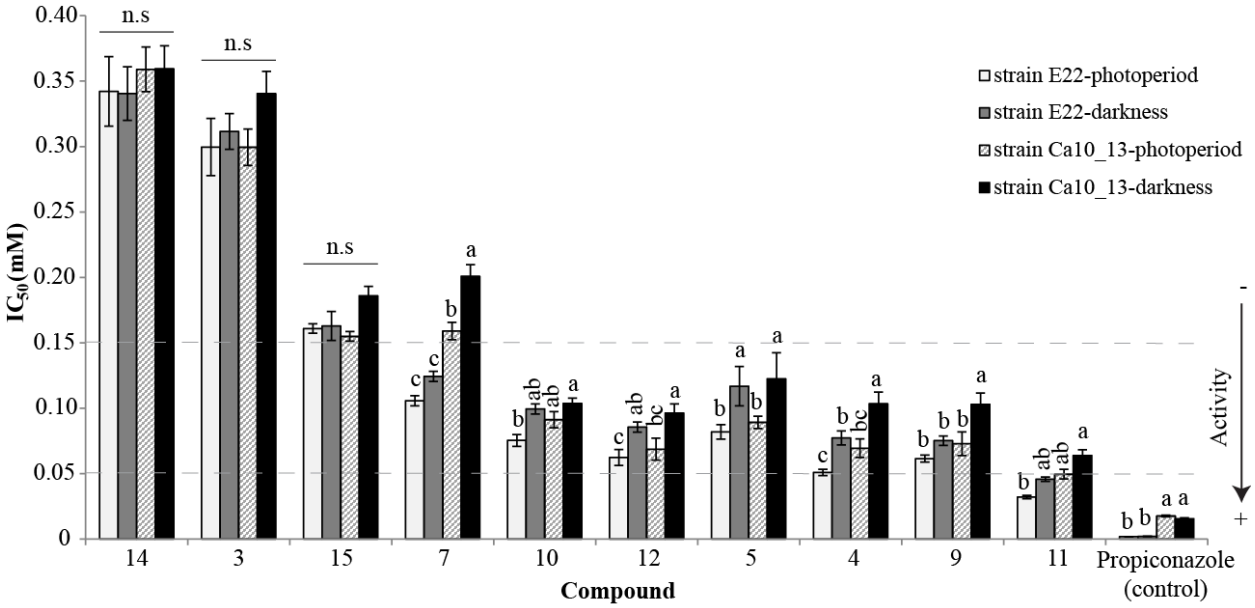

Fig. 8. Half maximal inhibitory concentration (IC_{50}) of the major inducible metabolites found in both *Musa* varieties during infection with *M. fijiensis*. Letters a - c indicate significant differences among treatments within the specified compound (Two-Way ANOVA, Holm-Sidak *post hoc* test: $P<0.001$; n.s: not significant). For chemical structures of compounds **3** – **5**, **7**, **9** – **12**, **14** and **15**, see Table 2.

Metabolism of phenylphenalenones by the fungus

Motivation. The finding that, despite of the induced production of antifungal phenylphenalenones, the BLSD symptoms caused by *M. fijiensis* strains E22 and Ca10_13

increased not only on the leaves of the susceptible *Musa* variety 'Williams' but also on the leaves of the resistant variety 'KTR' (for the case when the infection experiments were carried out with the strain Ca10_13), raised the question about the mechanism which enables the fungus to counteract the plant defense. The metabolism of defense chemicals is one of the most important ways the resistance of a plant is overcome by the pathogen (Morrissey & Osbourn 1999; Pedras & Ahiahonu 2005). The decreasing concentration of some of the most active antifungal compounds, especially anigorufone (**9**), during the progressing disease supported the suggestion that metabolic deactivation might be involved in the virulence mechanism of *M. fijiensis*. Therefore, selected phenylphenalenones were incubated under *in vitro* conditions with the fungus, and the mycelium and the fungal medium were screened for potential metabolites. Strain Ca10_13 was used in these experiments because of its stronger virulence compared to strain E22. Phenylphenalenones were applied at a concentration of 50% of the IC_{50}. In addition to chemical analysis of phenylphenalenone-derived metabolites, clues for the plant-fungus interaction such as the fungal biomass, the extracellular protein level and ergosterol concentration were determined.

Fungal biomass production during incubation with phenylphenalenones. Seven phenylphenalenone-type compounds were incubated at three different concentrations (10, 20 and 40 ppm) with the *M. fijiensis* strain Ca10_13. The results showed that anigorufone (**9**), 4′-*O*-methylirenolone (**12**) and 2-phenyl-1,8-naphthalic anhydride (**3**) did not affect the production of biomass in comparison with the control (Fig. 9). However, incubation with isoanigorufone (**11**), hydroxyanigorufone (**5**) and 4′-*O*-methylanigorufone (**10**) resulted in a biomass production up to ~ 80% in comparison with the control. The inhibition of the growth of fungal mycelium by compounds **5** and **10** was significantly dose-dependent (Fig. 9). Interestingly, already the lowest applied concentration (10 ppm) of methoxyanigorufone (**7**) significantly inhibited the biomass production to approximately 80% of the control. At concentrations of 20 and 40 ppm, biomass production was dramatically reduced to approximately 30% of the control, demonstrating that the microorganism was enormously affected by this particular compound but not the other compounds.

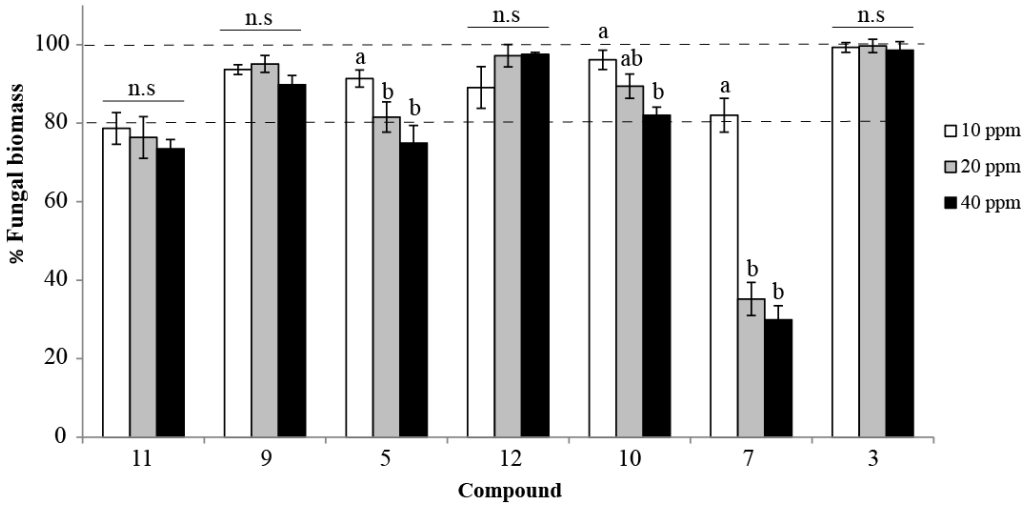

Fig. 9. Biomass produced by *M. fijiensis* strain Ca10_13 under *in vitro* treatment with different phenylphenalenone-type compounds assessed at 10, 20 and 40 ppm. Data were normalized for final biomass determination based on the growth of the non-treated fungus (control). Letters a - b indicate significant differences among treatments with the specified compound (Two-Way ANOVA, Holm-Sidak *post hoc* test: $P<0.001$; n.s: not significant). For chemical structures of compounds **3**, **5**, **7**, and **9** – **11**, see Table 2.

Extracellular protein production. Extracellular microbial proteins can be involved in the degradation and deactivation of chemical defenses of competing organisms (Morrissey & Osbourn 1999; Pedras & Ahiahonu 2005). Therefore, the production of soluble extracellular proteins was analyzed in the culture medium in which the fungus was incubated with phenylphenalenone-type compounds found in both *Musa* varieties. The aim of the analysis was to find out whether individual phenylphenalenones have a promoting or inhibiting effect on the protein production of the microorganism. The results showed clearly that isoanigorufone (**11**) and methoxyanigorufone (**7**) significantly induced the production of extracellular proteins in a dose-dependent manner and caused pronounced increase when concentrations of 20 and 40 ppm were applied (Fig. 10). However, no significant differences in comparison with the control were found when the fungal culture was incubated with anigorufone (**9**), 4′-*O*-methylirenolone (**12**), 4′-*O*-methylanigorufone (**10**) and 2-phenyl-1,8-naphthalic anhydride (**3**). Interestingly, hydroxyanigorufone (**5**) reduced the production of extracellular proteins to approximately 50% that of the control.

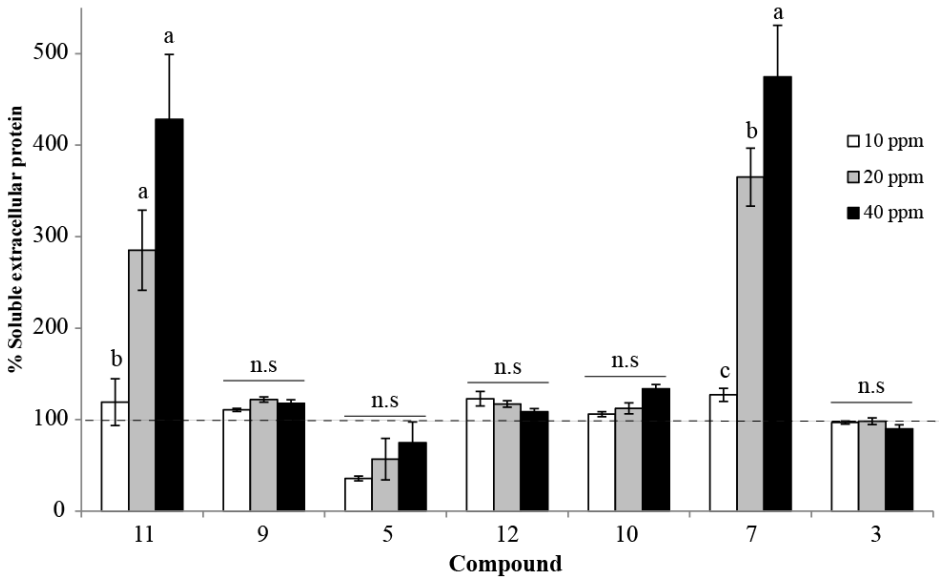

Fig. 10. Soluble extracellular protein produced in *in vitro* culture medium of *M. fijiensis* strain Ca10_13 after incubation with phenylphenalenone-type compounds at 10, 20 and 40 ppm. Data were normalized based on the total soluble extracellular protein determined to the non-treated fungal incubation (control). Letters a - c indicate significant differences among treatments with the specified compound (Krustal-Wallis One-way ANOVA on Ranks, Tukey test: $P<0.05$; n.s: not significant). For chemical structures of compounds **3**, **5**, **7**, and **9** – **11**, see Table 2.

Quantification of ergosterol by ^{1}H NMR analysis. Ergosterol is the major sterol of the fungal cell membranes and an important target molecule for many fungicides which exert their mode of action through the inhibition of its biosynthesis (Debieu *et al.* 1998, 2013; Spotts & Cervantes 1986). In order to test whether phenylphenalenones affect ergosterol biosynthesis in *M. fijiensis*, a ^{1}H NMR-based quantification approach was used. Again, isoanigorufone (**11**) and methoxyanigorufone (**7**) were the metabolites that differ in their activity from the other compounds assessed. For **11**, a significant increase was observed when the compound was assessed at 10 and 20 ppm, but this was not the case for the concentration of 40 ppm, where the production of ergosterol was only slightly above the control level (Fig. 11). During the incubation with hydroxyanigorufone (**5**) an increase of the ergosterol concentration of 40% in comparison with that of the control was observed only when 20 ppm of the phenylphenalenone was applied. A similar increase of the ergosterol concentration was detected with 4′-*O*-methylirenolone (**12**), but no dose-dependence was observed in this case. In contrast to treatment

with compounds **5** and **12**, and especially with isoanigorufone (**11**), which all resulted in an enhanced ergosterol concentration, incubation of the fungus with methoxyanigorufone (**7**) drastically inhibited the production of ergosterol since it was not detectable at concentrations of 20 and 40 ppm. Anigorufone (**9**) and 2-phenyl-1,8-napthalic anhydride (**3**) did not show significant differences in comparison with the control, and no dose-dependence was detected.

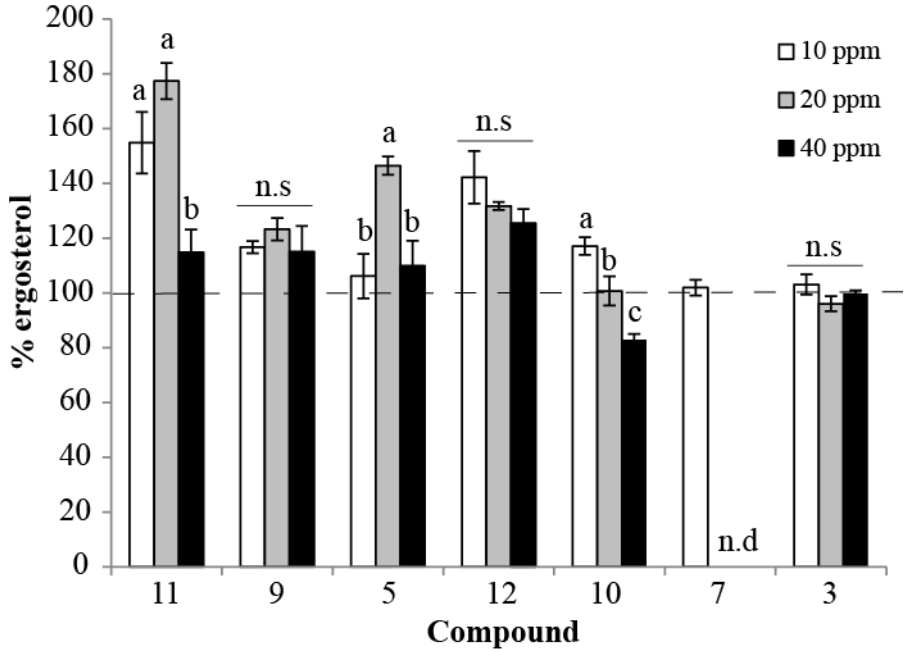

Fig. 11. Ergosterol production by *M. fijiensis* strain Ca10_13 after *in vitro* incubation with different phenylphenalenone-type compounds at 10, 20 and 40 ppm. Data were normalized based on the total ergosterol production determined for the non-treated fungal culture (control without phenylphenalenones). Letters a - c indicate significant differences among treatment (concentration) with the specified compound (Two-Way ANOVA, Holm-Sidak *post hoc* test: $P<0.001$; n.s: not significant). n.d: not detected. For chemical structures of compounds **3**, **5**, **7**, and **9** – **11**, see Table 2.

Quantification of phenylphenalenones in M. fijiensis *cultures.* The question of whether phenylphenalenone-type compounds are taken up by the mycelial tissue or persist in the medium during incubation with the fungus was assessed by HPLC. Fungal cultures of strain Ca10_13 were incubated for 8 days with three different concentrations (10, 20 and 40 ppm) of the corresponding phenylphenalenones, as described above. Each phenylphenalenone was then

quantitatively determined in the medium as well as in the mycelium. The results showed a very different distribution of the phenylphenalenones between the medium, the mycelium, and a non-recovered portion of the compounds (Fig. 12).

A considerable portion of most compounds persisted in the medium. For compounds **9** - **12**, this portion was between 27 and 45 % at the lowest concentration tested and increased up to approximately 70 to 80 % at the highest concentration. Simultaneously, a certain percentage of compounds **9** – **12** accumulated in the mycelium biomass and showed a tendency to decline at higher doses of the applied compounds. According to the data shown in Fig. 12, the portions of compounds **9** – **12** detected in the medium and in the fungal mycelium do not sum up to 100%: an essential portion was missing, exceeding 40% in some cases. Again, the non-recovered portion tends to decline with increasing doses of the applied compounds.

However, generalizing with regard to the data is problematic and an individualized consideration of the distribution pattern of most compounds seems to be reasonable, at least in the case of hydroxyanigorufone (**5**) and compounds **3** and **7**. Remarkably, compound **5** was no longer detectable after incubating a dose of 10 ppm with *M. fijiensis* strain Ca10_13, and even more than 70% of the highest applied dose of 40 ppm remained unrecovered. Unlike all other phenylphenalenones applied, methoxyanigorufone (**7**) and 2-phenyl-1,8-naphthalic anhydride (**3**) were taken up by the mycelium only to a relatively small (~ 10% for 7) or even negligible extent (**3**), that is, they remained mostly unchanged in the medium. For compound **3,** this finding coincided with its inactivity on the biomass production of *M. fijiensis* strain Ca10_13 as shown in Fig. 9.

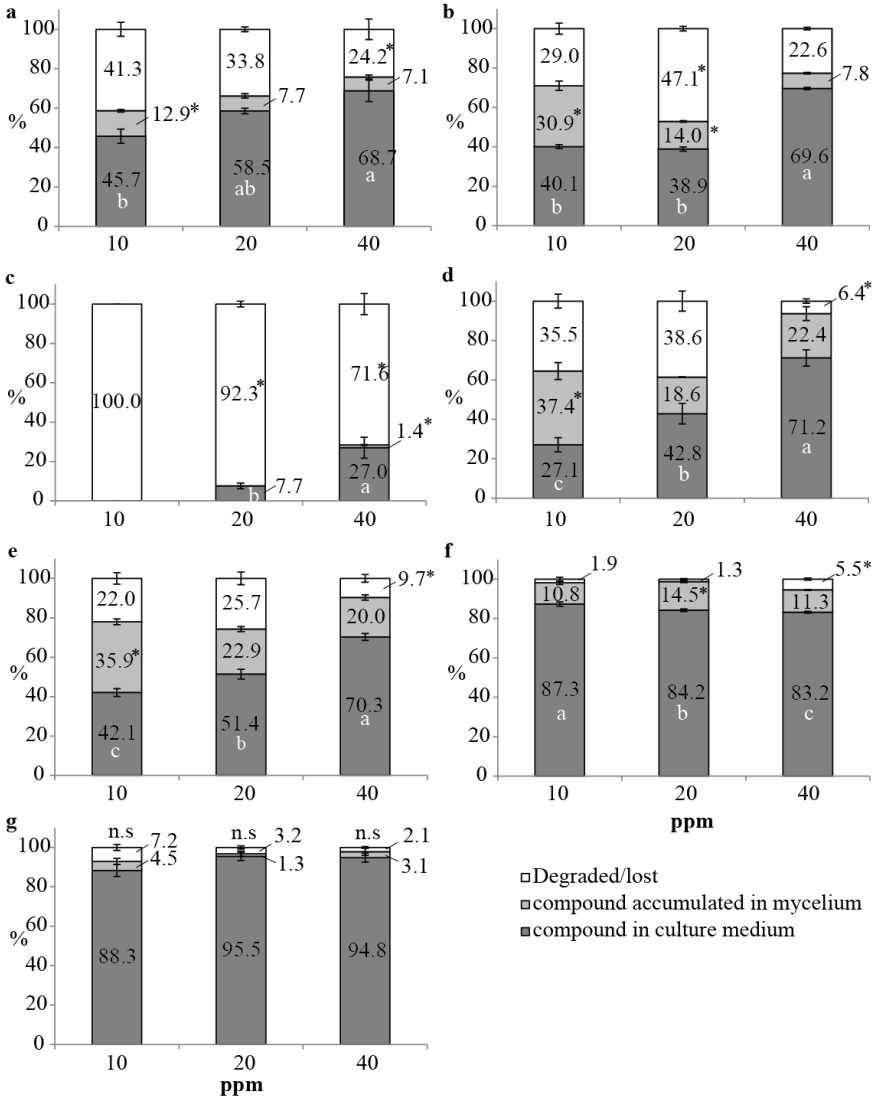

Fig. 12. Quantification of phenylphenalenones after incubation of *M. fijiensis* strain Ca10_13 with different doses (10, 20 and 40 ppm) of the specified compound. Data were normalized as a percentage based on the peak area generated by HPLC-DAD analysis of the negative controls of each compound. Phenylphenalenone recovery from culture medium (dark gray bars), mycelium (light gray bars) and the unrecovered portions of phenylphenalenones were determined as the difference between the applied dose and the concentration determined in the medium and the mycelium after 8 d of incubation (white bars). Panel **a**: isoanigorufone (**11**); **b**: anigorufone (**9**); **c**: hydroxyanigorufone (**5**); **d**: 4′-*O*-methylirenolone (**12**); **e**: 4′-*O*-methylanigorufone (**10**); **f**: methoxyanigorufone (**7**) and **g**: 2-phenyl-1,8-napthalic anhydride (**3**). Different letters or asterisks indicate significant differences among treatments (concentrations) of the compound analyzed (One-Way ANOVA, Holm-Sidak *post hoc* test: $P<0.05$; n.s: not significant).

Metabolism of phenylphenalenones by the fungus. The extensive (compounds **9** – **12**) or even complete (compound **5** at 10 ppm) disappearance of phenylphenalenones (Fig. 12) during incubation with the fungus could be explained by metabolic processes. Therefore, in the next step of this study, the mycelium and the culture medium were analyzed for potential metabolites of phenylphenalenones. In an up-scaled incubation experiment with *M. fijiensis* strain Ca10_13, synthetic anigorufone (**9**) was used as a model compound to study the metabolism. Except for the parent compound **9**, no phenylphenalenone-related compound was detected in the liquid culture medium, and the HPLC trace of the medium was identical with that of the control sample (data not shown).

However, an additional peak, which was not present in the control sample, emerged in the UV and selected ion chromatograms (LC-MS, positive ion mode) of the methanolic mycelium extract (Fig. 13). The mass spectrum of this peak (R_t = 7.95 min) displayed a molecular ion of *m/z* 353.2 $[M+H]^+$ and a fragment ion of *m/z* 273.2, suggesting a metabolite of compound **9**. HR-MS analysis confirmed the fragment ion as anigorufone (**9**) ($[M+H]^+$ found: *m/z* 273.0908, calc.: *m/z* 273.0916) and the molecular ion peak *m/z* 353.0475 ($[M+H]^+$) was consistent with a sulfated metabolite of **9** ($[M+H]^+$ calc.: *m/z* 353.0484). Since the hydroxyl group in position 2 of anigorufone (**9**) is the only place where a sulfate group could be attached to the molecule, the new metabolite must be anigorufone-2-sulfate (Fig. 13).

After anigorufone-2-sulfate was identified as a metabolite of anigorufone (**9**), the mycelia and extracts obtained after incubation of further phenylphenalenones were also analyzed by UPLC-HRMS for sulfate metabolites. While no such compounds were detected in the culture media, the mass spectra of the methanolic extracts of mycelia incubated with compounds **10** to **12** displayed not only peaks of the parent compounds but also characteristic peaks of corresponding sulfate conjugates (Table 3). Like anigorufone (**9**), compounds **10** to **12** have a single hydroxyl group at C-2 and therefore the sulfate unit of their conjugates must be attached to this particular position. A sulfate conjugate was also found for hydroxyanigorufone (**5**) (Table 3).

As in the conjugates of compounds **10** to **12**, the position of the sulfate in the hydroxyanigorufone conjugate was arbitrarily assigned to the ortho-hydroxyketone functionality,

although two hydroxyl groups, 2-OH and 4'-OH, are available in this special case. No sulfate conjugate was produced during incubation of the methoxyanigorufone (**7**) with the fungus. This was not unexpected because no free hydroxyl group was available in this structure. Furthermore, as shown in Fig. 12, the uptake of compound **7** into the mycelia was very limited.

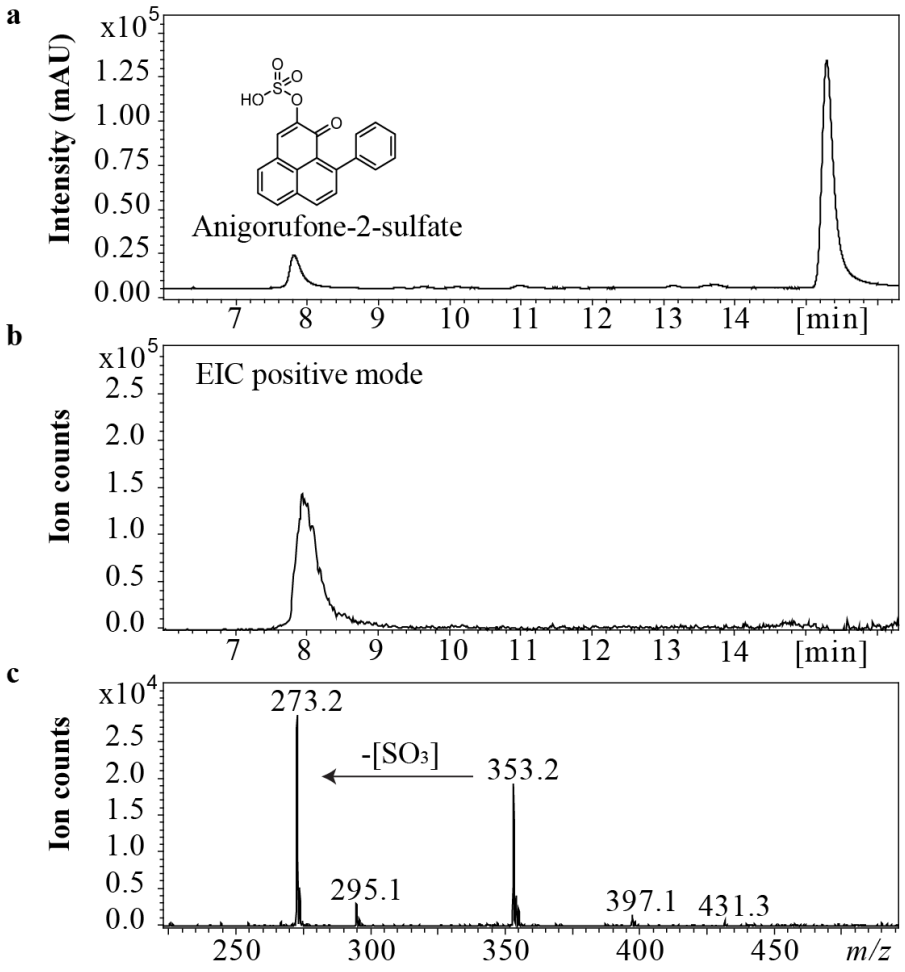

Fig. 13. LC-ESIMS analysis of anigorufone (**9**) and its metabolite in the methanolic extract of *M. fijiensis* Ca10_13 mycelium. Panel **a**: UV chromatogram at 254 nm displaying peaks of anigorufone (R_t = 15.3 min) and an anigorufone-derived metabolite (R_t = 7.8 min) identified as anigorufone-2-sulfate. Panel **b**: Extracted ion chromatogram (EIC) at *m/z* 353.2 $[M+1]^+$, the mass corresponding to anigorufone-2-sulfate; Panel **c**: Mass spectrum of anigorufone-2-sulfate obtained at R_t = 7.8 min showing the molecular ion peak *m/z* 353.2 $[M+H]^+$ and the fragment ion peak of *m/z* 273.2, corresponding to anigorufone (**9**).

Table 3. Phenylphenalenone sulfates identified in methanolic extracts of mycelia after incubation of the parent phenylphenalenones with *M. fijiensis* Ca10_13.

Entry (PP)	Parent compound	Product	t_R (min)*	HRMS (*m/z*, amu)	
				Calc.	Found
5	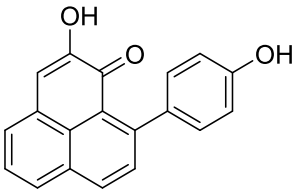	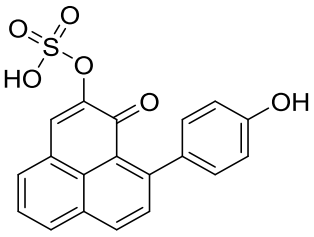 **	9.52	$[M+H]^+$ 369.0433	$[M+H]^+$ 369.0428
7	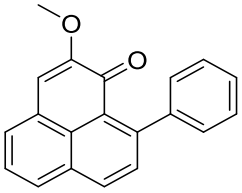	No metabolite detected	-	-	-
9	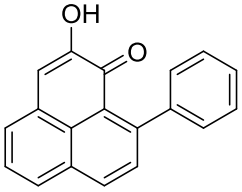	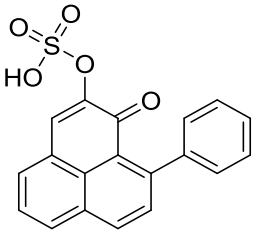	13.27	$[M+H]^+$ 353.0484	$[M+H]^+$ 353.0475
10	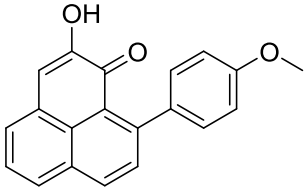	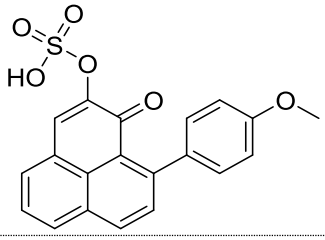	14.21	$[M-H]^-$ 381.0438	$[M-H]^-$ 381.0435
11	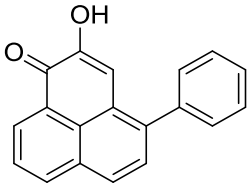	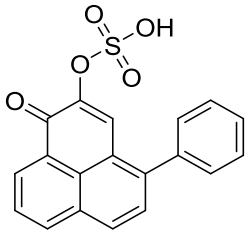	11.78	$[M+H]^+$ 353.0484	$[M+H]^+$ 353.0475
12	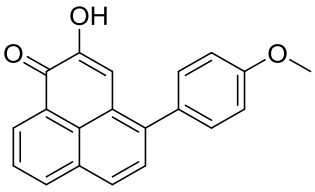	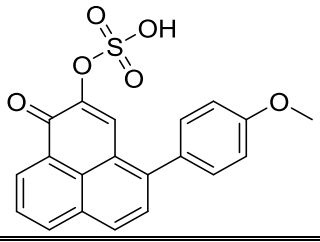	14.53	$[M-H]^-$ 381.0438	$[M-H]^-$ 381.0436

*Retention time of the phenylphenalenone sulfate-derivative (data from UHPLC-ESI-MS analysis).
**The isomeric hydroxyanigorufone-4'-sulfate cannot be excluded from the available HRMS data.

DISCUSSION

Monitoring *Musa's* metabolic responses during *M. fijiensis* attack

^{1}H NMR-based metabolomics revealed similar biochemical profiles for both *Musa* varieties, 'Williams' (susceptible) and 'Khai Thong Ruang' (resistant), in response to their interaction with the fungus *Mycosphaerella fijiensis*. Indeed, infection by this pathogen not only triggered the primary metabolism but also strongly affected the biosynthesis of specialized metabolites, especially aromatic compounds. These effects of infection were inferred from evaluating the group discrimination of each *Musa* plant part after the principal component analysis and the corresponding loading plots (Fig. 3). While the levels of carbohydrates, represented mainly by glucose and sucrose, rose in the infected plant tissue, the levels of most amino acids (such as L-alanine and L-threonine) declined. L-Methionine was an exception and tended to be more up-regulated in the infected *Musa* plants than in the non-treated plants. These findings confirm previous reports of plant-pathogen interactions that suggest that the translocation of sugars from the roots or other plant organs to the infected tissue may help counteract the metabolic imbalances caused by microbial invaders (Heil & Bostock 2002).

Carbohydrates are also involved in the biosynthesis of a broad spectrum of specialized metabolites and can mediate the gene expression of pathogenesis-related (PR) proteins (Aliferis *et al.* 2014; Herbers *et al.* 1996; Herbers *et al.* 2000; Scharte *et al.* 2005). Gene expression demands a substantial pool of amino acids for the synthesis of proteins commonly associated with the defense against pathogens. For example, chitinases and glucanases have been reported to play a role in the interaction between *Musa* and *M. fijiensis* and in other plant pathosystems (Harish *et al.* 2009; Torres *et al.* 2012). The production of defense-related proteins could explain the reduced content of amino acids found in the infected plant tissue of both *Musa* varieties. Surprisingly, L-methionine, which was the only amino acid positively regulated during the infection, may be associated with enzymatic reactions that make up the methionine *S*-methyltransferases involved in the *O*-methylation of some phenylpropanoids and phenylphenalenones-type compounds, as has been reported by Otálvaro et al. (Otálvaro, *et al.* 2010).

An enhanced number of signals in the ^{1}H NMR region from δ 6.0-9.0 were the most relevant features observed in the loading plots (Fig. 3) of both *Musa* varieties. Phenolic metabolites were more strongly up-regulated in the infected local tissue of the resistant variety 'KTR' than in the infected local tissue of the susceptible variety 'Williams', thus providing the first hints that the two varieties respond differently to the infection with the pathogen.

Dopamine, an animal neurotransmitter also occurring in plants (Kulma & Szopa 2007; Li *et al.* 2015), is a catecholamine identified previously in banana fruits (Kanazawa & Sakakibara 2000). In our experiments it was found in *Musa* leaves. We observed that it declined in the non-treated areas of infected plants (Fig. 2, samples B and D). Simultaneously, a positive correlation was observed for dopaol-β-D-glucoside, identified for the first time in healthy *Musa* plant tissue. Dopamine was thought to serve as a substrate in the biosynthesis of its glucoside, which then played a role as a phytoalexin. However, this assumption was ruled out since dopaol-β-D-glucoside (and dopamine as well) did not show any antifungal properties against *M. fijiensis* (Fig. S2). Thus, the role of those metabolites in *Musa* plant defense remains to be studied.

A group of phenylpropanoid conjugates was identified for the first time as constituents of *Musa* plants (Table 1, entries 14-17). 1'-*O*-(*E*-4-Coumaroyl)-β-glucoside may function as a depot compound which, after being hydrolyzed to *p*-coumaric acid by a putative cell wall-associated β-glucosidase (Chong *et al.* 1999; Chong *et al.* 2002), could be used as a precursor for the biosynthesis of phenylphenalenone-type compounds (Hölscher & Schneider 1995; Schmitt *et al.* 2000). This phenomenon could explain the reduced levels of such phenylpropanoids in the infected tissue. Moreover, phenylpropanoids are not only involved in the biosynthesis of phytoalexins of the phenylphenalenone-type but also play a role in lignification processes in order to counteract the invading pathogen (Liang *et al.* 2006).

Irenolone (**4**) and hydroxyanigorufone (**5**), the two major phenylphenalenones identified from the metabolomic analysis (Table 1), were induced only in the infected plant tissue; along with other phenolic compounds, these major phenylphenalenones constituted the chemical basis for the *Musa* response to *M. fijiensis*. Unfortunately, due to the overlapping ^{1}H NMR signals,

metabolic changes of the other phenolics could be not observed in the loading plots (Fig. 3) but, rather, required a conventional phytochemical approach.

Incompatible *Musa-M. fijiensis* interaction depends on the pathogen virulence

Phytochemical analysis of the infected *Musa* tissue led to identify fifteen phenylphenalenone-type compounds and structural analogs from the resistant variety 'KTR'. A smaller number (ten) of such metabolites appeared in the defense response of the susceptible variety 'Williams'. With the exception of 2-hydroxy-9-(4'-methoxyphenyl)-1*H*-phenalen-1-one (**10**), all other compounds had been previously reported in different varieties of *Musa,* and their occurrence has been correlated with the resistance phenotype exhibited by some *Musa* varieties against pathogens and herbivores (Hölscher, *et al.* 2014; Otálvaro, *et al.* 2007). Nonetheless, there has been little quantitative analysis of phenylphenalenones as BLSD progresses, and resistant traits have not been studied with isolates of *M. fijiensis* that differ in their virulence. Therefore, two strains of *M. fijiensis,* E22 and Ca10_13, were used as inoculum. According to the method proposed by Cañas et al. (Cañas-Gutierrez, *et al.* 2009), the strain E22 was classified as 'sensitive' and Ca10_13 as 'tolerant' to the fungicide propiconazole. It is important to note that sensitivity to the fungicide propiconazole does not necessarily correlate with a high degree of virulence of the pathogen. However, fungicide tolerance could help the microorganism overcome the plant's chemical defense and/or synthetic fungicides.

For the variety 'KTR', an early response was observed by the appearance of small specks on the lower surface of the infected leaf 7-9 dpi with the fungus, regardless of which *M. fijiensis* strain was used; no symptoms were detectable in the variety 'Williams' up to 15-17 dpi (Table S1). This difference between varieties is not surprising since an early recognition of virulence effectors from the pathogen triggers the defense mechanism in *Musa* (as they do in other plant-pathogen systems), conferring resistance on plants that are attacked (Hoss *et al.* 2000; Jacome *et al.* 2002; Torres, *et al.* 2012).

The resistance conferred on *Musa* 'KTR' in its interaction with *M. fijiensis* strain E22 was confirmed by the slow progress of BLSD determined at the two points of time. In contrast, *M.*

fijiensis Ca10_13 not only exhibited a higher degree of virulence than E22 but also was able to overcome the resistance of 'KTR' and cause severe foliar damages in the infected leaf (Fig. 5, Table S1). According to previous reports, the breakdown of the resistance in *Musa* caused by *M. fijiensis* has also been observed in other *Musa* varieties such as the variety 'Yangambi Km5', which is classified as highly resistant to this particular pathogen (Fullerton & Olsen 1995; Mouliom-Pefoura 1999).

For the variety 'Williams', the necrotic symptoms of BLSD were larger than those observed for 'KTR' during the progress of the fungal infection; this difference was expected for a susceptible variety. Nonetheless, leaf damage was increased when *M. fijiensis* Ca10_13 was used as a pathogen, confirming the strong virulence of this pathogen.

Priming defense mechanisms in plants at early stages of infection, after the recognition of the effectors signals produced by a pathogen, are crucial in the incompatible plant-pathogen interactions (Conrath *et al.* 2006; Frost *et al.* 2008). As demonstrated for some resistant *Musa* varieties, the production of pathogenesis-related proteins, lignification processes, hypersensitivity response (HR) and accumulation of phytoalexins must work in a concerted action in order to enable plants to block pathogenesis and herbivory (Harelimana *et al.* 1997; Hölscher *et al.* 2014; Otálvaro *et al.* 2002; Quiñones *et al.* 2000; Torres *et al.* 2012).

Here, the BLSD symptoms appearing on the leaves of the 'KTR' variety after infection with the strain Ca10_13 clearly demonstrated that resistance in this *Musa* variety could be overcome by a highly virulent pathogen. Analysis of the chemical composition of both *Musa* varieties during their responses to the two fungal strains showed that phenylphenalenone-type compounds constituted the major induced metabolites both in 'Williams' as well as in 'KTR'. The susceptible variety 'Williams' produced not only a smaller number but also lower levels of these metabolites (less than 10 nmol mg^{-1} DW) compared to 'KTR'. Hydroxyanigorufone (**5**) appeared to be the exception: it was the most prominent compound synthesized in 'Williams' in response to the strain Ca10_13. Nevertheless, as the disease developed, the concentration of hydroxyanigorufone (**5**) and anigorufone (**9**) decreased, while that of other compounds (e.g. **1**-**4**) stayed constant or even slightly increased. The reduced levels of compounds **5** and **9** at 50 dpi could be due to an

oxidative metabolic reaction and may result in the naphthalic anhydrides **1** and **3**, respectively. Reactive oxygen species like hydrogen peroxide, which have been reported to be produced in the infected tissue of *Musa* plants (Torres *et al.* 2012), could function as the oxidizing agent. In 'Williams', the susceptibility seemed to be associated with a late recognition of the pathogen which then successfully colonizes the plant tissue. This is consistent with a relatively low total level of phenylphenalenones (Fig. 7), although hydroxyanigorufone (**5**), which is one of the active phenylphenalenones (Fig. 8), was overproduced in comparison with the other metabolites (Fig. 6).

In contrast, the 'KTR' variety not only rapidly recognized the pathogen but it also responded with a burst of phenylphenalenones, providing an enhanced chemical response to both fungal strains. This variety produced a number of phenylphenalenones in concentrations over 10 nmol mg^{-1} DW; irenolone (**4**) was the most abundant compound (> 25 nmol mg^{-1} DW) (Fig. 6). Compound **4** and its congeners seemed to have a strong inhibiting effect on the fungal colonization of plant tissue infected by the strain E22 but not on tissue infected by Ca10_13 (Fig. 6). The response of the two *Musa* varieties to the two fungal strains E22 and Ca10_13 produced slight quantitative differences but no qualitative differences in the metabolic patterns (data not shown).

In 'KTR', the concentrations of compounds **2** - **4**, **12** and **14** increased significantly in response to Ca10_13 at 25 or 50 dpi but not in the response to the strain E22. Irenolone (**4**) was the metabolite with the highest response against Ca10_13 at 50 dpi in comparison with all other induced metabolites (Fig. 6a). This finding suggests that, at least from the chemical point of view, 'KTR' was able to distinguish between the virulence capacities of the fungal strains.

Pathogen virulence associated with metabolism of phenylphenalenones

The breakdown in the resistance of 'KTR' caused by the virulent strain Ca10_13 encouraged us to explore whether some phenylphenalenones (e.g. compounds **3**, **9**, **11**, **12**), although up-regulated in response to *M. fijiensis*, did not significantly inhibit the growth of this particular fungus in planta. The antifungal bioassay showed that phenylphenalenones were active against

both fungal strains (Fig. 8). The fungal pathogen E22 was more sensitive in comparison with Ca10_13 when irenolone (**4**), anigorufone (**9**), isoanigorufone (**11**) and methoxyanigorufone (**7**) were assessed under dark conditions. Furthermore, these compounds displayed an enhanced antifungal activity when light conditions were applied to the experimental system (Fig. 8). Phenylphenalenones (Flors & Nonell 2006; Lazzaro *et al.* 2004) and perinaphthenones (Hidalgo *et al.* 2009) have been reported to be light-dependent singlet oxygen producers, and these could significantly affect the fungal growth rate. Overall, the hypothesis that *M. fijiensis* strain Ca10_13 could tolerate higher concentrations of phenylphenalenones than the strain E22 was found to hold only for some compounds and under darkness.

Differences in the fungal growth rate between both *M. fijiensis* strains became more apparent when the incubation experiments were scaled-up to almost ten times the volume of liquid culture used for the microtiter bioassay. The growth rate of *M. fijiensis* strain E22 was much slower than that of strain Ca10_13 when phenylphenalenones in the range of 10 to 40 ppm were supplied in the incubation medium; hydroxyanigorufone (**5**) and 2-phenyl-1,8-naphthalic anhydride (**3**) were the exceptions (data not shown). Therefore, the strain Ca10_13 was selected for further experiments. Since some plant pathogens have developed strategies to evade plant defenses through a complex detoxification process (Barz & Welle 1992; Jeandet *et al.* 2010; Pedras & Taylor 1993), we wondered whether the resistance of *M. fijiensis* to some phenylphenalenones could be attributed to metabolic detoxification.

In fact, the strain Ca10_13 was able not only to metabolize most of the compounds into sulfate-derivatives (compounds **5, 9-12**; Table 3) but also to further degrade them into undetectable metabolites or even decompose them completely as in the case of hydroxyanigorufone (**5**) at the lowest concentration assessed. In general, the formation of sulfate conjugates through sulfotransferases constitutes a biochemical reaction which is involved in such physiological processes as intracellular signaling, extracellular interactions and detoxification of xenobiotics (Chapman *et al.* 2004; Zhang *et al.* 1996). The present work is the first report of an inactivation or detoxification of phenylphenalenones by *M. fijiensis* through sulfate conjugation. Also, to the best of our knowledge, ours is the first report of a detoxification reaction of any phenylphenalenone by a fungal organism. New strategies to control BLSD through inhibitors

that target sulfotransferases in the microorganism may result from this new understanding of the role of sulfate conjugates.

Interestingly, only phenylphenalenones containing a hydroxyl group attached to C-2 in the molecule were found to be sulfated (for hydroxyanigorufone, a sulfation in the free hydroxyl group at C–4' cannot be ruled out). Since conversion to sulfates seems to minimize the toxic effects of most phenylphenalenones, the fungal biomass production remained almost unaffected (Fig. 9). However, methoxyanigorufone (**7**), a metabolite which is missing a hydroxyl group (instead of the OH, an *O*-methyl group is attached to C-2), enormously affected growth and biomass production (Fig. 9). This supports the hypothesis that an α-hydroxyketone feature helps the molecule to be recognized by the aryl sulfotransferase. In addition, the chemical pressure generated by compound (**7**) on the metabolism of the strain Ca10_13 was confirmed by the overproduction of soluble extracellular proteins (Fig. 10) and the inhibited production of ergosterol (Fig. 11). Since no metabolites derived from phenylphenalenones were found in the liquid culture medium during the incubation with the fungus, the overexpression of extracellular proteins observed in response to compounds **7** and **11**, could not be associated with the external enzymatic detoxification of these metabolites. Instead, detoxification may suggest that these metabolites increase the physiological stress in the fungus, which then results in the overexpression of fungal proteins involved in the suppression of the plant defenses (Dodds & Rathjen 2010; Escobar *et al.* 2015). Identification of the proteins which were overexpressed by the interaction with specific phenylphenalenones would help explain the pathophysiological processes taking place during the interaction between *Musa* and *M. fijiensis*. Because of their role in the defense of *Musa* plants against *M. fijiensis*, methoxyanigorufone (**7**) and isoanigorufone (**11**) are considered the most relevant metabolites for further exploration of the molecular mode of phenylphenalenones.

ACKNOWLEDGMENTS

The authors thank Tamara Krügel and the greenhouse team of the Max Planck Institute for Chemical Ecology (Jena, Germany) for plant cultivation, Gert Kema (Plant Research International, Wageningen, The Netherlands) for kindly providing *M. fijiensis* strains and Emily

Wheeler for editorial assistance. This study was supported by the Max Planck Institute for Chemical Ecology and Colciencias (Bogotá, Colombia) by scholarships to W.H.

REFERENCES

Abadie C., Zapater M.F., Pignolet L., Carlier J. & Mourichon X. (2008) Artificial inoculation on plants and banana leaf pieces with *Mycosphaerella spp.* responsible for Sigatoka leaf spot diseases. *Fruits*, **63**, 319-323.

Ali K., Maltese F., Zyprian E., Rex M., Choi Y.H. & Verpoorte R. (2009) NMR metabolic fingerprinting based identification of grapevine metabolites associated with Downy mildew resistance. *Journal of Agricultural and Food Chemistry*, **57**, 9599-9606.

Aliferis K.A., Faubert D. & Jabaji S. (2014) A metabolic profiling strategy for the dissection of plant defense against fungal pathogens. *Plos One*, **9**, 1-13.

Arzanlou M., Abeln E.C.A., Kema G.H.J., Waalwijk C., Carlier J., de Vries I., Guzman M. & Crous P.W. (2007) Molecular diagnostics for the sigatoka disease complex of banana. *Phytopathology*, **97**, 1112-1118.

Banerjee N. & Delanghe E. (1985) A tissue-culture technique for rapid clonal propagation and storage under minimal growth-conditions of *Musa* (Banana and Plantain). *Plant Cell Reports*, **4**, 351-354.

Barz W. & Welle R. (1992) Biosynthesis and metabolism of isoflavones and pterocarpan phytoalexins in chickpea, soybean and phytopathogenic fungi. *Phenolic Metabolism in Plants*, **26**, 139-164.

Cañas-Gutierrez G.P., Angarita-Velasquez M.J., Restrepo-Florez J.M., Rodriguez P., Moreno C.X. & Arango R. (2009) Analysis of the CYP51 gene and encoded protein in propiconazole-resistant isolates of *Mycosphaerella fijiensis*. *Pest Management Science*, **65**, 892-899.

Carlier J., De Waele D. & Escalant J.V. (2002) Global evaluation of Musa germplasm for resistance to Fusarium wilt, Mycosphaerella leaf spot diseases and nematodes: in-depth evaluation. INIBAP, Montpellier (FRA)

Chabrier C. & Queneherve P. (2003) Control of the burrowing nematode (*Radopholus similis Cobb*) on banana: impact of the banana field destruction method on the efficiency of the following fallow. *Crop Protection*, **22**, 121-127.

Chapman E., Best M.D., Hanson S.R. & Wong C.H. (2004) Sulfotransferases: structure, mechanism, biological activity, inhibition, and synthetic utility. *Angewandte Chemie-International Edition*, **43**, 3526-3548.

Chong J., Baltz R., Fritig B. & Saindrenan P. (1999) An early salicylic acid-, pathogen- and elicitor-inducible tobacco glucosyltransferase: role in compartmentalization of phenolics and H_2O_2 metabolism. *FEBS Letters*, **458**, 204-208.

Chong J., Baltz R., Schmitt C., Beffa R., Fritig B. & Saindrenan P. (2002) Downregulation of a pathogen-responsive tobacco UDP-Glc : phenylpropanoid glucosyltransferase reduces scopoletin glucoside accumulation, enhances oxidative stress, and weakens virus resistance. *Plant Cell*, **14**, 1093-1107.

Conrath U., Beckers G.J.M., Flors V., Garcia-Agustin P., Jakab G., Mauch F.,… Mauch-Mani B. (2006) Priming: getting ready for battle. *Molecular Plant-Microbe Interactions*, **19**, 1062-1071.

Debieu D., Bach J., Lasseron A., Malosse C. & Leroux P. (1998) Effects of sterol biosynthesis inhibitor fungicides in the phytopathogenic fungus, *Nectria haematococca*: Ergosterol depletion versus precursor or abnormal sterol accumulation as the mechanism of fungitoxicity. *Pesticide Science*, **54**, 157-167.

Debieu D., Bach, J., Montesinos, E., Fillinger, S. & Leroux, P. (2013) Role of sterol 3-ketoreductase sensitivity in susceptibility to the fungicide fenhexamid in *Botrytis cinerea* and other phytopathogenic fungi. *Pest Management Science*, **69**, 642-651.

Dhakshinamoorthy S., Mariama K., Elsen A. & De Waele D. (2014) Phenols and lignin are involved in the defence response of banana (*Musa*) plants to *Radopholus similis* infection. *Nematology*, **16**, 565-576.

Dodds P.N. & Rathjen J.P. (2010) Plant immunity: towards an integrated view of plant-pathogen interactions. *Nature Reviews Genetics*, **11**, 539-548.

Escobar L., Guzmán M., Sandoval J. & Gómez M. (2015) Comparative analysis of the in vitro and in planta secretomes from *Mycosphaerella fijiensis* isolates. *British Mycological Society*, **119**, 447-470.

Etebu E. & Young-Harry W. (2011) Control of black sigatoka disease: Challenges and prospects. *African Journal of Agricultural Research*, **6**, 508-514.

FAO: Food and Agriculture Organization of the United Nations. (2013) Fight against Black Sigatoka must continue to save small Caribbean banana farms.

FAO (2014) Banana market review and banana statistic 2012-2013. *Intergovernmental group on bananas and tropical fruits*, pp. 39.

FAO (2015) http://www.statista.com/statistics/264001/worldwide-production-of-fruit-by-variety/

Flors C. & Nonell S. (2006) Light and singlet oxygen in plant defense against pathogens: Phototoxic phenalenone phytoalexins. *Accounts of Chemical Research*, **39**, 293-300.

Franzyk H., Olsen C.E. & Jensen S.R. (2004) Dopaol 2-keto- and 2,3-diketoglycosides from *Chelone obliqua*. *Journal of Natural Products*, **67**, 1052-1054.

Frost C.J., Mescher M.C., Carlson J.E. & De Moraes C.M. (2008) Plant defense priming against herbivores: Getting ready for a different battle. *Plant Physiology*, **146**, 818-824.

Fullerton R.A. & Olsen T.L. (1995) Pathogenic variability in *Mycosphaerella fijiensis* Morelet, cause of Black Sigatoka in Banana and Plantain. *New Zealand Journal of Crop and Horticultural Science*, **23**, 39-48.

Harelimana G., Lepoivre P., Jijakli H. & Mourichon X. (1997) Use of *Mycosphaerella fijiensis* toxins for the selection of banana cultivars resistant to black leaf streak. *Euphytica*, **96**, 125-128.

Harish S., Kavino M., Kumar N. & Samiyappan R. (2009) Differential expression of pathogenesis-related proteins and defense enzymes in banana: interaction between endophytic bacteria, Banana bunchy top virus and *Pentalonia nigronervosa*. *Biocontrol Science and Technology*, **19**, 843-857.

Heil M. & Bostock R.M. (2002) Induced systemic resistance (ISR) against pathogens in the context of induced plant defences. *Annals of Botany*, **89**, 503-512.

Herbers K., Meuwly P., Frommer W.B., Metraux J.P. & Sonnewald U. (1996) Systemic acquired resistance mediated by the ectopic expression of invertase: Possible hexose sensing in the secretory pathway. *Plant Cell*, **8**, 793-803.

Herbers K., Takahata Y., Melzer M., Mock H.P., Hajirezaei M. & Sonnewald U. (2000) Regulation of carbohydrate partitioning during the interaction of potato virus Y with tobacco. *Molecular Plant Pathology*, **1**, 51-59.

Heslop-Harrison J.S. (2011) Genomics, banana breeding and superdomestication. *International Ishs-Promusa Symposium on Global Perspectives on Asian Challenges*, **897**, 55-62.

Hidalgo W., Duque L., Saez J., Arango R., Gil J., Rojano B., Schneider B. & Otálvaro F. (2009) Structure activity relationship in the interaction of substituted perinaphthenones with *Mycosphaerella fijiensis*. *Journal of Agricultural and Food Chemistry*, **57**, 7417-7421.

Hirai N., Ishida H. & Koshimizu K. (1994) A phenalenone-type phytoalexin from *Musa-Acuminata*. *Phytochemistry*, **37**, 383-385.

Hölscher D. & Schneider B. (1995) The biosynthetic origin of the central one-carbon unit of phenylphenalenones in *Anigozanthos Preissii*. *Natural Product Letters*, **7**, 177-182.

Hölscher D., Dhakshinamoorthy S., Alexandrov T., Becker M., Bretschneider T., Buerkert, A., …, Swennen R.L. (2014) Phenalenone-type phytoalexins mediate resistance of banana plants (*Musa spp*.) to the burrowing nematode *Radopholus similis*. *Proceedings of the National Academy of Sciences of the United States of America*, **111**, 105-110.

Hölscher D., Fuchser J., Knop K., Menezes R., Buerkert A., Svatoš A., Schubert U. & Schneider B. (2015) High resolution mass spectrometry imaging reveals the occurrence of phenylphenalenone-type compounds in red paracytic stomata and red epidermis tissue of *Musa acuminata* ssp. *zebrina* cv. 'Rowe Red'. *Phytochemistry*, **116**, 239-245.

Hoss R., Helbig J. & Bochow H. (2000) Function of host and fungal metabolites in resistance response of banana and plantain in the Black Sigatoka disease pathosystem (*Musa* spp. *Mycosphaerella fijiensis*). *Journal of Phytopathology*, **148**, 387-394.

Huang S.X., Liao X., Nie Q.J., Ding L.S. & Peng S.L. (2004) Phenyl and phenylethyl glycosides from *Picrorhiza scrophulariiflora*. *Helvetica Chimica Acta*, **87**, 598-604.

Jacome L., Lepoivre P., Marin D., Ortiz R., Romero R. & Escalant J.V. (2002) *Mycosphaerella* leaf spot diseases of bananas: present status and outlook. In: Proceedings of the 2nd International workshop on *Mycosphaerella* leaf spot diseases San José, Costa Rica.

Jeandet P., Delaunois B., Conreux A., Donnez D., Nuzzo V., Cordelier S., Clement C. & Courot E. (2010) Biosynthesis, metabolism, molecular engineering and biological functions of stilbene phytoalexins in plants. *Biofactors*, **36**, 331-341.

Jitsaeng K. & Schneider B. (2010) Metabolic profiling of *Musa acuminata* challenged with Sporobolomyces salmonicolor. *Phytochemistry Letters*, **3**, 84-87.

Jones D.R. (2000) *Diseases of banana, Abacá and Enset.* CABI Publishing, Wallingford, Oxon (GBR).

Kamo T., Kato N., Hirai N., Tsuda M., Fujioka D. & Ohigashi H. (1998a) A biosynthetic intermediate of phytoalexins in banana fruits. *Phytochemistry*, **49**, 1617-1621.

Kamo T., Kato N., Hirai N., Tsuda M., Fujioka D. & Ohigashi H. (1998b) Phenylphenalenone-type phytoalexins from unripe Bungulan banana fruit. *Bioscience Biotechnology and Biochemistry*, **62**, 95-101.

Kanazawa K. & Sakakibara H. (2000) High content of dopamine, a strong antioxidant, in Cavendish banana. *Journal of Agricultural and Food Chemistry*, **48**, 844-848.

Kashiwada Y., Nonaka G.I., Nishioka I. & Yamagishi T. (1988) Galloyl and hydroxycinnamoylglucoses from Rhubarb. *Phytochemistry*, **27**, 1473-1477.

Kim H.K., Choi Y.H. & Verpoorte R. (2010) NMR-based metabolomic analysis of plants. *Nature Protocols*, **5**, 536-549.

Kovacs G., Sagi L., Jacon G., Arinaitwe G., Busogoro J.P., Thiry E., Strosse H., Swennen R. & Remy S. (2013) Expression of a rice chitinase gene in transgenic banana ('Gros Michel', AAA genome group) confers resistance to black leaf streak disease. *Transgenic Research*, **22**, 117-130.

Kulma A. & Szopa J. (2007) Catecholamines are active compounds in plants. *Plant Science*, **172**, 433-440.

Lazzaro A., Corominas M., Marti C., Flors C., Izquierdo L.R., Grillo T.A., Luis J.G. & Nonell S. (2004) Light- and singlet oxygen-mediated antifungal activity of phenylphenalenone phytoalexins. *Photochemical & Photobiological Sciences*, **3**, 706-710.

Li C., Sun X.K., Chang C., Jia D.F., Wei Z.W., Li C.Y. & Ma F.W. (2015) Dopamine alleviates salt-induced stress in *Malus hupehensis*. *Physiologia Plantarum*, **153**, 584-602.

Liang Y.S., Kim H.K., Lefeber A.W.M., Erkelens C., Choi Y.H. & Verpoorte R. (2006) Identification of phenylpropanoids in methyl jasmonate treated *Brassica rapa* leaves using two-dimensional nuclear magnetic resonance spectroscopy. *Journal of Chromatography A*, **1112**, 148-155.

Liu F., Zhang Y., Sun Q.Y., Yang F.M., Gu W., Yang J.,…, Long C.L. (2014) Diarylheptanoids and phenylphenalenones from *Musa itinerans* fruits. *Phytochemistry,* **103**, 171-177.

López-Gresa M.P., Maltese F., Belles J.M., Conejero V., Kim H.K., Choi Y.H. & Verpoorte R. (2010) Metabolic response of tomato leaves upon different plant-pathogen interactions. *Phytochemical Analysis*, **21**, 89-94.

Lu Y.R. & Foo L.Y. (2003) Polyphenolic constituents of blackcurrant seed residue. *Food Chemistry*, **80**, 71-76.

Luis J.G., Echeverri F., Quiñones W., Brito I., Lopez M., Torres F., Cardona G., Aguiar Z., Pelaez C. & Rojas M. (1993) Irenolone and emenolone - two new types of phytoalexin from *Musa Paradisiaca*. *Journal of Organic Chemistry*, **58**, 4306-4308.

Luis J.G., Fletcher W., Echeverri F., Abad T., Kishi M. & Perales A. (1995) New phenalenone-type phytoalexins from *Musa acuminata* (Colla AAA) Grand Nain. *Natural Product Letters*, **6**, 23-30.

Luis J.G., Fletcher W.Q., Echeverri F. & Grillo T.A. (1994) Phenalenone-type phytoalexins from *Musa acuminata*. Synthesis of 4-phenylphenalenones. *Tetrahedron*, **50**, 10963-10970.

Luis J.G., Lahlou E.H. & Andres L.S. (1999) 4 '-Dehydroxy-irenolone. A new phytoanticipin from the resistant *Musa* selected hybrid SH-3481. *Natural Product Letters*, **13**, 299-304.

Martinez-Bolanos L., Teliz-Ortiz D., Rodriguez-Maciel J.C., Mora-Aguilera J.A., Nieto-Angel D., Cortes-Flores J.I.,..., Silva-Aguayo G. (2012) Fungicides resistance on *Mycosphaerella fijiensis* populations of southeastern Mexico. *Agrociencia*, **46**, 707-717.

Morrissey J.P. & Osbourn A.E. (1999) Fungal resistance to plant antibiotics as a mechanism of pathogenesis. *Microbiology and Molecular Biology Reviews*, **63**, 708.

Mouliom-Pefoura A. (1999) First observation of the breakdown of high resistance in Yangambi km 5 (*Musa* sp.) to the black leaf sigatoka disease in Cameroon. *Plant Disease*, **83**, 78.

Munde T., Brand S., Hidalgo W., Maddula R.K., Svatos A. & Schneider B. (2013) Biosynthesis of tetraoxygenated phenylphenalenones in *Wachendorfia thyrsiflora*. *Phytochemistry*, **91**, 165-176.

Najbjerg H., Young J.F. & Bertram H.C. (2011) NMR-based metabolomics reveals that conjugated double bond content and lipid storage efficiency in HepG2 cells are affected by fatty acid cis/trans configuration and chain length. *Journal of Agricultural and Food Chemistry*, **59**, 8994-9000.

Otálvaro F., Echeverri F., Quiñones W., Torres F. & Schneider B. (2002) Correlation between phenylphenalenone phytoalexins and phytopathological properties in *Musa* and the role of a dihydrophenylphenalene triol. *Molecules*, **7**, 331-340.

Otálvaro F., Görls H., Hölscher D., Schmitt B., Echeverri F., Quiñones W. & Schneider B. (2002) Dimeric phenylphenalenones from *Musa acuminata* and various Haemodoraceae species. Crystal structure of anigorootin. *Phytochemistry*, **60**, 61-66.

Otálvaro F., Jitsaeng K., Munde T., Echeverri F., Quiñones W. & Schneider B. (2010) *O*-Methylation of phenylphenalenone phytoalexins in *Musa acuminata* and *Wachendorfia thyrsiflora*. *Phytochemistry*, **71**, 206-213.

Otálvaro F., Nanclares J., Vasquez L.E., Quiñones W., Echeverri F., Arango R. & Schneider B. (2007) Phenalenone-type compounds from *Musa acuminata* var. "Yangambi km 5" (AAA) and their activity against *Mycosphaerella fijiensis*. *Journal of Natural Products*, **70**, 887-890.

Otálvaro F., Quiñones W., Echeverri F. & Schneider B. (2004) Synthesis of [*phenyl*-$^{13}C_6$]lachnanthocarpone and other ^{13}C-labelled phenylphenalenones. *Journal of Labelled Compounds & Radiopharmaceuticals,* **47**, 147-159.

Parker D., Beckmann M., Zubair H., Enot D.P., Caracuel-Rios Z., Overy D.P., Snowdon S., Talbot N.J. & Draper J. (2009) Metabolomic analysis reveals a common pattern of metabolic re-programming during invasion of three host plant species by *Magnaporthe grisea*. *Plant Journal*, **59**, 723-737.

Pauli G.F., Jaki B.U. & Lankin D.C. (2005) Quantitative H-1 NMR: Development and potential of a method for natural products analysis. *Journal of Natural Products*, **68**, 133-149.

Pedras M.S.C. & Ahiahonu P.W.K. (2005) Metabolism and detoxification of phytoalexins and analogs by phytopathogenic fungi. *Phytochemistry*, 66, 391-411.

Pedras M.S.C. & Taylor J.L. (1993) Metabolism of the phytoalexin brassinin by the *Blackleg* fungus. *Journal of Natural Products*, **56**, 731-738.

Peláez J., Vásquez, L., Díaz, T., Castañeda, D., Rodríguez, E. and Arango, R. (2006) Use of micro titer plate dilution assay to measure activity of antifungal compounds against *Mycosphaerella fijiensis*, Morelet. *Rev. Fac. Nal. Agr. Medellín*, pp. 3425-3433.

Perrier X., De Langhe E., Donohue M., Lentfer C., Vrydaghs L., Bakry F.,…, Denham T. (2011) Multidisciplinary perspectives on banana (*Musa* spp.) domestication. *Proceedings of the National Academy of Sciences of the United States of America*, **108**, 11311-11318.

Ploetz R. (2000) Black sigatoka. *Pesticide Outlook*, **11**, 19-23.

Ploetz R.C. (2006) *Fusarium* wilt of banana is caused by several pathogens referred to as *Fusarium oxysporum* f. sp cubense. *Phytopathology*, **96**, 653-656.

Quiñones W., Escobar G., Echeverri F., Torres F., Rosero Y., Arango V., Cardona G. & Gallego A. (2000) Synthesis and antifungal activity of *Musa* phytoalexins and structural analogs. *Molecules*, **5**, 974-980.

Ramsay A., Fliniaux O., Fang J.J., Molinie R., Roscher A., Grand E., …, Mesnard F. (2014) Development of an NMR metabolomics-based tool for selection of flaxseed varieties. *Metabolomics*, **10**, 1258-1267.

Scharte J., Schoen H. & Weis E. (2005) Photosynthesis and carbohydrate metabolism in tobacco leaves during an incompatible interaction with Phytophthora nicotianae. *Plant, Cell and Environment*, **28**, 1421-1435.

Schmitt B., Hölscher D. & Schneider B. (2000) Variability of phenylpropanoid precursors in the biosynthesis of phenylphenalenones in *Anigozanthos preissii*. *Phytochemistry*, **53**, 331-337.

Sequeira L. (1998) Bacterial wilt: the missing element in international banana improvement programs. *Bacterial Wilt Disease*, 6-14.

Shimomura H., Sashida Y. & Adachi T. (1987) Phenolic glucosides from *Prunus Grayana*. *Phytochemistry*, **26**, 249-251.

Spotts R.A. & Cervantes L.A. (1986) Effects of fungicides that inhibit ergosterol biosynthesis on apple *Powdery Mildew* control, yield, and fruit-growth factors. *Plant Disease*, **70**, 305-306.

Strack D., Heilemann J., Wray V. & Dirks H. (1989) Structures and accumulation patterns of soluble and insoluble phenolics from *Norway Spruce Needles*. *Phytochemistry*, **28**, 2071-2078.

Torres J.M., Calderon H., Rodriguez-Arango E., Morales J.G. & Arango R. (2012) Differential induction of pathogenesis-related proteins in banana in response to *Mycosphaerella fijiensis* infection. *European Journal of Plant Pathology*, **133**, 887-898.

Vaganan M.M., Ravi I., Nandakumar A., Sarumathi S., Sundararaju P. & Mustaffa M.M. (2014) Phenylpropanoid enzymes, phenolic polymers and metabolites as chemical defenses to infection of *Pratylenchus coffeae* in roots of resistant and susceptible bananas (*Musa* spp.). *Indian Journal of Experimental Biology*, **52**, 252-260.

Vishnevetsky J., White T.L., Palmateer A.J., Flaishman M., Cohen Y., Elad Y.,…, Perl A. (2011) Improved tolerance toward fungal diseases in transgenic Cavendish banana (*Musa* spp. AAA group) cv. Grand Nain. *Transgenic Research*, **20**, 61-72.

Wang Z., Jia C.H., Li J.Y., Huang S.Z., Xu B.Y. & Jin Z.Q. (2015) Activation of salicylic acid metabolism and signal transduction can enhance resistance to *Fusarium* wilt in banana (*Musa acuminata* L. AAA group, cv. Cavendish). *Functional & Integrative Genomics*, **15**, 47-62.

Zhang D.L., Yang Y.F., Leakey J.E.A. & Cerniglia C.E. (1996) Phase I and phase II enzymes produced by *Cunninghamella elegans* for the metabolism of xenobiotics. *Fems Microbiology Letters*, **138**, 221-226.

Appendix. Supplementary information

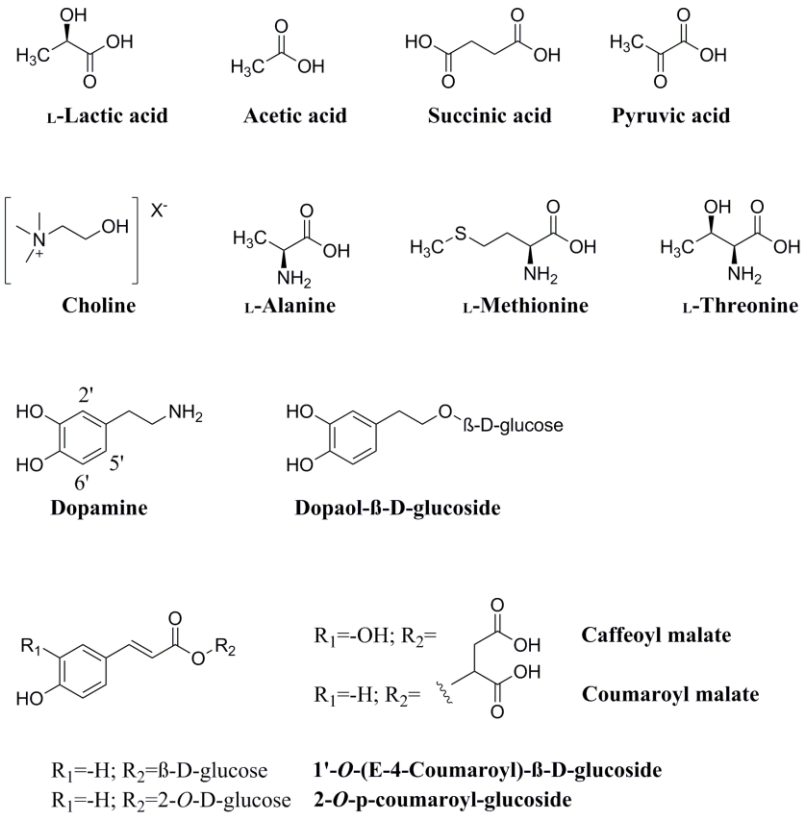

Fig. S1. Chemical structures of the metabolites identified by 1D- and 2D NMR analysis in 'Williams' and 'KTR' *Musa* varieties.

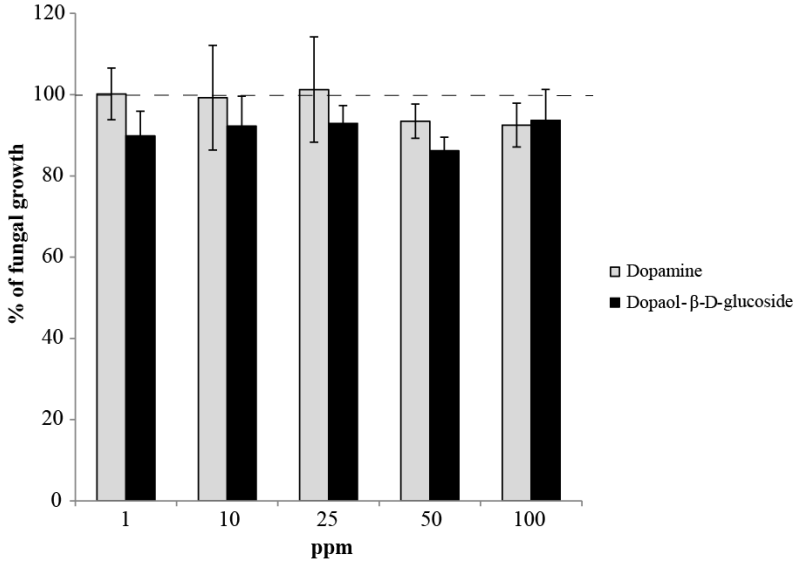

Fig. S2. Percentage of fungal growth of *M. fijiensis* strain Ca10_13 after treatment with different concentrations of dopamine and dopaol-β-D-glucoside.

Table S1. Black leaf streak disease symptoms developed by both *M. fijiensis* strains (E22 and Ca10_13) in 'Williams' and 'KTR' *Musa* varieties.

Symptoms of Black Leaf Streak Disease (BLSD) caused by *Mycosphaerella fijiensis*				
Time (days)	strain E22		strain Ca10_13	
	Musa variety 'Williams'	*Musa* variety 'KTR'	*Musa* variety 'Williams'	*Musa* variety 'KTR'
8	 No symptoms	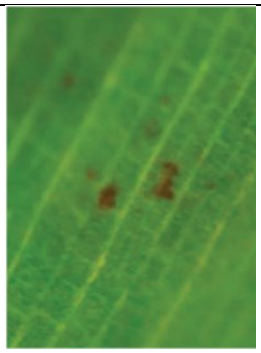 Red specks (0.5-1.0 mm diam.) on the abaxial side of the leaf	 No symptoms	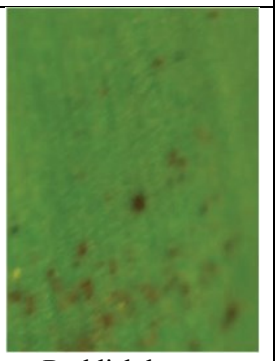 Reddish brown specks (0.5-2.0 mm diam.) on the abaxial side of the leaf
16	 Reddish brown specks (less than 0.5 mm diam.) on the abaxial part of the leaf	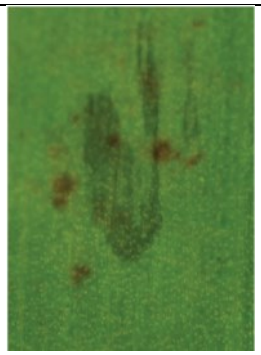 Small reddish brown spots (1-2 mm diam.) on the adaxial part of the leaf	 Brown dark spots (1-2 mm diam.) observed on the upper side of the leaf	 Reddish brown spots (1-3 mm diam.) on the upper side of the leaf

25	 Brown and black blotches (3-5 mm diam.) on the adaxial part of the leaf	 Brown dark spots (2-3 mm diam.) on the adaxial part of the leaf	 Brown and black spots (2-5 mm diam.) on the upper part of the leaf	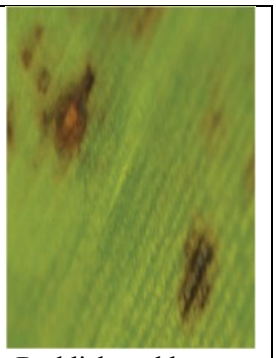 Reddish and brown dark spots (3-6 mm diam.) on the adaxial part of the leaf
50	 Asymmetric necrotic lesions (4-8 mm diam.) on the upper side of the leaf	 Reddish and brown spots (2-5 mm diam.) on the upper side of the leaf	 Necrotic lesions between 10-12 mm diam.	 Necrotic lesions between 10-15 mm diam.

.

Chapter 5

Synthesis of new antimicrobial compounds against *M. fijiensis*

5.1 Improved synthesis of 4-phenylphenalenones: the case of isoanigorufone and structural analogs. …… 111

5.2 4-Phenylphenalenones as a template for new photodynamic compounds against *Mycosphaerella fijiensis*…….. 121

Tetrahedron Letters 54 (2013) 351–354

Contents lists available at SciVerse ScienceDirect

Tetrahedron Letters

journal homepage: www.elsevier.com/locate/tetlet

Improved synthesis of 4-phenylphenalenones: the case of isoanigorufone and structural analogs

Marisol Cano [a], Carlos Rojas [a], William Hidalgo [b], Jairo Sáez [a], Jesús Gil [c], Bernd Schneider [b,*], Felipe Otálvaro [a,*]

[a] Instituto de Química-Universidad de Antioquia, Calle 67# 53-108, A.A. 1226 Medellín, Colombia
[b] Max-Planck Institut für Chemische Ökologie, Beutenberg Campus, Hans-Knöll-Strasse 8, 07745 Jena, Germany
[c] Universidad Nacional de Colombia sede Medellín, Autopista Norte, Calle 64 Cra 65, A.A. 1027 Medellín, Colombia

ARTICLE INFO

Article history:
Received 17 October 2012
Revised 7 November 2012
Accepted 12 November 2012
Available online 1 December 2012

Keywords:
Friedel–Crafts acylation
4-Phenylphenalenones
Suzuki–Miyaura coupling

ABSTRACT

2-Hydroxy-4-phenyl-1*H*-phenalen-1-one (isoanigorufone, **1**), a phytoalexin exclusive of Musaceae, was synthesized starting from 3-(2-hydroxynaphthalen-1-yl)propanenitrile in nine steps in an overall yield of 10%. Hydrolysis of ethyl 3-(2-phenylnaphthalen-1-yl)propanoate obtained from Suzuki–Miyaura coupling between the parent triflate and phenylboronic acid afforded the corresponding propionic acid which, after Friedel–Crafts acylation and bromine-mediated dehydrogenation, was subjected to Yang–Finnegan epoxidation to furnish **1**. The preparation of analogs using this procedure is also discussed.

Musa acuminata plants (bananas) exposed to chemical or biotic stress accumulate phenylphenalenones, which can be roughly divided into three types: 9-phenylphenalenones, 4-phenylphenalenones, and phenylnaphthalic anhydrides.[1] Similar or even identical compounds have been isolated from Haemodoraceae and Pontederiaceae plants as well; however, 4-phenylphenalenones remain exclusive to *Musa*.[2] Bioassay studies have suggested the involvement of a photooxidation component in the mode of action of phenalenones against *Fusarium oxysporum* and *Mycosphaerella fijiensis*.[3] Interestingly, these and other in vitro experiments have shown that the phenalenone isomer with a substitution at position C-4 is generally more active than corresponding phenalenones without a substitution in this position.[3,4] This fact can be partially rationalized in terms of the superior quantum yield of singlet oxygen production displayed by 4-phenylphenalenones in comparison with their 9-phenyl counterparts.[4a]

In spite of these results, no systematic study has been reported addressing structure–activity relationships among 4-phenylphenalenones, in part because only minute amounts can be isolated from natural sources with a minimum of structural variability.[1] In addition, there is only one report on the synthesis of 4-phenylphenalenones based on 9-phenylphenalenone carbonyl transposition via reduction–oxidation that leads to an isomeric mixture that is difficult to purify.[5] Moreover, the synthesis of 9-heterocyclic phenalenones, which can serve as educts for carbonyl transposition, is of limited success.[4c] Therefore, the development of other versatile and experimentally simpler synthetic routes for 4-phenylphenalenones is desirable.

Previously, we stated the plausibility of synthesizing 4-phenylphenalenones from 4-methoxyperinaphthenone via cross-coupling reactions.[6a] This strategy, however, is not free from pitfalls, as it implies the activation of 4-hydroxyperinaphthenone, a process that can afford a mixture of isomers due to the presence of its 7-hydroxyperinaphthenone tautomer.[6b] Here, we report the synthesis of 2-hydroxy-4-phenyl-1*H*-phenalen-1-one (isoanigorufone, **1**)[7] using a tactical variant in which the phenyl substituent was introduced prior to the formation of the perinaphthenone moiety in order to avoid the problem of tautomerism.

The general features of the isoanigorufone synthesis are outlined retrosynthetically in Scheme 1.

The Hardman[8] synthesis of 3-(2-hydroxynaphthalen-1-yl)propanenitrile (**9**) by means of refluxing acrylonitrile with a basic solution of 2-naphthol in benzene provided, after purification by flash column chromatography, the starting point for the synthesis of **1** in sufficient quantities (40 g) (Scheme 2).[8] Aqueous alkaline hydrolysis of **9**,[9] followed by Fisher esterification with ethanol according to the method of Nudelman, afforded ethyl 3-(2-hydroxynaphthalen-1-yl)propanoate (**7**) in 90% overall yield.[10] The treatment of **7** with trifluoromethanesulfonic anhydride in pyridine generated the corresponding triflate (**6**) in 62% (70% brsm) as a solid that can be chromatographed and set the stage for the cross-coupling reaction.[11] Coupling trimethyl(phenyl)tin and triflate **6**

* Corresponding authors. Tel.: +49 364 1571600; fax: +49 364 1571601 (B.S.); tel.: +57 421 95653; fax: +57 423 30120 (F.O.).
E-mail addresses: schneider@ice.mpg.de (B. Schneider), pipelion@quimica.udea.edu.co (F. Otálvaro).

0040-4039/$ - see front matter © 2012 Elsevier Ltd. All rights reserved.
http://dx.doi.org/10.1016/j.tetlet.2012.11.118

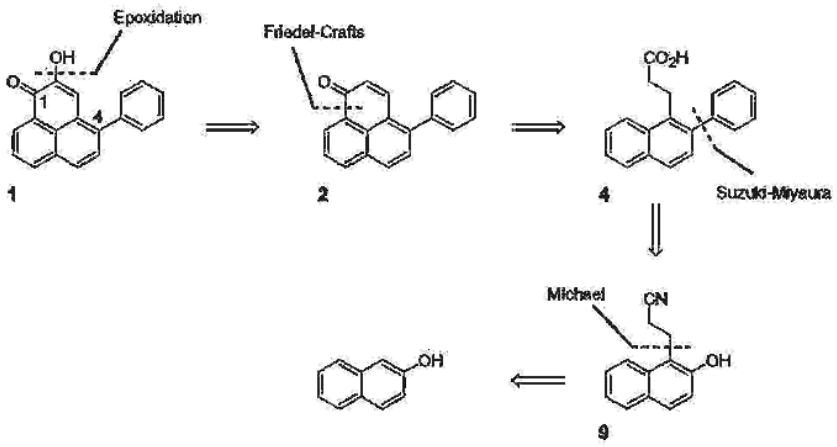

Scheme 1. Retrosynthetic analysis of isoanigorufone (1).[7]

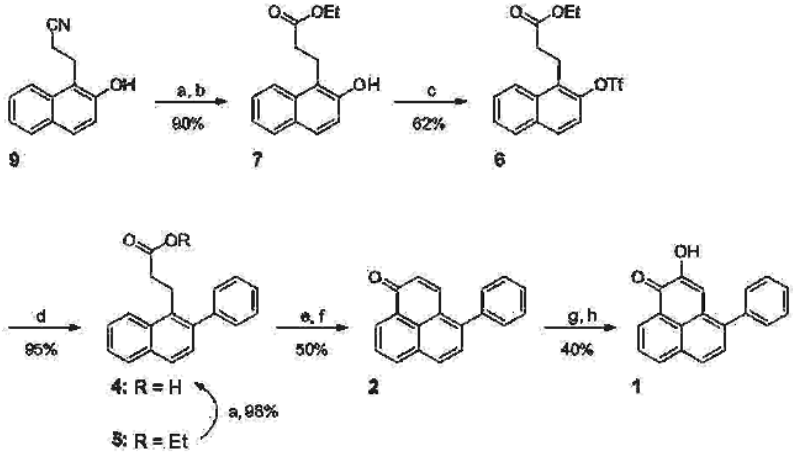

Scheme 2. Reagents and conditions: (a) NaOH 30%, 5 h reflux, then HCl until pH ~1; (b) EtOH, CH_3COCl (25 mol %), 4 h reflux; (c) Tf_2O (1.5 equiv), pyridine, 0 °C, 30 min, then 25 °C, 2.5 h; (d) $(PPh_3)_2PdCl_2$ (5 mol %), $PhB(OH)_2$ (1.5 equiv), $Na_2CO_{3(aq)}$ (2 M), dioxane, 22 h reflux; (e) $SOCl_2$, 30 °C until dryness, then CH_2Cl_2, $AlCl_3$ (3 equiv) 10 min; (f) NBS (1.2 equiv), CCl_4, 3 h reflux under irradiation (170 W UHE lamp, 1800 lumens); (g) *t*-BuOOH (80%), triton B, benzene, 0 °C, 5 min, then 25 °C, 18 h; (h) *p*-TSA, CH_2Cl_2, 25 °C, 1 h.

by means of the Stille reaction under a slight modification of Papadopoulos conditions proved successful after 20 h reflux (50% isolated yield).[12] However, superior yields were achieved using the Suzuki–Miyaura coupling under less demanding experimental conditions and without the use of additives.[12] Thus, the reaction of triflate **6** and phenylboronic acid mediated by bis(triphenylphosphine)palladium(II)chloride and Na_2CO_3 in dioxane–water afforded ethyl 3-(2-phenylnaphthalen-1-yl)propanoate (**5**) in a sufficiently pure, gratifying yield of 95% after 22 h reflux for the next step (Scheme 2).[12] Hydrolysis of **5** generated 3-(2-phenylnaphthalen-1-yl)propanoic acid (**4**) (98% yield) of sufficient purity for the anticipated regioselective Friedel–Crafts acylation.[13] Unfortunately, the reaction of **4** with thionyl chloride, followed by treatment with $AlCl_3$ and 2,3-dichloro-5,6-dicyanobenzoquinone (DDQ) in dichloromethane according to our previously reported one-pot procedure,[6] afforded 4-phenyl-1*H*-phenalen-1-one (**2**) in a disappointing 15% yield after many tedious purification steps. Stepwise execution of this methodology allowed the preparation of 4-phenyl-2,3-dihydro-1*H*-phenalen-1-one (**3**) in 80% yield and identified the DDQ-mediated dehydrogenation as the problematic step.[14] Similar dehydrogenation processes have been performed by means of benzylic bromination–dehydrobromination sequences. Therefore, it was hoped that the combination of *N*-bromosuccinimide (NBS) and white-light catalysis according to the method of Mills could afford the desired 4-phenyl-1*H*-phenalen-1-one (**2**) directly.[15]

Fortunately, this proved to be the case and compound **2** was obtained in 62% yield after flash chromatography. The Yang–Finnegan epoxidation of **2** (Scheme 2) went on to produce the epoxide which was treated with *p*-toluenesulfonic acid to afford 2-hydroxy-4-phenyl-1*H*-phenalen-1-one (isoanigorufone, **1**) in 40% combined yield.[16] The spectroscopic data of **1** were identical with those of the natural compound.[7a]

In order to check the diversification possibilities offered by the synthetic route, steps d–f (Scheme 2) were repeated using five different boronic acid derivatives under the same conditions (Tables 1 and 2). Table 1 illustrates some generality in the Suzuki–Miyaura coupling protocol developed for **1** independent of the electronic nature of the aromatic partner (all yields Y_1 between 88% and 97%). Execution of the Friedel–Crafts reaction on these propanoic

Table 1
Synthesis of 3-(naphthalene-1-yl)propanoic acid analogs using conditions developed for the synthesis of isoanigorufone

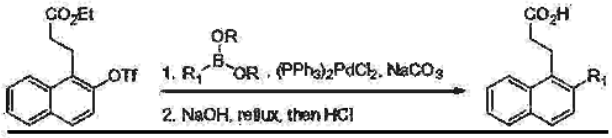

Entry	Boronic acid derivative	Product	Yield (%) Y_1, Y_2
1	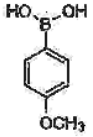	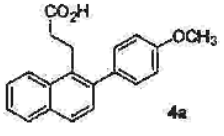 4a	97, 97
2	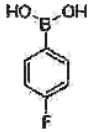	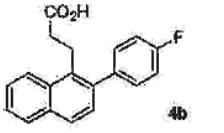 4b	88, 96
3	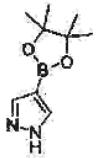	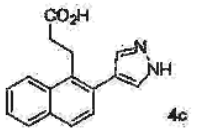 4c	95, 97
4	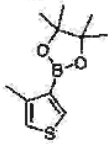	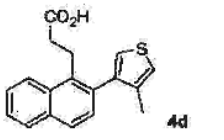 4d	94, 80
5	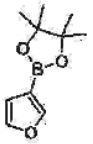	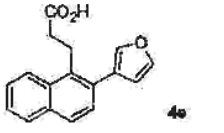 4e	97, 98

Y_1 = yield for step 1.
Y_2 = yield for step 2.
Experimental details can be found in Supplementary data.

Table 2
Synthesis of 4-phenylphenalenone analogs using conditions developed for the synthesis of isoanigorufone

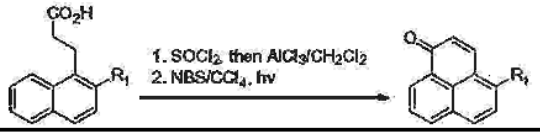

Entry	Educt	Product	Yield (%) Y_1, Y_2
1	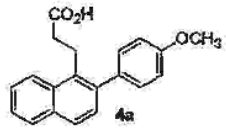 4a	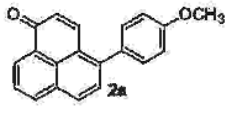 2a	94, 43 58[a]
2	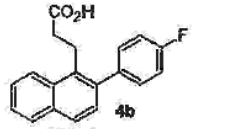 4b	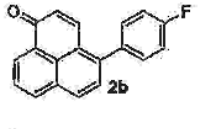 2b	97, 56
3	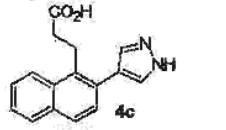 4c	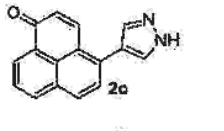 2c	66, 38[a]
4	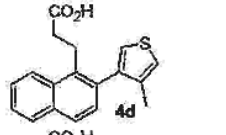 4d	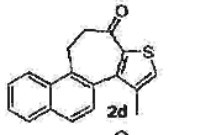 2d	68[b]
5	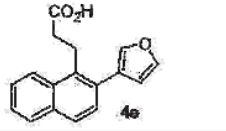 4e	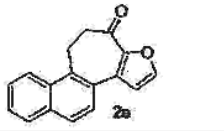 2e	72[b]

Y_1 = yield for step 1.
Y_2 = yield for step 2.
NBS = *N*-bromosuccinimide.
[a] NBS/light replaced by 2,3-dichloro-5,6-dicyano-1,4-benzoquinone (DDQ).
[b] Step 2 omitted. Experimental details can be found in Supplementary data.

acid substrates (Table 2) proved to be regioselective with preference for the six-member cyclization mode (Table 2, entries 1–3). However, electron rich five-member heterocycles displayed a tendency for a seven-member ring formation to give the 1,2-dihydro-3*H*-naphtho[2′,1′:3,4]cyclohepta[1,2-*b*]heterocyclic-3-one (Table 2, entries 4 and 5). This rather unexpected result represents the first synthetic entry to this type of nuclei but renders the synthesis unsuitable for the preparation of electron rich five-member heterocyclic analogs. It also shows the important influence the electron-density distribution of the lateral ring can exert on the ring size of the final product. Interestingly, execution of the Friedel–Crafts and DDQ mediated dehydrogenation as a one-pot procedure on substrate **4d** allowed the isolation of 4-(4-methylthiophen-3-yl)-1*H*-phenalen-1-one as a minor compound (4% yield, see Supplementary data). No phenalenone could be detected in the case of educt **4e**. Dehydrogenation of the Friedel–Crafts products using NBS/light (Table 2, entries 1–3) went as expected for the cases of phenyl analogs. However, no dehydrogenation occurred when this procedure was applied to the pyrazole derivative. This situation was partially remediated by the use of DDQ (Table 2, entry 3) albeit in low yield (38%, 44% brsm). Substrates **2d–2e** proved recalcitrant to the dehydrogenating conditions employed on the other substrates, probably due to the angular strain that would be introduced.

In conclusion, we have developed an operationally simple nine-step synthesis of 2-hydroxy-4-phenyl-1*H*-phenalen-1-one (isoanigorufone, **1**) starting from 3-(2-hydroxynaphthalen-1-yl)propanenitrile in a 10% global yield using the Suzuki–Miyaura and Friedel–Crafts reactions as key steps. The synthesis can be extrapolated to the preparation of 4-phenylphenalenone analogs with confidence.

Acknowledgments

We thank Marco Kai for mass spectrometric analyses, and Emily Wheeler for editorial assistance. This research was financially supported by Universidad de Antioquia (Grant CODI E01606) and the Max-Planck-Institut für Chemische Ökologie.

Supplementary data

Supplementary data associated with this article can be found, in the online version, at http://dx.doi.org/10.1016/j.tetlet.2012.11.118.

References and notes

1. (a) Luis, J. G.; Fletcher, W. Q.; Echeverri, F.; Grillo, T. *Tetrahedron* **1994**, *50*, 10963–10970; (b) Luis, J. G.; Quiñones, W.; Echeverri, F.; Grillo, T. A.; Kishi, M. P.; García-García, F.; Torres, F.; Cardona, G. *Phytochemistry* **1998**, *47*, 753–757; (c) Kamo, T.; Kato, N.; Hirai, N.; Tsuda, M.; Fujioka, D.; Ohigashi, H. *Biosci. Biotechnol. Biochem.* **1998**, *62*, 95–101; (d) Kamo, T.; Hirai, N.; Iwami, K.; Fujioka, D.; Ohigashi, H. *Tetrahedron* **2001**, *57*, 7649–7656; (e) Jitsaeng, K.; Schneider, B. *Phytochem. Lett.* **2010**, *3*, 84–87.
2. (a) Cooke, R. G.; Edwards, J. M. *Prog. Chem. Org. Nat. Prod.* **1981**, *40*, 153–190; (b) Greca, M. D.; Previtera, L.; Zarelli, A. *Tetrahedron Lett.* **2008**, *49*, 3268–3272; (c) Opitz, S.; Hölscher, D.; Oldham, N. J.; Bartram, S.; Schneider, B. *J. Nat. Prod.* **2002**, *65*, 1122–1130; (d) Fang, J.; Paetz, C.; Hölscher, D.; Munde, T.; Schneider, B. *Phytochem. Lett.* **2011**, *4*, 203–204.
3. (a) Lazzaro, A.; Corominas, M.; Martí, C.; Flors, C.; Izquierdo, L. R.; Grillo, T. A.; Luis, J. G.; Nonell, S. *Photochem. Photobiol. Sci.* **2004**, *3*, 706–710; (b) Hidalgo, W.; Duque, L.; Saez, J.; Arango, R.; Gil, J.; Rojano, B.; Schneider, B.; Otálvaro, F. *J. Agric. Food Chem.* **2009**, *57*, 7417–7421.
4. (a) Flors, C.; Ogilby, P. R.; Luis, J. G.; Grillo, T. A.; Izquierdo, L. R.; Gentili, P.; Bussotti, L.; Nonell, S. *Photochem. Photobiol.* **2006**, *82*, 95–103; (b) Quiñones, W.; Escobar, G.; Echeverri, F.; Torres, F.; Rosero, Y.; Arango, V.; Cardona, G.; Gallego, A. *Molecules* **2000**, *5*, 974–980; (c) Rosquete, L. I.; Cabrera-Serra, M. G.; Piñero, J. E.; Martín, P. R.; Fernández, L. P.; Luis, J. G.; McNaughton, G. S.; Grillo, T. A. *Bioorg. Med. Chem.* **2010**, *18*, 4530–4534.
5. Luis, J. G.; Fletcher, W. Q.; Echeverri, F.; Grillo, T. A. *Tetrahedron* **1994**, *50*, 10963–10970.
6. (a) Nanclares, J.; Gil, J.; Rojano, B.; Saez, J.; Schneider, B.; Otálvaro, F. *Tetrahedron Lett.* **2008**, *49*, 3844–3847; (b) In fact, triflation of 4-hydroxyperinaphthenone (prepared as described in Ref. 3b) afforded a 60:22:18 mixture of 1,1-dioxo-1*H*,1′*H*-[2,2′-biphenalene]-4,4′-diyl bis(trifluoromethanesulfonate), 1-oxo-1*H*-phenalen-7-yl trifluoromethanesulfonate, and 1-oxo-1*H*-phenalen-4-yl trifluoromethanesulfonate, respectively (for experimental details see Supplementary data).
7. (a) Luis, J. G.; Lahlou, E. H.; Andrés, L. S. *Nat. Prod. Lett.* **1999**, *13*, 299–304; (b) Otálvaro, F.; Nanclares, J.; Vásquez, L. E.; Quiñones, W.; Echeverri, F.; Arango, R.; Schneider, B. *J. Nat. Prod.* **2007**, *70*, 887–890.
8. (a) Hardman, A. F. *J. Am. Chem. Soc.* **1948**, *70*, 2119–2120; (b) Duque, L.; Restrepo, C.; Sáez, J.; Gil, J.; Schneider, B.; Otálvaro, F. *Tetrahedron Lett.* **2010**, *51*, 4640–4643.
9. Hydrolysis of **9** (32 g) was performed according to Ref. 8a using aqueous NaOH (30%, 100 mL, 5 h reflux) to obtain 38 g of crude 3-(2-hydroxynaphthalen-1-yl)propanoic acid (**8**) as a white solid after acidic workup. ^{1}H NMR (C_5D_5O, 500.13 MHz) δ 7.95 (d, J = 8.1 Hz, H-5′), 7.92 (d, J = 8.5 Hz, H-8′), 7.67 (d, J = 8.9 Hz, H-4′), 7.44 (ddd, J = 8.5, 6.9, 1.2 Hz, H-7′), 7.26 (ddd, J = 8.1, 6.9, 1.2 Hz, H-6′), 7.18 (d, J = 8.9 Hz, H-3′), 3.31 (t, J = 7.5 Hz, H-3), 2.66 (t, J = 7.5 Hz, H-2); ^{13}C NMR (C_5D_5O, 125.75 MHz) δ 177.4 C-1), 153.6 (C-2′), 131.7 (C-8a′), 130.0 (C-4a′), 129.3 (C-5′), 128.7 (C-4′), 127.1 (C-7′), 123.3 (C-6′), 123.2 (C-8′), 119.9 (C-1′), 119.7 (C-3′), 35.2 (C-2), 21.3 (C-3). HREIMS: *m/z* 216.07904 (calcd for $C_{13}H_{12}O_3$, 216.07864).
10. Nudelman, A.; Bechor, Y.; Falb, E.; Fischer, B.; Wexler, B.A.; Nudelman, A. *Synth. Commun.* **1998**, *28*, 471–474. *Experimental procedure*: 3-(2-Hydroxynaphthalen-1-yl)propanoic acid (**8**) (38.0 g, 0.2 mol), dissolved in 200 mL of distilled EtOH (not anhydrous), was treated with 3 mL of acetyl chloride and refluxed. Addition of acetyl chloride (1 mL) was repeated after 2 h and the mixture was kept under reflux for another 2 h. Evaporation of the reaction mixture and purification by column chromatography (CH_2Cl_2) afforded 35 g (90% from 9) of ethyl 3-(2-hydroxynaphthalen-1-yl)propanoate (**7**) as a yellow oil. ^{1}H NMR (C_5D_5O, 500.13 MHz) δ 7.95 (d, J = 8.1 Hz, H-5′), 7.78 (d, J = 8.5 Hz, H-8′), 7.67 (d, J = 8.9 Hz, H-4′), 7.47 (ddd, J = 8.5, 6.9, 1.2 Hz, H-7′), 7.29 (ddd, J = 8.1, 6.9, 1.2 Hz, H-6′), 7.20 (d, J = 8.9 Hz, H-3′), 4.10 (q, J = 7.1 Hz, –OCH_2CH_3), 3.36 (t, J = 7.7 Hz, H-3), 2.63 (t, J = 7.7 Hz, H-2), 1.19 (t, J = 7.1 Hz, –OCH_2CH_3); ^{13}C NMR (C_5D_5O, 125.75 MHz) δ 174.1 C-1), 153.1 (C-2′), 134.2 (C-8a′), 130.2 (C-4a′), 129.5 (C-5′), 128.9 (C-4′), 127.3 (C-7′), 123.5 (C-6′), 123.3 (C-8′), 119.2 (C-1′), 119.0 (C-3′), 60.9 (–OCH_2CH_3), 34.7 (C-2), 21.2 (C-3), 14.5 (–OCH_2CH_3). HREIMS: *m/z* 244.10888 (calcd for $C_{15}H_{16}O_3$, 244.10994).
11. *Experimental procedure*: A solution of **7** (12.87 g, 56.4 mmol) in pyridine (10 mL) was cooled to −10 °C and treated with triflic anhydride (18.8 mL, 112.8 mmol, 20 min addition). The reaction mixture was allowed to warm (room temperature) and stirred for an additional 2.5 h. The crude mixture was partitioned between saturated aqueous $CuSO_4$ and ethyl acetate, and the organic fraction was dried (Na_2SO_4), concentrated and submitted to column chromatography (AcOEt–*n*-hexane (1:9)) to give 13.2 g (62%) of ethyl 3-(2-(((trifluoromethyl)sulfonyl)oxy)naphthalene-1-yl)propanoate (**6**) as a white solid. ^{1}H NMR (C_5D_5O, 500.13 MHz) δ 8.25 (d, J = 8.5 Hz, H-8′), 8.05 (d, J = 8.1 Hz, H-5′), 8.02 (d, J = 9.1 Hz, H-4′), 7.72 (ddd, J = 8.3, 6.9, 1.4 Hz, H-7′), 7.55 (ddd, J = 8.1, 6.9, 1.2 Hz, H-6′), 7.50 (d, J = 9.1 Hz, H-3′), 4.11 (q, J = 7.1 Hz, –OCH_2CH_3), 3.53 (t, J = 7.7 Hz, H-3), 2.71 (t, J = 7.7 Hz, H-2), 1.20 (t, J = 7.1 Hz, –OCH_2CH_3); ^{13}C NMR (C_5D_5O, 125.75 MHz) δ 172.3 C-1), 146.0 (C-2′), 134.0 (C-4a′), 133.2 (C-8a′), 130.1 (C-1′), 130.7 (C-4′), 130.0 (C-5′), 128.9 (C-7′), 128.1 (C-6′), 125.4 (C-8′), 120.9 (q, J_{C-F} = 319.3 Hz, –SO_3CF_3), 120.3 (C-3′), 61.1 (–OCH_2CH_3), 34.8 (C-2), 22.3 (C-3), 14.5 (–OCH_2CH_3). HREIMS: *m/z* 376.06340 (calcd for $C_{16}H_{15}F_3O_5S$, 376.05923).
12. *The Stille reaction was performed as described in* Crisp, G.T.; Papadopoulus, S. *Aust. J. Chem.* **1988**, *41*, 1711–1715, using tris(dibenzylideneacetone) dipalladium instead of bis(dibenzylideneacetone)palladium. *Experimental procedure for the Suzuki–Miyaura reaction*: Compound **6** (3.08 g, 8.0 mmol), phenylboronic acid (1.94 g, 16.0 mmol), and bis(triphenylphosphine) palladium(II)chloride (281 mg, 5 mol %) were dissolved in dioxane (50 mL), mixed with a Na_2CO_3 solution (12 mL, 2 M) and refluxed for 22 h. Liquid partition with AcOEt/H_2O, dryness (Na_2SO_4) and concentration of the organic phase afforded 2.3 g (95%) of ethyl 3-(2-phenylnaphthalen-1-yl)propanoate (**5**). ^{1}H NMR (C_5D_5O, 500.13 MHz) δ & 16 (d, J = 8.5 Hz, H-8′), 7.95 (d, J = 8.1 Hz, H-5′), 7.82 (d, J = 8.5 Hz, H-4′), 7.61 (ddd, J = 8.5, 6.9, 1.2 Hz, H-7′), 7.55 (ddd, J = 8.1, 6.9, 1.2 Hz, H-6′), 7.37–7.47 (m, H-2″–H-6″), 7.32 (d, J = 8.5 Hz, H-3′), 4.03 (q, J = 7.1 Hz, –OCH_2CH_3), 3.33 (t, J = 7.7 Hz, H-3), 2.73 (t, J = 7.7 Hz, H-2), 1.15 (t, J = 7.1 Hz, –OCH_2CH_3); ^{13}C NMR (C_5D_5O, 125.75 MHz) δ 172.8 C-1), 143.4 (C-1″), 140.6 (C-2′), 134.5 (C-4a′), 134.4 (C-1′), 132.7 (C-8a′), 130.1 (C-2″/6″), 129.8 (C-5′), 129.2 (C-3″/5″), 129.0 (C-3′), 128.0 (C-4″), 127.6 (C-7′), 127.6 (C-4′), 126.5 (C-6′), 125.0 (C-8′), 60.8 (–OCH_2CH_3), 37.0 (C-2), 28.7 (C-3), 14.5 (–OCH_2CH_3). HREIMS: *m/z* 304.14510 (calcd for $C_{21}H_{20}O_2$, 304.14633).
13. Hydrolysis of **5** (2.3 g, 7.6 mmol) was performed using aqueous NaOH (30%, 50 mL, 5 h reflux) to obtain 2.0 g (98%) of crude 3-(2-phenylnaphthalen-1-yl)propanoic acid (**4**) as a white solid after acidic workup. ^{1}H NMR (C_5D_5O, 500.13 MHz) δ 8.24 (d, J = 8.5 Hz, H-8′), 7.87 (d, J = 8.1 Hz, H-5′), 7.73 (d, J = 8.5 Hz, H-4′), 7.56 [ddd, J = 8.5, 6.9, 1.2 Hz, H-7′), 7.48 (ddd, J = 8.1, 6.9, 1.2 Hz, H-6′), 7.36–7.44 (m, H-2″–H-6″), 7.28 (d, J = 8.5 Hz, H-3′), 3.29 (t, J = 7.7 Hz, H-3), 2.46 (t, J = 7.7 Hz, H-2); ^{13}C NMR (C_5D_5O, 125.75 MHz) δ 181.7 (C-1), 144.2 (C-1″), 140.5 (C-2′), 136.4 (C-1′), 134.8 (C-4a′), 133.2 (C-8a′), 130.4 (C-2″/6″), 129.7 (C-5′), 129.3 (C-3″), 129.3 (C-3″/5″), 127.9 (C-4″), 127.4 (C-4′), 127.1 (C-7′), 126.5 (C-6′), 125.6 (C-8′), 40.4 (C-2), 27.4 (C-3). HREIMS: *m/z* 276.11528 (calcd for $C_{19}H_{16}O_2$, 276.11503).
14. *Experimental procedure*: Compound **4** (1.4 g, 5.0 mmol) was treated with 1 mL of $SOCl_2$ and the flask was air-dried after gas evolution. This process was repeated four times. The product was dissolved in CH_2Cl_2 (15 mL) and $AlCl_3$ (2.0 g, 15.0 mmol) was added in one portion (the solution turns red). After 10 min, the reaction mixture was dried and immediately submitted to column chromatography using CH_2Cl_2 as eluent to give 1.0 g (80%) of 4-phenyl-2,3-dihydro-1*H*-phenalen-1-one (**3**) as a pale yellow oil. Compound **3** decomposes rapidly upon exposure to open air. ^{1}H NMR (C_5D_5O, 500.13 MHz) δ 8.19 (dd, J = 8.1, 1.1 Hz, H-9), 8.14 (dd, J = 7.2, 1.1 Hz, H-7), 7.92 (d, J = 8.4 Hz, H-6), 7.65 (dd, J = 8.1, 7.2 Hz, H-8), 7.48 (d, J = 8.4 Hz, H-5), 7.42–7.50 (m, H-2″–H-6″), 3.34 (t, J = 6.8 Hz, H-3), 2.81 (t, J = 6.8 Hz, H-2); ^{13}C NMR (C_5D_5O, 125.75 MHz) δ 198.8 C-1), 142.9 (C-1′), 140.8 (C-4), 135.7 (C-9), 134.8 (C-6a), 133.6 (C-9b), 132.1 (C-9a), 132.0 (C-3a), 131.1 (C-2′/6′), 130.6 (C-5), 130.2 (C-3′/5′), 129.1 (C-4′), 128.1 (C-6), 127.4 (C-8), 126.8 (C-7), 39.8 (C-2), 28.3 (C-3). HREIMS: *m/z* 258.10515 (calcd for $C_{19}H_{14}O$, 258.10447).
15. Mills, F.D. *J. Org. Chem.* **1981**, *46*, 2389–2393. *Experimental procedure*: To a refluxing solution (PYREX® glassware) of compound **3** (450 mg, 1.7 mmol) in CCl_4 (15 mL) irradiated with an EPSON Powerlite S4 video beam (170 W UHE lamp, 1800 lumens) were added 3 mg of benzoyl peroxide and 100 mg of *N*-bromosuccinimide (NBS). NBS addition was repeated twice over 30 min intervals (1.7 mmol total). The mixture was refluxed for another hour (a change in color to intense yellow was noticed). Evaporation of the solvent and purification by column chromatography (CH_2Cl_2–*n*-hexane (1:1)) afforded 270 mg (62%) of 4-phenyl-1*H*-phenalen-1-one (**2**) as a yellow solid. ^{1}H NMR (C_5D_5O, 500.13 MHz) δ 8.57 (dd, J = 7.5, 1.3 Hz, H-9), 8.39 (dd, J = 8.0, 1.3 Hz, H-7), 8.23 (d, J = 8.5 Hz, H-6), 7.87 (dd, J = 7.9, 7.5 Hz, H-8), 7.83 (d, J = 10.1 Hz, H-3), 7.66 (d, J = 8.5 Hz, H-5), 7.53–7.58 (m, H-2″–H-6″), 6.60 (d, J = 10.1 Hz, H-2); ^{13}C NMR (C_5D_5O, 125.75 MHz) δ 184.9 C-1), 145.7 (C-4), 140.2 (C-3), 140.1 (C-1′), 135.9 (C-7), 132.8 (C-6), 132.8 (C-6a), 131.3 (C-2′/6′), 131.0 (C-9), 130.6 (C-9a), 130.3 (C-5), 129.6 (C-2), 129.5 (C-3′/5′), 129.2 (C-4″), 128.8 (C-9b), 128.0 (C-8), 125.1 (C-3a). HREIMS: *m/z* 256.08960 (calcd for $C_{19}H_{12}O$, 256.08882).
16. *Experimental procedure*: A solution of compound **2** (68 mg, 0.3 mmol) in benzene (4 mL) was treated with benzyltrimethylammonium hydroxide (40 μL of a 40% triton B solution in MeOH) and *t*-BuOOH (40 μL of an 80% solution in water) at 0 °C. The mixture was allowed to warm to room temperature, after which the same addition of triton B and *t*-BuOOH was repeated twice at intervals of 50 min and the reaction was stirred for additional 2 h. The crude mixture was submitted to flash column chromatography (CH_2Cl_2–*n*-hexane (1:4)). This last step was found to ameliorate complications in the purification of isoanigorufone (**1**) if the epoxide was treated in the same flask with *p*-toluenesulfonic acid (*p*-TSA). 1-Phenyl-7a,8a-dihydro-7*H*-phenaleno[1,2-*b*]oxiren-7-one: ^{1}H NMR (C_5D_5O, 500.13 MHz) δ 8.40 (dd, J = 7.3, 1.2 Hz, H-6), 8.37 (dd, J = 8.2, 1.2 Hz, H-4), 8.17 (d, J = 8.5 Hz, H-3), 7.79 (dd, J = 8.2, 7.3 Hz, H-5), 7.66 (d, J = 8.5 Hz, H-2), 7.53–7.64 (m, H-2″–H-6″), 4.61 (d, J = 3.9 Hz, H-7a), 4.05 (d, J = 3.9 Hz, H-8a); ^{13}C NMR (C_5D_5O, 125.75 MHz) δ 193.4 C-7), 145.7 (C-1), 141.1 (C-1′), 137.0 (C-4), 134.5 (C-3a), 131.8 (C-2′/6′), 131.4 (C-3), 131.3 (C-8c), 130.7 (C-2), 130.5 (C-3′/5′), 130.1 (C-6), 129.9 (C-4′), 129.0 (C-6a), 128.3 (C-5), 126.2 (C-8b), 58.6 (C-8a), 56.7 (C-7a). HREIMS: *m/z* 272.08198 (calcd for $C_{19}H_{12}O_2$, 272.08373). The purified product (epoxide) was dissolved in CH_2Cl_2 (10 mL) and treated with *p*-TSA (5 mg) under stirring (30 min) at room temperature to give 33 mg (40% from 2) of 2-hydroxy-4-phenyl-1*H*-phenalen-1-one (isoanigorufone, **1**). HREIMS: *m/z* 272.08308 (calcd for $C_{19}H_{12}O_2$, 272.08373). Other spectroscopic data were identical with those of the natural compound.[7a]

Appendix. Supplementary information

General Methods: All reactions were monitored by thin-layer chromatography (TLC) carried out on 0.25 mm Merck silica gel plates (60-F_{254}) using UV light (254 nm) as visualizing agent and vanillin solution and heat as developing agent. Yields refer to heighted chromatographically homogeneous samples. NMR spectroscopic analyses were performed on a Bruker AV 500 NMR spectrometer operating at 500.13 MHz (^{1}H) and 125.75 MHz (^{13}C). Chemical shifts are reported relative to residual solvent peaks. Signals were assigned with the aid of HMQC, HMBC and HH-COSY spectra. ESI-HRMS was measured in the positive ion mode on a Micromass Quattro II tandem quadrupole mass spectrometer (Micromass Ltd., Manchester, UK) except for the carboxylic acids which were measured in the negative ion mode. All reagents were purchased from Aldrich and used without further purification.

Experimental procedures:

Triflation of 4-hydroxyperinaphthenone: 4-hydroxyperinaphthenone (809 mg, 2.7 mmol) was disolved in pyridine (2 mL) and treated with trifluoromethanesulfonic anhydride (682 μL, 2.7 mmol) at 0 ^{o}C for 10 min. The reaction mixture was sonicated (VWR international cleaning bat, model 150T) for 3 hours (no product was detected without sonication on a 4 hour period at room temperature). Evaporation of the solvent and flash column chromatography on silica gel (AcOEt/Hexane 2:11) afforded 323 mg of a chromatographically homogeneous sample containing a 60:22:18 mixture (measured by NMR) of 1,1-dioxo-1*H*,1′*H*-[2,2′-biphenalene]-4,4′-diyl bis(trifluoromethanesulfonate), 1- oxo-1*H*-phenalen-7-yl trifluoromethanesulfonate and 1-oxo-1*H*-phenalen-4-yl trifluoromethanesulfonate respectively. 1,1-dioxo-1*H*,1′*H*-[2,2′-biphenalene]-4,4′-diyl bis(trifluoromethanesulfonate): ^{1}H NMR (C_3D_6O, 500.13 MHz) δ 8.77 (dd, *J* = 7.5, 1.1 Hz, H-9-9′), 8.61 (dd, *J* = 8.3, 1.1 Hz, H-7-7′), 8.55 (d, *J* = 9.2 Hz, H-6-6′), 8.52 (s, H-3-3′), 8.05 (dd, *J* = 8.3, 7.5 Hz, H-8-8′), 7.84 (d, *J* = 9.2 Hz, H-5-5′); ^{13}C NMR (C_3D_6O, 125.75 MHz) δ 178.8 (C-1-1′), 148.4 (C-4-4′), 138.2 (C-7-7′), 137.2 (C-6-6′), 136.2 (C-3-3′), 135.3 (C-9-9′), 133.3 (C-6a-6a′), 130.7 (C-8-8′), 130.4 (C-9a-9a′), 130.1 (C-2-2′), 129.3 (C-9b-9b′), 123.0 (C-5-5′), 121.5 (C-3a-3a′). 1-

Oxo-1*H*-phenalen-7-yl trifluoromethanesulfonate: ^{1}H NMR (C_3D_6O, 500.13 MHz) δ 8.62 (d, *J* = 8.3 Hz, H-9), 8.28 (d, *J* = 8.8 Hz, H-6), 8.12 (d, *J* = 7.2 Hz, H-4), 8.03 (d, *J* = 9.9 Hz, H-3), 8.00 (d, *J* = 8.3 Hz, H-8), 7.95 (dd, *J* = 8.8, 7.2 Hz, H-5), 6.70 (d, *J* = 9.9 Hz, H-2). 1-Oxo-1*H*- phenalen-4-yl trifluoromethanesulfonate: ^{1}H NMR (C_3D_6O, 500.13 MHz) δ 8.63 (dd, *J* = 7.3, 1.1 Hz, H-9), 8.51 (dd, *J* = 7.5, 1.1 Hz, H-7), 8.45 (d, *J* = 9.0 Hz, H-6), 8.07 (d, *J* = 10.1 Hz, H-3), 7.99 (dd, *J* = 7.5, 7.3 Hz, H-8), 7.78 (d, *J* = 9.0 Hz, H-5), 6.86 (d, *J* = 10.1 Hz, H-2).

3-(2-(4-Methoxyphenyl)naphthalen-1-yl)propanoic acid: Prepared from ethyl 3-(2-(((trifluoromethyl)sulfonyl)oxy)naphthalen-1-yl)propanoate (**6**) (200 mg, 0.53 mmol) and (4-methoxyphenyl)boronic acid (83 mg, 0.55 mmol) and bis(triphenylphosphine)palladium(II)chloride (19 mg, 0.098 mmol, 5 mol%), 4 h reflux. The reaction mixture was partitioned between EtOAc/H_2O, the organic phase was dried and immediately submitted to hydrolysis (25 mL, aq. NaOH 30%, 3 h reflux) to afford 153 mg (94% for the two steps) of the acid as a white solid after acidification (HCl, pH~1), EtOAc/H_2O extraction and silica gel column chromatography (AcOEt/Hexane 1:8 then AcOEt). ^{1}H NMR (C_3D_6O, 500.13 MHz) δ 8.18 (d, *J* = 8.6 Hz, H-8′), 7.95 (d, *J* = 8.3 Hz, H-5′), 7.81 (d, *J* = 8.3 Hz, H-4′), 7.62 (ddd, *J* = 8.6, 6.6, 1.3 Hz, H-7′), 7.53 (ddd, *J* = 8.6, 6.8, 1.1 Hz, H-6′), 7.33 (d, *J* = 8.3 Hz, H-3′), 7.32 (d, *J* = 8.6 Hz, H-2′′-6′′), 7.05 (d, *J* = 8.6 Hz, H-3′′-5′′) 3.87 (s, -OCH_3), 3.34 (t, *J* = 8.4 Hz, H-3), 2.60 (t, *J* = 8.4 Hz, H-2); ^{13}C NMR (C_3D_6O, 125.75 MHz) δ 173.7 (C-1), 159.9 (C-4′′), 140.2 (C-2′), 135.5 (C-1′′), 134.7 (C-1′), 134.3 (C-4a′), 132.7 (C-8a′), 131.1 (C-2′′-6′′), 129.7 (C-5′), 129.5 (C-3′), 127.5 (C-7′), 127.3 (C-4′), 126.3 (C-6′), 124.9 (C-8′), 114.6 (C-3′′-5′′), 35.5 (C-2), 25.4 (C-3). HREIMS: *m/z* 306.1247 (calcd for $C_{20}H_{18}O_3$, 306.1256).

4-(4-Methoxyphenyl)-1*H*-phenalen-1-one (2a): Prepared from 3-(2-(4-methoxyphenyl)naphthalen-1-yl)propanoic acid (410 mg, 1.30 mmol), $SOCl_2$ (3 mL) and $AlCl_3$ (620.7 mg, 4.70 mmol) to obtain 363 mg (94%) of 4-(4-methoxyphenyl)-2,3- dihydro-1*H*-phenalen-1-one after Sephadex LH-20 column chromatography (Hexane/CH_2Cl_2/MeOH 5:3:1). This compound (68 mg) was submitted to NBS /light bromination-dehydrobromination (49 mg NBS, 1.20 mmol distributed in 2 additions, the last one at 30 min after initial reflux, 3 h

reflux) to afford 28 mg (43%) of the desired compound after silica gel column chromatography (CH_2Cl_2/Hexane 3:1). When the above perinaphthanone (68 mg) was refluxed for 1 h with DDQ (52 mg) in CH_2Cl_2 (7 mL), compound **2a** was isolated in 58% (39 mg) after Sephadex LH-20 column chromatography (Hexanes/CH_2Cl_2/MeOH 5:3:1) followed by preparative TLC (CH_2Cl_2/Hexane 3:1, R_f = 0.3). ^{1}H NMR (C_3D_6O, 500.13 MHz) δ 8.59 (dd, *J* = 7.3, 1.1 Hz, H-9), 8.42 (dd, *J* = 8.1, 1.1 Hz, H-7), 8.24 (d, *J* = 8.6 Hz, H-6), 7.92 (d, *J* = 10.1 Hz, H-3), 7.89 (dd, *J* = 8.1, 7.3 Hz, H-8), 7.69 (d, *J* = 8.6 Hz, H-5), 7.50 (d, *J* = 8.6 Hz, H-2′-6′), 7.16 (d, *J* = 8.6 Hz, H-3′-5′), 6.63 (d, *J* = 10.1 Hz, H-2), 3.92 (s, -OCH_3); ^{13}C NMR (C_3D_6O, 125.75 MHz) δ 185.9 (C-1), 161.9 (C-4′), 146.6 (C-4), 141.4 (C-3), 136.8 (C-7), 133.7 (C-6), 133.6 (C-2′-6′), 133.1 (C-1′), 131.8 (C-9), 131.5_0 (C-5), 131.5_3 (C-9a), 130.3 (C-8), 129.9 (C-9b), 128.8 (C-2), 125.9 (C-3a), 115.9 (C-3′-5′), 56.8 (-OCH_3). HREIMS: *m/z* 286.0990 (calcd for $C_{20}H_{14}O_2$, 286.0994).

3-(2-(4-Fluorophenyl)naphthalen-1-yl)propanoic acid: Prepared from ethyl 3-(2-(((trifluoromethyl)sulfonyl)oxy)naphthalen-1-yl)propanoate (**6**) (600 mg, 1.60 mmol) and (4-fluorophenyl)boronic acid (217 mg, 1.60 mmol) and bis(triphenylphosphine)palladium(II)chloride (56 mg, 0.080 mmol, 5 mol%), 2 h reflux. The reaction mixture was partitioned between EtOAc/H_2O, the organic phase was dried and submitted to silica gel column chromatography (AcOEt/Hexanes 1:15) to obtain 452 mg (88%) of the coupled product. This compound (435 mg, 1.40 mmol) was submitted to hydrolysis (25 mL, aq. NaOH 20%, 3 h reflux) to afford 382 mg (96%) of the acid as a white solid after acidification (HCl, pH~1). ^{1}H NMR (C_3D_6O, 500.13 MHz) δ 8.20 (d, *J* = 8.1 Hz, H-8′), 7.97 (d, *J* = 8.1 Hz, H-5′), 7.85 (d, *J* = 8.4 Hz, H-4′), 7.64 (ddd, *J* = 8.1, 6.8, 1.5 Hz, H-7′), 7.56 (ddd, *J* = 8.1, 6.8, 1.1 Hz, H-6′), 7.44 (dd, *J* = 9.0, 5.3 Hz, H-2′′-6′′), 7.34 (d, *J* = 8.4, H-3′), 7.26 (dd, *J* = 9.4, 9.0 Hz, H-3′′-5′′), 3.32 (t, *J* = 8.6 Hz, H-3), 2.58 (t, *J* = 8.6 Hz, H-2); ^{13}C NMR (C_3D_6O, 125.75 MHz) δ 173.6 (C-1), 162.9 (C-4′′, d, $J_{C\text{-}F}$ = 246.8 Hz), 139.5 (C-1′′, d, $J_{C\text{-}F}$ = 3.5 Hz), 139.4 (C-2′), 134.9 (C-1′), 134.4 (C-4a′), 132.7 (C-8a′), 132.0 (C-2′′-6′′, d, $J_{C\text{-}F}$ = 8.0 Hz), 129.7 (C-5′), 129.1 (C-3′), 127.6 (C-7′), 127.5 (C-4′), 126.6 (C-6′), 125.0 (C-8′), 115.9 (C-3′′-5′′, d, $J_{C\text{-}F}$ = 21.2 Hz), 35.4 (C-2), 25.4 (C-3); ^{19}F NMR (C_3D_6O, 125.75 MHz) δ –117.2. HREIMS: *m/z* 294.0969 (calcd for $C_{19}H_{15}FO_2$, 294.1056).

4-(4-Fluorophenyl)-1*H*-phenalen-1-one (2a): Prepared from 3-(2-(4-fluorophenyl)naphthalen-1-yl)propanoic acid (382 mg, 1.30 mmol), $SOCl_2$ (3 mL) and $AlCl_3$ (607 mg, 4.6 mmol) to obtain 348 mg (97%) of 4-(4-fluorophenyl)-1*H*-phenalen-1- one after silica gel column chromatography (CH_2Cl_2). This compound (348 mg) was submitted to NBS (254 mg, 1.40 mmol) /light bromination-dehydrobromination (2 h reflux) to afford 187 mg (54%) of the desired compound after silica gel column chromatography (AcOEt/Hexanes 1:7). ^{1}H NMR (C_3D_6O, 500.13 MHz) δ 8.60 (dd, *J* = 7.3, 1.3 Hz, H-9), 8.44 (dd, *J* = 8.1, 1.3 Hz, H-7), 8.27 (d, *J* = 8.4 Hz, H-6), 7.92 (dd, *J* = 8.1, 7.3 Hz, H-8) 7.86 (d, *J* = 10.1 Hz, H-3), 7.69 (d, *J* = 8.6 Hz, H-5), 7.62 (dd, *J* = 8.8, 5.5 Hz, H-2′-6′), 7.38 (dd, *J* = 9.0, 8.8 Hz, H-3′-5′), 6.64 (d, *J* = 10.1 Hz, H-2); ^{13}C NMR (C_3D_6O, 125.75 MHz) δ 185.9 (C-1), 145.5 (C-4), 141.0 (C-3), 136.9 (C-7), 134.4 (C-1′), 134.2 (C-2′′-6′′, d, $J_{C\text{-}F}$ = 8.0 Hz), 133.8 (C-6), 133.8 (C-6a), 132.0 (C-9), 131.5 (C-9a), 131.3 (C-5), 130.7 (C-2), 129.8 (C-9b), 129.0 (C-8), 126.2 (C-3a), 117.3 (C-3′′-5′′, d, $J_{C\text{-}F}$ = 21.2 Hz). HREIMS: *m/z* 274.0868 (calcd for $C_{19}H_{11}FO$, 274.0794).

3-(2-(1*H*-Pyrazol-4-yl)naphthalene-1-yl)propanoic acid: Prepared from ethyl 3-(2-(((trifluoromethyl)sulfonyl)oxy)naphthalen-1-yl)propanoate (**6**) (200 mg, 0.54 mmol) and 4-pyrazoleboronic acid pinacol ester (126 mg, 0.65 mmol) and bis(triphenylphosphine)palladium(II)chloride (19 mg, 5 mol%), 22 h reflux, to afford 151 mg of ethyl 3-(2-(1*H*-pyrazol-4-yl)naphthalen-1-yl)propanoate (95%). The product was submitted to hydrolysis (25 mL, aq. NaOH 30%, 16 h reflux) to afford 132 mg (97%) of the acid after acidification and extraction with ether. ^{1}H NMR (C_3D_6O, 500.13 MHz) δ 8.19 (d, *J* = 8.4 Hz, H-8′), 7.92 (d, *J* = 7.5 Hz, H-5′), 7.86 (s, H-3′′-5′′), 7.81 (d, *J* = 8.4 Hz, H-4′), 7.60 (ddd, *J* = 8.4, 7.0, 1.3 Hz, H-7′), 7.51 (ddd, *J* = 7.5, 7.0, 1.0 Hz, H-6′), 7.50 (d, *J* = 8.4 Hz, H-3′), 3.51 (t, *J* = 8.6 Hz, H-3), 2.68 (t, *J* = 8.6 Hz, H-2); ^{13}C NMR (C_3D_6O, 125.75 MHz) δ 174.9 (C-1), 135.6 (C-1′), 135.0 (C-4a′), 134.9 (C-3′′-5′′), 134.0 (C-8a′), 132.2 (C-2′), 130.7 (C3′), 130.6 (C-5′), 128.6 (C-4′), 128.4 (C-6′), 127.2 (C-7′), 125.8 (C-8′), 123.0 (C-4′′), 36.6 (C-2), 26.7 (C-3). HREIMS: *m/z* 266.1051 (calcd for $C_{16}H_{14}N_2O_2$, 266.1055).

4-(1-*H*-Pyrazol-4-yl)-1*H*-phenalen-1-one (2c): For this compound, DDQ dehydrogenation was followed due to unsatisfactory results using NBS/light. 3-(2-(1*H*-Pyrazol-4- yl)naphthalene-

1-yl)propanoic acid (132 mg, 0.50 mmol) was treated with $SOCl_2$ (2 mL) and the residual $SOCl_2$ was evaporated by means of a heat gun. The reaction mixture was diluted with CH_2Cl_2 (8 mL) and $AlCl_3$ (220 mg, 1.65 mmol) was added in one portion with agitation for 20 min. The reaction crude was dried and picked with 2 mL of a Hexane/CH_2Cl_2/MeOH 5:3:1 solution, filtered with a cotton plug and submitted to Sephadex LH-20 column chromatography (Hexane/CH_2Cl_2/MeOH 5:3:1) to give 82 mg (66%) of the 4-pyrazolperinaphthanone. Dehydrogenation of the 4-pyrazolperinaphthanone (82 mg) with DDQ (75 mg, 0.33 mmol) in CH_2Cl_2 (10 mL, 1.5 h reflux) afforded 31 mg (38%, 44% bsrm) of 4-(1-*H*-pyrazol-4-yl)-1*H*-phenalen-1-one (**2c**) after Sephadex LH-20 column chromatography (Hexane/CH_2Cl_2/MeOH 5:3:1). ^{1}H NMR (MeOH-d_4, 500.13 MHz) δ 8.64 (dd, *J* = 7.5, 1.1 Hz, H-9), 8.36 (dd, *J* = 7.7, 1.1 Hz, H-7), 8.30 (d, *J* = 9.9 Hz, H-3), 8.19 (d, *J* = 8.6 Hz, H-6), 8.02 (s, H-3′-5′), 7.84 (dd, *J* = 7.7, 7.5 Hz, H-8), 7.76 (d, *J* = 8.6 Hz, H-5), 6.75 (d, *J* = 9.9 Hz, H-2). ^{13}C NMR (MeOH-d_4, 125.75 MHz) δ 187.3 (C-1), 142.0 (C-3), 138.7 (C-4), 137.1 (C-7), 134.1 (C-6), 132.8 (C-6a), 132.1 (C-9), 130.8 (C-5), 130.5 (C-9a), 129.2 (C-9b), 129.1 (C-2), 128.0 (C-8), 124.7 (C-3a), 120.7 (C-4′). HREIMS: *m/z* 246.0787 (calcd for $C_{16}H_{10}N_2O$, 246.0793).

3-(2-(4-Methylthiophen-3-yl)naphthalene-1-yl)propanoic acid: Prepared from ethyl 3-(2-(((trifluoromethyl)sulfonyl)oxy)naphthalen-1-yl)propanoate (**6**) (666 mg, 1.8 mmol) and 4-methyl-3-thiopheneboronic acid pinacol ester (400 mg, 1.8 mmol) and bis(triphenylphosphine)palladium(II)chloride (60 mg, 5 mol%), 4 h reflux. To afford 550 mg of ethyl 3-(2-(4-methylthiophen-3-yl)naphthalene-1-yl)propanoate (94%). The product was immediately submitted to hydrolysis (25 mL, aq. NaOH 30%, 3 h reflux) to afford 400 mg (80%) of the acid. ^{1}H NMR (C_3D_6O, 500.13 MHz) δ 8.19 (d, *J* = 8.4 Hz, H-8′), 7.96 (d, *J* = 8.3 Hz, H-5′), 7.83 (d, *J* = 8.6 Hz, H-4′), 7.62 (ddd, *J* = 8.4, 7.7, 1.5 Hz, H-7′), 7.55 (ddd, *J* = 8.3, 7.7, 1.1 Hz, H-6′), 7.33 (d, *J* = 3.1 Hz, H-2′′), 7.26 (d, *J* = 8.6 Hz, H-3′), 7.24 (dd, *J* = 3.1, 0.9 Hz, H-5′′), 3.3 (brm, H-3), 2.52 (t, *J* = 8.4 Hz, H-2), 2.00 (d, *J* = 0.9 Hz, - CH_3); ^{13}C NMR (C_3D_6O, 125.75 MHz) δ 174.7 (C-1), 144.4 (C-3′′), 138.5 (C-2′), 137.2 (C-1′), 136.1 (C-4′′), 135.5 (C-4a′), 133.7 (C-8a′), 130.7 (C-5′), 130.1 (C-3′), 128.4$_3$ (C-7′), 128.3$_6$ (C-4′), 127.5 (C-6′), 125.9 (C-8′), 124.9 (C-2′′), 123.4 (C-5′′), 36.3 (C-2), 26.6 (C-3), 16.0 (-CH_3).

HREIMS: *m/z* 296.0864 (calcd for $C_{18}H_{16}O_2S$, 296.0871).

6-Methyl-1*H*-naphtho[2´,1´:3,4]cyclohepta[1,2-*b*]thiophen-3-(2*H*)-one (2d): Prepared from 3-(2-(4-methylthiophen-3-yl)naphthalene-1-yl)propanoic acid (400 mg, 1.4 mmol), $SOCl_2$ (1 mL) and $AlCl_3$ (628 mg, 4.7 mmol) to obtain 255 mg (68%) of **2d** after Sephadex LH-20 column chromatography (Hexane/CH_2Cl_2/MeOH 5:3:1). ^{1}H NMR (C_3D_6O, 500.13 MHz) δ 8.35 (d, *J* = 8.6 Hz, H-12), 7.96 (d, *J* = 8.1 Hz, H-9), 7.90 (d, *J* = 8.6 Hz, H-8), 7.66 (d, *J* = 0.9 Hz, H-5), 7.63 (d, *J* = 8.6 Hz, H-7), 7.60 (ddd, *J* = 8.6, 7.0, 1.7 Hz, H-11), 7.56 (ddd, *J* = 8.1, 7.0, 1.1 Hz, H-10), 3.53 (brm, H-1), 2.84 (brm, H-2), 2.40 (d, *J* = 0.9 Hz, -CH_3); ^{13}C NMR (C_3D_6O, 125.75 MHz) δ 197.3 (C-3), 145.3 (C-3a), 142.4 (C-5), 140.2 (C-12b), 138.8 (C-8a), 135.3 (C-6a), 132.7_2 (C-12a), 132.6_9 (C-6), 131.5 (C-9), 130.6 (C-8), 128.8 (C-6b), 128.5 (C-11), 128.3 (C-10), 128.1 (C-7), 126.0 (C-12), 46.3 (C-2), 24.6 (C-1), 18.0 (-CH_3). HREIMS: *m/z* 278.0755 (calcd for $C_{18}H_{14}OS$, 278.0765).

Research Article

Received: 19 February 2015 Revised: 28 April 2015 Accepted article published: 9 June 2015 Published online in Wiley Online Library:

(wileyonlinelibrary.com) DOI 10.1002/ps.4055

4-Phenylphenalenones as a template for new photodynamic compounds against *Mycosphaerella fijiensis*

William Hidalgo,[a] Marisol Cano,[b] Manuela Arbelaez,[b] Edwin Zarrazola,[c] Jesús Gil,[d] Bernd Schneider[a*] and Felipe Otálvaro[b*]

Abstract

BACKGROUND: Evaluation of 4-phenylphenalenones and structural analogues against the fungal pathogen *Mycosphaerella fijiensis* (causal agent of black sigatoka disease in bananas) under light-controlled conditions uncovered some key structural features for the design of photodynamic compounds.

RESULTS: Structure–activity relationship analysis revealed the importance of a chromophoric aryl-ketone and a steroidomimetic structural motif in the activity of the assayed compounds. The results pointed to 1,2-dihydro-3*H*-naphtho[2′,1′:3,4]cyclohepta[1,2-b]furan-3-one, which displayed an activity in the range of propiconazole but with photodynamic behaviour.

CONCLUSION: The present work demonstrates that 1,2-dihydro-3*H*-naphtho[2′,1′:3,4]cyclohepta[1,2-*b*]heterocyclic-3-one derivatives can be used as potential lead compounds for the development of fungicides, relying on a dual mode of action.

Supporting information may be found in the online version of this article.

Keywords: photodynamic activity; 4-phenylphenalenones; *Mycosphaerella fijiensis*; structure–activity relationship

1 INTRODUCTION

Fungal infections can be considered to pose the biggest threat to *Musa acuminata* (banana) cultivars.[1,2] Among these, *Fusarium oxysporum* and *Mycosphaerella fijiensis* (causal agents of Panama and Black Sigatoka diseases respectively) stand out as the most virulent, causing enormous economic losses and even potentially undermining the future of the Cavendish cultivar (the global-trade dominant variety).[1,2] Although strategies based on conventional breeding and genetic modification have been formulated, chemical treatment continues to be the main way of dealing with these infections.[1,3,4] However, the appearance of resistant fungal strains and the increasing need for environmentally friendly control measures call for new fungicidal compounds.[5]

Finding a lead structure constitutes the first step in the development of any agrochemical. In this regard, natural products are more likely than synthesised products to deliver new active motifs.[6] In the present case, phenylphenalenone-type phytoalexins have been used as template structures to design fungitoxic agents.[7–9]

Phenylphenalenones are natural products isolated mainly from the Haemodoraceae and Musaceae families.[10,11] In Musa plants, these compounds are clearly involved in the defence mechanism against nematodes,[12] and their accumulation is elicited by *Colletotrichum musae*,[13] *Fusarium oxysporum*,[14] *Mycosphaerella fijiensis*,[15] *Radopholus similis*[16] and *Sporobolomyces salmonicolor*,[17] meeting the definition of phytoalexins.[7] The phenyl group can be found attached to phenalenone positions C-9 or C-4, and some identical 9-phenylphenalenones have been reported in both families.[10] However, 4-phenylphenalenones remain exclusive to Musaceae. In addition, phenalenones with diverse substituents (including C-4) have been shown to enhance their antifungal activity through photosensitisation.[8,9]

This evidence suggests that C-4-substituted phenalenones might be used as interesting photodynamic templates for biological explorations, a statement that contrasts with the few studies conducted to date.[8,9,18,19]

Recently, we reported a nine-step synthesis of 4-phenylphenalenones, starting with 2-naphthol, that allows for the preparation of structural analogues in sufficient quantities

* *Correspondence to: B Schneider, Max-Planck Institut für Chemische Ökologie, Beutenberg Campus, Hans-Knöll-Strasse 8, 07745 Jena, Germany, E-mail: schneider@ice.mpg.de; or F Otálvaro, Instituto de Química-Universidad de Antioquia, Calle 67# 53–108, A.A. 1226, Medellín, Colombia. E-mail: leon.otalvaro@udea.edu.co*

a *Max-Planck Institut für Chemische Ökologie, Jena, Germany*

b *Instituto de Química-Universidad de Antioquia, Medellín, Colombia*

c *Instituto de Matemáticas-Universidad de Antioquia, Medellín, Colombia*

d *Universidad Nacional de Colombia sede Medellín, Autopista Norte, Medellín, Colombia*

for biological assays.[20] Here, the results of such assays conducted on *Mycosphaerella fijiensis* in the dark and under light-controlled conditions are reported.

2 MATERIALS AND METHODS

2.1 General

All reactions were monitored by thin-layer chromatography (TLC) carried out on 0.25 mm Merck silica gel plates (60-F_{254}) (Merck, Darmstadt, Germany) using UV light (254 nm) as a visualising agent and vanillin solution and heat as developing agents. NMR spectroscopic analyses were performed on a Bruker Avance 500 NMR spectrometer (Bruker, Billerica, MA) operating at 500.13 MHz (^{1}H) and 125.75 MHz (^{13}C). Chemical shifts were reported relative to residual solvent peaks. Signals were assigned with the aid of HMQC, HMBC and ^{1}H,^{1}H-COSY spectra. HREMIS was run on a Micromass MasSpec mass spectrometer at 70 eV with a direct insertion probe and in positive ion mode, except for fluorinated compounds, for which negative ion mode was used. All reagents were purchased from Sigma-Aldrich (St Louis, MO) and used without further purification. Yields refer to chromatographically homogeneous samples. The R_f values for compounds **8** to **12** were measured using petroleum ether (bp 55–68 °C) as eluent.

2.2 Synthetic procedures

Compounds **1** to **7**, **13** and **14** were prepared and purified as described earlier.[20] Compounds **8** to **12** are also known;[21–24] however, these were prepared by a different method.

2.2.1 *General method for the preparation of arylnaphthalenes (8 to 12)*

A 10 mL round-bottomed flask was charged with 2-bromonaphthalene (62 mg, 0.30 mmol), arylboronic acid (0.34 mmol), $Pd(PPh_3)_2Cl_2$ (11 mg, 5 mol%), dioxane (5 mL) and $Na_2CO_{3(aq)}$ (0.5 mL, 2 M) and refluxed for 24 h. After solvent partition between CH_2Cl_2 (30 mL × 3)/H_2O (50 mL), the organic layer was dried (Na_2SO_4), concentrated and purified by preparative TLC (silica gel 60 GF_{254}; Merck) using petroleum ether (bp 55–68 °C) as an eluent, except for compounds **10** and **11**, for which a Sephadex LH-20 column chromatography was conducted using petroleum ether/CH_2Cl_2/MeOH (5:3:1). Yields were as follows: compound **8** (56 mg, 82%, R_f = 0.5), compound **9** (22 mg, 31%, R_f = 0.3), compound **10** (38 mg, 60%, R_f = 0.4), compound **11** (5 mg, 8%, R_f = 0.4) and compound **12** (28 mg, 47%, R_f = 0.5). No attempt was made to optimise the reactions.

2-(4-Fluorophenyl)naphthalene (8). ^{1}H NMR (C_3D_6O, 500.13 MHz): δ 8.17 (d, J = 1.8 Hz, H-1), 8.00 (d, J = 8.6 Hz, H-4), 7.99 (d, J = 7.7 Hz, H-5), 7.94 (dd, J = 8.4, 1.5 Hz, H-8), 7.85 (m–dd, $^3J_{H-F}$ = 9.9, J_{H-H} = 8.8 Hz, H-3′–5′), 7.82 (dd, J = 8.6, 1.8 Hz, H-3), 7.55 (ddd, J = 7.7, 6.9, 1.5 Hz, H-6), 7.52 (ddd, J = 8.4, 6.9, 1.5 Hz, H-7), 7.28 (m–dd, $^4J_{H-F}$ = 5.3, J_{H-H} = 8.8 Hz, H-3′–5′). ^{13}C NMR (C_3D_6O, 125.75 MHz): δ 162.8 (d, $^1J_{C-F}$ = 244 Hz, C-4′), 139.1 (C-1′), 135.7 (C-4a), 134.6 (C-8a), 130.9 (d, $^3J_{C-F}$ = 8, C-2′-6′), 130.4 (C-4), 130.1 (C-5), 129.4 (C-8), 128.3 (C-6), 127.9 (C-7), 127.3 (C-1), 127.0 (C-3), 117.5 (d, $^2J_{C-F}$ = 21, C-3′–5′). HREIMS: *m/z* 221.0757 [M – H] (calcd for $C_{16}H_{11}F$, 222.08448).

2-(4-Methoxyphenyl)naphthalene (9). ^{1}H NMR (C_3D_6O, 500.13 MHz): δ 8.13 (d, J = 2.0 Hz, H-1), 7.98 (d, J = 8.6 Hz, H-4), 7.97 (d, J = 8.1 Hz, H-5), 7.92 (d, J = 7.9 Hz, H-8), 7.82 (dd, J = 8.6, 2.0 Hz, H-3), 7.76 (d, 2H, J = 9.0 Hz, H-2′–6′), 7.48–7.54 (m, 2H, H-6–H-7), 7.08 (d, 2H, J = 9.0 Hz, H-3′–5′), 3.87 (s, –OMe). ^{13}C NMR (C_3D_6O, 125.75 MHz): δ 161.4 (C-4′), 139.8 (C-2), 135.8 (C-8a), 134.9 (C-4a), 134.3 (C-1′), 130.3 (C-5), 130.0 (C-2′–6′), 129.9 (C-8), 129.4 (C-4), 128.1, 127.5, 126.9 (C-3), 126.5 (C-1), 116.2 (C-3′-5′), 56.6 (–OMe). HREIMS: *m/z* 235.1117 [M + H] (calcd for $C_{17}H_{14}O$, 234.1045).

2-Phenylnaphthalene (10). ^{1}H NMR (C_3D_6O, 500.13 MHz): δ 8.19 (d, J = 1.8 Hz, H-1), 8.00 (d, J = 8.6 Hz, H-4), 7.99 (d, J = 7.3 Hz, H-5), 7.94 (d, J = 7.7 Hz, H-8), 7.84 (dd, J = 8.6, 1.8 Hz, H-3), 7.81 (m, 2H, H-2′–6′), 7.52–7.54 (m, 2H, H-6–H-7), 7.52 (m, 2H, H-3′–5′), 7.40 (tt, J = 7.3, 1.3 Hz, H4′). ^{13}C NMR (C_3D_6O, 125.75 MHz): δ 142.6 (C-1′), 140.1 (C-2), 135.7 (C-8a), 134.6 (C-4a), 130.8 (C-2′–6′), 130.4 (C-1), 130.3 (C-5), 130.1 (C-4), 129,4 (C-8), 129.3 (C-4′), 129.0 (C-3′–5′), 128.2, 127.8, 127.1 (C-3). HREIMS: *m/z* 205.1017 [M + H] (calcd for $C_{16}H_{12}$, 204.0939).

4-(Naphthalen-2-yl)-1H-pyrazole (11). ^{1}H NMR (CD_3OD, 500.13 MHz): δ 8.05 (d, J = 1.8 Hz, H-1), 7.85 (d, J = 8.6 Hz, H-4), 7.85 (d, J = 8.6 Hz, H-5), 7.82 (d, J = 8.1 Hz, H-8), 7.74 (dd, J = 8.6, 1.8 Hz, H-3), 7.47–7.40 (m, 2H, H-6–H-7). ^{13}C NMR (CD_3OD, 125.75 MHz): δ 135.5 (C-8a′), 133.8 (C-4a′), 131.5 (C-2′), 129.5, 128.8, 128.7 (C-8′), 127.4, 126.5, 125.6 (C-3′), 123.2 (C-4). HREIMS: *m/z* 195.0917 [M + H] (calcd for $C_{13}H_{10}N_2$, 194.0844).

3-(Naphthalene-2-yl)furan (12). ^{1}H NMR (C_3D_6O, 500.13 MHz): δ 8.17 (dd, J = 1.5, 0.92 Hz, H-2), 8.12 (d, J = 1.8 Hz, H-1′), 7.91 (d, J = 8.6 Hz, H-4′), 7.90 (d, J = 8.1 Hz, H-5′), 7.88 (d, J = 8.3 Hz, H-8′), 7.78 (dd, J = 8.6, 1.8 Hz, H-3′), 7.69 (dd, J = 1.83, 1.5 Hz, H-5), 7.48 (m, 2H, H-6′–H-7′), 7.05 (dd, J = 1.83, 0.92 Hz, H-4). ^{13}C NMR (C_3D_6O, 125.75 MHz): δ 146.1 (C-5), 141.4 (C-2), 135.8 (4a′), 134.5 (8a′), 131.8 (C-2′), 130.3, 129.6, 129.5, 128.3 (C-3), 128.2 (C-6′), 127,5 (C-7′), 126.2 (C-3′), 125.6 (C-1′), 110.5 (C-4). HREIMS: *m/z* 195.0810 [M + H] (calcd for $C_{14}H_{10}O$, 194.0732).

2.3 Fungicidal assay

The *M. fijiensis* strain (voucher Ca10_13) was kindly donated by Dr Gert Kema (Plant Research International, Wageningen, The Netherlands).

A microtitre well method developed by Peláez *et al.*[25] was used, with some modifications.[9] Specifically, *M. fijiensis* strain (voucher Ca10_13) grown over a period of 15–17 days at 26 ± 1 °C in potato dextrose agar (PDA) (Fluka Analytical, Steinheim, Germany) was used for preparing the fungal inoculum. Mycelium of the culture was scraped with a smear loop using sterile water, and the dense suspension obtained was then fragmented in a vortex mixer with glass beads of 4 ± 0.3 mm diameter (Carl Roth GmbH, Karlsruhe, Germany). Filtration through four layers of sterile cheesecloth followed, in order to obtain uniform mycelial fragments. The concentration of the inoculum was counted under a light microscope using a Neubauer haematocytometer (Marienfeld, Lauda-Königshofen, Germany) and adjusted to 2×10^5 mycelial fragments mL^{-1} with sterile water. Sterile microtitre plates 96 well-F (Sarstedt AG & Co, Nümbrecht, Germany) were used for biological incubation. Each well was filled with 50 µL of Sabouraud broth (Fluka Analytical), 50 µL of the inoculum solution and 50 µL of compound solutions. Concentrations ranging from 1 to 100 ppm of each compound were prepared in 50% aqueous dimethyl sulfoxide (DMSO) (BioReagent, for molecular biology, ≥99.9%; Sigma-Aldrich) and passed through a filter (0.1 µm, hydrophilic polyethersulfone membrane sterile; PALL Life Sciences, Harbor Park Drive, NY) before administration to the incubation system. For control purposes, a solution of culture medium (50 µL; Sabouraud), 50 µL of inoculum and 50 µL of aqueous DMSO (50%, sterile) was used. The effect of DMSO was tested, replacing it with sterile water. Propiconazole (98.4%; Fluka

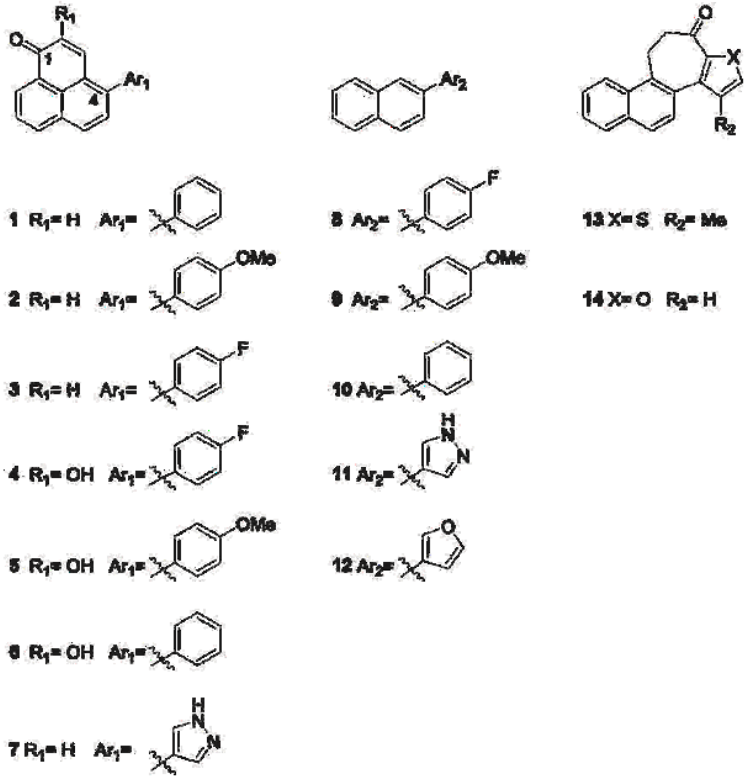

Figure 1. Synthetic compounds **1** to **14** assayed in this work. Compounds **5** and **6** occur as natural products in *Musa acuminata*.[26]

Analytical) was used as a positive control. The same procedure was applied for negative control, replacing the inoculum solution with sterile water. The microplates were incubated under darkness or photoperiod for 8 days (for the logarithmic growth phase of the fungi, see the supporting information) at 25 °C in an incubation chamber. For light-controlled experiments, plates were placed at a distance of 1 m from the light source (two cool white light tubes, Sylvania Luxline Plus T8 36 W/840; Osram Sylvania, Munich, Germany) and subjected to a 12 h photoperiod treatment per day. Both experiments (darkness and photoperiod) were carried out simultaneously. Optical density ($OD_{595\,nm}$) was recorded on a Tecan Infinite M200 spectrophotometer (Tecan, Männedorf, Switzerland) with a multimode microplate reader (Molecular Devices, Silicon Valley, CA) at 0 and 8 days after incubation in order to measure the mycelial growth. The experimental design comprised three biological replicates (including three technical replicates). The IC_{50} value was calculated by plotting the mycelial growth (data previously normalised to the reference control) against the logarithm of each concentration of the compound assessed. A one-way ANOVA (Statgraphics® centurion XVI v.16.1.11; Statpoint Technologies, Warrenton, VA) with a 95% confidence was employed in order to determine whether there were statistically significant differences between two samples (dark versus photoperiod for each compound).

3 RESULTS AND DISCUSSION

3.1 Synthetic chemistry

Compounds **1** to **7** (Fig. 1) were prepared according to our previously reported method.[20] Briefly, the Michael addition of cyanoacrylate to 2-naphthol followed by hydrolysis and Fisher esterification afforded ethyl 3-(2-hydroxynaphthalen-1-yl)propanoate which, upon triflation, generated ethyl 3-(2-{[(trifluoromethyl)sulfonyl]oxy}naphthalene-1-yl)propanoate. The latter compound served as a branching point in the generation of the title compounds throughout the application of a Suzuki–Miyaura – Friedel–Crafts sequence. Compounds **8** to **12** (Fig. 1) were prepared under the same Suzuki–Miyaura conditions using 2-bromonaphthalene as substrate.

3.2 Fungicidal activities and structure–activity relationship analysis

Figure 2 presents the antifungal activity of compounds **1** to **15** (*M. fijiensis* mycelial growth inhibition) measured in the dark and under light-controlled conditions.[9] Propiconazole (**15**) was tested for reference purposes.

At first glance, all arylperinaphthenones (compounds **1** to **7**) displayed significant photodynamic behaviour (see the supporting information for statistical analysis). Interestingly, comparing compounds **1** to **3** with compounds **4** to **6** points to the relevance of the α-hydroxyenone moiety for the activity of these compounds. This is intriguing, considering that natural 4-phenylphenalenones ubiquitously contain this substitution.[10,11] Pyrazole derivative **7** displays an extreme difference between IC_{50} values of 72 ± 8 ppm in the dark and 20 ± 1 ppm under the photoperiod.

To clarify this further, compounds **8** to **11** (completely lacking the chromophoric enone) were prepared and tested under the same conditions. Interestingly, these compounds displayed activities in the same range or in an even greater range than

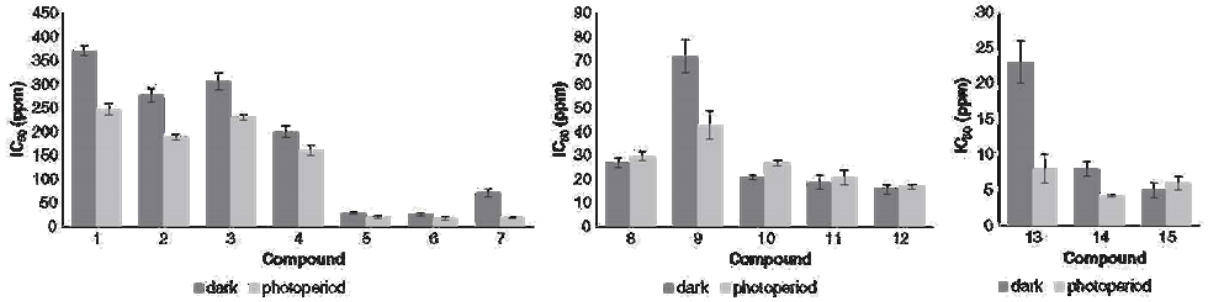

Figure 2. Antifungal activity of compounds **1** to **15** on *Mycosphaerella fijiensis*. The effect on mycelial growth was measured in the dark and under photoperiods of 12 h during 8 days of incubation. Propiconazole (**15**) was tested for reference purposes.

their enone-containing counterparts. However, the lack of the chromophore rendered compounds **8** and **11** photodynamically inactive. These data reveal the topological importance of the 2-arylnaphthalene moiety. The structural motif is recognised as steroidomimetic owing to resemblance with rings A–B–D.[27] The above evidence draws our attention to compounds **13** and **14** (Fig. 1). These compounds were obtained as products of different regioselectivity in the Friedel–Crafts reaction during the synthesis of 4-phenylphenalenones.[20] Compounds **13** and **14** contain the necessary 2-arylnaphthalene moiety in a conformationally restricted configuration, in agreement with the A–B–D spatial distribution of the steroid nuclei. Moreover, compounds **13** and **14** possess an intrinsic aryl-ketone, which hopefully could induce photodynamic behaviour.

To our gratification, compounds **13** and **14** displayed activities in the range of propiconazole but with significant photodynamic activity. Compound **14**, being the most active compound assayed ($IC_{50\text{-dark}} = 8 \pm 1$ ppm; $IC_{50\text{-light}} = 4 \pm 1$ ppm), was compared with 3-(naphthalene-2-yl)furan (**12**) in order to establish the role of the chromophore (Fig. 2). The results ($IC_{50\text{-dark}} = 16 \pm 2$ ppm; $IC_{50\text{-light}} = 17 \pm 1$ ppm for compound **12**) clearly demonstrate the role of the aryl-ketone in compound **14** as an inducer of photodynamic activity, and reinforce the importance of the ethylene bridge in fixing the arylnaphthalene conformation.

4 CONCLUSION

We have shown the photodynamic activity of 4-phenylphenalenones and structural analogues against *M. fijiensis*, which relies on a dual mode of action. In particular, the combination of 2-heteroarylnaphthalene with a conjugated ketone as a chromophore seems to be relevant, especially if a rigid steroidomimetic conformation can be acquired, as in compound **14** (Fig. 3).

These requirements can be found in other phenylphenalenone-related compounds, such as naphthoxanthenones, that have yet to be explored.[28]

ACKNOWLEDGEMENTS

We thank Emily Wheeler for editorial assistance. This research was financially supported by Universidad de Antioquia (Grant IN651CE), Fundación para la Promoción de la Investigación y la Tecnología (Convenio 201327) and the Max-Planck-Institut für Chemische Ökologie.

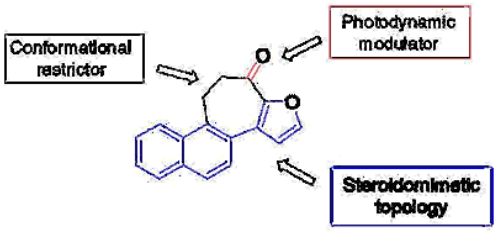

Figure 3. Structural characteristics of compound **14** relevant for fungicidal activity against *Mycosphaerella fijiensis*.

SUPPORTING INFORMATION

Supporting information may be found in the online version of this article.

REFERENCES

1 Marín DH, Romero RA, Guzmán M and Sutton TB, Black Sigatoka: an increasing threat to banana cultivation. *Plant Dis* **87**:208–222 (2003).
2 Butler D, Fungus threatens top banana. *Nature* **504**:195–196 (2013).
3 Jones D, Novel and conventional path to a better banana. *Nature* **421**:889–889 (2003).
4 Grube A, Donaldson D, Kiely T and Wu L, *Pesticides Industry Sales and Usage, 2006 and 2007 Market Estimates*. [Online]. Biological and Economic Analysis Division, Office of Pesticide Programs, Office of Chemical Safety and Pollution Prevention, US Environmental Protection Agency, Washington, DC (2011). Available: http://www.epa.gov/opp00001/pestsales/07pestsales/market_estimates2007.pdf [29 October 2014].
5 Harrison W, Agrochemical research and development in the 21st century: bloom or bust. *J Biomol Screen* **4**:61–65 (1999).
6 Peng J, Shen X, El Sayed K, Dunbar DC, Perry TL, Wilkins SP *et al.*, Marine natural products as prototype agrochemical agents. *J Agric Food Chem* **51**:2246–2252 (2003).
7 Essenberg M, Prospects for strengthening plant defenses through phytoalexin engineering. *Physiol Mol Plant Pathol* **59**:71–81 (2001).
8 Lazzaro A, Corominas M, Martí C, Flors C, Izquierdo LR, Grillo TA *et al.*, Light- and singlet oxygen-mediated antifungal activity of phenylphenalenone phytoalexins. *Photochem Photobiol Sci* **3**:706–710 (2004).
9 Hidalgo W, Duque L, Sáez J, Arango R, Gil J, Rojano B *et al.*, Structure–activity relationship in the interaction of substituted perinaphthenones with *Mycosphaerella fijiensis*. *J Agric Food Chem* **57**:7417–7421 (2009).
10 Fang J, Paetz C, Hölscher D, Munde T and Schneider B, Phenylphenalenones and related natural products from *Wachendorfia thyrsiflora* L. *Phytochem Lett* **4**:203–208 (2011).
11 Kamo T, Hirai N, Iwami K, Fujioka D and Ohigashi H, New phenylphenalenones from banana fruit. *Tetrahedron* **57**:7649–7656 (2001).

12 Hölscher D, Dhakshinamoorthy S, Alexandrov T, Becker M, Bretschneider T, Buerkert A *et al.*, Phenalenone-type phytoalexins mediate resistance of banana plants (*Musa* spp.) to the burrowing nematode *Radopholus similis*. *PNAS* **111**:105–110 (2014).
13 Kamo T, Kato N, Hirai N, Tsuda M, Fujioka D and Ohigashi H, Phenylphenalenone-type phytoalexins from unripe Buñgulan banana fruit. *Biosci Biotechnol Biochem* **62**:95–101 (1998).
14 Luis JG, Fletcher WQ, Echeverri F, Abad T, Kishi MP and Perales A, New phenalenone-type phytoalexins from *Musa acuminata* (colla AAA) Gran nain. *Nat Prod Lett* **6**:23–30 (1995).
15 Luis JG, Echeverri F, Quiñones W, Brito I, López M, Torres F *et al.*, Irenolone and emenolone: two new types of phytoalexin from *Musa paradisiaca*. *J Org Chem* **58**:4306–4308 (1993).
16 Blinks RH, Greenham JR, Luis JG and Gowen SR, A phytoalexin from roots of *Musa acuminata* var. *Pisang sipulu*. *Phytochemistry* **45**:47–49 (1997).
17 Jitsaeng K and Schneider B, Metabolic profiling of *Musa acuminata* challenged with *Sporobolomyces salmonicolor*. *Phytochem Lett* **3**:84–87 (2010).
18 Rosquete LI, Cabrera-Serra MG, Piñero JE, Martín-Rodríguez P, Fernández-Pérez L, Luis JG *et al.*, Synthesis and *in vitro* antiprotozoal evaluation of substituted phenalenone analogues. *Bioorg Med Chem* **18**:4530–4534 (2010).
19 Quiñones W, Escobar G, Echeverri F, Torres F, Rosero Y, Arango V *et al.*, Synthesis and antifungal activity of *Musa* phytoalexins and structural analogs. *Molecules* **5**:974–980 (2000).
20 Cano M, Rojas C, Hidalgo W, Sáez J, Gil J, Schneider B *et al.*, Improved synthesis of 4-phenylphenalenones: the case of isoanigorufone and structural analogs. *Tetrahedron Lett* **54**:351–354 (2013).
21 Chung KH, So CM, Wong SM, Luk CH, Zhou Z, Lau CP *et al.*, An efficient palladium–benzimidazolyl phosphine complex for the Suzuki–Miyaura coupling of aryl mesylates: facile ligand synthesis and metal complex characterization. *Chem Commun* **48**:1967–1969 (2012).
22 Agrawal T and Cook SP, Iron-catalyzed coupling of aryl sulfamates and aryl/vinyl/tosylates with aryl Grignards. *Org Lett* **16**:5080–5083 (2014).
23 Guan BT, Lu XY, Zheng Y, Yu DG, Wu T, Li KL *et al.*, Biaryl construction through Kumada coupling with diaryl sulfates as one-by-one electrophiles under mild conditions. *Org Lett* **12**:396–399 (2010).
24 Vashkevich EV, Potkin VI and Kozlov NG, Uncommon heterocyclization into a pyrazole system of *Z*-3-(2-naphthyl)-3-chloro-2-propenal semicarbazone and thiosemicarbazone. *Russ J Org Chem* **41**:739–741 (2005).
25 Peláez J, Vásquez L, Díaz T, Castañeda D, Rodríguez E and Arango R, Use of micro titer plate dilution assay to measure activity of antifungal compounds against *Mycosphaerella fijiensis*, Morelet. *Rev Fac Nal Agr Medellin* **59**:3425–3433 (2006).
26 Otálvaro F, Nanclares J, Vásquez LE, Quiñones W, Echeverri F, Arango R *et al.*, Phenalenone-type compounds from *Musa acuminata* var. 'Yangambi Km 5' (AAA) and their activity against *Mycosphaerella fijiensis*. *J Nat Prod* **70**:887–890 (2007).
27 Mendieta MAEP-B, Negri M, Jagusch C, Hille UE, Müller-Vieira U, Schmidt D *et al.*, Synthesis, biological evaluation and molecular modelling studies of novel ACD- and ABD-ring steroidomimetics as inhibitors of CYP17. *Bioorg Med Chem Lett* **18**:267–273 (2008).
28 Opitz S, Otálvaro F, Echeverri F, Quiñones W and Schneider B, Isomeric oxabenzochrysenones from *Musa acuminata* and *Wachendorfia thyrsiflora*. *Nat Prod Lett* **16**:335–338 (2002).

Chapter 6

Discussion

6.1 General discussion

Plant secondary metabolites, which do not appear to participate directly in growth and development of the plant, have gained much attraction by the scientific community during the last decades in order to figure out their possible role in the plant, especially in the context of ecological functions. In this sense, secondary metabolites are now well recognized for playing a role in direct and indirect plant defense against microbial pathogens and herbivores, as attractants of pollinators and as allelopathic agents (Buchanan et al. 2000). According to the specific occurrence in individual plant families or species, the term "secondary metabolites" nowadays is going to be replaced by the term "specialized metabolites". Phenylphenalenones, a group of polycyclic aromatic compounds, are specialized metabolites found in the Haemodoraceae, Pontederiaceae, Strelitziaceae and Musaceae plant families (Munde et al. 2013). After the first plant phenalenone "Haemocorin" was isolated from *Haemodorum corymbosum* (Haemodoraceae) (Cooke & Segal 1955), to date, more than 140 phenylphenalenone-type compounds have been characterized from these related plant families (Hölscher et al. 2015). Furthermore, their biosynthesis (Thomas 1971; Hölscher & Schneider 1995; Schmitt et al. 2000; Munde et al. 2011) as well as their role in the plant protection has been studied during the last decades (Luis et al. 1993; Luis et al. 1995; Otálvaro et al. 2007; Hölscher et al. 2014).

However, several questions remain to be addressed towards exploring the precursor-product relationship in the biosynthesis of phenylphenalenones as well as their role in *Musa* plant protection against pathogens. Thus, these topics were encompassed in the present doctoral thesis along with chemical synthesis of phenylphenalenones and structural analogues for being probed as antimicrobial agents.

6.2 Biosynthesis of phenylphenalenones in Haemodoraceae plants

In vitro root cultures of *Anigozanthos preissii* and *Wachendorfia thyrsiflora* (Haemodoraceae plants) are suitable biological systems for studying the biosynthesis of phenylphenalenones under sterile conditions since these metabolites are constitutively synthesized in root cultures and allow facile administration of precursors via the liquid nutrient medium. Furthermore, it is well known that phenylphenalenones are formed by condensation of two phenylpropanoids units with one malonate unit (Hölscher & Schneider 1995). Previous studies in *A. preissii* have shown that the substitution pattern of the lateral phenyl ring attached to C-9 in the phenylphenalenone depends on the intact incorporation of a specific phenylpropanoid with the same substitution motif (Schmitt et al. 2000).

Therefore, our hypothesis was to probe whether phenylpropanoids differing in their substitution pattern can be successfully incorporated into the phenylphenalenone skeleton as result of promiscuous enzymatic machinery. Thus, ^{13}C-labelled phenylpropanoids differing in the substitution pattern at the lateral phenyl ring were administered to root cultures of *A. preissii* and *W. thyrsiflora*, followed by ^{13}C NMR-guided analysis of ^{13}C-labelled phenylphenalenones. Successful incorporation of two of the precursors (ferulic acid, 4-methoxycinnamic acid) into phenylphenalenones was achieved in *A. preissii* but not in *W. thyrsiflora*. For root cultures of the latter, previous phytochemical studies have shown that phenylphenalenone-type compounds were characterized for bearing an unsubstituted lateral phenyl ring (Fang et al. 2011). Therefore, the biosynthetic origin of the lateral phenyl ring attached to the phenylphenalenone scaffold seems to be almost restricted to cinnamic acid pointing out a highly specific substrate-enzyme relationship. In the other hand, ferulic acid and the unusual 4-methoxycinnamic acid were successfully incorporated into the phenylphenalenones musanolone F and 4'-*O*-methylanigorufone, respectively, in *A. preissii.* Here, we demonstrated that the substitution pattern in the lateral phenyl ring of the phenylphenalenone depends exclusively on the specific phenylpropanoid found in the plant. Although the phenylphenalenone-type compounds in both species are derived from the general phenylpropanoid pathway, at least one of the enzymes involved in the phenylphenalenone biosynthesis in *A. preissii* (e.g. the CoA ligase, the diarylheptanoid synthase, or the putative "Diels-Alderase") seems to be more promiscuous than

the corresponding enzyme in *W. thyrsiflora*. Thus, *A. preissii* is able to produce phenylphenalenones with different substitution pattern in the lateral phenyl ring while *W. thyrsiflora* produces almost only phenylphenalenones with an unsubstituted lateral phenyl ring. Furthermore, isotope dilution approach along with ^{13}C NMR spectroscopy was demonstrated to be an excellent system not only in precursor-product relationship studies but also in the detection and identification of trace metabolites in plants. Using this approach, 4-methoxycinnamic acid was identified as a natural product in root cultures of *A. preissii* (Chapter 3.1). As most of the enzymes of the phenylphenalenone pathway, the putative *O*-methyltransferase catalyzing the biosynthetic formation of 4-methoxycinnamic acid from *p*-coumaric acid remains to be studied.

Whereas the phenylphenalenone-type compounds in *A. preissii* displayed their characteristic features in the ring A and D, phenylphenalenones of *W. thyrsiflora* reflect their diversity by oxygenated functional groups on both ring A and B (so-called 7-phenylphenalenones, see Fig. 9) and also by bearing a nitrogen in position 2 of ring B of the 7-phenylphenalenones (Fang et al. 2011). Until the publication of our study (Chapter 3.2, Munde et al., 2011), the oxidation sequences in the biosynthesis of 1,2,5,6-tetraoxygenated phenylphenalenones occurring in *W. thyrsiflora* was unknown. Incubation of *W. thyrsiflora* root cultures in an atmosphere of $^{18}O_2$ along with administration of ^{13}C-labelled precursors allowed to explore the origin of the oxygen functionalities in the tricyclic phenalenone part of tetraoxygenated phenylphenalenones. As in *A. preissii*, the oxygen functionalities in the ring A of the phenylphenalenones in *W. thyrsiflora* originated from the parent phenylpropanoid *p*-coumaric acid followed by an o-hydroxylation at the stage of an diarylheptanoid intermediate (Chapter 3.2, Fig. 9) (Munde et al. 2011). Furthermore, we demonstrated that the oxygen functionality in the position C-5 of tetraoxygenateded phenylphenalenones from *W. thyrsiflora*, is formed downstream during the biosynthesis. Thus, the "early hydroxylation" hypothesis about the involvement of an α-hydroxyl in the starter phenylpropanoid was ruled out. Overall, the general biosynthetic formation of the phenylphenalenone skeleton seems to be closely related not only in both of the Haemodoraceae plant species (*A. preissii* and *W. thyrsiflora*) but also in *Musa* plants. The major diversification likely occurs after the phenalenone tricycle has been closed. Such structural modifications are responsible for the species-specific metabolic profiles of phenylphenalenone-producing plants.

Although the ecological role of phenylphenalenone-type compounds in Haemodoraceae plants is poorly understood, they could protect the plant against biotic challenges (pathogens such bacteria or fungi) and abiotic factors (in oxidative stress due to the antioxidant activities found of some phenylphenalenones) (Otálvaro et al. 2007; Duque et al. 2013; Hölscher et al. 2014). Phenylphenalenones may also have allelopathic effects which would be an interesting subject for future studies. In contrast to the Haemodoraceae, the role of phenylphenalenone-type compounds in the economically important *Musa* genus has been studied in some detail and will be discussed in the next paragraph.

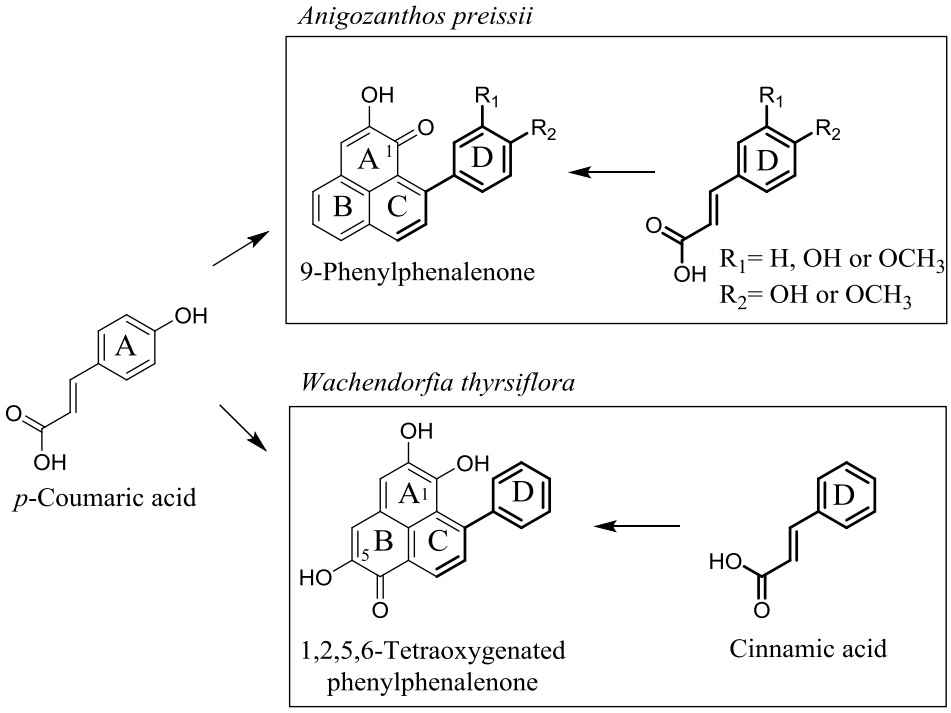

Fig. 9. Biosynthesis of phenylphenalenones in *A. preissii* and *W. thyrsiflora* and their potential precursors.

6.3 Phenylphenalenones involved in chemical defense of *Musa*

A general overview on the current situation that threat both smallholders as well as banana industry worldwide was presented in special attention to the pathogen *Mycosphaerella fijiensis*, one of the most detrimental pathogens of banana crops. In this regard, application of fungicides has been the effective method for maintaining the crop free of this microorganism or at least reduces the losses caused by it. Nevertheless, the use of pesticides in the banana production is

not only costly but also risky in the health care both for the farmers as well as consumers of the fruit. In fact, there is a tendency to reduce the fruit import into several countries, mainly due to the concern generated by the abuse in the application of fungicides in the commercial banana crops. Nonetheless, the concomitant fungicide resistance developed by *M. fijiensis* which prompted to search for new reliable and effective antifungal compounds is one of the urgent issues to be resolved. As an alternative to the chemical control, the conventional or genetic breeding of banana is nowadays more attractive in terms of searching for an ecological solution that can contribute to the agriculture sustainability. Basically, the last strategy has been performed by using *Musa* varieties which have shown to be highly resistant to this pathogen. Although some hybrids of *Musa*, derived from conventional breeding, have shown satisfying resistance against *M. fijiensis*, there are still issues regarding to the fruit quality and the genetic stability of the clone in the *in vitro* plant propagation. However, the role of pathogenesis-related proteins (PR-proteins) (Vishnevetsky et al. 2011; Torres et al. 2012; Kovacs et al. 2013), early recognition of effector proteins by the host (Stergiopoulos et al. 2010), activation of enzymes involved in the phenylpropanoid pathway (such as phenylalanine-ammonia-lyase, PAL) (Wuyts et al. 2006; Alvarez et al. 2013) and early accumulation of phytoalexins in the plant (Luis et al. 1993; Luis et al. 1995; Otálvaro et al. 2002; Otálvaro et al. 2007) are among the main strategies which could result in or contribute to resistance of *Musa*.

Although there are several studies about the identification of phytoalexins in *Musa*, to the best of our knowledge there are no reports about the metabolic changes initiated in the plant during the interaction with *M. fijiensis*. This gap in the knowledge about the effect of the fungus on the plant metabolism motivates us to study the chemical aspects of the plant-fungus interaction in this part of the doctoral project (Chapter 4).

Nowadays, metabolomics studies have gained extremely much attention due to the useful information that can be extracted in a wide range of topics, such as in medicine (Moazzami et al. 2011; Mastrangelo et al. 2014; Guo et al. 2015), food quality control (Thissen et al. 2011; Oms-Oliu et al. 2013) and plant physiology. Studies on the plant's natural product variations under biotic or abiotic stress conditions has contributed in a deeper understanding of the plant defense mechanisms (Mandavi et al. 2015; Noctor et al. 2015; Ordoudi et al. 2015; Sade et al. 2015).

Therefore, we analyzed the chemical responses of the susceptible 'Williams' and the resistant 'KTR' *Musa* varieties during the interaction with *M. fijiensis* by using ^{1}H NMR-based metabolomics as a suitable approach. In fact, the principal component analysis (PCA) proved to be useful in this study. A high discrimination between infected versus non-infected plant tissue was observed and the corresponding loading plots analysis allowed us to distinguish some of the metabolic changes after infection with the microbial pathogen. In both *Musa* varieties, changes in the primary metabolism, especially an increasing level of carbohydrates (glucose and sucrose), were observed in the infected leaf area whereas a negative correlation (decreasing level) was found for the identified amino acids L-alanine and L-threonine, but not for L-methionine. Several studies have already reported that, according to high biosynthetic consumption of carbohydrates, accelerated translocation from roots or systemic leafs to the infected areas take place (Herbers et al. 1996; Herbers et al. 2000). In parallel, carbohydrates can mediate gene expression in the biosynthesis of pathogenesis-related proteins, such as chitinases and glucanases, which are hydrolytic enzymes that break glucosidic bonds in the chitin and glucans, respectively, fundamental components of the fungal cell walls (Herbers et al. 1994; Herbers et al. 2000; Adams 2004). Additional, it has also been reported that sugars can influence the biosynthesis of specialized metabolites, especially phytoalexins (Hara et al. 2003; Morkunas et al. 2013; Formela et al. 2014). Therefore, an activation of the plant defense mediated by accumulation of sugars cannot be ruled out in the *Musa* - *M. fijiensis* pathosystem but, it needs to be further studied.

A plausible explanation for the downregulation of L-alanine and L-threonine could be attributed to the high demand for free amino acids needed for the synthesis of overexpressed pathogenesis-related (PR) proteins, which can led to successful plant defense. Intriguing, L-methionine was upregulated in the chemical response of both *Musa* varieties. This is not surprising since this amino acid is required for to synthesis of *S*-adenosylmethionine (SAM), which is the classical methyl donor for methyltransferases involved in *O*-methylation of phenylpropanoids and likely in *O*-methylation of phenylphenalenone-type compounds (Otálvaro et al. 2010).

It must be highlighted the strong influence that ^{1}H NMR signals in the aromatic region had on the analysis performed by PCA and the corresponding loading plots. The data demonstrated that the synthesis of inducible defense metabolites (phytoalexins) takes place locally only in the infected tissue. Thus, it was the main challenge for us to identify these induced metabolites.

At first, we identified dopamine for being present both in control leaves of *Musa* plants and in those leaf areas of infected plants where the infection took place. Dopamine occurs in banana fruit (Kanazawa & Sakakibara 2000) but, to the best of our knowledge, to date there is no report on the occurrence of this metabolite in leaves of *Musa*. Interestingly, the PCA analysis between "control plant samples" versus "healthy leave tissue of infected plants" addressed the question to figure out the metabolite (s) responsible for the group discrimination observed between these plant tissues. Detailed inspection of the whole set of ^{1}H NMR spectra allowed to detect some candidates signals that were enhanced in spectra of "healthy tissue of infected plants" but not in the spectra of "untreated control plants". By using 1D- and 2D NMR experiments and confirmed by HRMS, we identified dopaol-β-D-glucoside as the compound mainly responsible for the result observed in PCA analysis. Dopaol-β-D-glucoside is reported here for the first as a metabolite occurring in *Musa* plants (Chapter 4).

The biological function of catecholamines such as dopamine in plants is not completely understood but its synthesis seems to be regulated by stress conditions. Overall, catecholamines have been reported to affect the action of several plant hormones, regulate carbohydrate metabolism and protect plants against pathogens (Kulma & Szopa 2007). On the other hand, the chemical structure of dopaol-β-D-glucoside is closely related to dopamine. Therefore, the idea that dopamine may serve as substrate for the biosynthesis of its glucoside through an oxidation/reduction step followed by the enzymatic reaction by a β-glucosyltransferase could be reasonable (Strack et al. 2003; Satoh et al. 2012) (Fig. 10). Thus, conversion into dopaol-β-D-glucoside would explain the low level of dopamine found in the healthy areas of the infected plants. In order to investigate if these metabolites play a role as phytoalexins in *Musa*, we assessed them under *in vitro* conditions against *M. fijiensis* but no growth inhibition of the fungus at all was observed even at the highest concentration evaluated (100 ppm). Therefore, their biological function in the *Musa* - *M. fijiensis* interaction is open for being explored.

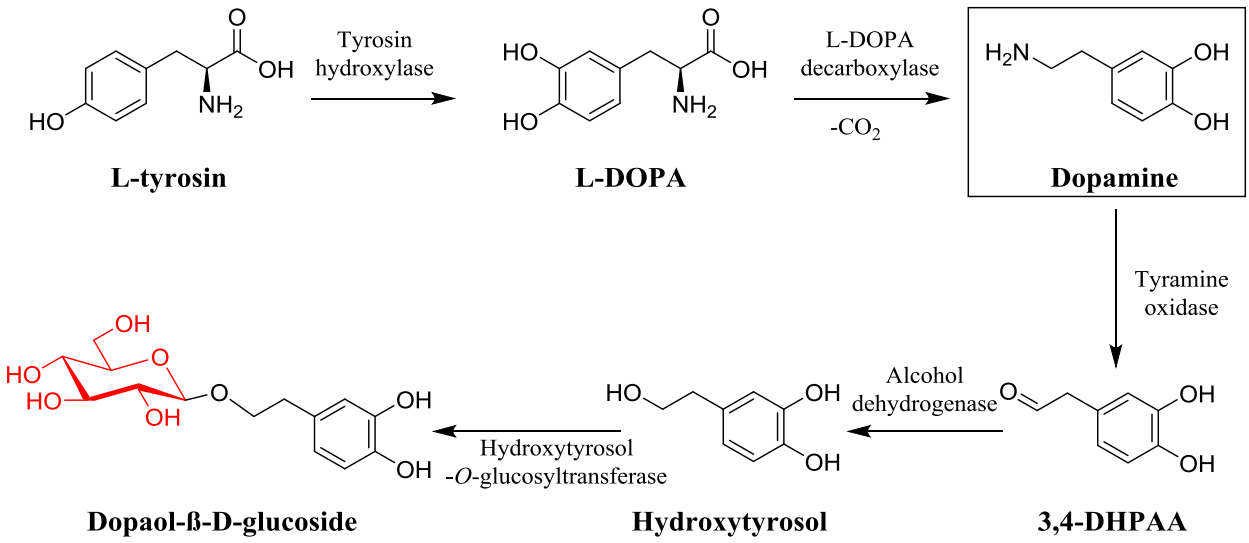

Fig. 10. Pathway for oxidation of dopamine to hydroxytyrosol followed by 1-*O*-glucosyltransfer in the synthesis of dopaol-β-D-glucoside (initial steps starting from L-tyrosin are shown). 3,4-DHPAA: 3,4-dihydroxyphenylacetaldehyde.

Among other metabolites identified from comparing the infected plant tissue with control ones, it becomes important to highlight 1'-*O*-(*E*)-4-coumaroyl-β-glucoside. In both *Musa* varieties, a downregulation of this metabolite in the infected areas of the leaf suggested a high consumption of this phenylpropanoid in the biosynthesis of specialized metabolites such as phenylphenalenones (Luis et al. 1993; Luis et al. 1994; Luis et al. 1995). Indeed, two phenylphenalenone-type compounds (irenolone and hydroxyanigorufone) were identified by means of the ^{1}H NMR spectra (and confirmed by 2D NMR) of infected leafs from 'Williams' and 'KTR' *Musa* varieties. In addition, the loading plots confirmed that these metabolites were strongly upregulated only in the infected areas of the leaves which was associated with the low levels of its precursor *p*-coumaric acid simultaneously found in the same plant tissue (Hölscher & Schneider 1995). *p*-Coumaric acid may be released by a β-glucosidase from 1'-*O*-(*E*)-4-coumaroyl-β-glucoside, which may function as a depot compound (Chong et al. 1999).

NMR spectroscopy is a powerful tool for structure elucidation of organic compounds. We used this analytical technique for screening the chemical profile of *Musa* plants during biotic stress in response to the infection with *M. fijiensis*. Nonetheless, most of the induced metabolites

were difficult to assign through ^{1}H NMR, basically because of heavily overlapping signals as shown in Fig. 11. 2D NMR represents a good alternative to overcome such drawback as has been reported in several studies and summarized in excellent reviews focused on direct identification of metabolites from complex mixture of crude plant extracts (Kim et al. 2010; Bingol & Bruschweiler 2014; Man et al. 2014; Guennec et al. 2015; Mahrous & Farag 2015). Therefore, as an attempt to elucidate the secondary metabolites in infected *Musa* plants, 2D NMR was applied without much success since the overlapping signals were not only an issue in the ^{1}H NMR but even in 2D NMR spectra. Therefore, a conventional phytochemical study was necessary in order to figure out the chemical profile of both *Musa* varieties in their interaction with the fungal pathogen.

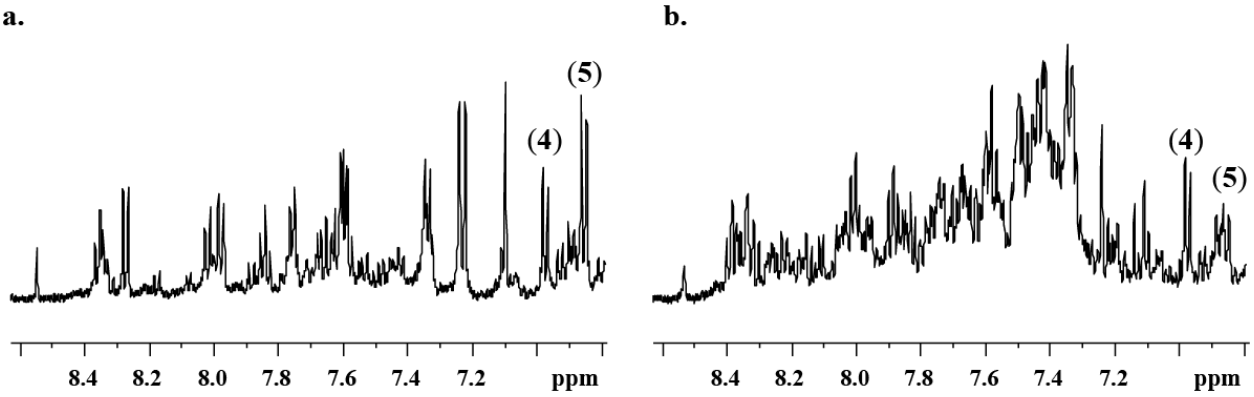

Fig. 11. ^{1}H NMR region from δ 6.8-8.6 (500 MHz, MeOH-d_4) of crude extracts of infected *Musa* leaf tissue from 'Williams' (panel a) and 'Khai Thong Ruang' (panel b). Numbers represent the signal of H/C-3'/5' of irenolone (**4**) and hydroxyanigorufone (**5**) identified in the plant extract (for details, see Chapter 4)

Identification of induced phenylphenalenones in Musa - M. fijiensis interaction

NMR/PCA analysis proved to be a valuable tool for exploring metabolic variations in the *Musa – M. fijiensis* pathosystem and left open several findings which need to be studied in more detail, as for example, the physiological role of dopaol-β-glucoside and dopamine, and the accumulation of sugars during the plant responses against biotic stress. It turned out that most of the metabolic changes take place in the infected leaf areas, with the production of specialized compounds, mainly phenylphenalenone-type phytoalexins, as the major metabolites (Luis et al. 1993; Quiñones et al. 2000). Furthermore, the chemical responses of the resistant variety 'KTR'

was stronger than that of the susceptible variety 'Williams', since many more signals appeared in the aromatic region of the ^{1}H NMR spectra of the infected samples of 'KTR' than in infected samples of 'Williams' (Fig 11).

The phytochemical study of both *Musa* varieties by using NMR and MS analyses allowed us to identify a total of fifteen phenylphenalenones or structural analogues from 'KTR'. In contrast, 'Williams' variety produced a smaller number of these metabolites (ten compounds), displaying a weaker chemical defense (details in Chapter 4, Table 2). Due to the diversity of phenylphenalenones induced during the response of the 'KTR' variety against *M. fijiensis*, we hypothesized that the resistant phenotype could be largely correlated with the expression of phytoalexins, especially, phenylphenalenones as has been reported previously (Otálvaro et al. 2002; Otálvaro et al. 2007). In order to test this hypothesis in more detail, an experimental design involving two strains of *M. fijiensis* E22 and Ca10_13 differing in their tolerance to the fungicide propiconazole (Cañas-Gutierrez et al. 2009) were used as fungal inoculum for both *Musa* varieties. We assumed that the fungicide tolerance of the microorganism could correlate with the virulence of the fungal strain, and thus the plant could respond differentially to each pathogen. Therefore, three factors were evaluated and correlated in this experiment: time after infection, progress of the disease (Black Leaf Sigatoka Disease) and concentration of the phenylphenalenones found in different part of the plant (Chapter 4, Table 2).

The results showed that the *Musa* 'Williams' variety was susceptible to the pathogen attack independently of the strain of *M. fijiensis* used. This susceptibility was attributed to some extend to the late recognition of the pathogen, the disease symptoms progression during the time evaluated and low quantities of phenylphenalenones produced in the response to the biotic stress caused by the fungus (except hydroxyanigorufone whose concentration was over 25 nmol mg^{-1} DW) (Chapter 4, Fig. 6b). Nevertheless, it was observed that the BLSD symptoms were slightly stronger when the plant was treated with the strain Ca10_13.

On the other hand, the resistance of the 'KTR' variety was demonstrated when the plant was infected with *M. fijiensis* strain E22 (small size of the symptomatic areas and slowly progressing disease after 25 dpi); however, in contrast to our expectations, the resistance in this variety was

overcome when the experiment was performed with the strain Ca10_13 (tolerant to propiconazole) since large necrotic symptoms and a time-depending progress of the disease were observed. In this case, the necrotic lesions were even worse in comparison with those of the susceptible 'Williams' variety. These results draw our attention basically to two aspects:

- Some plant pathogens have developed strategies to circumvent the activation of plant defenses through effector proteins that interfere with a wide range of physiological processes in the host (Alba et al. 2011; Doehlemann & Hemetsberger 2013).
- Plant pathogens can even degrade preformed and induced antimicrobial compounds (Bouarab et al. 2002) into substances less toxic to the microorganism (Pedras & Ahiahonu 2005; Pedras et al. 2011).

Regarding the first hypothesis, it has to be stated that effector proteins from *M. fijiensis* that can suppress plant defenses are still unexplored. Only few reports refer to two effector proteins that can trigger plant defenses (see Chapter 1, section 1.4) (Stergiopoulos et al. 2010). Therefore, the second hypothesis, namely exploring possible detoxification mechanism of phenylphenalenones by the microorganism, became a major aim of this work. The results are discussed in the following section.

Metabolism of phenylphenalenones by the ascomycete fungus M. fijiensis

Interestingly the breakdown resistance of the 'KTR' variety by the virulent *M. fijiensis* strain Ca10_13 raised the question, how this fungus was able to survive against the plant defenses (specifically phenylphenalenone-type phytoalexins) and cause larger foliar damage than observed with the strain E22. Therefore, a series of experiments was conducted in which the fungus was incubated with specific phenylphenalenones (at 10, 20 and 40 ppm) under *in vitro* conditions. Variables such as biomass, soluble extracellular proteins, ergosterol concentration and phenylphenalenone concentration both in mycelial biomass and fungal medium were determined after 8 days of incubation. The major results can be summarized as follows:

M. fijiensis strain Ca10_13 was able to metabolize most of the tested phenylphenalenones in a concentration-dependent manner. Hydroxyanigorufone (**5**), for example, disappeared completely at a concentration of 10 ppm in the culture medium. This observation led us to analyze both the fungal medium and the mycelium for possible phenylphenalenone-derived metabolites. The occurrence of sulfate conjugates in the well-growing mycelium cells suggested that *M. fijiensis* was able to transform the phenylphenalenones into products which could be less toxic for the fungus than the parent compounds. In this regard, we could hypothesize that a typical 3'-phosphoadenosine-5'-phosphosulfate (PAPS) was used as a sulfate donor during the sulfation reaction (Fig. 12). Nevertheless, the sulfate transfer by an arylsulfate sulfotransferases (ASSTs) could not be ruled out since these enzymes have been reported for some microorganism (Kaysser et al. 2010). In addition to sulfate conjugation, a considerable amount of the parent phenylphenalenones seemed to be converted into structures not detectable by UV, i.e. the tricyclic aromatic system must have been degraded into a non-chromophoric system or completely decomposed.

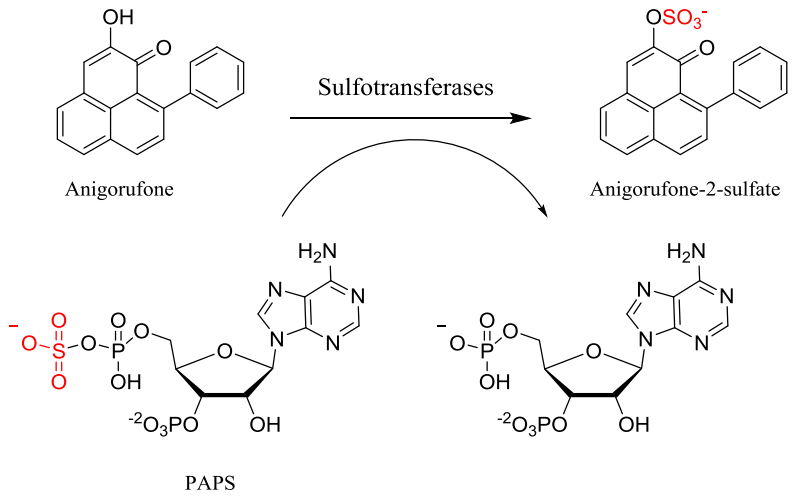

Fig. 12. Hypothetical reaction catalyzed by sulfotransferases for anigorufone. PAPS: 3'-phosphoadenosine 5'-phosphosulfate

As already mentioned above, hydroxyanigorufone (**5**) was completely metabolized at 10 ppm and had only a slightly negative effect on the fungal biomass and soluble extracellular protein production. Since hydroxyanigorufone (**5**) was the major compound produced by the susceptible *Musa* variety 'Williams' in response to the pathogen infection, the chemical defense of this variety seems to be easily counteracted by the *M. fijiensis* Ca10_13 and likely, also by the strain E22.

An interesting result was indeed that metabolites such as 2-phenyl-1,8-naphthalic anhydride (**3**) did not cause any negative effect on the fungus. All the *in vitro* experimental variables analyzed were similar to those obtained from untreated fungal control. Therefore, oxidized phenylphenalenones seem to be not toxic for the fungus. Since the major structural difference between phenylphenalenones and naphthalic anhydrides is the presence of an α-hydroxyenone moiety in the first group of compounds and its absence in the second group, such a structural feature seems to be essential for the antimicrobial activity. Previous biosynthetic studies have suggested that the formation of naphthalic anhydrides from the corresponding 4- or 9-phenylphenalenones seems to occur by the action of an unidentified decarboxylase (Edwards & Weiss 1974; Kamo et al. 2000). Curiously, in most of the cases such oxidized-phenylphenalenones have been reported once the plant material – *Musa* plants or banana fruits – were treated with fungal inoculum of pathogens such as *Colletotrichum musae* (Hirai et al. 1994; Kamo et al. 2000) with non-pathogenic fungus as *Sporobolomyces salmonicolor* (Jitsaeng & Schneider 2010) or, in another case, with the burrowing nematode *Radopholus similis* (Hölscher et al. 2014). Here, not only is reported for the first time such class of compounds produced by *Musa* plants in response to *M. fijiensis* but also it is proposed to gain future insights into the possible role of decarboxylases as potentially responsible enzymes in the metabolization of phenylphenalenones during plant-microbe or plant-nematode interactions. Deactivation of such enzymes *in vivo* could result in a plant resistant against pathogens such as *M. fijiensis.* Therefore, decarboxylases may be considered as a target for further genetic *Musa* breeding.

On the other hand, metabolites such as methoxyanigorufone (**7**) and isoanigorufone (**11**) were the most relevant metabolites among the compounds assessed under *in vitro* conditions. They influenced the overproduction of fungal extracellular proteins by above threefold in comparison with the control sample. In addition, they reduced the biomass production by levels below 70% and 20%, respectively, when compared with the control sample. While methoxyanigorufone (**7**) inhibited enormously the production of ergosterol (ergosterol was not detectable at all when the fungus was treated at 20 and 40 ppm) isoanigorufone (**11**) influenced positively the production of this fungal cell wall component. Here, it was shown that the undetectability of ergosterol in the samples treated with methoxyanigorufone (7) is correlated with the reduced levels of fungal biomass produced. Due to the results observed with this

metabolite, it seems to represent a special case, which deserves to be studied in more detail. Methoxyanigorufone (**7**) does not possess a free hydroxyl group at C-2 and therefore, it cannot be conjugated with a sulfate group for further degradation/metabolism by the fungus as occurred with the other phenylphenalenones tested. This could explain to some extent the recovery rates of more than 94.5% of this metabolite during the *in vitro* bioassays performed with the fungus (Chapter 4). To the best of our knowledge, isoanigorufone (**11**) and/or methoxyanigorufone (**7**) have been reported for being induced metabolites mainly in resistant *Musa* varieties such as Yangambi km5 (Otálvaro et al. 2007; Hölscher et al. 2014), the resistant cultivar hybrid SH 3481 (Luis et al. 1999), *Musa balbisiana* 'Thepanom' (Jitsaeng et al. 2010) and, in very low quantities (~ 0.016µg of methoxyanigorufone per gram fresh weight), in the susceptible *Musa* variety 'Gran Nain' (Luis et al. 1995). However, in our study both compounds were found in the resistant *Musa* variety 'KTR' but not in the susceptible 'Williams' variety. Recently it has been reported that the biosynthesis of *O*-methylated phenylphenalenones is mediated by *S*-adenosyl-methionine-dependent *O*-methyltransferases (OMT) both in Haemodoraceae and Musaceae plants (Otálvaro et al. 2010). The role of OMT enzymes in disease-resistance against pathogens has been reported for several plant systems (Busam et al. 1997; Christensen et al. 1998; Berr et al. 2010) and insects (Meihls et al. 2013). Therefore, a specific *O*-methylation occurring at OH-2 of the 9-phenylphenalenones in *Musa* during the pathogen attack seems to be an important trait that mediates an ecologically relevant trade-off between susceptibility and resistance of the plant against pathogens and pests, perhaps as a result of a co-evolutionary process. Thus, an overexpression of OMT's could improve the defensive traits of susceptible *Musa* varieties against microbial pathogens, which opens another possibility for further investigations in genetic breeding of *Musa* plants.

6.4 Design of new antimicrobial compounds against *M. fijiensis*

Several efforts have been addressed in order to develop ecologically friendly ways to control BLSD in banana plants. Breeding resistant *Musa* varieties would help to reduce the extensive application of fungicides and other chemicals in banana production. However, no resistant *Musa* varieties are available so far, which are meeting the quality requirements for commercial purposes. Therefore, chemical control is still the most effective method among the management

practices of banana crops as was described in the introduction part of the thesis. However, the use of such chemicals has resulted in the development of fungicide resistance and thus led to another serious issue for the control of this disease. The development of new and effective therapeutic agents is therefore still highly desirable in order to treat the infection caused by *M. fijiensis*. Since natural products have demonstrated to be the main source of inspiration for developing new medicines and drugs (Newman & Cragg 2012), here we used the structure of phenylphenalenones as a template scaffold for chemically synthesizing new molecules with improved antimicrobial properties against the pathogen *M. fijiensis*.

The Chapters 5.1 and 5.2 describe the chemical approaches used for synthesizing a series of 4-phenylphenalenones along with 2-arylnaphthalene derivatives. The modes of action of phenylphenalenones are so far not yet completely understood and therefore, studies towards understanding the mechanisms behind the antimicrobial properties exerted against fungal pathogens should be undertaken. However, we have found that some phenylphenalenone-type compounds displayed an enhanced antifungal activity when controlled light conditions were used during the *in vitro* bioassay, suggesting a photodynamic behavior. As a first hypothesis, the absorption of light energy by the compound can led to the production of singlet oxygen, a toxic substance, as has been reported for several phenylphenalenones in previous work (Lazzaro et al. 2004). Nevertheless, it is not clear how phenylphenalenones act under darkness conditions. Since an α-hydroxyenone moiety is present in the phenylphenalenone molecule, a Michael-type 1,4-addition with nucleophilic active site residues of proteins or other biomolecules to form a covalent linkage between the phenylphenalenone and the biomolecule could interfere thus with the normal physiological fungal growth. It is intriguing to investigate how these compounds deploy their activities and further synthetic, mechanistic, and bioassay studies could contribute to better understand the biochemical reactions, which happen in the phenylphenalenone - *M. fijiensis* interaction.

Chapter 7

Summary

Phenylphenalenones are polycyclic phenolic natural products occurring in the four monocotyledoneous plant families Musaceae (banana plants), Haemodoraceae, Pontederiaceae and Strelitziaceae. Overall, their biosynthesis involves the condensation of two phenylpropanoids with one malonate unit through the diarylheptanoid pathway. Labelling experiments using ^{13}C-labelled substrates have demonstrated to be an elegant and suitable approach for establishing new insights into the precursor-product relationship in the biosynthesis of phenylphenalenones. Some Hamodoraceae plants constitutively produce phenylphenalenones and therefore, they have become highly useful plant systems for exploring the biosynthesis of these specialized metabolites. Previous studies have hypothesized that the substitution pattern at the lateral phenyl ring attached to the phenalenone nucleus depends on the intact incorporation of the precursor used. Therefore, ^{13}C-labeled phenylpropanoids with different substitution at that phenyl ring were synthesized and administered to Haemodoraceae root cultures. In *A. preissii* but not in *W. thyrsiflora,* ferulic acid and the unusual phenylpropanoid 4-methoxycinnamic acid were incorporated into phenylphenalenones bearing the same substitution at the phenyl ring as the precursor. This result suggested a certain promiscuity of the enzymes involved in phenylphenalenone biosynthesis in *Anigozanthos*. The unsubstituted lateral phenyl ring of most of the phenylphenalenones from *W. thyrsiflora* could be explained by the preference of the biosynthetic machinery of this plant for the precursor cinnamic acid. One of the phenylphenalenones biosynthetically produced in *A. preissii*, 4'-*O*-methylanigorufone, is reported here for the first time as a natural product (Chapter 3.1).

Another intriguing feature of the biosynthesis of phenylphenalenones is the sequence in which the oxygen functionalities are introduced. This is of special interest for 1,2,5,6-tetraoxygenated phenylphenalenones produced, for example, by *W. thyrsiflora*. Incubating root cultures under an $^{18}O_2$ atmosphere, simultaneous administration of ^{13}C-labelled phenylpropanoids and diarylheptanoids, and introduction of O$^{13}CH_3$ groups by *O*-methylation with $^{13}CH_2N_2$ generated isotopologues, which were analysed by HRMS and NMR. Especially the

detection of ^{18}O-induced effects on the NMR chemical shifts of the *O*-$^{13}CH_3$ groups allowed conclusions about the sequence of oxygenation of the phenylphenalenone molecule. The results suggest that the oxygen atoms decorating the phenalenone tricycle are introduced at different biosynthetic stages in the sequence *O*-1 → *O*-2 → *O*-5. Oxygen atoms ending up C-1 and C-6 are incorporated from the activated precursor 4-coumaroyl-CoA and the oxygen group attached to C-5 was determined to occur late in the biosynthesis of phenylphenalenone, once lachnanthocarpone, a trioxygenated phenylphenalenone, has been biosynthesized (Chapter 3.2).

Little is known about the role of the phenylphenalenones in plants of the Haemodoraceae family. However, due to the antimicrobial, nematicidal and antioxidant activities exhibited by these metabolites, a protective function of the plant against biotic and abiotic stresses could be suggested. In this sense, plants of the Musaceae (banana) family provide a good experimental system for exploring the ecological role of phenylphenalenones in plant chemical defense. In fact, phenylphenalenones are considered as phytoalexins of the *Musa* genus since these specialized metabolites are induced in response to attack by pathogens and herbivores. In addition, the level of their biosynthesis has been correlated to some extent with the resistance against pathogens and pests. Therefore, the metabolic changes in the chemical responses of the susceptible 'Williams' and the resistant 'Khai Thong Ruang' ('KTR') *Musa* varieties were studied (Chapter 4). *Mycosphaerella fijiensis*, the causing agent of the most devastating disease in banana crops named Black Leaf Sigatoka Disease (BLSD), has been used as the fungal pathogen. Principal component analysis displayed a strong discrimination of the metabolic pattern between infected versus non-infected plant tissue. Phenylphenalenones were identified as the major induced metabolites in the infected tissue, confirming data reported by other authors. In addition, the number and turnover of phenylphenalenones biosynthesized in the local infected tissue together with the slow progression of the disease was correlated with the resistance level observed for the 'KTR' *Musa* variety. However, a virulent strain of *M. fijiensis* was able to overcome plant resistance by converting fungitoxic phenylphenalenones to sulfate conjugates. Phenylphenalenone sulfates are reported here for the first time. They are metabolic detoxification products to evade the chemical defense of *Musa* plants. Further studies are in progress in order to get new insights about this hypothesis.

Currently, pest management of banana crops is exclusively depending on the application of fungicides and pesticides. However, the excessive use of these chemicals has become a serious problem for the health and safety of the banana farmers. The extensive treatment with fungicides generates environmental contaminations and facilitates development of resistance by the fungus. Therefore, searching for more efficient control strategies with an environmentally friendly value are the challenges assumed by several scientific groups in crop protection worldwide. In this sense, new antifungal agents were synthesized based on the phenylphenalenones moiety and assessed against *M. fijiensis* under *in vitro* conditions. 4-Phenylphenalenones and structural analogues displayed good antifungal activities and enhanced antimicrobial properties were observed when the fungal incubation system was irradiated with light, suggesting a photodynamic activity by the phenylphenalenones assessed. It has been demonstrated that phenylphenalenones can be used as potential compounds for the development of fungicides, relying on a dual mode of action (Chapter 5.1 and 5.2).

Zusammenfassung

Phenylphenalenone sind polyzyklische phenolische Naturstoffe, die in den vier monokotylen Pflanzenfamilien Musaceae (Bananenpflanzen), Haemodoraceae, Pontederiaceae und Strelitziaceae vorkommen. Ihre Bildung erfolgt grundsätzlich durch Kondensation von zwei Phenylpropanoiden mit einer Malonyleinheit über die Diarylheptanoid-Biosyntheseroute. Es ist bekannt, dass Fütterungsexperimente mit ^{13}C-angereicherten Substanzen einen eleganten und geeigneten Ansatz darstellen, um neue Einblicke in die Edukt-Produkt-Beziehung während der Biosynthese von Phenylphenalenonen zu eröffnen. Haemodoraceae-Pflanzen mit konstitutiver Phenylphenalenon-Produktion sind dabei besonders gute Modellsysteme für die Erforschung der Biosynthese dieser spezialisierten Metaboliten. Frühere Studien gingen davon aus, dass das Substitutionsmuster des lateralen Phenylrings, der an den Phenalenon-Kern gebunden ist, vom Einbau der eingesetzten, intakten Vorstufe abhängt. Deswegen wurden ^{13}C-markierte Phenylpropanoide mit unterschiedlicher Substitution am Phenylring synthetisiert und den Haemodoraceae-Wurzelkulturen zugeführt. In *A. preisii*, aber nicht in *W. thyrsiflora,* konnte ein solcher Einbau ohne Veränderung des Substitutionsmusters nach Fütterung von Ferulasäure und der ungewöhnlichen 4-Methoxyzimtsäure beobachtet werden. Dieses Ergebnis wies auf eine gewisse Indifferenz der Enzyme hin, die an der Biosynthese der Phenylphenalenone in *Anigozanthos* beteiligt sind. Der unsubstituierte, laterale Phenylring der meisten Phenylphenalenone von *W. thyrsiflora* konnte durch die Präferenz des Biosyntheseapparates dieser Pflanze für die Zimtsäure-Vorstufe erklärt werden. Außerdem gelang in diesem Zusammenhang die Identifizierung eines neuen Phenylphenalenones, des 4'-*O*-Methylanigorufons, in *A. preisii* (Kapitel 3.1)

Ein weiterer faszinierender Aspekt der Phenylphenalenon-Biosynthese ist jener Schritt, in dem Sauerstoff-Funktionalitäten eingeführt werden. Dies ist von speziellem Interesse für 1,2,5,6-tetraoxygenierte Phenylphenalenone, wie sie beispielsweise *W. thyrsiflora* produziert. Inkubation von Wurzelkulturen in einer $^{18}O_2$-Atmosphäre, gleichzeitige Verabreichung von ^{13}C-markierten Phenylpropanoiden bzw. Diarylheptanoiden sowie Einführung von O$^{13}CH_3$-Gruppen durch *O*-Methylierung mit $^{13}CH_2N_2$ erzeugten Isotopologe, die mittels HRMS und NMR analysiert wurden. Speziell die Detektion von ^{18}O-induzierten Isotopieeffekten auf die chemischen

Verschiebungen der O-$^{13}CH_3$-Gruppen erlaubte Rückschlüsse auf die Abfolge der Oxygenierungen des Phenylphenalenonmoleküls. Die Ergebnisse legen nahe, dass die Sauerstoffatome am Phenalenon-Trizyklus in verschiedenen Biosynthesestadien in der Reihenfolge O-1 → O-2 → O-5 eingeführt werden. Sauerstoffatome an Position C-1 und C-6 werden aus der aktivierten Vorstufe 4-Cumaryl-CoA bezogen, wohingegen der an C-5 gebundene Sauerstoffsubstituent im Verlauf der Biosynthese erst spät auftritt, nämlich nachdem Lachnanthocarpon, ein trioxygeniertes Phenylphenalenon, gebildet wurde (Kapitel 3.2)

Über die Rolle der Phenylphenalenone in den Pflanzen aus der Familie der Haemodoraceae ist wenig bekannt. Aufgrund ihrer antimikrobiellen, nematiziden und antioxidanten Aktivität liegt es jedoch nahe, dass diese Metabolite dem Schutz der Pflanze gegen biotischen und abiotischen Stress dienen. In diesem Sinne stellen die Pflanzen der Musaceae-Familie (Bananen) ein gutes experimentelles Modellsystem dar, um die ökologische Funktion der Phenylphenalenone in der chemischen Verteidigung zu untersuchen. Tatsächlich gelten die Phenylphenalenone als Phytoalexine des Musa-Genus, weil ihre Bildung als Abwehrreaktion gegen den Befall durch Pathogene oder Herbivore induziert wird. Des Weiteren besteht zu einem gewissen Grad eine Korrelation zwischen dem Level ihrer Biosynthese und der Resistenz gegen Pathogene und Schädlinge. Aus diesem Grund erfolgte die Untersuchung der metabolomischen Änderungen während der chemischen Antwort bei zwei Musa-Varietäten, der empfindlichen „Williams“ und der resistenten „Khai Thong Ruang“ (KTR) (Kapitel 4). Als fungaler Erreger wurde *Mycosphaerella fijiensis* eingesetzt. Er verursacht die für Bananenpflanzen verheerendste Krankheit, die sogenannten Schwarzen Blattmasern. Die Auswertung einer Hauptkomponentenanalyse zeigte, dass deutliche Unterschiede im Metabolitenprofil von gesunden und erkrankten Pflanzen bestehen. Die Bildung der Phenylphenalenone wurde im infizierten Gewebe am stärksten induziert, womit sich die Ergebnisse anderer Autoren bestätigten. Weiterhin korrelieren Anzahl und Menge der biosynthetisierten Phenylphenalenone im Bereich der Infektion sowie die langsame Ausbreitung der Krankheit mit dem Resistenzgrad der Musa-Varietät „KTR“. Jedoch überwand der virulente Erregerstamm *M. fijiensis* diese Resistenz durch die Umwandlung der fungiziden Phenylphenalenone in ihre Sulfatkonjugate, deren Auftreten in dieser Arbeit erstmals nachgewiesen wurde. Es handelt sich offensichtlich um metabolische Entgiftungsprodukte, die

dazu dienen, die chemische Verteidigung der Musa-Pflanzen zu überwinden. Aktuell laufen weitere Studien, um neue Einblicke zu diesem Thema zu ermöglichen.

Gegenwärtig erfolgt die Schädlingsbekämpfung an Bananenpflanzen ausschließlich durch das Aufbringen von Fungiziden und Pestiziden. Unterdessen ist der exzessive Gebrauch dieser Chemikalien zu einem ernsthaften Problem für die Gesundheit und Sicherheit der Bananenfarmer geworden. Die ausgiebige Verwendung von Fungiziden kontaminiert die Umwelt und erleichtert dem Pilz gleichzeitig die Resistenzentwicklung. Aus diesem Grund zählt die Suche nach einer effizienteren Bekämpfungsstrategie zur Erntesicherung mit umweltfreundlichen Eigenschaften zu den Herausforderungen, der sich weltweit viele wissenschaftliche Gruppen stellen. Zu diesem Zweck erfolgte die Synthese von antifungalen Substanzen basierend auf dem Strukturmotiv der Phenylphenalenone, deren Wirkung gegen *M. fijiensis* unter *in vitro* Bedingungen untersucht wurde. Die 4-Phenylphenalenone und ihre Strukturanaloge zeigten eine gute antifungale Wirkung und erhöhte antimikrobielle Eigenschaften, wenn das Inkubationssystem Licht ausgesetzt wurde, woraus sich eine mögliche photodynamische Aktivität der Phenylphenalenone ableitet. Das demonstriert die Eignung der Phenylphenalenone zur Entwicklung von Fungiziden, die auf einem dualen Wirkmechanismus beruhen (Kapitel 5.1 und 5.2).

References

Adams D.J. (2004) Fungal cell wall chitinases and glucanases. *Microbiology*, **150**, 2029-2035.

Alba J.M., Glas J.J., Schimmel B.C.J. & Kant M.R. (2011) Avoidance and suppression of plant defenses by herbivores and pathogens. *Journal of Plant Interactions*, **6**, 221-227.

Albuquerque G.M.R., Santos L.A., Felix K.C.S., Rollemberg C.L., Silva A.M.F., Souza E.B.,…, Mariano R.L.R. (2014) Moko disease-causing strains of *Ralstonia solanacearum* from Brazil extend known diversity in Paraphyletic Phylotype II. *Phytopathology*, **104**, 1175-1182.

Alvarez J., Rodriguez A., Rodriguez-Arango E., Monsalve Z., Morales J. & Arango R. (2013) Characterization of a differentially expressed Phenylalanine Ammonia-Lyase gene from Banana induced during *Mycosphaerella fijiensis* infection. *Journal of Plant Studies*, **2**, 35-46.

Arzanlou M., Abeln E.C.A., Kema G.H.J., Waalwijk C., Carlier J., de Vries I., Guzman M. & Crous P.W. (2007) Molecular diagnostics for the sigatoka disease complex of banana. *Phytopathology*, **97**, 1112-1118.

Bairu M.W., Fennell C.W. & van Staden J. (2006) The effect of plant growth regulators on somaclonal variation in Cavendish banana (*Musa* AAA cv. 'Zelig'). *Scientia Horticulturae*, **108**, 347-351.

Berr A., McCallum E.J., Alioua A., Heintz D., Heitz T. & Shen W.H. (2010) Arabidopsis histone methyltransferase SET DOMAIN GROUP8 mediates induction of the Jasmonate/Ethylene pathway genes in plant defense response to Necrotrophic Fungi. *Plant Physiology*, **154**, 1403-1414.

Beveraggi A., Mourichon X. & Salle G. (1995) Comparative-study of the first stages of infection in sensitive and resistant Banana plants with *Cercospora-fijiensis* (*Mycosphaerella fijiensis*), responsible for Black Leaf Streak Disease. *Canadian Journal of Botany*, **73**, 1328-1337.

Bingol K. & Bruschweiler R. (2014) Multidimensional approaches to NMR-Based metabolomics. *Analytical Chemistry*, **86**, 47-57.

Bouarab K., Melton R., Peart J., Baulcombe D. & Osbourn A. (2002) A saponin-detoxifying enzyme mediates suppression of plant defences. *Nature*, **418**, 889-892.

Buchanan B., Gruissem W. & Jones R. (2000) Natural products (secondary metabolites). In: Biochemistry & Molecular Biology of Plants. Courier Companies, Inc., USA.

Bucher G., Bresoli-Obach R., Brosa C., Flors C., Luis J.G., Grillo T.A. & Nonell S. (2014) Beta-Phenyl quenching of 9-phenylphenalenones: a novel photocyclisation reaction with biological implications. *Physical Chemistry Chemical Physics*, **16**, 18813-18820.

Busam G., Junghanns K.T., Kneusel R.E., Kassemeyer H.H. & Matern U. (1997) Characterization and expression of caffeoyl-coenzyme A 3-O-methyltransferase proposed for the induced resistance response of *Vitis vinifera* L. *Plant Physiology*, **115**, 1039-1048.

Cañas-Gutierrez G.P., Angarita-Velasquez M.J., Restrepo-Florez J.M., Rodriguez P., Moreno C.X. & Arango R. (2009) Analysis of the CYP51 gene and encoded protein in propiconazole-resistant isolates of *Mycosphaerella fijiensis*. *Pest Management Science*, **65**, 892-899.

Capanoglu E., Beekwilder J., Matros A., Boyacioglu D., Hall R.D. & Mock H.P. (2012) Correlation of rutin accumulation with 3-O-Glucosyl transferase and Phenylalanine ammonia-lyase activities during the ripening of tomato fruit. *Plant Foods for Human Nutrition*, **67**, 371-376.

Carlier J., De Waele D. & Escalant J.V. (2002) Global evaluation of *Musa* germplasm for resistance to *Fusarium Wilt*, *Mycosphaerella* Leaf Spot Diseases and Nematodes: In-Depth Evaluation.

Castro R., Pesantez M., Lema P., Quevedo J., Arichabala P. & Alvarado-Capo Y. (2015) Potential use of *Trichoderma*-based bioproduct for black leaf streak disease (*Mycosphaerella fijiensis*) management in the field. *Biocontrol Science and Technology*, **25**, 481-486.

Chandra A., Saxena R., Dubey A. & Saxena P. (2007) Change in phenylalanine ammonia lyase activity and isozyme patterns of polyphenol oxidase and peroxidase by salicylic acid leading to enhance resistance in cowpea against *Rhizoctonia solani*. *Acta Physiologiae Plantarum*, **29**, 361-367.

Chang P.F.L., Hsu C.C., Lin Y.H., Chen K.S., Huang J.W. & Liou T.D. (2008) Histopathology comparison and phenylalanine ammonia lyase (PAL) gene expressions in *Fusarium wilt* infected watermelons. *Australian Journal of Agricultural Research*, **59**, 1146-1155.

Chong J., Baltz R., Fritig B. & Saindrenan P. (1999) An early salicylic acid-, pathogen- and elicitor-inducible tobacco glucosyltransferase: role in compartmentalization of phenolics and H_2O_2 metabolism. *FEBS Lett*, **458**, 204-208.

Christelova P., Valarik M., Hribova E., De Langhe E. & Dolezel J. (2011) A multi gene sequence-based phylogeny of the Musaceae (banana) family. *BMC Evolutionary Biology*, **11**, 103.

Christensen A.B., Gregersen P.L., Olsen C.E. & Collinge D.B. (1998) A flavonoid 7-O-methyltransferase is expressed in barley leaves in response to pathogen attack. *Plant Molecular Biology*, **36**, 219-227.

Churchill A.C.L. (2011) *Mycosphaerella fijiensis*, the black leaf streak pathogen of banana: progress towards understanding pathogen biology and detection, disease development, and the challenges of control. *Molecular Plant Pathology*, **12**, 307-328.

Cieplik F., Spath A., Regensburger J., Gollmer A., Tabenski L., Hiller K.A.,…, Schmalz G. (2013) Photodynamic biofilm inactivation by SAPYR-An exclusive singlet oxygen photosensitizer. *Free Radical Biology and Medicine*, **65**, 477-487.

Cooke R.G. & Segal W. (1955) Colouring Matters of Australian Plants. 4. Haemocorin - a unique glycoside from Haemodorum-Corymbosum Vahl. *Australian Journal of Chemistry*, **8**, 107-113.

Cruz-Cruz C.A., Ramirez-Tec G., Garcia-Sosa K., Escalante-Erosa F., Hill L., Osbourn A.E. & Pena-Rodriguez L.M. (2010) Phytoanticipins from banana (*Musa acuminata* cv. Grand Naine) plants, with antifungal activity against *Mycosphaerella fijiensis*, the causal agent of black Sigatoka. *European Journal of Plant Pathology*, **126**, 459-463.

D'Hont A., Denoeud F., Aury J.M., Baurens F.C., Carreel F., Garsmeur O.,…, Wincker P. (2012) The banana (*Musa acuminata*) genome and the evolution of monocotyledonous plants. *Nature*, **488**, 213-217.

Dita M.A., Garming H., van den Bergh I., Staver C. & Lescot T. (2013) Banana in Latin America and the Caribbean: Current State, Challenges and Perspectives. International Ishs-Promusa Symposium on Bananas and Plantains: Towards Sustainable Global Production and Improved Use, **986**, 365-380.

Doehlemann G. & Hemetsberger C. (2013) Apoplastic immunity and its suppression by filamentous plant pathogens. *New Phytologist*, **198**, 1001-1016.

Duque L., Zapata C., Rojano B., Schneider B. & Otálvaro F. (2013) Radical scavenging capacity of 2,4-Dihydroxy-9-phenyl-1*H*-phenalen-1-one: A functional group exclusion approach. *Org Lett*, **15**, 3542-3545.

Edwards J.M. & Weiss U. (1974) Pigments of *L Tinctoria* Ell .5. Phenalenone pigments of root system of *Lachnanthes Tinctoria*. *Phytochemistry*, **13**, 1597-1602.

Elayabalan S., Subramaniam S. & Selvarajan R. (2015) Banana bunchy top disease (BBTD) symptom expression in banana and strategies for transgenic resistance: A review. *Emirates Journal of Food and Agriculture*, **27**, 55-74.

Elsebai M.F., Kehraus S., Lindequist U., Sasse F., Shaaban S., Gutschow M., Josten M., Sahl H.G. & Konig G.M. (2011) Antimicrobial phenalenone derivatives from the marine-derived fungus *Coniothyrium cereale*. *Organic & Biomolecular Chemistry*, **9**, 802-808.

Elsebai M.F., Saleem M., Tejesvi M.V., Kajula M., Mattila S., Mehiri M., Turpeinen A. & Pirttila A.M. (2014) Fungal phenalenones: chemistry, biology, biosynthesis and phylogeny. *Natural Product Reports*, **31**, 628-645.

Etebu E. & Young-Harry W. (2011) Control of black Sigatoka disease: Challenges and prospects. *African Journal of Agricultural Research*, **6**, 508-514.

Fang J.J., Paetz C., Holscher D., Munde T. & Schneider B. (2011) Phenylphenalenones and related natural products from *Wachendorfia thyrsiflora*. *Phytochemistry Letters*, **4**, 203-208.

FAO (2013a) Fight against Black Sigatoka must continue to save small Caribbean banana farms. Food and Agriculture Organization of the United Nations (FAO)

FAO (2013b) http://faostat.fao.org/default.aspx?lang=en. Food and Agriculture Organization of the United Nations (FAO)

FAO (2015) http://www.statista.com/statistics/264001/worldwide-production-of-fruit-by-variety/

Flors C. & Nonell S. (2006) Light and singlet oxygen in plant defense against pathogens: Phototoxic phenalenone phytoalexins. *Accounts of Chemical Research*, **39**, 293-300.

Formela M., Samardakiewicz S., Marczak L., Nowak W., Narozna D., Bednarski W., Kasprowicz-Maluski A. & Morkunas I. (2014) Effects of endogenous signals and *Fusarium oxysporum* on the mechanism regulating genistein synthesis and accumulation in *Yellow Lupine* and their impact on plant cell cytoskeleton. *Molecules*, **19**, 13392-13421.

Fouré E. (1987) Varietal reactions of bananas and plantains to Black Leaf Streak disease. In: Banana and plantain breeding strategies: Proceedings of an International workshop", pp. 110-113.

Fouré E. (1993) Characterization of the reaction of banana cultivars to *Mycosphaerella fijiensis* Morelet in Cameroon and genetics of resistance. In: Breeding Banana and Plantain for Resistance to Diseases and Pests (ed J. Ganry), pp. 159-170. CIRAD/INIBAP, Montpellier, France.

FRAC (2014) Fungicide Resistance Action Committee. Banana workin group. In: http://www.frac.info/working-group/banana-group/general-use-recommendations.

Garcia-Bastidas F., Ordoñez N., Konkol J., Al-Qasim M., Naser Z., Abdelwali M.,..., Kema G.H.J. (2014) First report of *Fusarium oxysporum* f. sp cubense tropical race 4 associated with Panama disease of Banana outside Southeast Asia. *Plant Disease*, **98**, 694-694.

González R., Bustamante E., Shannon P., Okumoto S. & Leandro G. (1996) Evaluación de microorganismos quitinolíticos en el control de la Sigatoka Negra (*Mycosphaerella fijiensis*) en banano. *Manejo Integrado de Plagas*, **40**, 12-16.

Guennec A., Dumez J., Giraudeaub P. & Caldarelli S. (2015) Resolution-enhanced 2D NMR of complex mixtures by non-uniform sampling. *Magnetic Resonance in Chemistry*. Early View.

Guo J.M., Lu Y.W., Shang E.X., Li T., Liu Y., Duan J.A., Qian D.W. & Tang Y.P. (2015) Metabolite identification strategy of non-targeted metabolomics and its application for the identification of components in Chinese multicomponent medicine Abelmoschus manihot L. *Phytomedicine*, **22**, 579-587.

Gutierrez D., Flores N., Abad-Grillo T. & McNaughton-Smith G. (2013) Evaluation of substituted phenalenone analogues as antiplasmodial agents. *Experimental Parasitology*, **135**, 456-458.

Gutiérrez M., Holguín F., Dunn M., Guillén K. & Huerta G. (2015) Antifungal activity of Serratia marcescens CFFSUR-B2 purified chitinolytic enzymes and prodigiosin against *Mycosphaerella fijiensis*, causal agent of black Sigatoka in banana (*Musa spp.*). *Biocontrol*, **60**, 565-572.

Hara M., Oki K., Hoshino K. & Kuboi T. (2003) Enhancement of anthocyanin biosynthesis by sugar in radish (*Raphanus sativus*) hypocotyl. *Plant Science*, **164**, 259-265.

Herbers K., Meuwly P., Frommer W.B., Metraux J.P. & Sonnewald U. (1996) Systemic acquired resistance mediated by the ectopic expression of invertase: Possible hexose sensing in the secretory pathway. *Plant Cell*, **8**, 793-803.

Herbers K., Takahata Y., Melzer M., Mock H.P., Hajirezaei M. & Sonnewald U. (2000) Regulation of carbohydrate partitioning during the interaction of potato virus Y with tobacco. *Molecular Plant Pathology*, **1**, 51-59.

Heslop-Harrison J.S. & Schwarzacher T. (2007) Domestication, genomics and the future for banana. *Annals of Botany*, **100**, 1073-1084.

Hidalgo W., Duque L., Saez J., Arango R., Gil J., Rojano B., Schneider B. & Otálvaro F. (2009) Structure activity relationship in the interaction of substituted perinaphthenones with *Mycosphaerella fijiensis*. *Journal of Agricultural and Food Chemistry*, **57**, 7417-7421.

Hirai N., Ishida H. & Koshimizu K. (1994) A phenalenone-type phytoalexin from *Musa acuminata*. *Phytochemistry*, **37**, 383-385.

Hölscher D., Dhakshinamoorthy S., Alexandrov T., Becker M., Bretschneider T., Buerkert A.,…, Swennen R.L. (2014) Phenalenone-type phytoalexins mediate resistance of banana plants (*Musa spp.*) to the burrowing nematode *Radopholus similis*. *Proceedings of the National Academy of Sciences of the United States of America*, **111**, 105-110.

Hölscher D., Fuchser J., Knop K., Menezes R., Buerkert A., Svatoš A., Schubert U. & Schneider B. (2015) High resolution mass spectrometry imaging reveals the occurrence of phenylphenalenone-type compounds in red paracytic stomata and red epidermis tissue of *Musa acuminata* ssp. zebrina cv. 'Rowe Red'. *Phytochemistry*, **116**, 239-245.

Hölscher D. & Schneider B. (1995) A diarylheptanoid intermediate in the biosynthesis of phenylphenalenones in *Anigozanthos preissii*. *Journal of the Chemical Society-Chemical Communications*, 525-526.

Hölscher D. & Schneider B. (1995) The biosynthetic origin of the central one-carbon unit of phenylphenalenones in *Anigozanthos preissii*. *Natural Product Letters*, **7**, 177-182.

Hoss R., Helbig J. & Bochow H. (2000) Function of host and fungal metabolites in resistance response of banana and plantain in the Black Sigatoka disease pathosystem (*Musa* spp.-*Mycosphaerella fijiensis*). *Journal of Phytopathology*, **148**, 387-394.

Hyam R. & Pankhurst R. (1995) Plants and their names: A concise Dictionary, pp. 545. Oxford University Press.

IITA (2015) Banana and plantain. International Institute of Tropical Agriculture. http://www.iita.org/banana-and-plantain.

INIBAP (1989) Annual Report. International Network for the Improvement of Banana and Plantain.

Jacome L.H. & Schuh W. (1992) Effects of Leaf Wetness Duration and Temperature on Development of Black Sigatoka Disease on Banana Infected by *Mycosphaerella fijiensis* Var Difformis. *Phytopathology*, **82**, 515-520.

Jitsaeng K., Paetz C. & Schneider B. (2010) Phenylphenalenones from *Musa* cv. 'Thepanom' (BBB). *Records of Natural Products*, **4**, 26-30.

Jitsaeng K. & Schneider B. (2010) Metabolic profiling of *Musa acuminata* challenged with *Sporobolomyces salmonicolor*. *Phytochemistry Letters*, **3**, 84-87.

Kamo T., Hirai N., Iwami K., Fujioka D. & Ohigashi H. (2001) New phenylphenalenones from banana fruit. *Tetrahedron*, **57**, 7649-7656.

Kamo T., Hirai N., Tsuda M., Fujioka D. & Ohigashi H. (2000) Changes in the content and biosynthesis of phytoalexins in banana fruit. *Bioscience Biotechnology and Biochemistry*, **64**, 2089-2098.

Kamo T., Kato N., Hirai N., Tsuda M., Fujioka D. & Ohigashi H. (1998) Phenylphenalenone-type phytoalexins from unripe Bungulan banana fruit. *Bioscience Biotechnology and Biochemistry*, **62**, 95-101.

Kanazawa K. & Sakakibara H. (2000) High content of dopamine, a strong antioxidant, in Cavendish banana. *Journal of Agricultural and Food Chemistry*, 48, 844-848.

Kaysser L., Eitel K., Tanino T., Siebenberg S., Matsuda A., Ichikawa S. & Gust B. (2010) A new arylsulfate sulfotransferase involved in liponucleoside antibiotic biosynthesis in *Streptomycetes*. *Journal of Biological Chemistry*, **285**, 12684-12694.

Kim H.K., Choi Y.H. & Verpoorte R. (2010) NMR-based metabolomic analysis of plants. *Nat Protoc*, **5**, 536-549.

Kovacs G., Sagi L., Jacon G., Arinaitwe G., Busogoro J.P., Thiry E.,…, Remy S. (2013) Expression of a rice chitinase gene in transgenic banana ('Gros Michel', AAA genome group) confers resistance to black leaf streak disease. *Transgenic Research*, **22**, 117-130.

Kulma A. & Szopa J. (2007) Catecholamines are active compounds in plants. *Plant Science*, **172**, 433-440.

Langfelder K., Streibel M., Jahn B., Haase G. & Brakhage A.A. (2003) Biosynthesis of fungal melanins and their importance for human pathogenic fungi. *Fungal Genetics and Biology*, **38**, 143-158.

Lazzaro A., Corominas M., Marti C., Flors C., Izquierdo L.R., Grillo T.A., Luis J.G. & Nonell S. (2004) Light- and singlet oxygen-mediated antifungal activity of phenylphenalenone phytoalexins. *Photochemical & Photobiological Sciences*, **3**, 706-710.

Lepoivre P., Acuna P. & Riveros A.S. (1993) Screening procedure from improving resistance to banana black leaf streak disease. In: Breeding Bananas for Resistance to Disease and Pest (ed J. Ganry). CIRAD/INIBAP, Montpellier, France.

Lepoivre P., Busogoro J.P., El Hadrami A., Carlier J., Harelimana G., Mourichon X.,…, Swenen R. (2002) Banana-*Mycosphaerella fijiensis* (black leaf streak disease) interactions. In: Proceedings of the 2nd International Workshop on *Mycospharella fijiensis* leaf spot diseases of bananas. INIBAP. CORBANA, pp. 317, San José, Costa Rica.

Li L.F., Hakkinen M., Yuan Y.M., Hao G. & Ge X.J. (2010) Molecular phylogeny and systematics of the banana family (Musaceae) inferred from multiple nuclear and chloroplast DNA fragments, with a special reference to the genus *Musa*. *Molecular Phylogenetics and Evolution*, **57**, 1-10.

Liu A.Z., Kress W.J. & Li D.Z. (2010) Phylogenetic analyses of the banana family (Musaceae) based on nuclear ribosomal (ITS) and chloroplast (trnL-F) evidence. *Taxon*, **59**, 20-28.

Luis J.G., Echeverri F., Quiñones W., Brito I., Lopez M., Torres F.,..., Rojas M. (1993) Irenolone and Emenolone - 2 new types of phytoalexin from *Musa paradisiaca*. *Journal of Organic Chemistry*, **58**, 4306-4308.

Luis J.G., Fletcher W., Echeverri F., Abad T., Kishi M. & Perales A. (1995a) New phenalenone-type phytoalexins from *Musa acuminata* (Colla AAA) Grand Nain. *Natural Product Letters*, **6**, 23-30.

Luis J.G., Fletcher W.Q., Echeverri F. & Grillo T.A. (1994) Phenalenone-type phytoalexins from *Musa acuminata.* Synthesis of 4-phenylphenalenones. *Tetrahedron*, **50**, 10963-10970.

Luis J.G., Fletcher W.Q., Echeverri F., Grillo T.A., Perales A. & Gonzalez J.A. (1995b) Intermediates with biosynthetic implications in *de novo* production of phenylphenalenone-type

phytoalexins by *Musa acuminata* - Revised Structure of Emenolone. *Tetrahedron*, **51**, 4117-4130.

Luis J.G., Lahlou E.H. & Andres L.S. (1999) 4 '-dehydroxy-irenolone. A new phytoanticipin from the resistant *Musa* selected hybrid SH-3481. *Natural Product Letters*, **13**, 299-304.

Luque-Ortega J.R., Martinez S., Saugar J.M., Izquierdo L.R., Abad T., Luis J.G.,..., Rivas L. (2004) Fungus-elicited metabolites from plants as an enriched source for new leishmanicidal agents: Antifungal phenylphenalenone phytoalexins from the banana plant (*Musa acuminata*) target mitochondria of Leishmania donovani promastigotes. *Antimicrobial Agents and Chemotherapy*, **48**, 1534-1540.

Mahrous E. & Farag M.A. (2015) Two dimensional NMR spectroscopic approaches for exploring plant metabolome: A review. *Journal of Advanced Research*, **6**, 3-15.

Malencic D., Cvejic J., Tepavcevic V., Bursac M., Kiprovski B. & Rajkovic M. (2013) Changes in L-phenylalanine ammonia-lyase activity and isoflavone phytoalexins accumulation in soybean seedlings infected with *Sclerotinia sclerotiorum*. *Central European Journal of Biology*, **8**, 921-929.

Man T., Tessem M.B., Bathen T.F., Bertilsson H., Angelsen A., Hedenstrm M. & Andreassen T. (2014) Identification of metabolites from 2D ^{1}H-^{13}C HSQC NMR using peak correlation plots. *BMC Bioinformatics*, **15**:413

Mandavi V., Farimani M.M., Fathi F. & Ghassempour A. (2015) A targeted metabolomics approach toward understanding metabolic variations in rice under pesticide stress. *Analytical Biochemistry*, **478**, 65-72.

Manosalva P.M., Tonnessen B.W., Lang J.M., Baraoidan M., Bordeos A., Leung H. & Leach J.E. (2013) Rice phenylalanine ammonia lyase 4 gene (OsPAL4) is associated with broad spectrum disease resistance. *Phytopathology*, **103**, 89-89.

Marín D., Romero R., Guzmán M. & Sutton T. (2003) Black Sigatoka: an increasing threat to banana cultivation. *Plant Disease*, **87**, 208-222.

Martínez-Bolaños L., Teliz-Ortiz D., Rodriguez-Maciel J.C., Mora-Aguilera J.A., Nieto-Angel D., Cortes-Flores J.I.,..., Silva-Aguayo G. (2012) Fungicides resistance on *Mycosphaerella fijiensis* populations of Southeastern Mexico. *Agrociencia*, **46**, 707-717.

Mastrangelo A., Armitage E.G., Garcia A. & Barbas C. (2014) Metabolomics as a tool for drug discovery and personalised medicine. A Review. *Current Topics in Medicinal Chemistry*, **14**, 2627-2636.

Meihls L.N., Handrick V., Glauser G., Barbier H., Kaur H., Haribal M.M.,…, Jander G. (2013) Natural variation in maize aphid resistance is associated with 2,4-Dihydroxy-7-methoxy-1,4-benzoxazin-3-one glucoside methyltransferase activity. *Plant Cell*, **25**, 2341-2355.

Meredith D.S. & Lawrence J.S. (1969) Black leaf streak disease of bananas (*Mycosphaerella fijiensis*): Symptoms of disease in Hawaii, and notes on the conidial state of the causal fungus. *Transactions of the British Mycological Society*, **52**, 459-476.

Moazzami A.A., Zhang J.X., Kamal-Eldin A., Aman P., Hallmans G., Johansson J.E. & Andersson S.O. (2011) Nuclear magnetic resonance-based metabolomics enable detection of the effects of a whole grain rye and rye bran diet on the metabolic orofile of plasma in prostate cancer patients. *Journal of Nutrition*, **141**, 2126-2132.

Morkunas I., Formela M., Floryszak-Wieczorek J., Marczak L., Narozna D., Nowak W. & Bednarski W. (2013) Cross-talk interactions of exogenous nitric oxide and sucrose modulates phenylpropanoid metabolism in yellow lupine embryo axes infected with *Fusarium oxysporum*. *Plant Science*, **211**, 102-121.

Munar-Vivas O., Morales-Osorio J.G. & Castaneda-Sanchez D.A. (2010) Use of field-integrated information in GIS-based maps to evaluate Moko disease (*Ralstonia solanacearum*) in banana growing farms in Colombia. *Crop Protection*, **29**, 936-941.

Munde T., Brand S., Hidalgo W., Maddula R.K., Svatos A. & Schneider B. (2013) Biosynthesis of tetraoxygenated phenylphenalenones in *Wachendorfia thyrsiflora*. *Phytochemistry*, **91**, 165-176.

Munde T., Maddula R.K., Svatos A. & Schneider B. (2011) The biosynthetic origin of oxygen functions in phenylphenalenones of *Anigozanthos preissii* inferred from NMR- and HRMS-based isotopologue analysis. *Phytochemistry*, **72**, 49-58.

Narasimhachari, N., Joshi V.B., Krishnan S., Panse M.V. & Wamburka.Mn (1968) Antibacterial properties of perinaphthenone derivatives. *Current Science*, **37**, 288.

Nazir M., Maddah F., Kehraus S., Egereva E., Piel J., Brachmannb A. & König G. (2015) Phenalenones: insight into the biosynthesis of polyketides from the marine alga-derived fungus *Coniothyrium cereale*. *Organic & Biomolecular Chemistry*, In press.

Newman D.J. & Cragg G.M. (2012) Natural products as sources of new drugs over the 30 Years from 1981 to 2010. *Journal of Natural Products*, **75**, 311-335.

Noctor G., Lelarge-Trouverie C. & Mhamdi A. (2015) The metabolomics of oxidative stress. *Phytochemistry*, **112**, 33-53.

OECD (2009) Organisation for Economic Co-operation and Development (OECD). Consensus document of the biology of bananas and plantains (*Musa spp.*). Series on Harmonisation of Regulatory Oversight in Biotechnology No. 48, Paris, France.

OGTR (2008) Department of Health and Ageing Office of the Gene Technology Regulator. The biology of *Musa L*. (banana), pp. 73, Australia.

Oms-Oliu G., Odriozola-Serrano I. & Martin-Belloso O. (2013) Metabolomics for assessing safety and quality of plant-derived food. *Food Research International*, **54**, 1172-1183.

Opitz S. (2002) Phenylphenalenones and related phenolic pigments of the Haemodoraceae: Structure, biosynthesis and accumulation patterns in *Xiphidium caeruleum* and *Wachendorfia thyrsiflora*. Ph.D thesis, Friedrich Schiller Universität Jena.

Ordoudi S.A., Cagliani L.R., Lalou S., Naziri E., Tsimidou M.Z. & Consonni R. (2015) ^{1}H NMR-based metabolomics of saffron reveals markers for its quality deterioration. *Food Research International*, **70**, 1-6.

Ortiz R. & Vuylsteke D. (1994) Inheritance of Black Sigatoka Disease Resistance in plantain-Banana (*Musa Spp*) Hybrids. *Theoretical and Applied Genetics*, **89**, 146-152.

Osbourn A. & Lanzotti V. (2009) Plant-derived Natural Products: Synthesis, Function, and Application. 597p.

Otálvaro F. (2004) Structural, phytopathological and biosynthetic aspects of phenylphenalenones isolated from *Musa*. Ph.D thesis, Universidad de Antioquia.

Otálvaro F., Echeverri F., Quinones W., Torres F. & Schneider B. (2002) Correlation between phenylphenalenone phytoalexins and phytopathological properties in *Musa* and the role of a dihydrophenylphenalene triol. *Molecules*, **7**, 331-340.

Otálvaro F., Jitsaeng K., Munde T., Echeverri F., Quinones W. & Schneider B. (2010) *O*-Methylation of phenylphenalenone phytoalexins in *Musa acuminata* and *Wachendorfia thyrsiflora. Phytochemistry*, **71**, 206-213.

Otálvaro F., Nanclares J., Vasquez L.E., Quiñones W., Echeverri F., Arango R. & Schneider B. (2007) Phenalenone-type compounds from *Musa acuminata* var. "Yangambi km 5" (AAA) and their activity against *Mycosphaerella fijiensis*. *Journal of Natural Products*, **70**, 887-890.

Pedras M.S.C. & Ahiahonu P.W.K. (2005) Metabolism and detoxification of phytoalexins and analogs by phytopathogenic fungi. *Phytochemistry*, 66, 391-411.

Pedras M.S.C., Hossain S. & Snitynsky R.B. (2011) Detoxification of cruciferous phytoalexins in Botrytis cinerea: Spontaneous dimerization of a camalexin metabolite. *Phytochemistry*, **72**, 199-206.

Pérez-Vicente L. (2012) A holistic integrated management approach to control Black Sigatoka Disease of banana caused by *Mycosphaerella fijiensis*. Technical manual. FAO.

Perpelescu M., Kobayashi J., Furuta M., Ito Y., Izuta S., Takemura M., Suzuki M. & Yoshida S. (2002) Novel phenalenone derivatives from a marine-derived fungus exhibit distinct inhibition spectra against eukaryotic DNA polymerases. *Biochemistry*, **41**, 7610-7616.

Ploetz R. (2000) Black sigatoka. *Pesticide outlook*, **11**, 19-23.

Ploetz R. (2001) Black Sigatoka of Banana: the most important disease of a most important fruit. In: American Phytopathological Society. http://www.apsnet.org/publications/apsnetfeatures/Pages/blacksigatoka.aspx.

Ploetz R.C., Kepler A.K. & Daniells J.W.N., S.C. (2007) Banana and plantain: an overview with emphasis on Pacific island cultivars Musaceae (banana family) In: Species profiles for Pacific Island agroforestry (ed C.R. Elevitch), pp. 27. Permanent Agriculture Resources, Holualoa (USA).

Potts J., Lynch M., Wilkings A., Huppé G., cunningham M. & Voora V. (2014) The state of sustainability initiatives review 2014 standards and the green economy. SSI Review pp. 354.

Quiñones W., Escobar G., Echeverri F., Torres F., Rosero Y., Arango V.,..., Gallego A. (2000) Synthesis and antifungal activity of *Musa* phytoalexins and structural analogs. *Molecules*, **5**, 974-980.

Ramawat K. & Mérillon J. (2013) Natural products phytochemistry, botany and metabolism of alkaloids, phenolics and terpenes. Springer Berlin Heidelberg. 4159 p.

Rosquete L.I., Cabrera-Serra M.G., Pinero J.E., Martin-Rodriguez P., Fernandez-Perez L., Luis J.G., McNaughton-Smith G. & Abad-Grillo T. (2010) Synthesis and in vitro antiprotozoal evaluation of substituted phenalenone analogues. *Bioorganic & Medicinal Chemistry*, **18**, 4530-4534.

Sade D., Shriki O., Cuadros-Inostroza A., Tohge T., Semel Y., Haviv Y.,..., Brotman Y. (2015) Comparative metabolomics and transcriptomics of plant response to Tomato yellow leaf curl virus infection in resistant and susceptible tomato cultivars. *Metabolomics*, **11**, 81-97.

Sági L. (2003) Engineering resistance to pathogenic fungi. In: Genetic transformation strategies to address the major constraints to banana and plantain production in Africa, pp. 1-38. International Network for the Improvement of Banana and Plantain, Montpellier, France.

Sarah J.L. (1999) Diseases of banana, Abacá and Enset. (ed D.R. Jones), pp. 295-303. CABI Publishing Wallingford (GBR), United Kingdom.

Satoh Y., Tajima K., Munekata M., Keasling J.D. & Lee T.S. (2012) Engineering of L-tyrosine oxidation in Escherichia coli and microbial production of hydroxytyrosol. *Metabolic Engineering*, **14**, 603-610.

Schmitt B., Hölscher D. & Schneider B. (2000) Variability of phenylpropanoid precursors in the biosynthesis of phenylphenalenones in *Anigozanthos preissii*. *Phytochemistry*, **53**, 331-337.

Schwenk E. (1962) Tumor action of some quinonoid compounds in the Cheekpouch Test. Arzneim. *Forsch*., **12**, 1143.

Simmonds N.W. & Shepherd K. (1955) Taxonomic and origins of cultivated bananas. *Journal of the Linnean Sciety of London Botany*, **55**, 302-312.

Spath A., Leibl C., Cieplik F., Lehner K., Regensburger J., Hiller K.A.,…, Maisch T. (2014) Improving photodynamic inactivation of bacteria in dentistry: Highly effective and fast killing of oral key pathogens with novel tooth-colored Type-II photosensitizers. *Journal of Medicinal Chemistry*, **57**, 5157-5168.

Stergiopoulos I., van den Burg H., Ökmen B., Beenen H., van Liere S., Kema G. & de Wit P. (2010) Tomato Cf resistance proteins mediate recognition of cognate homologous effectors from fungi pathogenic on dicots and monocots. *Proceeding of the National Academy of Science of the United States of America*, **107**, 7610-7615.

Stierle A.A., Upadhyay R., Hershenhorn J., Strobel G.A. & Molina G. (1991) The Phytotoxins of *Mycosphaerella fijiensis*, the causative agent of Black Sigatoka Disease of Bananas and Plantains. *Experientia*, **47**, 853-859.

Strack D., Vogt T. & Schliemann W. (2003) Recent advances in betalain research. *Phytochemistry*, **62**, 247-269.

Swennen R., Vuylsteke D. & Ortiz R. (1995) Phenotypic diversity and patterns of variation in West and Central African Plantains (*Musa* spp, Aab Group Musaceae). *Economic Botany*, **49**, 320-327.

Thissen U., Coulier L., Overkamp K.M., Jetten J., van der Werff B.J.C., van de Ven T. & van der Werf M.J. (2011) A proper metabolomics strategy supports efficient food quality improvement: A case study on tomato sensory properties. *Food Quality and Preference*, **22**, 499-506.

Thomas R. (1971) Biosynthesis of plant phenalenone Haemocorin. *Journal of the Chemical Society D-Chemical Communications*, 739.

Torres J.M., Calderon H., Rodriguez-Arango E., Morales J.G. & Arango R. (2012) Differential induction of pathogenesis-related proteins in banana in response to *Mycosphaerella fijiensis* infection. *European Journal of Plant Pathology*, **133**, 887-898.

Upadhyay R.K., Strobel G.A., Coval S.J. & Clardy J. (1990) Fijiensin, the first phytotoxin from *Mycosphaerella fijiensis*, the causative agent of Black Sigatoka Disease. *Experientia*, **46**, 982-984.

Vishnevetsky J., White T.L., Palmateer A.J., Flaishman M., Cohen Y., Elad Y.,…, Perl A. (2011) Improved tolerance toward fungal diseases in transgenic Cavendish banana (*Musa* spp. AAA group) cv. Grand Nain. *Transgenic Research*, **20**, 61-72.

Wada K.C., Mizuuchi K., Koshio A., Kaneko K., Mitsui T. & Takeno K. (2014) Stress enhances the gene expression and enzyme activity of phenylalanine ammonia-lyase and the endogenous

content of salicylic acid to induce flowering in pharbitis. *Journal of Plant Physiology*, **171**, 895-902.

Wen P.F., Chen J.Y., Wan S.B., Kong W.F., Zhang P., Wang W.,…, Huang W.D. (2008) Salicylic acid activates phenylalanine ammonia-lyase in grape berry in response to high temperature stress. *Plant Growth Regulation*, **55**, 1-10.

Wuyts N., De Waele D. & Swennen R. (2006) Activity of phenylalanine ammonia-lyase, peroxidase and polyphenol oxidase in roots of banana (*Musa acuminata* AAA, cvs Grand Nain and Yangambi km5) before and after infection with *Radopholus similis*. *Nematology*, **8**, 201-209.

Acknowledgements

Finally, after more than 150 pages of my Ph.D dissertation, I am glad to arrive at this section and say thanks to many people whom greatly support and contribute to make my PhD unforgettable through scientific guidance and discussion as well as friendship.

First to all, I sincerely thank my main supervisor Dr. Bernd Schneider for giving me the opportunity to be part of his research group, for his guidance through the knowledge in NMR spectroscopy as well as by his motivation, support and discussion of all the ideas and hypothesis that were part of my doctoral project. It was a pleasant and unforgettable trip into my scientific carreer. Thank you so much Dr. Schneider!

I am greaful to two other co-supervisors, Prof. Georg Pohnert and Dr. Aleš Svatoš, for their suggestions about my Ph.D project.

I would like to thanks to all my colleagues of the Biosynthesis/NMR group, Renate Ellinger for helping me a lot with NMR issues and her friendship; Christian Paetz for sharing greatful discussions, knowledge and ideas to my projects. Other former and current colleagues, Jingjing Fang, Evangelous Tatsis, Sara Agnolet, Kati Barthold, Kusuma Jitsaeng, Tobias Munde, Kamel H. Shaker, Felix Feistel, Anne-Christin Warskulat, Fernanda Ocampos, Bettina Dudek, Jima Chandram amd Yu Chen, for all your contributions, discussions and nice working atmosphere during my doctoral staying. It was really nice to meet and share time with all you!

I would like to thanks MS group, especially Marco Kai, Sybille Lorenz and Riya Menezes for helping me with all the MS measurements of labelled and unlabeled compounds. Thanks to Jerrit Weißflog for being always willing to help me for sharing many standard compounds as well as solvents when they were running short in our lab. I am thankful to Dr. Michael Reichelt from Biochemistry Department for helping me with the phytohormone analysis in *Musa* plants, although these results were not included in the present dissertation. Nevertheless, it gave us new insights for further investigations. Thanks to Dr. Tamara Krügel and greenhouse team for their

support in cultivation and maintenance of the *Musa* plants. Many thanks to Dr. Karin Groten for her support in all the IMPRS stuffs.

I would like to express my gratitude to Dr. Felipe Otálvaro, to whom I owe my first steps into my scientific research in natural products. I really appreciate not only his friendship but also to be part of his current research team in Colombia whereby some results of a great networking collaboration are stamped in the present thesis. In the same way, I want to thanks to all the coauthors of the manuscripts for sharing their scientific experience with me and made wonderful contributions in my projects. Thanks to Emily Wheeler for her editorial assistance with all the manuscripts.

Thanks to all my friends in Jena, especially Diana, Andrea, Ricardo, Paola, Marcela, Jorge, Stephanie, Monique and Susana for sharing with me an awesome time here. I will never forget our discussions, journeys, dancing, and picnics along with some beers, whisky and tequila.

A special thanks to my parents, José and Stella, my brothers, Javier and Mario and my grandparents, for their love and unconditional support in all my personal and professional life (Muchas gracias familia por todo su apoyo incondicional para lograr mis metas tanto en lo personale como profesional, Dios los bendiga, los amo mucho).

I truly thank my girlfriend, Alexandra Ortíz, for her love, patience and unconditional support for carrying out our dreams and professional goals (Gordita, no solo eres parte fundamental de mi vida sino también, fruto de inspiración por quien decidí continuar con mi carrera científica, te amo!).

I would like to thank Max Planck Institute for Chemical Ecology and Colciencias (Colombia) for supporting me with a Ph.D scholarships and the German Academic Exchange Service (DAAD) for travel grant for attending conferences.

Curriculum Vitae

Mr. William Fernando Hidalgo Bucheli (M.Sc)
Biosynthesis/NMR research Group
Max Planck Institute for Chemical Ecology, Hans-Knöll-Straße 8, 07745, Jena
Tel.: +49 (0)3641 57 1609 – Mobile phone: +49 (0)176 2659 9505
E-mail: whidalgo@ice.mpg.de
williamhidalgob@hotmail.com

Education

2010-present:	Ph.D student, Friedrich Schiller University, Jena, Germany.
2007-2009:	Master in Science Biotecnology, Universidad Nacional de Colombia, Medellín, Colombia.
1999-2005:	Chemist, Universidad de Nariño, Pasto, Colombia

Research experience

Ph.D thesis: Biosynthesis of phenylphenalenone-type compounds in Haemodoraceae plants and their phytopathological role in the interaction *Musa-Mycosphaerella fijiensis*

Duration: Sept 2010 – present. Supervisor: Dr. Bernd Schneider
Biosynthesis/NMR research group, Max Planck Institute for Chemical Ecology, Hans-Knöll-Straße 8, D-07745, Jena, Germany.

Master thesis: Structure-activity relationship of perinaphthenone-type compounds in the biological system *Mycosphaerella fijiensis*

Duration: Jan 2007-Dec 2008. Supervisor: Dr. Felipe Otálvaro Tamayo
Synthesis and biosynthesis of natural metabolites research group, Universidad de Antioquía, Medellín, Colombia.

Underdegree thesis: Characterization of bacteria producing polyhydroxyalkanoates (PHAs) isolated of soils of Andean region of Nariño Department.

Duration: Jan 2004-Aug 2005. Supervisor: Dr. Pablo Fernández Izquierdo
Microbial Biotechnology, Universidad de Nariño, Pasto

Professional experience

Jan 2009- Sep 2010 Lecturer, Faculty of Medicine, Universidad Cooperativa de Colombia, Pasto, Colombia.

Jan 2009- Dec 2009 Lecturer, Faculty of Chemistry, Universidad de Nariño, Pasto, Colombia.

Aug 2007-Dec 2008 Lecturer, Postgrade Biotechnology, Universidad Nacional de Colombia, Medellín, Colombia.

Publications record

1. **Hidalgo W**., Chandran J., Menezes R., Otálvaro F. & Schneider B. (2015) Phenylphenalenones protect banana plants from infection by *Mycosphaerella fijiensis* and are deactivated by metabolic conversion. Plant, Cell & Environment (in press). doi: 10.1111/pce.12630
2. **Hidalgo W**., Kai M. & Schneider B. (2015) 4-Methoxycinnamic acid – An unusual phenylpropanoid involved in phenylphenalenone biosynthesis in *Anigozanthos preissii*. *Phytochemistry*, **13**, 68-73.
3. **Hidalgo W**., Cano M., Arbelaez M., Zarrazola E., Gil J., Schneider B. & Otálvaro F. (2015) 4-phenylphenalenones as a template for new photodynamic compounds against *Mycosphaerella fijiensis*. *Pest Manag. Sci.* (in press). doi: 10.1002/ps.4055
4. Munde T., Brand S., **Hidalgo W**., Maddula R., Svatos A. & Schneider B. (2013) Biosynthesis of tetraoxygenated phenylphenalenones in *Wachendorfia thyrsiflora*. *Phytochemistry*, **91**, 165-176.
5. Cano M., Rojas C., **Hidalgo W**., Sáez J., Gil J., Schneider B. & Otálvaro, F. (2012). Improved synthesis of 4-phenylphenalenones: the case of isoanigorufone and structural analogs. *Tetrahedron Letters*, **54**, 351-354

6. Fang J., Reichelt M., **Hidalgo W**., Agnolet S. & Schneider B. (2012). Tissue-specific distribution of secondary metabolites in rapeseed (*Brassica napus*). PLoS One, 7(10).
7. **Hidalgo W**, Duque L, Saez J, Arango R, Gil J, Rojano B, Schneider B, Otálvaro F. (2009) Structure-activity relationship in the interaction of substituted perinaphthenones with *Mycosphaerella fijiensis*. *J. Agric. Food Chem*. **57**, 7417-7421.

Oral presentations:

1. Hidalgo W. (2014) From the precursor towards understanding the structural dynamic in the biosynthesis of phenylphenalenones. 13th IMPRS Symposium, MPI for Chemical Ecology, Dornburg, Deutschland.
2. Hidalgo W. (2013) Phenylphenalenones: The weapons of banana plants against its enemy *Mycosphaerella fijiensis*. ICE Symposium, MPI for Chemical Ecology, Jena, Deutschland
3. Hidalgo W. (2013) Phenylphenalenone-type compounds and its role as phytoalexins in the pathosystem *Musa- M. fijiensis*. Trends in natural products research: a young scientists meeting of PSE and ÖPhG, Austrian Pharmaceutical Society (ÖPhG); Phytochemical Society of Europe (PSE); Innsbruck University, University Centre Obergurgl, Obergurgl, Austria.

Poster presentations:

1. Hidalgo W., Chandran J., Menezes R., Otálvaro F. & Schneider B. (2015) Unraveling the role of phenylphenalenones as key metabolites in Musa plants against the attack by the pathogen *Mycosphaerella fijiensis*. International Society of Chemical Ecology (ISCE 2015), Stockholm, Sweden.
2. Hidalgo W. (2014) Unraveling the role of phenylphenalenones as key metabolites in *Musa* plants against the attack by the pathogen *Mycosphaerella fijiensis*. III Congress of the Latin American Association of Chemical Ecology (ALAEQ), Bogotá, Colombia.
3. Hidalgo W.*, Kai M., Schneider B. (2014) New insights on the structural dynamic in the biosynthesis of phenylphenalenones in Haemodoraceae plants. Workshop "Challenges and Advances in the Annotation and de novo Identification of Small Biological Molecules" (AISBN), National Center for Scientific Research (CNRS), Gif-sur-Yvette, FR

4. Hidalgo W.*, Reichelt M., Schneider B. (2013) Phenylphenalenone-type compounds and its role as phytoalexins in the pathosystem *Musa* - *M. fijiensis*. 1st European Conference on Natural Products, DECHEMA, Frankfurt/Main, DE
5. Hidalgo W. (2013) Phenylphenalenone-type compounds and its role as phytoalexins in the pathosystem *Musa* - *M. fijiensis*. 12th IMPRS Symposium, MPI for Chemical Ecology, Jena, DE.
6. Hidalgo W. (2012) Metabolic profile of the fungi *Mycosphaerella fijiensis* and its role in the interaction with *Musa* plants. 11th IMPRS Symposium, MPI for Chemical Ecology, Dornburg, DE
7. Hidalgo W.*, Sáez J., Arango R., Gil J., Schneider B., Otálvaro L.F. (2009) Structure-activity relationship studies in the perinaphthenone series. The *Mycosphaerella fijiensis* pathosystem. XV Latinamerican Congress of Plant Pathology, Pontificia Universidad Catolica de Chile, Santiago, CL

Honors, awards and fellowships:

1. Distinction best student Faculty of Chemistry, Universidad de Nariño, Dec 2005
2. Distinction Meritor Under degree thesis, Universidad de Nariño, Sep 2005
3. Distinction Meritor Master thesis, Universidad Nacional de Colombia, Dec 2008
4. Distinction Best master project, Pontificia Universidad Católica de Chile, Jan 2009
5. Distinction qualify lecturer Faculty of Medicine, Universidad Cooperativa de Colombia, May 2010
6. Master Fellowship, Universidad Nacional de Colombia, Jan 2007- Dec 2008

William F. Hidalgo Bucheli

Signature

Erklärung zu den Eigenanteilen des Promovenden/der Promovendin sowie der weiteren Doktoranden/Doktorandinnen als Koautoren an den Publikationen und Zweitpublikationsrechten bei einer kumulativen Dissertation (in die kumulative Dissertation aufzunehmen)

Für alle in dieser kumulativen Dissertation verwendeten Manuskripte liegen die notwendigen Genehmigungen der Verlage („Reprint permissions") für die Zweitpublikation vor.

Die Co-Autoren der in dieser kumulativen Dissertation verwendeten Manuskripte sind sowohl über die Nutzung, als auch über die oben angegebenen Eigenanteile informiert und stimmen dem zu (es wird empfoh-len, diese grundsätzliche Zustimmung bereits mit Einreichung der Veröffentlichung einzuholen bzw. die Gewichtung der Anteile parallel zur Einreichung zu klären).

Die Anteile der Co-Autoren an den Publikationen sind in der Anlage aufgeführt (Musterbeispiel).

Ich bin mit der Abfassung der Dissertation als publikationsbasiert, d.h. kumulativ, einverstanden und bestätige die vorstehenden Angaben. Eine entsprechend begründete Befürwortung mit Angabe des wissenschaftlichen Anteils des Doktoranden/der Doktorandin an den verwendeten Publikationen werde ich parallel an den Rat der Fakultät der Chemisch-Geowissenschaftlichen Fakultät richten.

MAX - PLANCK - INSTITUT
FÜR CHEMISCHE ÖKOLOGIE
Dr. B. Schneider
Beutenberg Campus
Hans-Knöll-Str. 8
D - 07745 Jena

Name Erstbetreuer(in) Datum Ort Unterschrift

Prof. Dr. Georg Pohnert
Institut für Anorganische und Analytische Chemie
Lehrstuhl für Instrumentelle Analytik
Bioorganische Analytik
Friedrich-Schiller-Universität Jena
Lessingstr. 8
D-07743 Jena
Germany

Name Zweitbetreuer(in) Datum Ort Unterschrift

Jena, 13.07.2015

Selbständigkeitserklärung

Jena, 21.10.2015

Ich erkläre, dass ich die vorliegende Arbeit selbständig und unter Verwendung der angegebenen Hilfsmittel, persönlichen Mitteilungen und Quellen angefertigt habe.

.....

William Fernando Hidalgo Bucheli

Jena, 21.10.2015

Erklärung:

Ich erkläre,

dass mir die geltende Promotionsordnung der Fakultät bekannt ist;

dass ich die Dissertation selbst angefertigt, keine Textabschnitte eines Dritten oder eigener Prüfungsarbeiten ohne Kennzeichnung übernommen und alle von mir benutzten Hilfsmittel, persönlichen Mitteilungen und Quellen in meiner Arbeit angegeben habe;

dass mich folgende Personen bei der Auswahl und Auswertung des Materials sowie bei der Herstellung des Manuskripts unterstützt haben: Bernd Schneider, Felipe Otálvaro, Marco Kai, Jima Chandran, Riya Menezes, Marisol Cano, Carlos Rojas, Jesús Gil, Jairo Sáez, Edwin Zarrazola, Manuela Arbelaez.

dass die Hilfe eines Promotionsberaters nicht in Anspruch genommen wurde und dass Dritte weder unmittelbar noch mittelbar geldwerte Leistungen von mir für Arbeiten erhalten haben, die im Zusammenhang mit dem Inhalt der vorgelegten Dissertation stehen;

dass ich die Dissertation noch nicht als Prüfungsarbeit für eine staatliche oder andere wissenschaftliche Prüfung eingereicht habe,

dass ich nicht die gleiche, eine in wesentlichen Teilen ähnliche oder eine andere Abhandlung bei einer anderen Hochschule als Dissertation eingereicht habe (wenn ja, bitte Ergebnis angeben).

……

William F. Hidalgo Bucheli